APPLICATIONS OF POPULATION AND OTHER ANALYTICAL APPROACHES TO PHARMACOKINETIC AND PHARMACOKINETIC/PHARMACODYNAMIC MODELLING

by

Maria C. P. Rosario, B.Sc.Pharm., M.Sc., M.R.Pharm.S.

This being a thesis submitted for the degree of Doctor of Philosophy in the Faculty of Medicine, University of Glasgow

Department of Medicine and Therapeutics

ProQuest LLC.
789 East Eisenhower Parkway
P.O. Box 1346
Ann Arbor, MI 48106 – 1346

TABLE OF CONTENTS

ACKNOWLEDGEMENTS

I would like to extend my gratitude to each of the following persons who helped me in the preparation of this thesis:

Professor John Reid for allowing me to undertake this work in his department.

Dr. Peter A. Meredith for his infinite intellectual and mental support while supervising throughout the course of my PhD.

Dr Alison H. Thomson for her teaching and enthusiasm, which led me into this area of drug research.

Dr. Murray and Dr. Elliott for their encouragement, interest, good advice and constant willingness to discuss any aspect of the thesis.

Professor Jose Morais who first taught me pharmacokinetics and who has encouraged me to pursue my interest in pharmacokinetics and pharmacodynamics.

Many heartfelt thanks go to JNICT (and Praxis Programme) for giving the fellowship that made it possible for me to be sponsored during the three years of research work. I am also grateful to Fundacao Calouste Gulbenkian for having sponsored the first months of my work.

I also feel deeply indebted to recognition to my friends Mrs and Mr Wagg for their support, interest and willingness to read my thesis.

Finally and most owingly I would like to thank my parents and sisters whose understanding, support and affection have been essential throughout these years.

DECLARATION

I declare that this thesis has been written by myself and is a record of work performed by myself. It has not been submited previously for a higher degree. The research was carried out in the Department of Medicine and Therapeutics, University of Glasgow, under the supervision of Doctor Peter A. Meredith and Doctor Alison H. Thomson.

Maria C. P. Rosario

November 1999

LIST OF TABLES

LIST OF FIGURES

LIST OF ABBREVIATIONS AND SYMBOLS

AIC	Akaike Information Criterion
Ce	concentration in the effect compartment
CL	clearance
CL/F	clearance/bioavailability
cv	coefficient of variation
Cmax	maximal concentration
DBP	diastolic blood pressure
DF	degrees of freedom
ELS	extended least squares
Emax	maximal effect
EC50	concentration eliciting half of the maximal effect
Exp	exponential
f(.)	vector function, e.g. pharmacokinetic model
g	escalar function e.g. mathematical function
HR	heart rate
k10	first-order rate constant for drug elimination from compartment 1
k01/Ka	first-order absorption rate constant
k12/k21	first-order constant rate for movement of drug from compartment 1 to 2 and vice-versa.
Keo	first-order elimination rate constant representing the loss from the effect compartment and accounting for the hysteresis
i^{th}	individual data
j^{th}	measurement data
ITS	iterated two-stage method
m	slope of a linear model
NP	number of parameters
N	number of individuals in a study
n	number of measurements from an individual
NONMEM	nonlinear mixed effects model
NPD	naïve pooled data method
NPEM	non-parametric expectaction maximization
OFV	objective function value
ΔOFV	changes in objective function value
POSTHOC	empirical Bayesian parameter estimate
Q/Q_1	intercompartmental clearance
P_i	individual pharmacokinetic parameter
P	population pharmacokinetic parameter
R^2adj	coefficient of determination adjusted
SC	Schwarz criterion
S0	parameter denoting Emax/EC50
STS	standard two-stage method
SE	standard error
$T_{1/2}$	half-life

Tlag	lag time
Tmax	time taken to reach the maximum concentration
WRES	weighted residuals
Var(.)	variance of a scalar random variable
V_1	volume of distribution of compartment 1
V_2	volume of distribution of compartment 2
Vss	volume of distribution at steady state
V/F	volume/bioavailability
Wss	weighted sum of squares
Wssr	weighted residuals sum of squares
Y	measured response
$\hat{Y}$	predicted response
η	random interindividual error
ε	residual error (between measured data and model predictions)
Ω	variance-covariance matrix of the random parameters η; collection of ω^2
λ_n	exponent of the n^{th} exponential
Σ	variance-covariance matrix of the random parameters ε; collection of σ^2
γ	Hill coefficient
θ	parameter to be estimated
σ^2	variance of ε
ω^2	variance of η

SUMMARY

In spite of being in use for more than 50 years, the pharmacokinetics of gentamicin still remain controversial. Advances in analytical techniques during the 70s made it possible to identify a long elimination phase of gentamicin. At that time several studies were published documenting accumulation of gentamicin for a long period of time and the inadequacy of a mono-exponential decline model to describe the elimination phase. Since then, several studies investigating the pharmacokinetics of gentamicin have been carried out. These studies involved either a general patient population or specific subgroups of the patient population. It is only in the last decade that the first report documenting an increased volume of distribution in patients with cancer was published. To date only eight studies have been performed to investigate the volume of distribution of gentamicin. They have all used a mono-exponential decline model and the parameters were estimated either by a Bayesian technique, by the Sawchuck-Zaske method or by the non-parametric expectation maximization (NPEM) algorithm. The nonlinear mixed effects approach has never been employed to characterize the population pharmacokinetics of gentamicin. Most of these studies enrolled a small number of patients and the results obtained were compared with values assumed for the rest of population. A matched control group was used in only a few studies. Therefore the conclusion drawn by these investigators was contradictory. In this thesis the population pharmacokinetics of gentamicin were investigated in patients with cancer using a nonlinear mixed effects approach (NONMEM) using data collected from routine therapeutic drug monitoring.

The data were best fit with a bi-exponential disposition model with a combined residual error structure. Several covariates were examined for a possible influence on the pharmacokinetics of gentamicin. The best covariate model related clearance to estimates of creatinine clearance (minimum creatinine value 60 $\mu mol\ L^{-1}$) and volume of the central compartment to body surface area and albumin concentration.

Since gentamicin is mainly eliminated by glomerular filtration, creatinine clearance estimates are often used to determine initial doses of gentamicin. However, there are limitations to the value of creatinine concentration as a measure of renal function. Disease states that affect the normal production of creatinine will yield estimates of creatinine clearance that do not represent the renal function of the patient, putting patients at risk of overdosing and toxicity. Several strategies have been proposed in the literature to overcome this problem. In this study the influence of low creatinine concentration by deriving three new covariates corresponding to three different minimum creatinine values of 60, 70 and 88.4 μmol L^{-1} was investigated. In this study it was found that setting concentrations less than or equal to 60 μmol L^{-1} to 60 μmol L^{-1}or concentrations less than or equal to 70 μmol L^{-1} to 70 μmol L^{-1} was superior to using either actual creatinine concentration or minimum value of 88.4 μmol L^{-1}.

The usefulness of linear regression as a complementary technique in the covariate model building process was evaluated. It performed well when the relationship between individual parameter estimates and covariate was close to a straight line.

The best model obtained in the population analysis was then used to simulate concentration-time profiles in two simulated "patients" with different clinical characteristics according to two published nomograms: one that used a 'once daily' regimen and one based on traditional target ranges. In the context of published nomograms this analysis indicated that both nomograms achieve satisfactory concentrations in cancer patients. These results confirm the wide interpatient variability in aminoglycoside pharmacokinetics and the need for dosage optimisation of this drug.

Mibefradil is a new calcium antagonist used for the treatment of hypertension. Several studies have been published comparing the efficacy and tolerability of mibefradil with other calcium antagonists. However, comparative studies between mibefradil and slow release formulations of verapamil and diltiazem were lacking. This analysis was carried out aiming to characterise the pharmacokinetics and pharmacodynamics of mibefradil relative to verapamil and diltiazem after a single dose and also to characterise the

concentration-effect relationships of single and multiple doses of mibefradil and verapamil in hypertensive patients. Data collected during a phase II clinical trial from patients with mild to moderate hypertension were used in this analysis. Pharmacodynamic endpoints were changes in diastolic blood pressure, heart rate and PQ prolongation.

An Emax pharmacokinetic/pharmacodynamic model best described the concentration-effect relationship for diastolic blood pressure (DBP) and heart rate (HR) for the three drugs whereas a linear model was used for PQ prolongation.

For mibefradil, as far as DBP is concerning, the concentration-effect relationships were best described by an Emax model for some patients and a linear model for other patients, rendering the comparison impossible. This was caused by the fact that drug concentrations were not high enough to fully characterise the Emax model. The parameters were poorly estimated. An investigator recently proposed a solution to this problem which consisted of introducing a new parameter (S0 equal to Emax/EC50) that could be used to evaluate the potency of a drug even when the maximal effect was not attained. In this thesis, the parameterisation mentioned above was applied and the results obtained were compared with those from the Emax model using a standard parameterisation.

Mibefradil produced sustained effects on blood pressure and heart rate. Diltiazem produced a greater effect on blood pressure and a similar effect on heart rate. The effect of verapamil on blood pressure was similar to diltiazem. However, the effect on heart rate was more pronounced. At steady state, both mibefradil and verapamil produced antihypertensive responses consistent with those characterised after the first dose. For mibefradil the effect on heart rate was also consistent. In both the single, and multiple dose studies, mibefradil showed the weakest effect on PQ prolongation compared with diltiazem and verapamil. For all three calcium antagonist drugs there were close and reproducible relationships between plasma drug concentrations and the effects on blood pressure, heart rate and PQ interval. Important differential effects were observed

between the compounds, which should be of value in determining optimal dosage regimens.

There are several ways of combining pharmacokinetic and pharmacodynamic information during the modelling process. The pharmacokinetic and pharmacodynamic data as well as the link between them can either be modelled separately or simultaneously. The data may be analysed sequentially; the pharmacokinetic model is first described and the results from that can be included in the pharmacodynamic analysis. Alternatively, the data may be analysed simultaneously. In the present analyses, the data sets used in Chapter 3, were collected after the administration of 150 mg of mibefradil as a single dose. The data were analysed in four different ways 1) pharmacokinetic data were fitted and then the population pharmacokinetic parameters were fixed during the pharmacodynamic data fitting, only pharmacodynamic measurements were included in the data set. 2) pharmacokinetic data were fitted and then the population pharmacokinetic parameters were fixed during the pharmacodynamic data fitting, using a full data set. 3) pharmacokinetic and pharmacodynamic data were analysed simultaneously. 4) individual predicted concentrations from the pharmacokinetic analysis were used as independent variable in the pharmacodynamic analysis. Since in most cases the pharmacokinetic model is better known than the pharmacodynamic model, a subsequent, stepwise modelling approach is often preferred, avoiding pitfalls due to poor pharmacodynamic data or a wrong model selection. It was concluded that the pharmacokinetic data should be left in the data set while estimating pharmacodynamic parameters.

CHAPTER 1 INTRODUCTION

1.1 SUMMARY

First an overview of the reason for modelling is given. Particular emphasis is given to the role of modelling in clinical pharmacology. Differences in the various analytical approaches are highlighted as they were applied in the thesis. Finally, technical concepts used in the analyses presented in the thesis are reviewed.

1.2 OUTLINE OF THE THESIS

The aim of this thesis is to apply different techniques to pharmacokinetic-pharmacodynamic modelling.

The advantages and disadvantages of applying these techniques are explored through application to different types of data. In Chapter 2 the nonlinear mixed effects approach is applied to a sparse data set obtained from therapeutic drug monitoring. In Chapter 3, the standard two-stage approach is used to analyse rich data obtained from Phase II clinical trials of the development of a new compound. Finally, in Chapter 4 different methods of combining pharmacokinetic and pharmacodynamic data are explored and the results are compared.

The conclusions from all the chapters are presented in Chapter 5.

1.3 MODELLING METHODOLOGY

The reasons for modelling have been discussed from a philosophical point of view by Boxenbaum (1992). Biological processes are very complex and difficult to understand. Complications arising from the analyses of biological data from pharmacokinetic and metabolism studies have also been recognised. To overcome the problem, one can represent the system being analysed by a model. Models provide a conceptual framework for phenomena by taking into account the structural and operational characteristics of the system. Nonetheless, models that completely explain and predict the process are complex and limited in their applications. One way to approach the problem is to simplify the process by assuming that the model is a representation and typifies a class of similar systems. From that perspective the overall function of a model is to assist in characterising and explaining phenomena.

During pharmacokinetic and/or pharmacodynamic studies, an enormous amount of data may be generated. Mathematical models are then used to extract information and the results are summarised by the parameters estimated from fitting the model to the data. The model parameter functions as a measure of comparison of results both within and between experiments. Mathematical modelling can also help in exploring the mechanism involved in the process. The modelling process can lead to an empirical representation and from this empirical representation a theoretical basis can be developed to explain the observations. Once a model is selected and parameter values estimated, it can be used to make predictions. In conclusion, the ultimate goal of pharmacokinetic and pharmacodynamic modelling is to learn something about the parameters of the study population so as to allow generalisation of results to the wider population, or to predict alternative scenarios such as the effect of different dosage regimens.

1.3.1 MODELLING APPLICATIONS IN CLINICAL PHARMACOLOGY

The use of population pharmacokinetic/pharmacodynamic models has been an object of researchers' attention over the last decades, and has been discussed in detail in the

literature. Applications include the development of dosing recommendations, the optimisation of dosage adjustments, drug regulatory agency submissions, and guidance for future research.

Academic research is the driving force in this field and two main areas benefit from those applications and they are: therapeutic drug monitoring in hospitals and drug development in industry.

1.3.1.1 Optimisation of Dosage Regimens

The establishment of appropriate dosage regimens has attracted the attention of investigators for many years. Theoretically, dosage regimens for drugs with a low therapeutic index should be determined from the pharmacokinetic and pharmacodynamic parameters for each individual. This implies that for these drugs a complete concentration-time profile should be available for each patient when selecting a dosage regimen. A full pharmacokinetic profile involves obtaining several blood samples, which would be both costly and cumbersome for the patient and impractical to carry out in routine patient care.

In the literature, different approaches have been proposed to establishing ideal dosage regimens. Initially, individual pharmacokinetic parameters estimated from a specific population were used to relate pharmacokinetic parameters such as clearance to patient characteristics such as age and sex. These relationships were used to develop nomograms (Siersbaek-Nielsen et al., 1971; Chan et al., 1972; Cockcroft and Gault, 1976). The selection of a maintenance dosage regimen for an individual patient based on nomograms gained popularity as it reduced the chances of overdosing or underdosing patients. The limitations of this approach are that the relationship between the physiological and pharmacokinetic parameters may differ widely among individuals and that the approach does not make use of pharmacokinetic information directly obtained from an individual patient. Another aspect to note is that, in many cases, the nomograms were obtained from classic pharmacokinetic studies of small, relatively homogeneous groups of volunteers or patients who were not representative of the whole

patient population. The extrapolation of such results to different patient populations is not recommended.

Other methods have been proposed to select more accurately the dosage regimen for an individual patient. For example, Sawchuk et al. (1977) suggested using 3 measured concentrations of gentamicin *per* patient. However, although this approach served well for gentamicin, it is not generally applicable to a wide variety of drugs. Another approach, described by Slattery, was to adjust dosage on the basis of a single test dose. This 'one point method' gave a maintenance dose to achieve a desired trough concentration at steady state (Slattery, 1980). The method did not aid in the selection of the first dose and dosing interval, which had to be obtained from a nomogram. Chiou et al. (1978) proposed the estimation of theophylline clearance based on two drug concentrations. One advantage of this method was that it only requires minimal pharmacokinetic information and it selected the safe and effective dose early in the course of treatment.

The generalised use of computers on the one hand and the development of reliable drug assays on the other have helped in the application of feedback control methods in clinical pharmacokinetics. A detailed description of the concept for drug dosage optimisation was presented by Vozeh et al. (1985). Technological advances have also led to the development of nonlinear least squares regression programs (Peck and Barret, 1979). One of the most widely used methods for dosage optimisation is the Bayesian algorithm. The Bayesian algorithm allows the combination of population pharmacokinetic information as 'a priori' information with patient drug concentration information to determine individual dosage regimens. Ideally, the information to be used as 'a priori' for dosage recommendations should be derived from data collected from the patient population (Sheiner et al., 1979b) who will receive the drug treatment. Several Bayesian software packages have been developed (Sheiner et al., 1979b; Peck et al., 1980; Kelman et al., 1982; Sheiner and Beal, 1982) and a review of commonly used dosing methods has been published (Burton et al., 1985).

With the advent of these techniques, the pharmacokinetic information from a specific patient was no longer the object of interest as far as dosage recommendation is concerned. The knowledge of mean values and variances of the parameters of a specific patient population became the main aim of research. Therefore an alternative approach to population pharmacokinetic data analysis was implemented: that of the nonlinear mixed effect model (Sheiner et al., 1977; Sheiner and Grasela, 1984).

1.3.1.2 Drug Development

The implemention of population pharmacokinetic/pharmacodynamic modelling to drug development was first advocated by Sheiner & Benet (1985) but it was only in 1991 that a conference was held to discuss the topic (Peck et al., 1992). During this conference the integration and roles of pharmacokinetics, pharmacodynamics and toxicokinetics in rational drug development were identified and discussed. Since then the topic has expanded. The European Commission, through the COST B1 project, supported the realization of two important meetings, the first in 1992 and the second in 1997, and several conferences of experts in the field. The FDA has also encouraged the implementation of the population approach during drug development by producing guidance documents on the topic (Sun et al., 1999).

The application of pharmacokinetic and pharmacodynamic principles in drug development can be seen as tools for scientific and strategic decision making. Ideally, the application of the approach should start in phase I, tolerability trials. It should continue with PK/PD investigations in phase II to provide guidance on dose selection to be used in subsequent clinical trials. In addition, in phase II, a full pharmacokinetic screen is a potential alternative to detect possible clinically relevant drug-drug interactions and to study the drug in sub-groups of patients.

PK/PD modelling from phase II and phase III studies has been sucessfully applied during drug development using the population approach (Vozeh et al., 1996). Some examples showing the merits of PK/PD modelling in drug development have been published (Reigner et al., 1997). The population approach can be a valuable

complement to conventional approaches for collection of PK/PD data for assessment of efficacy and tolerability in relation to drug plasma concentration and to help in the selection of drug dosage in the target population, including special sub-groups. Today, most pharmaceutical companies, to different extents, are using this approach during development of drugs in a wide variety of therapeutic areas.

1.3.2 STUDY DESIGN

One of the points to consider when implementing any clinical trial is the selection of appropriate subjects to be included in the study. Ideally, the population who will need the drug should be included in the trials. Conducting pharmacokinetic studies only in 'healthy volunteers' or 'selected patients' excludes special patient populations, such as geriatric, paediatric and critically ill patients from being investigated. Since the collection of data from such patients by conventional methods gives rise to ethical questions, the use of sparse information obtained during the routine care of patients was advocated (Sheiner, 1984). Data collected during routine care comprises few data *per* individual and therefore traditional methods of data analysis cannot be applied. Difficulties encountered in the analysis of these data motivated investigators to implement an alternative approach using a nonlinear mixed effect model (Sheiner et al., 1977).

These type of data are characterised by having few design restrictions and are collected at a wide range of times and under a variety of circumstances. This contrasts with experimental data in which sampling times are fixed and all subjects are handled in exactly the same manner. A major criticism of using observational data is the uncertainty of conclusions drawn from such data. Firstly there is a lack of balance, resulting from different numbers of data points in different individuals. Usually it is the more critically ill patients who have more samples collected. Secondly, the sparseness of data may present a problem as very few data points are obtained from each individual.

1.4 NONLINEAR REGRESSION MODELLING

1.4.1 GENERAL MODEL

The pharmacokinetic/pharmacodynamic modelling process can be represented by a general function. Considering all individuals, i = 1, ..., N, each individual will have n_i observations. The general model can then be represented by:

$$Y_{ij} = M_i (\Theta, \eta_i, \varepsilon_{ij}) \qquad \text{Eq. 1.1}$$

where Y_{ij} denotes the vector of observations for individual i^{th} at time j. M_i includes the dosing history and covariates. Θ represents the mean parameter estimates. η_i represents the i^{th} individual vector of η where η are the values of the interindividual variability, and ε_{ij} is diference between the measured and model predicted observations.

1.4.2 ESTIMATION ALGORITHMS

Nonlinear regression involves parameter estimation. The parameters are estimated based on a mathematical criterion. The best known is the least squares estimation. The least squares objective function is based on minimising the sum of squared differences between the measured and model predicted responses.

1.4.2.1 Ordinary Least Squares (OLS)

The ordinary least squares method computes the model parameters at a value that minimises the sum of the squared deviations from the measured (Y_{ij}) and model predicted $\hat{Y}_{ij}$ responses. The least squares objective function (O_{OLS}) is given by:

$$O_{ols} = \sum_{i=1}^{N} \sum_{j=1}^{n} (Y_{ij} - \hat{Y}_{ij})^2 \qquad \text{Eq. 1.2}$$

where n is the number of observations. Ordinary least squares estimates assume that that all errors have the same magnitude. Inspection of the plots of residuals (measured-

chosen by the analyst but estimated by the method. ELS is a generalisation of WLS and it is reduced to ordinary least squares when the variance is 1.

The performance of ELS has been evaluated and compared with the other minimisation methods. Some investigators concluded that ELS estimates the parameters with greater accuracy and precision than WLS (Peck et al., 1984). However, Metzler (1987) and van Houwelingen (1988) did not find the ELS method superior to the other methods but found that the IRLS method was almost always better than WLS. They did not recommend the routine use of ELS.

1.4.3 METHODS TO ESTIMATE POPULATION PARAMETERS

Population parameter estimation can be carried out by a number of different methods. All the methods are associated with a minimisation of a least squares objective function as a fitting criterion.

1.4.3.1 Standard Two-Stage (STS)

The standard two-stage approach proceeds in two steps. First, the data from each individual is analysed and the individual parameters estimated, then the individual parameter values are combined to derive the population parameters. For example, the mean can be calculated as follows:

$$\hat{\theta} = \frac{1}{N}\sum_{i=1}^{N}\hat{\theta}_i \qquad \text{Eq. 1.5}$$

where $\hat{\theta}$ is the estimate of the population mean vector of parameters, $\hat{\theta}_i$ are estimates of the individual pharmacokinetic or pharmacodynamic parameters and N represents the number of individuals. The final stage of STS can also include the analysis of dependencies between parameters and covariates using classical statistical approaches (linear stepwise regression, cluster analysis, covariance analysis). The interindividual variability is given by the standard deviation of the individual values.

Studies carried out on simulated data concluded that STS yielded good estimates of mean parameter values and residual variability but imprecise estimates of interindividual variability (Sheiner and Beal, 1980; Sheiner and Beal, 1981; Sheiner, 1984). STS performs well provided the residual error is low (Sheiner and Beal, 1983).

1.4.3.2 Naïve Pooled Data (NPD)

The data from all individuals are pooled as if they all came from one individual and was analysed simultaneously. The ordinary least squares objective function with respect to the parameters is described as follows:

$$O_{NPD}(\theta) = \sum_{i=1}^{N}\sum_{j=1}^{n}(Yij - \hat{Y}_{ij})^2 \qquad \text{Eq. 1.6}$$

where Y_{ij} represents the measured response for the i^{th} individual at the j^{th} time data point and $\hat{Y}_{ij}$ is the model predicted measurement. N represents the number of individuals and n the number of data points for each individual. The least squares function is minimised with respect to parameters.

The NPD has the advantage that it can deal easily with non-standardised data, i.e. different number of data points per individual, and data sets with few data points can be used. It is easy and fast to perform as all the parameters are estimated in one fitting. However, it is associated with some drawbacks. This approach fails to recognise that the information arises from different individuals and consequently it does not estimate the random inter and intraindividual variability. It performs well when the variability between subjects is small but its use has been discouraged (Sheiner, 1984). Studies on simulated data indicate that this approach produces imprecise estimates of mean kinetics, either with sparse data (Sheiner and Beal, 1980) or experimental data (Sheiner and Beal, 1981). That contrasts with the conclusions of others investigators, who recommended its use (Egan et al., 1993; Kataria et al., 1994).

1.4.3.3 Nonlinear Mixed Effects

In the nonlinear mixed effects method, as with NPD, the data from all individuals are analysed at once. In contrast to NPD, the information from each individual is explicitly kept and the interindividual random effects are taken into account. Nonlinear mixed effects uses information from each individual to estimate typical values for the population.

An advantage of the mixed effect model technique is that it uses data pooled from several different studies. Because a mixed effect model allows a different magnitude of residual error variance to be estimated for the data from different sources, they can be combined appropriately to estimate their common structural model parameters.

The first algorithm proposed for estimation of population parameters in a nonlinear mixed effect model was the First Order method (Sheiner et al., 1977) implemented in the NONMEM software. The nonlinear mixed effect model has been implemented in different maximum likelihood algorithms, available through several software packages. Parametric maximum likelihood methods are implemented in software such as NONMEM, in NLME (Pinheiro and Bates, 1989), expectation maximization (EM) and in P-Pharm (Gomeni et al., 1994). Non-parametric approaches are implemented in non-parametric maximum likelihood (NPML) (Steimer et al., 1985; Mallet, 1986) and non-parametric expectation maximization (NPEM) (Schumitzky, 1991). The semi- or smooth non-parametric approach was implemented by Davidian and collaborators, in NLMIX (Davidian and Gallant, 1992; Davidian, 1993). The Bayesian approach to estimate population pharmacokinetic modelling was available in the POPKAN software package (Wakefield and Racine-Poon, 1995). POPKAN uses a Gibbs sampler technique to estimate parameters. A paper reporting a study designed to compare the estimates of seven population pharmacokinetic modelling methods discusses the validity of some of the methods (Roe, 1997) and demonstrated that NONMEM yielded satisfactory results compared to other methods.

1.4.3.4 Comparison of Methods to Estimate Population Parameters

Several studies have reviewed these approaches to the estimation of population parameters (Sheiner and Beal, 1980; Sheiner and Beal, 1981; Sheiner and Beal, 1983; Steimer et al., 1984; Hashimoto and Sheiner, 1991). The standard two-stage approach can only be used if the number of observations *per* individual is sufficiently large (rich-data) to allow an estimation of individual parameters. From a theoretical point of view, the STS population parameter estimates should agree well with the true value provided the study is well designed and performed. However the interindividual variability estimates are expected to be biased upward. This is because the standard deviations include not only the true biological interindividual variability but also the variability due to imprecision in the individual parameter estimation. Improved methods have been proposed that take into account imprecision in parameter estimates. Steimer and collaborators implemented a global two-stage approach and the iterated two-stage approach (Steimer et al., 1984). Another improved method is the Bayesian two-stage proposed by Racine-Poon (1985). In a study to compare the performance of the STS approach with NONMEM in the analysis of simulated data, Sheiner and Beal (1981) found that both approaches yielded acceptable (nonbiased and precise) estimates for the fixed effect parameters. The same conclusion, however, cannot be made with regard to the estimates of interindividual variability. In the same study, Sheiner and Beal found that the STS approach systematically overestimated these parameters. This error accounts for the residual error and interindividual variability and therefore adds variability to the parameter estimates that is not biological in origin, resulting in an upward-biased estimate of interindividual variability. NONMEM estimates of interindividual variability tend to be more reliable because they are not contaminated with the error involved in the estimation of individual parameters. Although NONMEM estimates of these parameters have been shown to be relatively unbiased, they become increasingly imprecise as the number of subjects decreases.

1.4.4 NONMEM - NONLINEAR MIXED EFFECTS

The best-documented and most widely used method of parameter estimation is the

nonlinear mixed-effects model proposed by Sheiner and Beal (1992) and implemented in the software package NONMEM. NONMEM is a Fortran 77 software most extensively used for mixed effect modelling and is the acronym of Nonlinear Mixed Effects Model. NONMEM minimises the extended least squares objective function from Equation 1.4, which, under Gaussian conditions, provides maximum likelihood estimates.

1.4.4.1 First-Order Method

In certain cases, the extended least squares method has difficulties in computing $\hat{Y}_i$ and the var ($\hat{Y}_i$) rendering the minimisation of the objective function impossible. To overcame this problem an approximation of this method is used, the first-order method (FO). The FO method is the default algorithm in NONMEM. It consists of a linearization of the ELS equation through a first-order Taylor series expansion around zero, the expected values of the η's and ε' (Beal and Sheiner, 1992). The first-order estimation method produces estimates of the typical population parameters Θ, Ω and Σ but it does not produce estimates of the individual random interindividual effects, η_i. During the search for the best parameter combination, all subjects have the same parameter values. However, η_i can be estimated after the population parameters have been obtained.

Beal investigated the effect of the approximation involved in the first-order method on parameter estimates and he acknowledged that linearization can affect the accuracy of the estimates. However, where accuracy was affected, this was by not more than 10 per cent (Beal, 1984). In this study, the STS was also compared with the FO method and it was concluded that the STS method performed poorly when there are just a few observations per individual but behaves as well as the FO method when there are as many as seven observations per individual.

1.4.4.2 First-Order Conditional Estimation Method

Version IV of NONMEM (Beal and Sheiner, 1992) incorporated the First-Order

Conditional Estimation method (FOCE) first investigated by Lindstrom & Bates (1990). The difference between these methods and the FO method lies in the way the linearization is done. The FOCE method uses a first order Taylor series expansion around the conditional estimates of ηs. This is done in an iterative way: first, equation 1.4 is fitted to the data using the conditional η's based on the current value of θ, Ω and Σ and second, new conditional estimates are calculated using the updated θ, Ω and Σ. The parameter values η are calculated for each individual during each step of the parameter search. The FOCE method produces estimates of the population parameters and, simultaneously, estimates of the random interindividual effects.

1.4.5 ERROR MODELS

Two types of error models can be defined under the nonlinear mixed effects approach. One type, the residual error model, accounts for the difference between the measured observation and that predicted by the model. The second type of error model, the interindividual error model, accounts for differences between individuals.

1.4.5.1 Residual Error Models

In the general model, as described by equation Eq.1.1, ($Y_{ij} = M_i(\Theta, \eta_i, \varepsilon_{ij})$), Θ can include the estimated model's parameters and the fixed effects. This can be represented by the following mathematical expressions:

$$Y_{ij} = f(P_i, X_{ij}, \varepsilon_{ij}) \qquad \text{Eq. 1.7}$$

where Y_{ij} represents the jth observation for the ith individual, $f(\,)$ is a vector-function that represents the structural model (PK or PD) and relates the independent variables, X_{ij} (e.g. time and dose) to the response given the vector of model parameters of the i^{th} individual P_i. ε_{ij} is the residual error and accounts for the errors due to the assay, model misspecification and intraindividual variability. ε_{ij} are assumed to be independently symmetrically distributed around zero and with variance σ^2.

The residual error can be modelled by several mathematical expressions. Under the NONMEM nomenclature, F represents $\hat{Y}_{ij}$, and EPS is the ε_{ij}. Examples of residual error models are:

Additive error model

Y=F+EPS (1) Eq. 1.8

the variability, σ is constant, expressed as a SD.

Proportional error model

Y=F*(1+EPS (1)) Eq. 1.9

the variability, σ is proportional to the $\hat{Y}_{ij}$, expressed as % CV.

Exponential error model

Y=F*EXP(EPS (1)) Eq. 1.10

The FO method does not distinguish the exponential and the proportional model.

These models can be combined in more complex structures such as:

Y=F*(1+EPS (1)) + EPS (2) Eq. 1.11

Y=F* EXP (EPS (1)) + EPS (2) Eq. 1.12

where EPS(1) and EPS (2) represent two independent errors, ε_{ij1} ε_{ij2}. The combined error model has some advantages as it allows the expression of two models within the same model. This produces a variance at the lower limit of the assay that tends towards an additive error structure and at high concentrations tends towards a proportional (exponential) structure. From these model structures two independent variances σ^2_{add} and $\hat{Y}_{ij}{}^2\sigma^2_{exp}$ are estimated. The additive component of the error is expressed as a SD whereas the proportional component of the error is expressed as %CV. In NONMEM, the variance and covariance for the ε_{ij}'s are estimated as a block matrix (Σ).

1.4.5.2 Interindividual Variability Error Model

P_i, the vector of the individual parameters, is distributed around the typical values (TV), θ_k. These relationships can be described by the equation:

$P_i = \theta_k, + \eta_{ki}$ representing the interindividual error Eq. 1.13

where η_{ki} is the difference between the typical values and the individual parameters. The η_{ki} are assumed to arise from a Gaussian distribution, independent and identically distributed (i.i.d.) with mean zero and variance-covariance matrix, ω^2.

For each parameter, several interindividual error models can be used under the NONMEM terminology. For example:

Additive

CL = TVCL + ETA (1) Eq. 1.14

Where CL represents the individual parameter, and TVCL is the typical value. ETA represents η.

Proportional

CL = TVCL * (1+ ETA (1)) Eq.1.15

Exponential

CL = TVCL * EXP (ETA(1)) Eq.1.16

The FO model does not distinguish between proportional and exponential models.

1.4.6 BAYESIAN ESTIMATES

Information about the distribution of the parameters in a population can be used to determine the most likely set of pharmacokinetic parameters for an individual by applying Bayes' theorem. The Bayesian technique merges the pre-existing population

information (mean and variances) of pharmacokinetic parameters with the measured plasma concentrations from an individual. Population parameters are estimated by setting to 0 the interindividual random effects (η set at 0). This information is used as 'a priori' information for the Bayesian technique to calculate the individual pharmacokinetic parameters, also called 'POSTHOC estimates'. The extended least square objective function is minimised with respect to the interindividual random effects parameters (η) in the estimation of the posterior POSTHOC estimates of the parameters.

The relative contributions of the individual and population data depend on how much information is supplied by the individual and the magnitude of the interindividual variability. If an individual has a large number of accurate data points the empirical POSTHOC estimates for that individual will mainly be determined by that individual alone. The information from population parameters will predominate if the individual only has a few data points.

1.4.7 MODEL SELECTION

Model selection in NONMEM analyses has been based on several criteria. The difference in objective function value (ΔOFV) obtained when two hierarchical models are fitted to the same data set has been used as a criterion to compare the two models when one model is a sub-model from the other. A sub-model is defined as a model that is identical to the full model except that one or more parameters of the latter are set to a fixed value. ΔOFV is minus twice the difference in the log likelihood (-2 log likelihood) of the two models, each likelihood evaluated at its maximum. Minimisation of the objective function is equivalent to maximising the probability of the data. The ΔOFV is asymptotically distributed as χ^2, with degrees of freedom equal to the number of parameters of the full model that are fixed in the reduced model. If the difference in log likelihood exceeds the critical value, the reduced model can be rejected in favour of the full one at whatever p value was used (Sheiner et al., 1977).

The magnitude of the standard error (SE) of the parameter estimates denotes the

confidence in the parameter estimates and can give an indication about the goodness of fit.

Analysis of residuals is designed to test the adequacy of a model and check assumptions made during non-linear regression analysis. Residuals are assumed to be independent, with a zero mean, constant variance, and to follow a normal distribution. If the assumptions are verified, residuals and weighted residuals should be randomly distributed and scattered within a lower and upper horizontal band along the predicted values of dependent variable and time. A change in the sign of the residuals when displayed in time order is called a run. It can be determined whether runs arise at random or whether they are systematic. Systematic deviations are an indication of model misspecification (Boxenbaum et al., 1974).

Inspection of the plots is a very useful tool for model selection. Basic plots include the measured concentration against the model-predicted concentration based on the typical population parameters and on predictions based on the POSTHOC parameter estimates.

1.4.8 COVARIATES

The principal aims of the population pharmacokinetic and pharmacodynamic approaches are to estimate the typical values of the population parameters and to identify the factors (covariates) that have an influence on PK/PD parameters. Models try to minimise the extent of unexplained variability present in the data by incorporating covariates. Covariates are factors such as patient characteristics (age, weight, height, and sex) or pathology (such as renal or hepatic impairment) or other factors that can influence drug disposition, such as concomitant drug therapy, smoking habits and alcohol intake.

The sequences of NONMEM runs which are necessary to determine relationships can become very complicated and time-consuming as the structural model becomes more complex and the number of covariates increases. The use of statistical techniques like linear regression and generalized additive modelling (GAM) and graphical examination

outside NONMEM have been advocated to help in the identification of the structure of the relationships between covariates and parameter estimates. As regression analysis assumes that covariates are not correlated, the existence of collinearity that might influence the model building has to be excluded. Therefore an exploratory analysis should be performed on covariates to examine the distribution and correlation between covariates. The shape of the relationship between POSTHOC parameter estimates and covariates can be identified by mean of bivariate scatterplots. Plots of population residuals and weighted residuals (WRES) provide an indication as to whether a covariate should be included in the model.

Covariates can be incorporated in the model in a stepwise manner, one at a time, starting with the one with the strongest influence until the best model is obtained. Categorical covariates can be included as a "step model". For each NONMEM analysis, the improvement in fit obtained by the addition of one covariate in the regression model can be assessed by the change in the objective function value. Following the forward inclusion of parameter-covariate relationships is a backward elimination process. In each step, each parameter-covariate relationship in the model is replaced by the next lower model. The least important, given that it is not significant, is dropped in favour of the simpler model. This continues until no more terms can be dropped.

1.5 PHARMACOKINETIC AND PHARMACOLOGICAL RESPONSE RELATIONSHIPS

1.5.1 PHARMACOLOGICAL EFFECT

A pharmacological response is a result of the interaction between a drug molecule and a receptor. The pharmacological response is assumed to follow the law of mass action as long as the interaction between drug and receptor is reversible. The interaction between a single drug molecule and single binding site of the receptor causing a response (effect) can be represented by:

[Drug] + [Receptor] $\leftrightarrow$ [Drug-Receptor Complex] $\rightarrow$ Response

where the brackets represents molar concentrations.

The pharmacological response at the receptor site can be classified as:

i) Agonist – the molecule interacts with the receptor and produces a maximal pharmacological response

ii) Partial agonist – the drug interacts and produces a partial maximal effect

iii) Antagonist – the drug inhibits the interaction of another compound with the receptor.

The triggering of a pharmacological response is a result of intricate mechanisms. Modelling techniques are applied to simplify, quantify and help in the understanding of the pharmacological response. Pharmacological response is combined with pharmacokinetics in pharmacokinetic/pharmacodynamic modelling and has been used to predict the time course of action of several drugs.

The pharmacokinetic properties of a drug and the dose determine the onset, intensity and duration of the effect. Increasing the dose causes an increase in the drug concentration at the receptor site leading to an increase in the effect up to a maximum effect. The half-life of a drug affects the duration of activity. A prolonged half-life

causes the drug to remain longer in the body and thereby increasing the duration of effect. The drug action is also dependent on the fraction of the dose that reaches the receptor site. This process depends on the delivery rate of the drug. At the receptor site, the onset, duration and intensity of the pharmacological responses is controlled by concentration of the drug and its metabolites. By combining pharmacokinetics and pharmacodynamics, complex pharmacological responses have been described by pharmacodynamic models accounting for their onset, intensity and duration of action.

Once the pharmacodynamic models have been selected, it is possible to predict the time course of action obtained from different dosage regimens.

1.5.2 PHARMACODYNAMIC MODELS

Pharmacodynamic models correlate the time-course of pharmacological action with the concentration. These models are quite simple if the pharmacological effect of a drug is directly related to concentration (Holford and Sheiner, 1981).

1.5.2.1 Linear Model

The linear model assumes a direct proportionality between pharmacological effect and drug concentration. This relationship can be expressed as:

$$E = m * Y \qquad \text{Eq. 1.17}$$

where E is the effect measurement, m is a proportionality constant (the slope estimated by linear regression) and Y is the drug concentration.

1.5.2.3 Sigmoidal Emax Model

For some drugs the relationship between concentration and effect has a sigmoidal shape, an S-shape instead of a hyperbolic shape as described above. Hill first applied this model to describe the association of oxygen with haemoglobin (1910). The sigmoidal model is represented by:

$$E = \frac{Emax * Y^{\gamma}}{EC50^{\gamma} + Y^{\gamma}} \qquad \text{Eq. 1.21}$$

where E denotes the effect, γ is a factor, also known as the Hill coefficient, Emax is the maximal effect, Y is the drug concentration and EC50 represents the drug concentration that produces half of the maximal response. When γ is 1 the Hill model reduces to the Langmuir Emax model. The Hill coefficient determines the degree of sigmodicity of the curve and thus the value of γ influences the slope of the sigmoid curve.

PK/PD modelling was first developed in drugs with a reversible mechanism of action and with continuous effect data. Recently, these concepts have been successfully applied to drugs with an irreversible effect, like cancer chemotherapy (Jusko, 1971) as well as categorical or dichotomous responses, e.g. the analgesic effect of ketorolac (Mandema and Stanski, 1996).

1.5.3 PHARMACOKINETIC/PHARMACODYNAMIC MODELS

The PK/PD models can be categorised by different aspects. One is classified by the way PK data relates to the PD data, the link model. Another way is to classify PD models is by the mechanism of action of the drug (response models). Also they can be classified if the PD parameters change with the time or not.

1.5.3.1 Pharmacokinetic/Pharmacodynamic Link Models

a) Direct Link Models

Direct link models relate plasma concentrations in the central compartment to the pharmacological effect. In this case, the peak plasma concentration occurs at the same time as the peak effect. It is assumed that a rapid equilibrium between plasma concentration and concentration at the effect site is achieved under steady state as well as non steady-state conditions. The measured plasma concentrations serve as the independent variable in the PD model, as shown in Figure 1.4.3.a, panel A.

b) Indirect Link Models

The relationship between plasma concentration and effect can often show a delay that accounts for the time necessary to allow the equilibrium between concentrations in plasma and at the effect-site to be reached. This phenomenon is called hysteresis. When effect is plotted against plasma concentration, and points are connected in time order, a counterclockwise loop profile may be observed as shown in Figure 1.4.3.b, upper panel. This is removed when concentrations at the effect-site are used to draw the plots (Figure 1.4.3.b, lower panel). The incorporation of a link model between the pharmacokinetic and pharmacodynamic models will help in describing the relationship. The link can be established either by predicting the concentration in a peripheral compartment, or by predicting the concentration at the effect-site, including a hypothetical effect-compartment as shown in Figure 1.4.3.a panel B. The use of steady-state plasma concentration, when the concentration at the effect site is presumed to be in equilibrium with plasma concentration, also removes hysteresis.

Initially, Segre (1968) and later Dahlstrom et al. (1978) proposed the incorporation of a hypothetical link model, "effect-compartment" to simultaneously characterise the pharmacokinetics and pharmacodynamics of a drug. The effect-compartment accounts for the time delay between pharmacological effect and plasma drug concentration and it is a link between the pharmacokinetic model and effect. Hull et al. (1978) proposed the addition of an effect-compartment linked to the plasma by a first-order process represented by a rate constant. k_{eo} was estimated only with two time points (one time,

Figure 1.4.3.a Schematic representation of the relationship between pharmacokinetic, link and pharmacodynamic models of a drug

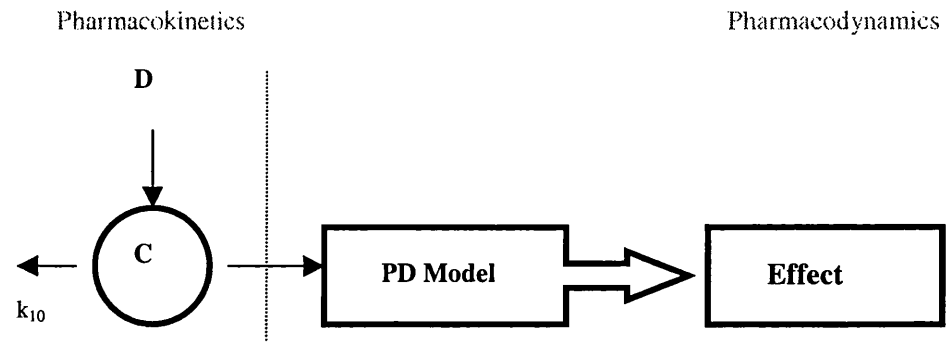

a Direct Link

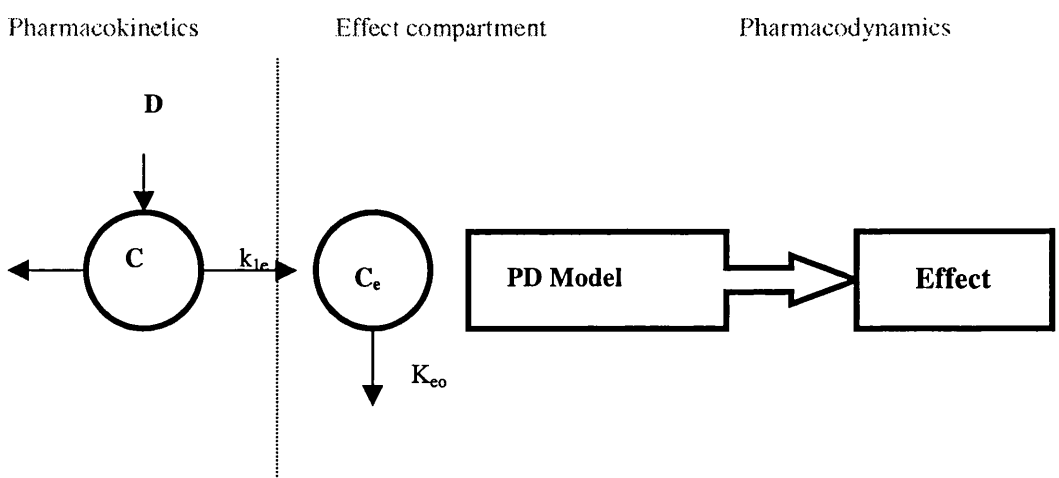

b Indirect Link

Key: D represents Dose; C is the drug concentration at the central compartment; C_e is the concentration at the effect site

Figure 1.4.3.b Representation of the relationship between effect and plasma concentration in the presence of hysteresis (upper panel) and effect and concentration at the effect site (lower panel)

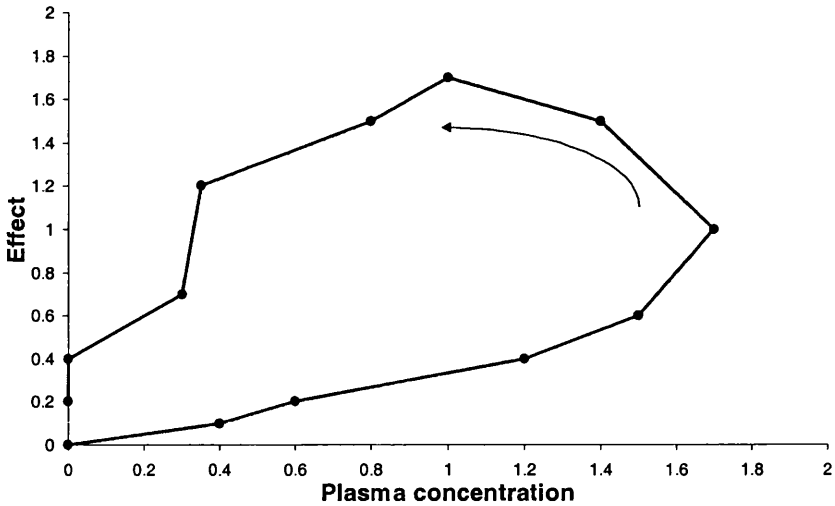

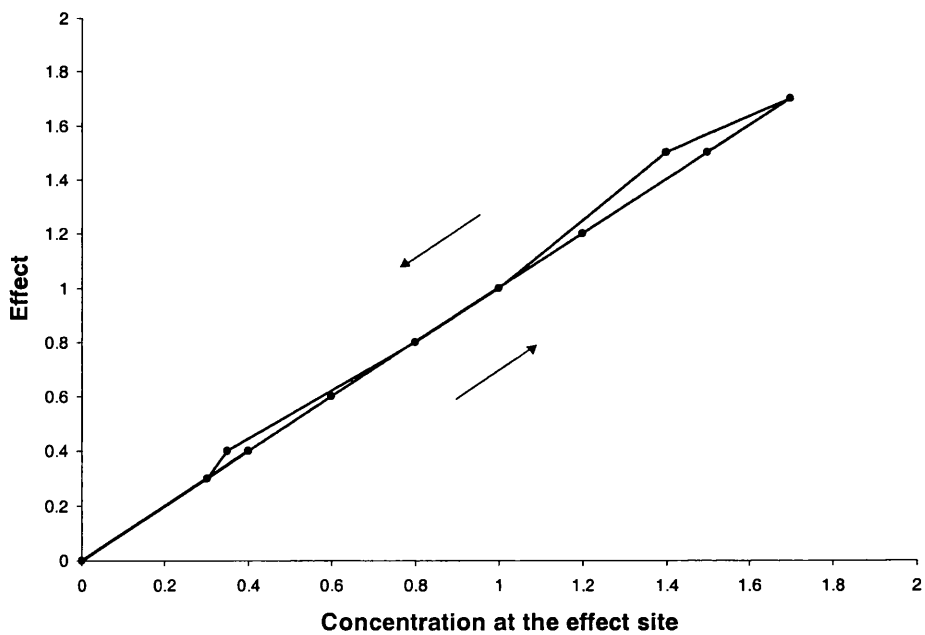

during drug input and one later, as drug concentration was falling). With the estimated k_{eo}, the C_e was predicted for all time points to obtain a full concentration-response curve. No assumption regarding the pharmacodynamic model was made.

Sheiner et al. (1979a) further developed this approach and proposed using all data points to calculate k_{eo}. A traditional pharmacokinetic model was used to describe the concentration-time data. The hypothetical compartment model is linked to the central compartment by a first-order rate constant (k_{1e}), in which the amount of drug transferred to the effect-compartment is negligible and therefore does not interfere with the properties of the pharmacokinetic model. The removal of the drug from the effect-compartment follows a first-order process, represented by the rate constant k_{eo}. It is assumed that the drug lost from the effect-compartment does not return to the central compartment but rather leaves the body. The time delay between effect and plasma drug concentration is determined by k_{eo}. The amount of drug in the effect compartment is given by the solution of the differential equation:

$$\frac{dA_e}{dt} = k_{1e} A_1 - k_{eo} A_e \qquad \text{Eq. 1.22}$$

where A_e is the amount of drug in the effect-compartment, A_1 represents the amount of drug in the central compartment, and k_{1e} and k_{eo} are the rate constants as described above. Pharmacodynamic models can be used to relate the pharmacologic effect to the hypothetical amount of drug in the effect-compartment.

Fuseau et al. (1984) proposed a variation of the approach proposed by Hull, which was a parametric pharmacodynamic model in which all the effect-time points were used to estimate k_{eo}. This variation chose k_{eo} so that the two limbs of the C_e-effect curve were superimposed. Another approach was developed by Unadkat et al. (1986), where the pharmacokinetic model was approximated nonparametrically.

The PK and PD data as well as the link between them can either be modelled separately or simultaneously. Since in most cases the pharmacokinetic model is better understood than the PD model, a subsequent, stepwise modelling approach is often preferred. This

avoids the pitfalls due to poor pharmacodynamic data or a wrong model selection.

1.5.3.2 Physiological Response Models

The Emax-type of models are empirical models and do not reflect the underlying physiological mechanism involved. Models using a mechanism-based approach offer an insight into the physiological process involved. The use of these types of model is increasing and has been advocated by Levy (1994). The physiological response models can be classified as direct response models or indirect response models. The effect of a drug can be a result of a direct relationship of the concentration at the effect site or might be an indirect effect that is secondary to one or several intermediate response steps, depending on the physiological mechanisms involved (Jusko and Ko, 1994). The link models discussed above are examples of direct response models. However when a delay in time between the peak concentration at the effect site and maximum drug effect occurs it can be described using an indirect response model, which results in a counterclockwise hysteresis for the observed response. The delay in time is not caused by a slow distribution but by an indirect response mechanism, such as stimulation or inhibition of a response variable.

1.5.3.3 Time Variant/ Time Invariant Models

PD models can also be classified according to the time dependency of their PD parameters.

a) Time Invariant Models

This type of model is characterised by the fact that the PD parameters stay constant over time. Most drugs follow this type of model, with changes in PD parameters related solely to the concentration at the effect site.

b) Time Variant Models

In some cases, the PD parameters, Emax and EC50, may change. This phenomenon is explained by the occurrence of tolerance or sensitization. Tolerance is a decrease in the response, caused by a decrease in the number of receptors or in the receptor affinity.

Tolerance causes a clockwise hysteresis loop for the concentration-effect relationship. Sensitisation is the increase in a response with time and results in a counterclockwise hysteresis.

Over the last years, pharmacokinetics has expanded from therapeutic drug monitoring services to a more complex PK/PD based dosage individualisation. The concepts of PK/PD modelling have been applied in clinical settings to provide a more rational basis for a specific patient individualised dosing regimen. In industry, the PK/PD based concepts can be applied as a decision making tools throughout all stages of drug development process leading to a reduction in the cost and time of the drug development.

CHAPTER 2 POPULATION PHARMACOKINETICS OF GENTAMICIN IN CANCER PATIENTS

2.1 SUMMARY

This chapter describes an approach to characterising the pharmacokinetics of gentamicin in cancer patients. A population pharmacokinetic model was developed and evaluated and the clinical factors that influence clearance and volume were explored.

The ability of creatinine clearance, estimated by the Cockroft-Gault equation, to accurately predict gentamicin handling was investigated.

Finally, the performance of existing nomograms was evaluated in the light of the population model developed in this section. Concentration-time profiles for two simulated patients (with low and high clearance) were obtained by simulation, using the derived population model.

2.2 INTRODUCTION

Gentamicin is an aminoglycoside antibiotic obtained from cultures of *Actinomycetes micromonospora* and has been in clinical use for over 30 years.

2.2.1 CHEMISTRY

Gentamicin consists of an aminocyclitol nucleus glycosidically linked to an amino sugar. 2-deoxystreptamine is the aminocyclitol nucleus of gentamicin, amikacin, kanamycin, neomycin, netilmicin and tobramycin

2.2.2 PHARMACOLOGY

2.2.2.1 Mechanism of Action

Gentamicin is a bactericidal antibiotic, and while important advances have been made in the understanding of the cellular mechanisms of its bactericidal action, the exact mechanism of action of gentamicin has not yet been fully elucidated. It appears to inhibit protein synthesis in susceptible bacteria by irreversible binding to the 30S ribosomal subunit, causing a disruption of protein synthesis eventually resulting in cell death. However, this mechanism does not completely explain the rapid bactericidal effect. The uptake of aminoglycosides into the bacterial cell is an irreversible, oxygen-dependent process. Aminoglycosides are therefore especially active against growing bacteria and practically inactive under anaerobic conditions (Janknegt, 1990).

2.2.2.2 Spectrum of Activity

Aminoglycosides have a broad spectrum of activity against gram-negative aerobic bacteria, including *Acinectobacter, Citrobacter, Enterobacter, Eschirichia coli, Klebsiella, Proteus, Providencia, Pseudomonas, Salmonella, Serratia* and *Shigella. In vitro,* susceptible organisms are generally inhibited by gentamicin concentrations of 1-8 mg L^{-1}. However, different species and different strains of the same species may exhibit

wide variations in susceptibility. In addition, *in vitro* susceptibility does not always correlate with *in vivo* activity. Aminoglycosides have little activity against anaerobic bacteria. Some gram-positive bacteria are relatively resistant. However, gentamicin is active against *Staphylococcus aureus* and *S. epidermidis*. When used alone, it has only minimal activity against streptococci and most strains of enterococci, but it has a synergistic effect when used in combination with a penicillin or vancomycin (Janknegt, 1990).

2.2.2.3 Toxicity

Ototoxicity and nephrotoxicity are the most serious adverse effects of the aminoglycosides. They are most likely to occur in geriatric or dehydrated patients, patients with renal impairment, patients who are receiving high doses or prolonged therapy, and patients who are receiving, or have received, other ototoxic and/or nephrotoxic drugs (Mattie et al., 1989).

The exact mechanism of aminoglycoside nephrotoxicity has not been fully characterised but several mechanisms have been proposed. Aminoglycosides are taken up into the cells lining the proximal tubule after they bind to cell membrane phospholipids. As a consequence of aminoglycoside digestion, some toxic enzymes are released into the cytoplasm of the cell causing cellular necrosis. Nephrotoxicity is usually a reversible phenomenon because the cells of the tubule have a regenerative capacity that completely restores the nephron activity. However, prolonged exposure to aminoglycosides causes loss of this regenerative capacity and leads to irreversible damage.

The occurrence of aminoglycoside nephrotoxicity has been reported to vary from 0.5 to 63 per cent (Garrison et al., 1990). This wide range is largely due to the way nephrotoxicity has been characterised and to the different criteria used in the studies. Creatinine clearance or creatinine serum concentrations are often used to report nephrotoxicity. For example, an increase of 45 μmol L^{-1} or 10 per cent over the baseline serum creatinine value is often used as an indicator or alternatively, a decrease in more than 50 per cent in the calculated creatinine clearance is also used. Aminoglycoside

nephrotoxicity can also be detected by the presence of some endogenous substances in the urine. While such detection has the advantage of giving an indication of nephrotoxicity at an early stage of its development, the measurements are imprecise and non-specific and therefore they cannot be used as specific indicators of aminoglycoside-associated nephrotoxicity. Other drugs, such as amphotericin B, vancomycin, frusemide, cisplatin, and cyclosporin may potentiate aminoglycoside-induced nephrotoxicity (Garrison et al., 1990).

Ototoxicity is also associated with aminoglycoside usage. It is manifested as auditory and/or vestibular toxicity that affects the eighth cranial nerve. Tinnitus is usually a sign of ototoxicity although it can also occur without any clinical signs. Auditory toxicity is frequently reversible if detected early. Vertigo, dizziness, nausea, and nystagmus are usually manifestations of vestibular toxicity. This kind of toxicity is irreversible and markedly affects the everyday lifestyle of the patient, especially the elderly (Garrison et al., 1990).

The exact mechanism of ototoxicity is unclear. It is thought that prolonged exposure to high concentrations of aminoglycosides is responsible for the destruction of the hair cells in the organ of Corti (Wersall et al., 1969). The incidence of aminoglycoside ototoxicity is generally reported to range from 0.5 to 5 per cent. Depending on the sensitivity of the detection method, however, the incidence of toxicity can be up to 43 per cent (Chan, 1989).

2.2.3 PHARMACOKINETICS

Traditionally, the disposition of gentamicin has been described by a one-compartment pharmacokinetic model, which assumes rapid distribution to the tissues (Wilson et al., 1973; Regamey et al., 1973; Siber et al., 1975; Barza et al., 1975). These studies were based on concentration data collected between 0 and 10 hours after dosing. Investigators who proposed a mono-exponential decline model probably did not collect data for long enough to characterise a late elimination phase and the limitations of the early bioassay methods prevented the detection of low concentrations.

It has been reported (Kaye et al., 1974; Barza et al., 1975) that there was considerable variability in serum concentrations following gentamicin administration. A study (Kahlmeter and Kamme, 1975) revealed the case of a patient with normal renal function who excreted gentamicin for 20 days after therapy had been discontinued. Later, other investigators (Schentag et al., 1977) reported a slow increase in sequential serum concentration peaks throughout the course of treatment even although no change was noted in renal function.

A progressive increase in concentrations, and the incomplete recovery of doses of the drug in the urine of patients with normal renal function (Kahlmeter and Kamme, 1975) are all incompatible with a mono-exponential elimination phase and indicate that gentamicin persists in serum and tissues for relatively long periods. In 1977, a two-compartment model was used to describe gentamicin elimination from the body (Schentag and Jusko, 1977a). They reported an initial decline phase followed by a second, slower phase, which corresponded to an average terminal half-life of 112 hours (range, 27-693 hours).

2.2.3.1 Absorption

Gentamicin, which is a highly polar molecule, is minimally absorbed from the gastrointestinal tract and penetration of the central nervous system is poor. It is rapidly absorbed following topical administration and it is rapidly and completely absorbed after intramuscular administration, reaching peak levels in 30 to 60 minutes. However, the rate of absorption is erratic and usually associated with a high variability in serum concentrations. Furthermore, absorption is reduced by decreased perfusion at the site of administration, as can occur in critically ill patients. Therefore, the intravenous route, either bolus or short infusion is recommended.

2.2.3.2 Distribution

Gentamicin is primarily distributed in the extracellular fluid with a volume of distribution of 0.25 L kg^{-1} (range 0.1-0.5 Lkg^{-1}) which approximates to the extracellular compartment (Zaske, 1992). Due to poor lipid solubility, it distributes well in lean body tissues but the extent of the distribution in tissues varies enormously from patient to patient. Following administration, gentamicin is widely distributed into body fluids including ascitic, pericardial, peritoneal, pleural, synovial and abscess fluids. It diffuses poorly into the central nervous system and it is minimally protein bound.

A wide range of factors such as age, pyrexia (Pennington et al., 1975), body weight, anaemia, albumin (Davis et al., 1991), platelet count (Phillips et al., 1988) and disease states can influence the distribution of the aminoglycosides. Oncology and haematology patients have been reported to have higher volumes of distribution. However, these studies were undertaken either without a control group (Manny and Huston, 1986; Higa and Murray, 1987) and assuming a control value of 0.25 - 0.30 L kg^{-1} or without reporting creatinine clearance or other renal function indices (Phillips et al., 1988). Thus, it is difficult to assess whether or not a true difference in renal function could explain the differences in the pharmacokinetic parameters. Nevertheless, several mechanisms have been proposed to explain the apparent increase in the volume of distribution in cancer patients. Zeitany et al (1990) reported an increased volume of distribution of 0.40 L kg^{-1} in patients with haematological malignacy compared to 0.27 L kg^{-1} in the control group, but patients in the control group were matched only for age and gender. More recently Bertino et al. (1991) reported a volume of distribution of 0.34 or 0.35 L kg^{-1} for haematology or oncology, respectively. These authors found no statistically significant differences from the control group. Table 2.2.3 summarises the results carried out to evaluate volume of distribution in oncology patients.

Studies using gentamicin indicate that febrile patients may have slightly lower serum gentamicin concentrations than afebrile patients (Pennington et al., 1975). However, the clinical importance of this effect is unclear (Zeitany et al., 1990).

Table 2.2.3 Summary of studies carried out to evaluate the volume of distribution of gentamicin in cancer patients

Reference	Volume of Distribution (L kg^{-1})	Range	Number of Patients	Pathology	Comments	Model	Method
(Higa and Murray, 1987)	1.14 x (0.25 TBW)	-	35	Haematology & Oncology	No matched control; assumed a control of 0.25-0.30 L kg^{-1}	1-compartment model	Sawchuck-Zaske
(Manny and Huston, 1986)	0.41	0.20-0.65	6	Haematology & Oncology	No matched control; assumed a control of 0.20-0.30 L kg^{-1}	1-compartment model	Bayesian
(Inciardi and Batra, 1993)	0.30	-	28	Haematology & Oncology		1-compartment model	NPEM algorithm,
(Ordovas et al., 1994)	0.32	-	13	ORL cancer	No control. Assumed a control of 0.25L kg^{-1}	1-compartment model	NPEM algorithm
(Bertino et al., 1991)	0.34 Haematology 0.35 Oncology	-	235	Haematology & Oncology	Matched control of 645 patients ; V = 0.33L kg^{-1}	1-compartment model	Sawchuck-Zaske
(Zeitany et al., 1990)	0.40	-	14	Haematology	Not matched control group of 15 patients . V = 0.27L kg^{-1}	1-compartment model	Sawchuck-Zaske
(Phillips et al., 1988)	0.42	-	24	Haematology	Matched for age and gender; V = 0.25 Lkg^{-1}	1-compartment model	Winter Equations

Key: TBW represents the total body weight; ORL is ear, nose and throat; NPEM is non-parametric estimation

Serum gentamicin concentrations may also be lower and the elimination prolonged in patients with marked oedema or altered fluid distribution.

The disposition of gentamicin is described by an initial rapid phase, representing the distribution of gentamicin from the central to peripheral compartments, followed by an elimination phase. In the literature there are few data to document the duration of the initial distribution phase. It is common practice to administer gentamicin as a 30min intravenous infusion with peak serum concentrations obtained 30 minutes after the end of infusion. However, it was recently reported (Demczar et al., 1997) that distribution was not complete until approximately 30 minutes after the end of a 60 minute infusion with gentamicin. Previous studies (MacGowan et al., 1994) have also suggested that the distribution phase might not be complete by an hour after infusion.

2.2.3.3 Elimination

In adults with normal renal function, gentamicin is almost completely cleared unchanged from the body by glomerular filtration (GF). Only a small amount of drug undergoes renal tubular secretion. Very high concentrations are reached in urine: over 40-97 per cent of a dose is normally excreted in the urine within 24 hours. There may also be biliary excretion when the GFR is low (Sande and Mandell, 1996). Current evidence indicates that gentamicin elimination follows a biphasic decline. In adults with normal renal function, the initial elimination phase is characterised by a half-life of 2-3 hours. This contrasts with the terminal elimination phase associated with a half-life of 112 hours (Schentag and Jusko, 1977a). This slow elimination is caused by tissue accumulation and probably tissue binding. Despite its polarity, gentamicin is distributed into adipose tissue (Schwartz et al., 1978) and accumulates in body tissues where it is tightly bound intracellularly. It is then slowly released from these tissues. According to some authors, the complete recovery of the dose in urine requires approximately 10-20 days in patients with normal renal function (Schentag and Jusko, 1977b).

Patients with impaired renal function have elevated serum concentrations and prolonged elimination half-lives. Gender has been reported to influence gentamicin elimination,

but the clinical importance of this factor is a matter of debate (Zaske et al., 1982; Phillips et al., 1988).

2.2.4 PHARMACODYNAMICS

The therapeutic effect of gentamicin results from a combination of several factors. It has been demonstrated (Moore et al., 1987) that there is a strong association between the clinical response and the ratio of the peak concentration to the minimal inhibitory concentration for the infecting organism.

Gentamicin also has a marked concentration-dependent bactericidal activity. *In vitro* data document more extensive and rapid bactericidal killing and continually increasing post-antibiotic effects with increasing aminoglycoside peak concentrations (Barriere, 1988). This effect has practical consequences in the design of dosage regimens (Mattie et al., 1989).

Post-antibiotic effect (PAE) is a period of time after complete elimination of an antibiotic during which there is no growth of the organism. The mechanism by which the post-antibiotic effect occurs has not been completely clarified. It is thought to be the result of irreversible binding of the aminoglycoside to ribosomal subunits. The PAE of these agents for both gram-positive cocci and gram-negative bacilli is explained by this irreversible binding and the time needed to synthesize new proteins. Several factors influence the presence or duration of the PAE such as type of organism, type of antibiotic, concentration of antibiotic, duration of antibiotic exposure, and antibiotic combinations (Zhanel et al., 1991).

Recent studies suggest that antibiotic combinations have synergistic, additive, or indifferent effects on the duration of the PAE. A synergistic increase in the PAE of up to three hours was observed when *Enterococcus faecalis* was tested against penicillin G plus gentamicin. These data suggest that the combination of certain antibiotics can allow the choice of a different dosing regimen.

It has been demonstrated that gentamicin shows adaptive resistance when in the presence of *Pseudomonas aeruginosa*. Adaptive resistance involves reversible down regulation of gentamicin uptake into bacteria. It develops within 1 or 2 hours of initial exposure to an aminoglycoside and persists for 6 to 7 hours during growth in a drug-free medium. Adaptive resistance increases with continous exposure to gentamicin (Daikos et al., 1990). The aminoglycosides have a biphasic rate of bactericidal action on aerobic gram-negative bacilli. The passive ionic binding of the drug to bacterial lipopolysacharide induces an initial phase of rapid bacterial killing. A second phase of slower bacterial killing is associated with decreased energy-dependent uptake of aminoglycoside, and the rate is independent of the initial or persistent drug level. Those bacteria that survive first exposure develop adaptive resistance, which is characterised by impermeability to aminoglycoside. Adaptive resistance is reversed during growth in drug-free media (Barclay et al., 1992).

2.2.5 DOSAGE REGIMENS

Information related to the effect of the drug should be incorporated in the design of dosage regimens. The target plasma concentration-time profiles should be based on the pharmacodynamic characteristics of the drug. The associations between a) serum concentrations of aminoglycoside and therapeutic outcome, b) bactericidal activity and clinical efficacy, and c) *in vitro* inhibitory concentrations and clinical outcome have all been well documented. Thus high serum concentrations should be obtained early in therapy (Moore et al., 1984). It has been suggested that data on adaptive resistance should be considered when selecting the most effective dosing regimen for therapeutic use (Klastersky et al., 1974; Mattie et al., 1989).

Application of pharmacokinetic techniques may help in the choice of an individual drug regimen for a target concentration-time profile. Dosage regimens should be based on patient-specific pharmacokinetic parameters. The identification of subgroups of populations with particular pharmacokinetic characteristics is useful in the design of initial dosage regimens and individual dosage adjustments can be made after obtaining the first set of concentration measurements.

2.3 AIMS OF THE ANALYSIS

The aims of the analysis were:

i) To determine the population pharmacokinetic characteristics of gentamicin in patients with cancer.

ii) To investigate the influence of clinical factors on the pharmacokinetics of gentamicin.

iii) To investigate the influence of low creatinine concentrations on clearance estimates.

iv) To examine the relevance of existing dosage nomograms in the light of the population model developed in this particular patient population.

2.4 METHODS

2.4.1 PATIENTS

All patients with cancer, treated in the Beatson Oncology Centre, Western Infirmary in Glasgow, who received gentamicin and had at least one measured serum gentamicin concentration, were eligible for inclusion in the study. Patients on haemodialysis or continuous venovenous haemofiltration (CVVH) were excluded from the study. Data were collected prospectively from January 1993 to August 1996.

Gentamicin was administered intravenously either by a short infusion or bolus. The exact and complete dosing history as well as times of blood sampling were recorded as part of the routine drug monitoring using specialised recording charts. Dosage regimens were adjusted according to patients' renal function (Cockcroft and Gault, 1976) to achieve a peak concentration (1hour post dose) of 8-12 mg L^{-1} and trough less than 2 mgL^{-1}. For each patient the following information was also collected: gender; weight; age; height; creatinine; urea; albumin; platelets; haemoglobin; white cell count; and

temperature. Biochemical and haematological factors and temperature, were generally checked daily during therapy. Additional clinical factors such as ideal body weight, body surface area, body mass index and lean body mass, were determined using the equations shown in Table 2.4.1. Patients were classified as obese if the actual body weight exceeded the ideal body weight by 20% and pyrexia was defined as a temperature equal to or above 38 °C. The measurement of creatinine concentration closest in time to each measured gentamicin concentration was used to estimate creatinine clearance. Patients with missing clinical, dosage or sampling data and patients with rapidly changing renal function were excluded from the study.

2.4.2 ASSAY

Gentamicin serum concentrations were analysed by fluorescence polarisation immunoassay (TD_x, Abbott Laboratories) in the Microbiology Laboratory, Western Infirmary. The lower limit of detection of this method was 0.1 mg L^{-1} and the interassay coefficients of variation were 6.3% at 1 mg L^{-1}, 3.7% at 4.0 mg L^{-1} and 4.3% at 8 mg L^{-1}.

2.4.3 DATA ANALYSIS

The analysis was performed with the population pharmacokinetic package NONMEM (Non Linear Mixed Effects Model), version IV, level 2 (Beal and Sheiner, 1992). Data such as: patient identification; date; time; dose (mg); infusion rate (mg h^{-1}); duration of

Table 2.4.1 Equations used to derive clinical factors used in the analysis

CLINICAL FACTOR	EQUATION	REFERENCE
Creatinine clearance ($ml\ min^{-1}$)	$\frac{(140 - Age) * Ideal\ body\ weight\ (kg)}{Creatinine\ (\mu mol\ L^{-1})}$ Females * 1.04 and males * 1.23	(Cockcroft and Gault, 1976)
Ideal body weight (kg)	50 kg + 2.3 kg for every 1" > 5 ft for males; 45.5 kg + 2.3 kg for every 1" > 5 ft for females.	(Devine, 1974)
Body surface area (m^2)	$71.84 * Wt^{0.425}\ (kg) * Ht^{0.725}(cm)$	(Du Bois and Du Bois, 1916)
Body mass index ($kg\ m^{-2}$)	$Wt\ (kg) / Ht^2(m)$	
Lean body mass	Males $(1.1 * Wt) - (128 * Wt^2(kg)/Ht^2(cm))$ Females $(1.07 * Wt) - (148 * Wt^2/Ht^2)$	(Hallynck et al., 1981)

infusion (min); concentration (mg L^{-1}); age (years); sex; weight (kg); height (cm); ideal body weight (kg); creatinine concentration (μmol L^{-1}); urea (mmol L^{-1}); albumin (g L^{-1}); white cell count (*10^9 L^{-1}); haemoglobin (g dL^{-1}); platelets (*10^9 L^{-1}); temperature; obesity and lean body mass were entered into a spreadsheet package, Excel®, in the format required by NONMEM. Body surface area and body mass index were derived from NONMEM control files. FORTRAN subroutines were compiled using FORTRAN Power-Station® (version 1.0a, Microsoft Corporation). Both programs were implemented on an Opus personal computer with a Pentium processor.

The data file was investigated for possible errors or outliers. A control file was created using the "Checkout" option in NONMEM and scatter plots of data items against patient identification number were produced.

The data were then split into two sets: a population data set comprising two thirds of the patients and a test data set comprising the remaining one third of the patients. Patients were randomly allocated to the population or test data sets.

Data were fitted simultaneously by non-linear regression with NONMEM. Models were implemented using the data pre-processor NMTRAN and the PREDPP subroutines. Mono-, bi- and tri-exponential structural models were fitted to the gentamicin concentration-time data. The PREDPP subroutines ADVAN1/TRANS2 and ADVAN3/TRANS4, were implemented to run a mono- and bi-exponential model respectively, whereas for the tri-exponential model the subroutine ADVAN7 was chosen.

Models were parameterised to give estimates of clearance (CL), intercompartmental clearance (Q), and volumes of distribution (V_1, V_2, V_3). The mathematical equations for intravenous, bolus and infusion administration are shown in Appendix I. The microscopic rate constants represent the transfer rate from compartment 1 to 2 and vice-versa and they were derived from the macroparameters obtained from NONMEM output for a bi-exponential model as follows:

$k10 = CL/V_1$

$k12 = Q/V_1$

$k21 = Q/V_2$

and then the half-lives ($T_{1/2}$) were derived as follows:

$T_{1/2\ initial} = 0.693 / \lambda_1$

$T_{1/2\ terminal} = 0.693 / \lambda_2$

Where λ_1 and λ_2 are the roots of the quadratic equations calculated from:

$\lambda_1; \lambda_2 = 0.5*[(k_{12}+k_{21}+k_{10}) \pm ((k_{12} +k_{21} + k_{10})^2 - 4\ k_{21}\ k_{10})^{1/2}]$

Interindividual variability, ETA (η_i) was assumed to arise from a Gaussian distribution, i.e. to be a random variable, independent and identically distributed, with a mean zero and variance ($Var(\eta_i)$), expressed as ω_P^2.

Preliminary analysis revealed that the data were best fitted assuming a logarithmic Normal distribution on η_i. Therefore, P_{ik}, the individual estimates of the pharmacokinetic parameters, where k could be CL, Q, V_1, V_2, etc. of the i^{th} individual, were described by the following equation:

$$P_{ik} = P_k * Exp\ (\eta_i^{P_k})$$

where P_k is the typical population estimate of the parameter k, and $\eta_i^{P_k}$ is the difference between the population parameter and the parameter for the i^{th} individual.The residual error on concentrations was investigated using the additive, proportional and combined (exponential and additive) models. A description of these models is given in Chapter 1. The distributions of the POSTHOC parameter estimates obtained from the basic model were then examined by means of histograms. The distribution of each parameter was tested for normality using the Anderson-Darling test.

Another assumption made in regression analysis is that residuals and weighted residuals are random variables with zero-mean, and therefore are symmetrically distributed around zero and have unit variance. An indication of the shape of the residual distributions was obtained from distribution plots. Residual analyses were performed using both the residuals and weighted residuals.

In the present study a preliminary analysis was first carried out to examine distributions of all covariates and identify any abnormalities in clinical factors such as renal and hepatic function. This exploratory analysis was carried out on the following covariates: age; gender; weight; height; ideal body weight; creatinine concentration; urea concentration; albumin concentration; white cell count; haemoglobin; platelet count; temperature; obesity; lean body mass; body mass index; and body surface area. The frequency distributions of covariates were examined by means of histograms. Collinearity that might influence the model building was inspected graphically by a matrix scatter plots and by the correlation coefficient obtained by correlating each covariate against all the others.

Each covariate was plotted against POSTHOC parameter estimates of clearance and volume of the central compartment calculated from the basic model. The shape of the plots gave an indication about the possible mathematical form for the relationship when the covariate was added to the kinetic model. Similar plots were also produced using population residuals and weighted residuals (WRES). These plots provided an indication as to whether a covariate should be included in the model. Multiple linear regression was also used to examine the relationship between the POSTHOC parameter estimates and covariates. Firstly, one covariate at a time was regressed against each POSTHOC pharmacokinetic parameter. The judgement of goodness of fit was evaluated by the reduction in the residual sum of squares associated with the incorporation of each covariate in the model. The significance in the reduction in the residual sum of squares was formally tested by F-test and $p<0.01$ was used as the criterion for covariate inclusion or exclusion. Only those covariates associated with a significant change were then used in the "bestsubset" regression. This option first

selected the two covariates associated with the largest coefficient of determination (R^2). Using this model the next most significant covariate was included. This process was repeated until all significant covariates were included in the model. All the statistical analyses were carried out using the statistical software package Minitab (1996b).

The model was built up assuming no covariance between elements of η. Once the structural pharmacokinetic model was finalised, both the diagonal elements of the Ω-matrix and the covariance terms of the lower triangle of the Ω-matrix were estimated. Plots of η's against each other provide an indication of which covariance to consider for inclusion in the model.

Once the final model was obtained, the structural model was reinvestigated. The one-compartment model was re-run with the full covariate model. Covariates identified by this preliminary analysis were then investigated using NONMEM as described in section 1.4.8.

2.4.4 INVESTIGATION OF CREATININE CONCENTRATION

The influence of low creatinine concentrations was investigated by comparing the model obtained using creatinine clearance based on measured creatinine concentration with the models using new covariates derived from the corrected creatinine concentration. Three new covariates corresponding to the three different minimum creatinine values were derived as follows:

(i) All creatinine concentrations less than or equal to 60 μmol L^{-1} were set at 60 μmol L^{-1} (the lower limit of the reference range used in the hospital).

(ii) All creatinine concentrations less than or equal to 70 μmol L^{-1} were set at 70 μmol L^{-1} (an arbitrary intermediate value).

(iii) All creatinine concentrations less than or equal to 88.4 μmol L^{-1} were set at 88.4 μmol L^{-1} (equivalent to 1 mg dl^{-1}).

2.4.5 MODEL EVALUATION

Evaluation of the models obtained from the population analysis was performed using the test data set. Concentrations were predicted for each patient at each sampling time using the dosing history and the relevant clinical data. Prediction errors were then calculated to evaluate how well the population model predicted the measured concentrations. These prediction errors were obtained by subtracting the measured concentrations from the predicted concentrations as follows:

$$\% \text{ Prediction error (PE)} = 100*[\Sigma(\hat{Y}_{ij} - Y_{ij})/N]/\ \hat{Y}_{ij}$$

where $\hat{Y}_{ij}$ is the predicted and Y_{ij} is the measured concentration in the i^{th} individual at the j^{th} measurement. For each patient only the first peak and trough concentrations were used to calculate the prediction error. The mean prediction error for the two concentrations for each individual was first calculated and then the mean for all individuals. A t-test was used to test whether the prediction errors were significantly different from zero, when statistical significance was set at $p<0.05$. The prediction errors for peaks and troughs, calculated separately, were compared with the combined peak and trough results for each individual.

For each observed concentration the expected concentration distribution was obtained using the population derived parameter estimates by simulating 1000 data points. This allowed the probability of the measured concentration being within the 2.5-97.5 percentile ranges of the expected value to be determined.

2.4.6 DOSAGE GUIDELINES

The best model was then run using the data from a pooled data set including all patients, to obtain the most accurate parameter estimates. The results of this analysis were used to predict the concentration-time profile in simulated patients who were males, aged 50 years, weighed 70 kg, had heights of 1.7 m and albumin concentrations of 40 g L^{-1}. Three creatinine concentrations were used: 70 μmol L^{-1}, 112 μmol L^{-1} and 290 μmol L^{-1},

which corresponded to creatinine clearances of 25 ml min^{-1}, 65 ml min^{-1} and 105 ml min^{-1}, respectively. One thousand simulations were performed for each 'patient', and the median (25-75 percentile range) concentration-time profiles were determined according to two published nomograms: one that used a "once daily" regimen (Nicolau et al., 1995) and one based on traditional target ranges (Thomson et al., 1996).

2.5 RESULTS

2.5.1 PATIENTS

Data were collected from 210 patients. The exact dosing history, times of blood sampling and measured concentrations were recorded prospectively and demographic and clinical characteristics were recorded prospectively and retrospectively.

The option "Data Checkout" from NONMEM revealed no problems when scatter plots were produced of data items against patient identification number. Gentamicin was administered by intravenous bolus or by short infusion over 10-30 minutes. Doses ranged from 40 mg to 300 mg and the sampling times ranged from 1 to 26 hours after the dose. Five hundred and seventy four concentrations were available for analysis, ranging from 0.1 mg L^{-1} to 13.5 mg L^{-1} with a median of 1.7 mg L^{-1}.

Patients were given an identification number according to the chronological order of recruitment. A random number table was then generated using the statistical software Minitab (1996b). Patients whose identification numbers were within the first 140 random numbers were allocated to the population data set and the remaining 70 patients were allocated to the test data set.

The population data set comprised three hundred and seventy eight concentrations ranging from 1 to 9 for most patients. Three patients had 14, 17, and 22 concentrations measured over several treatment courses. Fifty-seven per cent of the measured concentrations were troughs and 92% were measured within the first 7 days of therapy.

A summary of the demographic and clinical characteristics of the patients included in both population and test data sets is presented in Table 2.5.1. There were no significant differences in characteristics between patients in the population and test data sets. According to the definition of obesity, 108 patients (81.8% of the concentrations) were not obese. Only 6 out of the 140 'population' patients weighed more than 100 kg and half of the patients weighed less than 66 kg. Twenty-two per cent of the concentrations used in the analysis were taken from pyrexial patients (flag = 1) but temperature was missing for 29% of the concentrations. Forty-nine per cent of the serum albumin concentrations were below the lower limit of the reference range, median 34 g L^{-1}, creatinine concentration was also low in many cases with a median of 71 μmol L^{-1}. The majority of patients had creatinine concentrations less than 100 μmol L^{-1}. The median albumin concentration was 34 g L^{-1} and 49% of the albumin concentrations were below 36 g L^{-1}, the lower limit of the reference range. Some patients in whom low creatinine concentrations were measured had creatinine clearance estimates from the Cockroft-Gault equation of 320 ml min^{-1} (greater than 200 ml min^{-1} is not physiological).

2.5.2 DATA ANALYSIS

The bi-exponential model was found to be superior to the mono-exponential, and the tri-exponential model offered no advantage, based in the criteria. Model selection was based in the analysis of residuals as described in the section 1.4.7. Figure 2.5.2.a shows the weighted residuals against time after the dose obtained from different structural

Figure 2.5.2.a Weighted residuals of gentamicin against time from last dose, obtained from mono-exponential and bi-exponential decline models

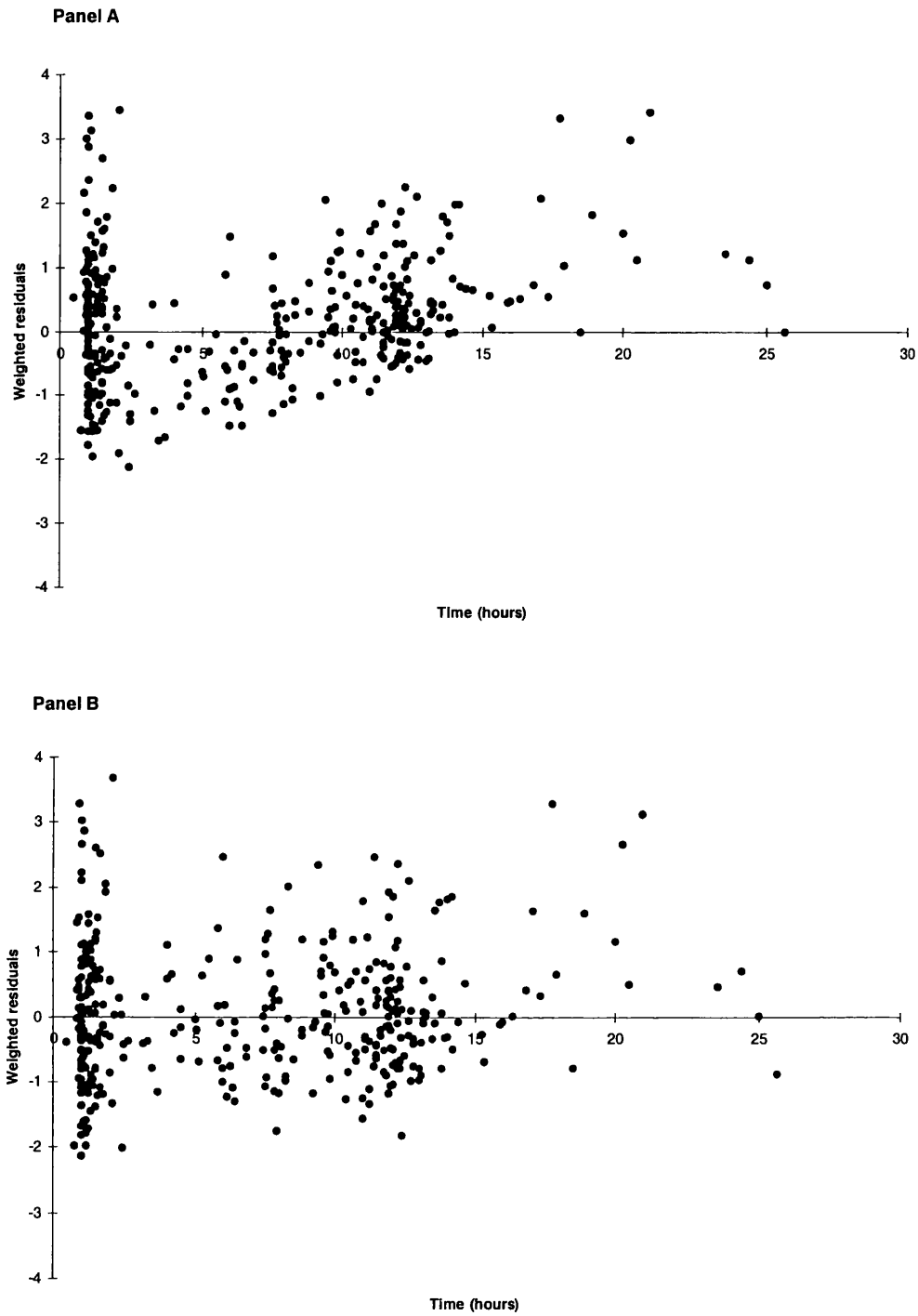

Key: Panel A - mono-exponential decline model; Panel B - bi-exponential decline model.

Table 2.5.1 Summary of demographic and clinical characteristics of patients included in the study

	Reference range	**Population set N=140** Median (range) or number (%) of patients/samples	**Test set N=70** Median (range) or number (%) of patients/samples
Females		70 (50%)	42 (60%)
Age (years)		50 (15 - 81)	53 (14 - 77)
Weight (kg)		66 (38 - 117)	65 (38 - 95)
Height (cm)		170 (146 - 188)	165 (147 - 188)
Ideal body weight (kg)		59.2 (38.0 - 82.2)	55.0 (38.0 - 77.6)
Lean body mass		49.5 (32.3 - 73.8)	47.1 (31.1 - 65.6)
Body mass index (kg m^{-2})		23.0 (14.8 - 36.9)	23.0 (16.2 – 33.2)
Body surface area (m^2)		1.7 (1.3 – 2.3)	1.7 (1.3 – 2.1)
Obesity (20% above IBW)		69 (18.2%)	64 (32.3%)
Urea (mmol L^{-1})	2.5 - 6.7	4.5 (0.8 - 22.1)	3.9 (1.1 - 17.0)
Creatinine (µmol L^{-1})	60 - 110	71 (26 - 258)	74 (38 - 292)
Creatinine clearance (ml min^{-1})[a]		89.7 (22.9 - 319.7)	77.2 (15.8 - 213.9)
Creatinine clearance (ml min^{-1})[b]		86.1 (22.9 -183.7)	74.9 (15.8 - 179.1)
Albumin (g L^{-1})	36 - 50	34.0 (17.0 - 53.0)	33.5 (18.0 - 52.0)
White cell count (* 10^9 L^{-1})	4.1 – 11.0	0.8 (0.04 - 194.1)	1.1 (0.1 - 57.0)
Haemoglobin (g dl^{-1})	13 - 18	10.4 (5.6 - 16.1)	10.3 (6.7 -15.4)
Platelets (*10^9 L^{-1})	150 - 400	52 (2 - 670)	79 (4 - 883)
Temperature (> 38°C)		84 (22.2%)	36 (18.2%)

Key: [a] *Calculated by Cockcroft Gault equation (Cockcroft and Gault, 1976);* [b] *creatinine concentrations ≤ 60µmol L^{-1} set at 60 µmol L^{-1}*

models. Weighted residuals produced from the monoexponential decline model were overestimated at early time points, whereas this was not observed with the bi-exponential model. However, towards later time points both models tended to underestimate the concentration. Bi- and tri-exponential models produced similar plots, the pharmacokinetic parameters were estimated with a similar degree of confidence and there was no decrease in the variability associated with the residual error. The objective function value dropped 83.7 points when the bi-exponential model was compared to the mono-exponential model but only 9 points between the bi- and tri-exponential models. The parameter estimates obtained from the mono- and bi-exponential models are shown in Table 2.5.2.a. The plot of measured against predicted data points for bi-exponential model showed a distribution along the line of identity (Figure 2.5.2.b). The weighted residuals against predicted concentrations for the bi-exponential decline model showed a more random scatter around zero (Figure 2.5.2.c) than for the mono-exponential decline.

Interindividual variability was assumed to follow a logarithmic-normal distribution. The shape of the distributions of η_j^{CL}, η_j^{V1}, ε_1 and ε_2 were investigated by an Anderson-Darling normality test. Figure 2.5.2.d shows scatter plots from η's in clearance against η's in volume obtained from the three residual error models. The combined error structure was associated with a more random pattern around the axis line than the other two models. The combined residual error model was also superior to both additive and proportional models when the objective function values were compared. The combined model was associated with a drop in objective function value of 177.4 points compared to the proportional and 76.7 points compared to the additive model. Weighted residuals obtained from the combined model were normally distributed.

The distributions of the POSTHOC η values for clearance and volume of the central compartments were tested for normality.

Figure 2.5.2.d Scatter plots of η^{CL} against η^{V1} obtained from three residual error models

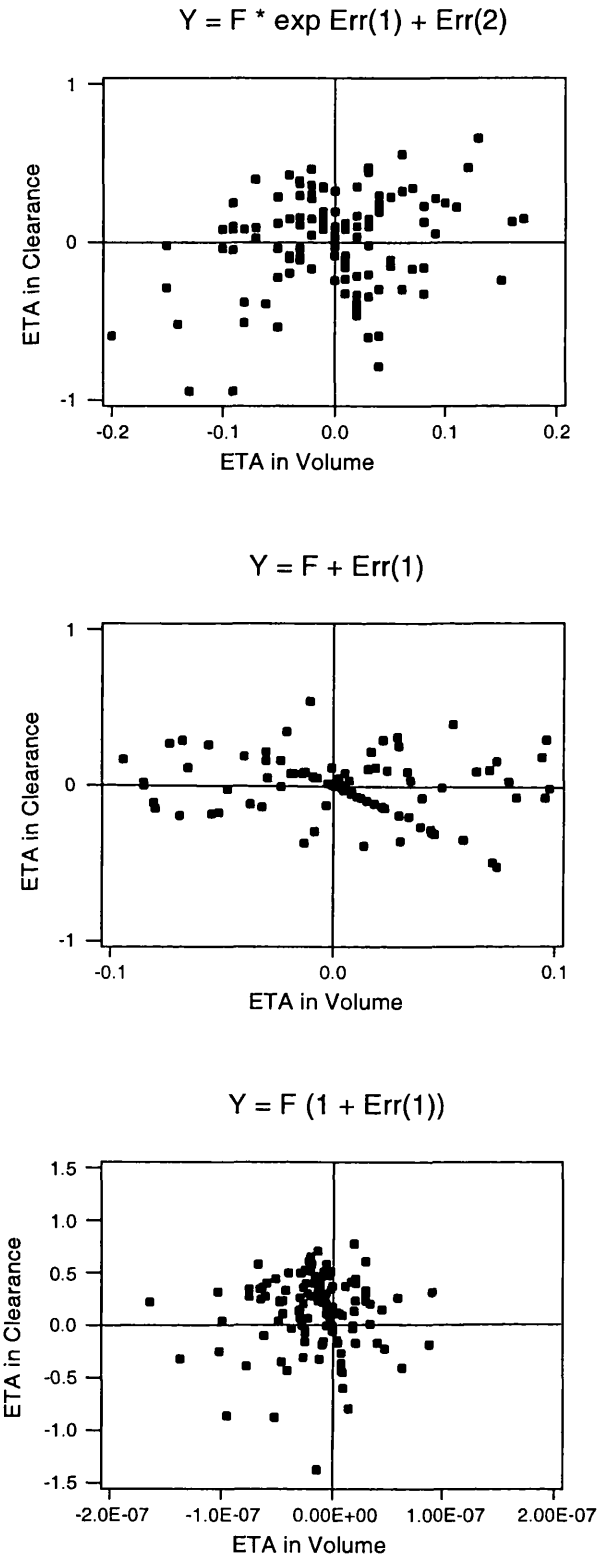

Figure 2.5.2.b Measured against predicted concentration obtained from the bi-exponential decline model

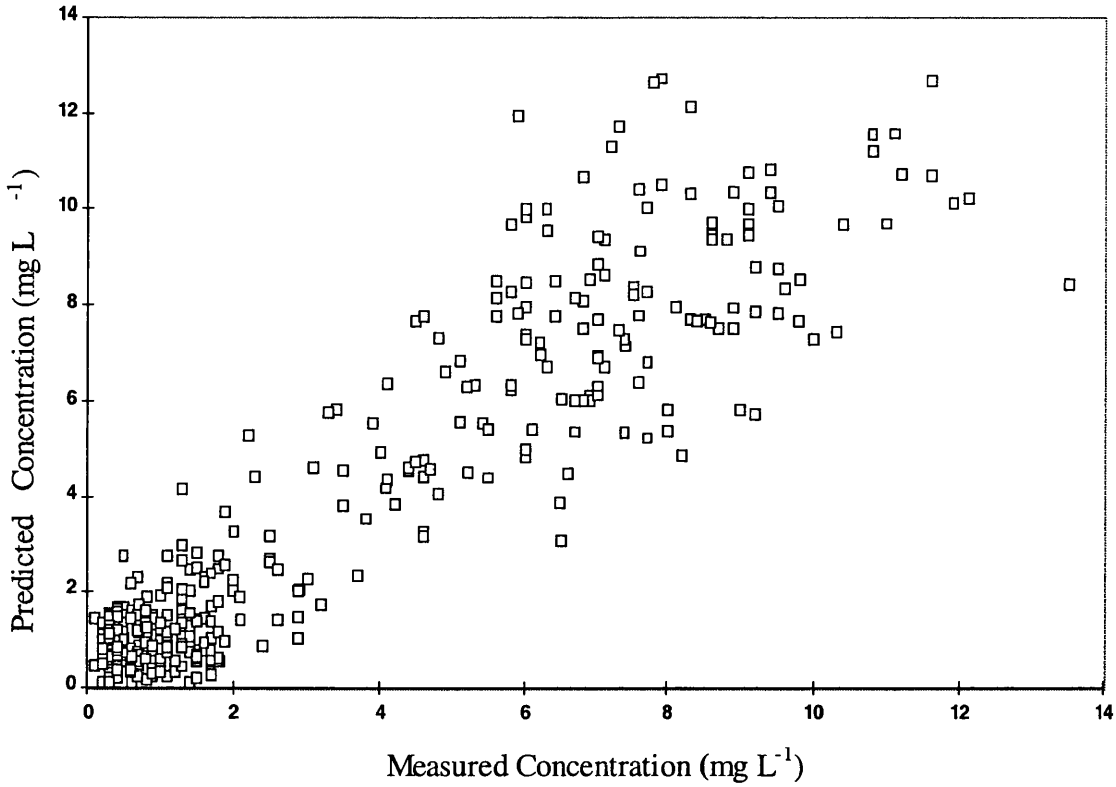

Figure 2.5.2.c Weighted residuals against predicted concentrations obtained from the bi-exponential decline model

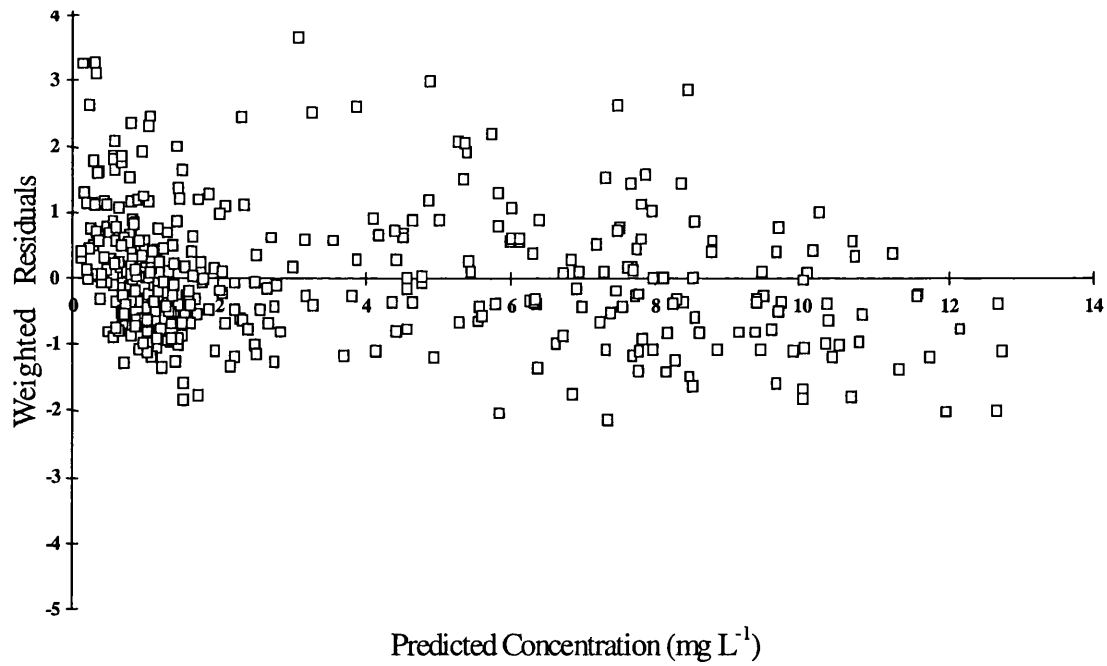

Table 2.5.2 a Gentamicin pharmacokinetic parameters estimated from two structural models, mono- and bi-exponential decline models

	Parameter Estimates *(SE%)*	
	Mono-exponential decline	**Bi-exponential decline**
Clearance ($L\ h^{-1}$)	3.86 *(4.1)*	3.98 *(4.1)*
V or V_1 (L)	17.2 *(2.9)*	13.9 *(5.8)*
V_2 (L)	-	13.4 *(22)*
Q ($L\ h^{-1}$)	-	2.2 *(19)*
Interindividual Variability		
CL	31.7% *(29)*	33.9% *(24)*
V or V_1	12.9% *(75)*	15.5% *(72)*
V2		indeterminate
Q		indeterminate
Residual variability		
at 1 $mg\ L^{-1}$	45.0%	38.4%
at 8 $mg\ L^{-1}$	16.3%	14.6%
OFV	322.0	238.3

Key: OFV - Objective Function Value; SE represents the standard error; V represents the volume of distribution; V1 is the volume of distribution of the central compartment; V_2 the volume of distribution of the peripheral compartment; Q is the intercompartmental clearance between the central and peripheral compartments.

The "basic model", a bi-exponential decline model with an exponential interindividual variability and a combined structure for residual error, was used to estimate population pharmacokinetic parameters. The mean of the individual (POSTHOC) clearance estimates using this model was 4.39 L h^{-1} (range 1.55 to 7.69 L h^{-1}), the mean intercompartmental clearance was 2.21 L h^{-1}, V_1 was 13.9 L and V_2 was 13.4 L. The intersubject variability was 33.9% on CL with a standard error of 23.8% and 15.5% on V_1 with a standard error of 72.3% but the intersubject variabilities on Q and V_2 were very low with wide standard errors, i.e. indeterminate. The standard deviations of the residual error were 0.38 mg L^{-1} at 1 mg L^{-1} and 1.17 mg L^{-1} at 8 mg L^{-1}.

Possible relationships between POSTHOC parameter estimates, residuals and weighted residuals and covariates such as age, ideal body weight, weight, lean body mass, height, gender, body surface area, urea, albumin, creatinine concentration and creatinine clearance were identified from the scatter plots. In Figure 2.5.2.e plots from the coavariates that showed a relationship are depicted. Haematological indices (haemoglobin, white cell count, and platelet count) showed no obvious trends nor did the presence or absence of pyrexia. Volume of distribution tended to increase with indices of body size: weight; height; body surface area; and lean body mass, and decrease with serum albumin concentration, as shown in Figure 2.5.2.e.

The results obtained from the linear regression analysis are presented in Table 2.5.2.b. Covariates associated with significant influence were used in a "bestsubset" multiple linear regression and the results are shown in Table 2.5.2.c. For clearance, creatinine clearance and urea were the two models selected with the highest R^2 for a single-covariate model. The second covariates for a two-covariate model were clearance of creatinine and age. Body surface area and ideal body weight were selected as the third covariate on a 3-covariate model. For volume of distribution, lean body mass and body surface area were the best single-covariate models selected. Albumin was selected a covariate for a 2-covariate model and creatinine for a 3-covariate model. Urea was not incorporated in the model because it was highly correlated with creatinine.

Figure 2.5.2.e Plots of individual pharmacokinetic parameters, residual and weighted residuals against covariate that show a relationship

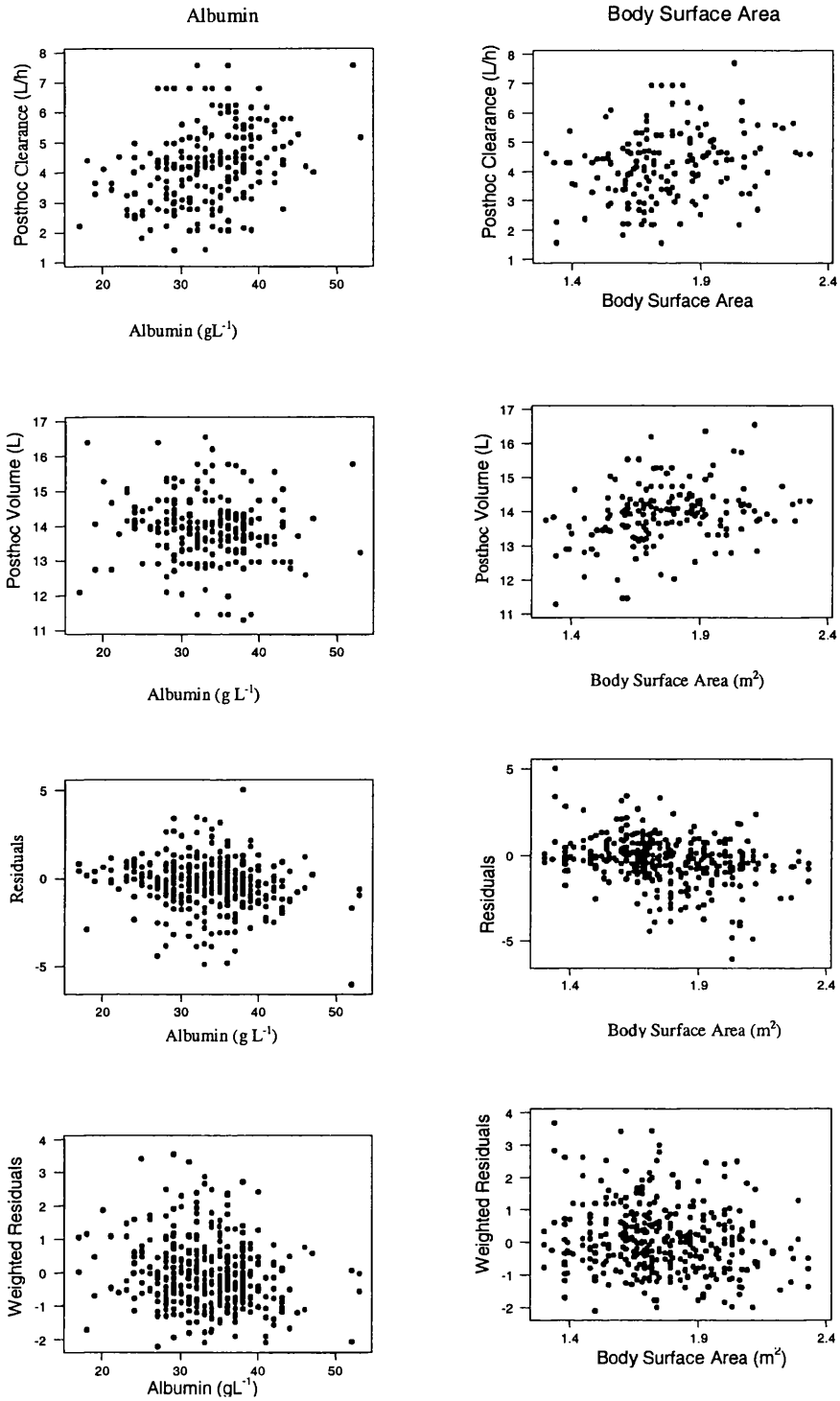

Figure 2.5.2.e Plots of individual pharmacokinetic parameters, residuals and weighted residuals against covariate that show a relationship

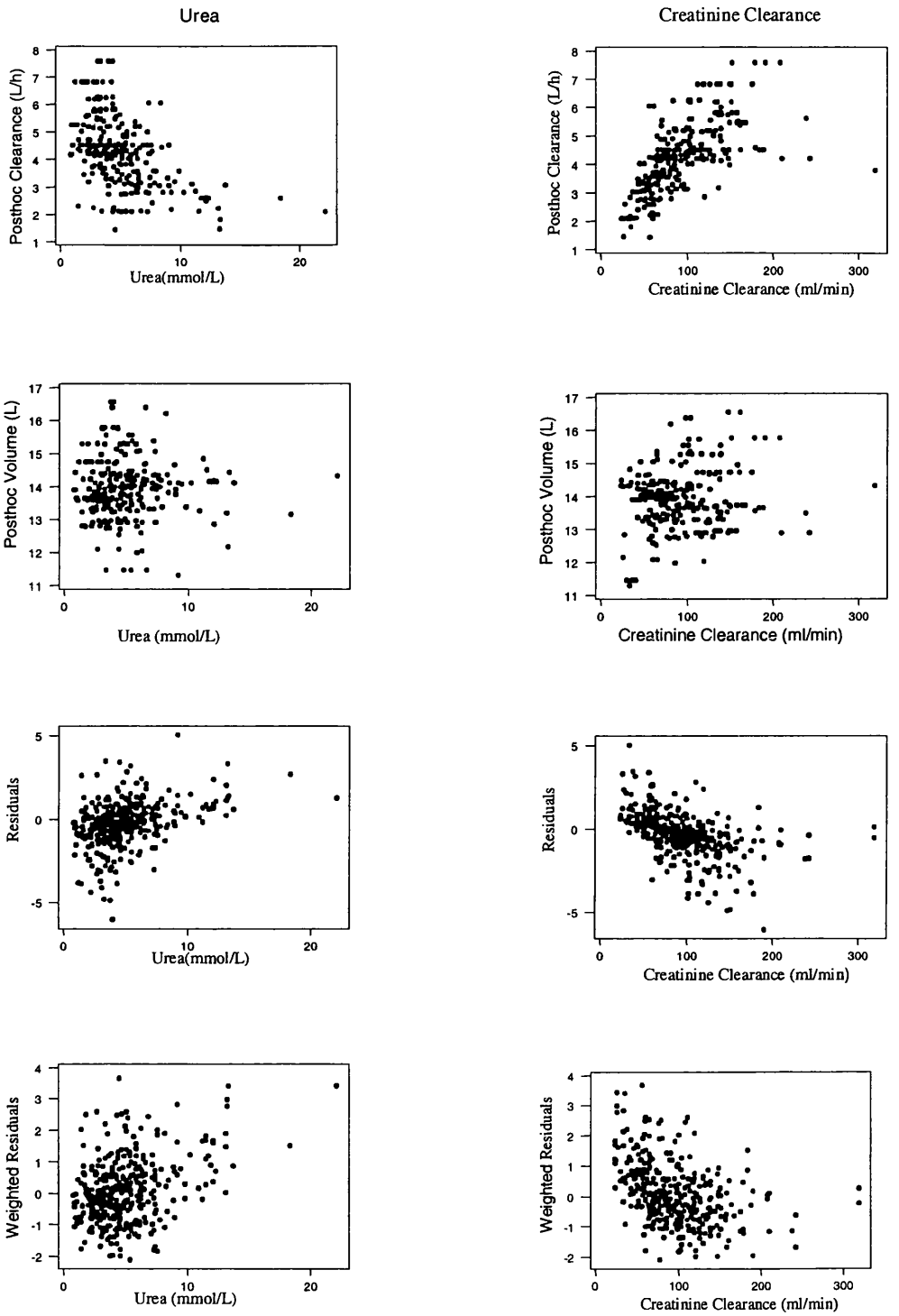

Table 2.5.2 b Summary of the results from the linear regression of POSTHOC pharmacokinetic parameter estimates against covariates values

	CLEARANCE *SS Total - 618.925*		VOLUME (V_1) *SS Total - 362.54*	
	SS error	p	SSerror	p
Age	450.6	<0.01	362.2	0.6
Height	542.9	<0.01	328.2	<0.01
Ideal body weight	568.9	<0.01	308.2	<0.01
Weight	592.9	<0.01	313.7	<0.01
Lean body mass	555.4	<0.01	303.6	<0.01
Body mass index	616.9	0.27	336.0	<0.01
Body surface area	571.6	<0.01	304.9	<0.01
Albumin	558.2	<0.01	360.6	0.159
White cell count	618.8	0.82	358.9	0.05
Haemoglobin	617.3	0.31	362.6	0.9
Platelets	616.0	0.18	359.6	0.08
Urea	448.3	<0.01	362.1	0.5
Creatinine	471.3	<0.01	361.3	0.3
Creatinine clearance	375.9	<0.01	351.6	0.01

Note: POSTHOC parameter estimates obtained from the 'basic model' were the response variables and covariates were the predictor variables.

Key: SS Total represents both residual sum of squares that is explained and not explained by the model; SS error represents the residual sum of squares that was not explained with the inclusion of a variable; p is the level of significance of the decrease in sum of squares.

Table 2.5.2 c Models obtained by "bestsubset" multiple linear regression of clinical factors and POSTHOC pharmacokinetic parameter estimates (clearance, CL and volume of the central compartment, V_1)

		Model	R^2 adj %
CL	~	Creatinine clearance	39.1
	~	Urea	27.4
	~	Urea + Creatinine clearance	47.8
	~	Creatinine + Age	43.6
	~	Creatinine + Body surface area + Age	53.9
	~	Creatinine + Ideal body weight + Age	53.8
	~	Urea + Creatinine + Ideal body weight + Age	56.0
	~	Creatinine + Body surface area + Weight + Age	56.0
V_1	~	Lean body mass	16.0
	~	Body surface area	15.6
	~	Lean body mass + Albumin	18.6
	~	Body surface area + Albumin	18.1
	~	Body surface area + Albumin + Creatinine	20.8
	~	Lean body mass + Albumin + Creatinine	20.8

Key: R^2 adj represents the coefficient of determination adjusted for a multicovariate model

Analysis of single covariates by NONMEM identified weight, age, height, ideal body weight, albumin, urea, creatinine clearance, gender, body surface area, lean body mass platelets and pyrexia as influencing clearance. A summary of the results is presented in Table 2.5.2.d. Creatinine clearance and creatinine concentration were the two covariates with the strongest influence on clearance. Two different approaches were then used in the analysis of these data. The first involved building the model from an estimate of creatinine clearance calculated from age, weight, creatinine concentration and gender. The second approach used the individual clinical characteristics such as age, body surface area and serum creatinine concentration.

With the 'creatinine clearance' approach, in addition to a linear relationship between creatinine clearance and clearance, a linear relationship was found between V_1, and BSA (or lean body mass and ideal body weight) and a nonlinear relationship with albumin. BSA was chosen for inclusion in the model as a measure of body size because it is widely used in oncology. Model building with the creatinine clearance approach produced the results presented in Table 2.5.2.e. The best model was represented by:

$CL = \theta_1 * (1 + \theta_3 \text{ Creatinine clearance})$

$$V_1 = \theta_2 * \text{Body surface area} * \left(\frac{\text{Albumin}}{34}\right)^{\theta 4}$$

$Q = \theta_5$

$V2 = \theta_6$

where θ_1, θ_2, θ_3, θ_4, θ_5 and θ_6 are typical population parameter estimates.

With the 'clinical factors' approach the inclusion of body surface area, ideal body weight or lean body mass as a second covariate caused similar drops in the objective function value. As BSA gave the same results as height and weight but required one less parameter, BSA was chosen as the covariate. A third covariate, age as a power model, was added to the previous model causing a further drop in objective function value.

Table 2.5.2 d Summary of results of individual covariates tested by NONMEM

Pharmacokinetic Parameter	Covariates Tested (reduction of OFV from basic model)			
	Significant addition	Δ OFV[a]	Insignificant addition	Δ OFV[a]
CL (L h^{-1})	Creatinine clearance	123.1	Body mass index	3.4
	Creatinine	67.2	Platelets	6.8
	Urea	59.7	Pyrexia	4.3
	Age	46.2	White cell count	2.3
	Lean body mass	23.1	Obesity	1.4
	Ideal body weight	20.6	Haemoglobin	0.5
	Body surface area	18.5		
	Gender	18.4		
	Height	18.2		
	Albumin	13.5		
	Weight	12.9		
V_1 (L)	Body surface area	20.1	Height	6.0
	Lean body weight	20.0	Obesity	3.7
	Ideal body weight	17.4	Platelets	1.9
	Albumin	9.5	Haemoglobin	0.2
	Weight	9.3	White cell count	0
	Gender	8.4	Urea	0

Key: OFV represents the objective function value; [a] *A reduction in OFV of more than 7.9 units was considered statistically significant, i.e.* $p < 0.05$.

Table 2.5.2 e Summary of covariate selection by NONMEM using the creatinine clearance approach

	Model	OFV	Model for comparison	ΔOFV
1.	$CL = \theta_1$ $V_1 = \theta_2$	238.3		
2.	$CL = \theta_1 * (1+ \theta_3 *$ Creatinine clearance) $V_1 = \theta_2$	115.2	1	123.1
3.	$CL = \theta_1 * (1 + \theta_3 *$ Creatinine clearance) $V_1 = \theta_2 *$ Weight	107.4	2	7.8
4.	$CL = \theta_1 * (1 + \theta_3 *$ Creatinine clearance) $V_1 = \theta_2 *$ (Albumin/34)$^{\theta 4}$	104.5	2	10.7
5.	$CL = \theta_1 * (1 + \theta_3 *$ Creatinine clearance) $V_1 = \theta_2 *$ Ideal body weight	90.1	2	25.1
6.	$CL = \theta_1 * (1 + \theta_3 *$ Creatinine clearance) $V1 = \theta_2 *$ Lean body mass	92.5	2	22.7
7.	$CL = \theta_1 * (1 + \theta_3 *$ Creatinine clearance) $V_1 = \theta_2 *$ Body surface area	91.9	2	23.3
8.	$CL = \theta_1 * (1 + \theta_3 *$ Creatinine clearance) $V_1 = \theta_2 *$ Body surface area * (Albumin/34)$^{\theta 4}$	73.9	7	18.0

Key: OFV Objective function value; Δ OFV - logarithmic likelihood difference asymptotically distributed as χ^2, with 1 degree of freedom; θ_n represent parameters estimated from the population analysis; significance set at 99.5%, corresponds to a difference of 7.9 in OFV.

The best fit of the data was achieved by modelling volume of the central compartment with body surface area as a linear, and albumin as a power model. Discrete covariates such as temperature, obesity and gender were incorporated as step models. The influence of gender on clearance was no longer statistically significant. Table 2.5.2.f shows a summary of the covariate models tested. The best model was:

$$CL = \theta_1 * \left(\frac{\text{Creatinine concentration}}{71}\right)^{\theta 5} * \left(\frac{\text{Age}}{46}\right)^{\theta 6} * \text{Body surface area}$$

$$V_1 = \theta_2 * \text{Body surface area} * \left(\frac{\text{Albumin}}{34}\right)^{\theta 7}$$

$$Q = \theta_3$$

$$V_2 = \theta_4$$

No covariates were found that influenced V_2 and Q and the interindividual variabilities in V_1 and V_2 were indeterminate using both approaches.

Backward stepping was then carried out on the full model such that each covariate was removed from the model one at a time to confirm its influence on the full model.

All covariates were associated with a significant increase in the objective function value when removed from the model. The analysis was carried out using a diagonal covariance matrix on the vector of η. A full covariance matrix on clearance and intercompartmental clearance was estimated using the best models obtained from the two approaches. From the model including the covariance matrix, the covariates were removed one at a time to check the influence of each one on the pharmacokinetic parameter estimates; thus the results showed that the choice of covariates was not influenced by correlation among the pharmacokinetic parameters. The inclusion of the covariance matrix did not affect the choice of the structural model.

Table 2.5.2 f Summary of covariate selection by NONMEM using the clinical factors approach

	Model	OFV	Model for comparison	ΔOFV
1	$CL = \theta_1$ $V1 = \theta_2$	238.3	-	-
9	$CL = \theta_1 * (Creatinine/71)^{\theta 3}$ $V1 = \theta_2$	171.1	1	67.2
10	$CL = \theta_1 * (Creatinine/71)^{\theta 3}$ * Body mass index $V1 = \theta_2$	177.4	9	60.9
11	$CL = \theta_1 * (Creatinine/71)^{\theta 3}$ * Height $V1 = \theta_2$	154.5	9	83.8
12	$CL = \theta_1 * (Creatinine/71)^{\theta 3}$ * Weight $V1 = \theta_2$	148.2	9	90.1
13	$CL = \theta_1 * (Creatinine/71)^{\theta 3}$ * Body surface area $V1 = \theta_2$	132.9	9	105.4
14	$CL = \theta_1 * (Creatinine/71)^{\theta 3}$ * Lean body mass $V1 = \theta_2$	122.1	9	116.2
15	$CL = CL = \theta_1 * (Creatinine/71)^{\theta 3}$ * Ideal body weight $V1 = \theta_2$	129.9	9	108.4
16	$CL = CL = \theta_1 * (Creatinine/71)^{\theta 3} * (Age/46)^{\theta 3}$ $V1 = \theta_2$	133.5	9	104.8
17	$CL = CL = \theta_1 * (Creatinine/71)^{\theta 3}$ * Weight * $(Age/46)^{\theta 4}$ $V1 = \theta_2$	113.5	12	34.7
18	$CL = CL = \theta_1 * (Creatinine/71)^{\theta 3}$ Ideal body weight * $(Age/46)^{\theta 4}$ $V1 = \theta_2$	100.1	15	29.9
19	$CL = \theta_1 * (Creatinine/71)^{\theta 3}$ * Lean body mass * $(Age/46)^{\theta 4}$ $V1 = \theta_2$	94.2	14	27.9
20	$CL = \theta_1 * (Creatinine/71)^{\theta 3}$ * Body surface area *$(Age/46)^{\theta 4}$ $V1 = \theta_2$	95.9	13	37.0
21	$CL = \theta_1 * (Creatinine/71)^{\theta 3}$ * Body surface area * $(Age/46)^{\theta 4}$ $V = \theta_2 * (Albumin/34)^{\theta 5}$	83.6	20	12.3
22	$CL = \theta_1 * (Creatinine/71)^{\theta 3}$ * Body surface area * $(Age/46)^{\theta 4}$ $V = \theta_2$ * Body mass index	88.5	20	7.4
23	$CL = \theta_1 * (Creatinine/71)^{\theta 3}$ * Body surface area * $(Age/46)^{\theta 4}$ $V = \theta_2$ * Weight	85.8	20	10.1
24	$CL = \theta_1 * (Creatinine/71)^{\theta 3}$ * Body surface area * $(Age/46)^{\theta 4}$ $V = \theta_2$ * Ideal body weight	74.4	20	21.5
25	$CL = \theta_1 * (Creatinine/71)^{\theta 3}$ * Body surface area * $(Age/46)^{\theta 4}$ $V = \theta_2$ * Lean body mass	73.9	20	22
26	$CL = \theta_1 * (Creatinine/71)^{\theta 3}$ * Body surface area * $(Age/46)^{\theta 4}$ $V = \theta_2$ * Body surface area	72.1	20	23.8
27	$CL = \theta_1 * (Creatinine/71)^{\theta 3}$ * Body surface area * $(Age/46)^{\theta 4}$ $V = \theta_2$ * Body surface area * $(Albumin/34)^{\theta 5}$	52.9	26	19.2

key: OFV - Objective Function Value; ΔOFV - logarithmic likelihood difference asymptotically distributed as χ^2, with 1 degree of freedom; θ_n represent parameters estimated from the population analysis; significance set at 99.5% corresponds a difference of 7.9 of OBV.

From the population analysis two models were obtained, one using clinical factors and the other using the estimated creatinine clearance. The residual error model was also reconfirmed.

2.5.3 INVESTIGATION OF CREATININE CONCENTRATION

The results obtained using the measured and three different minimum creatinine concentrations are presented in Table 2.5.3.a. With the creatinine clearance model there was no major difference between using a lower value of 60 μmol L^{-1} or 70 μmol L^{-1} but both were superior to 88.4 μmol L^{-1} and the measured concentration. In contrast, 70 μmol L^{-1} proved the optimal minimum with the clinical factor model. Figure 2.5.3 shows the POSTHOC clearance estimates against creatinine clearance obtained when the creatinine concentration was set at 60, 70 or 88.4 μmol L^{-1}. The best correlation between estimated creatinine clearance and gentamicin clearance was obtained when the creatinine concentration was set at 60 μmol L^{-1}. That observation is in agreement with the results obtained from NONMEM. The weighted residuals plots were also consistent with these results.

After comparing the plots and parameter estimates from the two best models, no firm conclusion could be drawn about which approach was better. Table 2.5.3.b shows the parameter estimates and the error associated with the two models.

Figure 2.5.3 Gentamicin clearance estimates against creatinine clearance (ml min^{-1}) obtained from creatinine concentration set at 60, 70 and 88.4 μmol L^{-1}

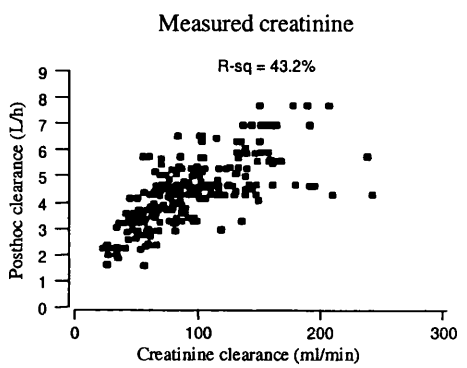

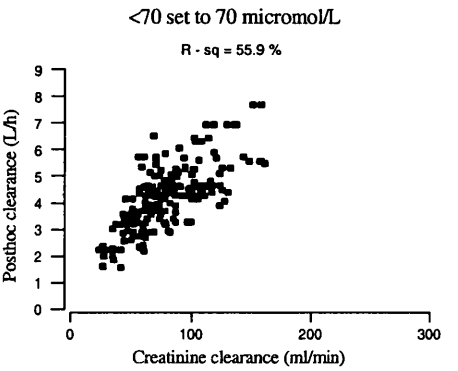

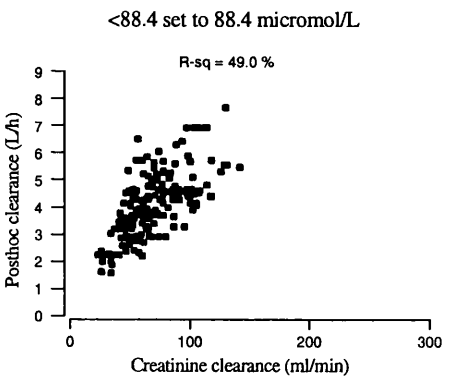

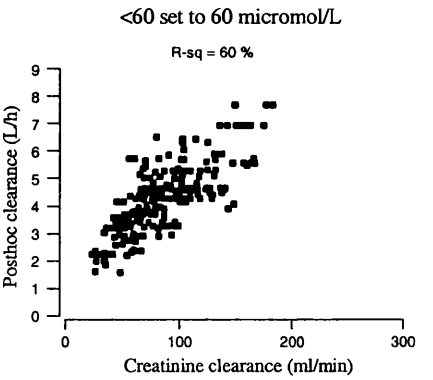

Table 2.5.3 a Summary of objective function values obtained using the best models with the creatinine concentration set to different minimum values

MODEL	CLEARANCE MODEL	CREATININE CONCENTRATION (μmol L^{-1})	OFV
8	Creatinine clearance	measured	73.9
	Creatinine clearance	≤ 60 set at 60	32.0
	Creatinine clearance	≤ 70 set at 70	28.9
	Creatinine clearance	≤ 88.4 set at 88.4	61.0
27	Creatinine, BSA, Age	measured	52.9
	Creatinine, BSA, Age	≤ 60 set at 60	24.5
	Creatinine, BSA, Age	≤ 70 set at 70	17.9
	Creatinine, BSA, Age	≤ 88.4 set at 88.4	31.6

Key: BSA - Body surface area; OBV– objective function value

Table 2.5.3 b Summary of the parameter estimates obtained from the two best models using the population data set (N=140)

		$CL = \theta_1 (1 + \theta_5 * CLcr)$ *cut off 60 μmoll^{-1}* $V_1 = \theta_2 * BSA (Alb/34)^{\theta 6}$			$CL = \theta_1 * (Cr/71)^{\theta 5} * (Age/46)^{\theta 6} * BSA$ *cut off 70 μmoll^{-1}* $V_1 = \theta_2 * BSA (Alb/34)^{\theta 7}$	
		Estimate	SE (%)		Estimate	SE (%)
CL	θ1	1.02	22.7	CL θ1	2.56	2.8
	θ5	0.037	30.6	θ5	- 0.86	8.8
				θ6	- 0.33	14.6
V_1	θ2	8.49	5.6	V_1 θ2	8.45	4.4
	θ6	- 0.61	24.2	θ7	- 0.63	22.0
Q	θ3	1.61	30.7	Q θ3	1.62	23.7
V_2	θ4	8.22	21.2	V_2 θ4	7.87	13.5
Intersubject variability						
ω_{CL} (CV%)		17.7	22.9		17.8	21.2
ω_{V1} (CV%)		indeterminate			indeterminate	
ω_Q (CV%)		29.5	222		33.6	142
ω_{V2} (CV%)		indeterminate			indeterminate	
Residual variability						
σ *at 1 mgL^{-1}(%)*		30.6	14.7		28.5	14.0
at 8 mgL^{-1}(%)		16.7	27.0		16.7	27.9
Derived Parameters						
$T_{1/2\alpha}$ (h)		1.5			1.4	
$T_{1/2\beta}$ (h)		6.2			6.0	
Vss (L kg^{-1})		0.37			0.36	

Key: Clcr - Creatinine clearance; alb - albumin; Cr - Creatinine concentration; BSA - Body surface area; CL -Clearance; V_1 - Central volume of distribution; V_2 - Peripheral volume of distribution; ω^2 - Variance of intersubject variability; σ^2 - Variance of residual variability; $T_{1/2}$ - Half life.

2.5.4 MODEL EVALUATION

The model evaluation was carried out with 70 patients and 132 concentrations.

The mean percentage prediction error was -7.2% for the model based on creatinine clearance and -6.6% for the model based on clinical factors. For the model using creatinine clearance, peak concentrations had a prediction error of -3.4% whereas troughs had a prediction error of -6.5%. For the model using clinical factors, the prediction error associated with the peak concentration was -3.7% whereas the trough concentrations had a mean error of -2.5%. There was no bias in the prediction errors. The probability that a measured concentration lay within the 2.5-97.5 percentile of the simulated concentration was 0.9 for both models. Figure 2.5.4 shows the 2.5-97.5 percentile range of the simulated concentration for each data point for all patients in whom peak and trough concentrations were measured.

2.5.5 DOSAGE GUIDELINES

The parameters obtained by fitting the full data set are shown in Table 2.5.5. Due to its simplicity, the model based on creatinine clearance was selected for the evaluation of dosage guidelines arising from two nomograms. Concentration-time profiles were simulated for 1000 patients for three values of creatinine clearance (105 $mlmin^{-1}$, 65 $mlmin^{-1}$ and 25 $mlmin^{-1}$) assuming the dose regimens recommended by Nicolau et al. (1995) and Thomson et al. (1996). The mean concentration time profiles, the dosage regimens, and the 25 – 75 percentile ranges are shown in Figure 2.5.5.

Figure 2.5.4 Measured concentrations, population predicted concentrations and 2.5-97.5 percentile range of 1000 simulations in the test data set.

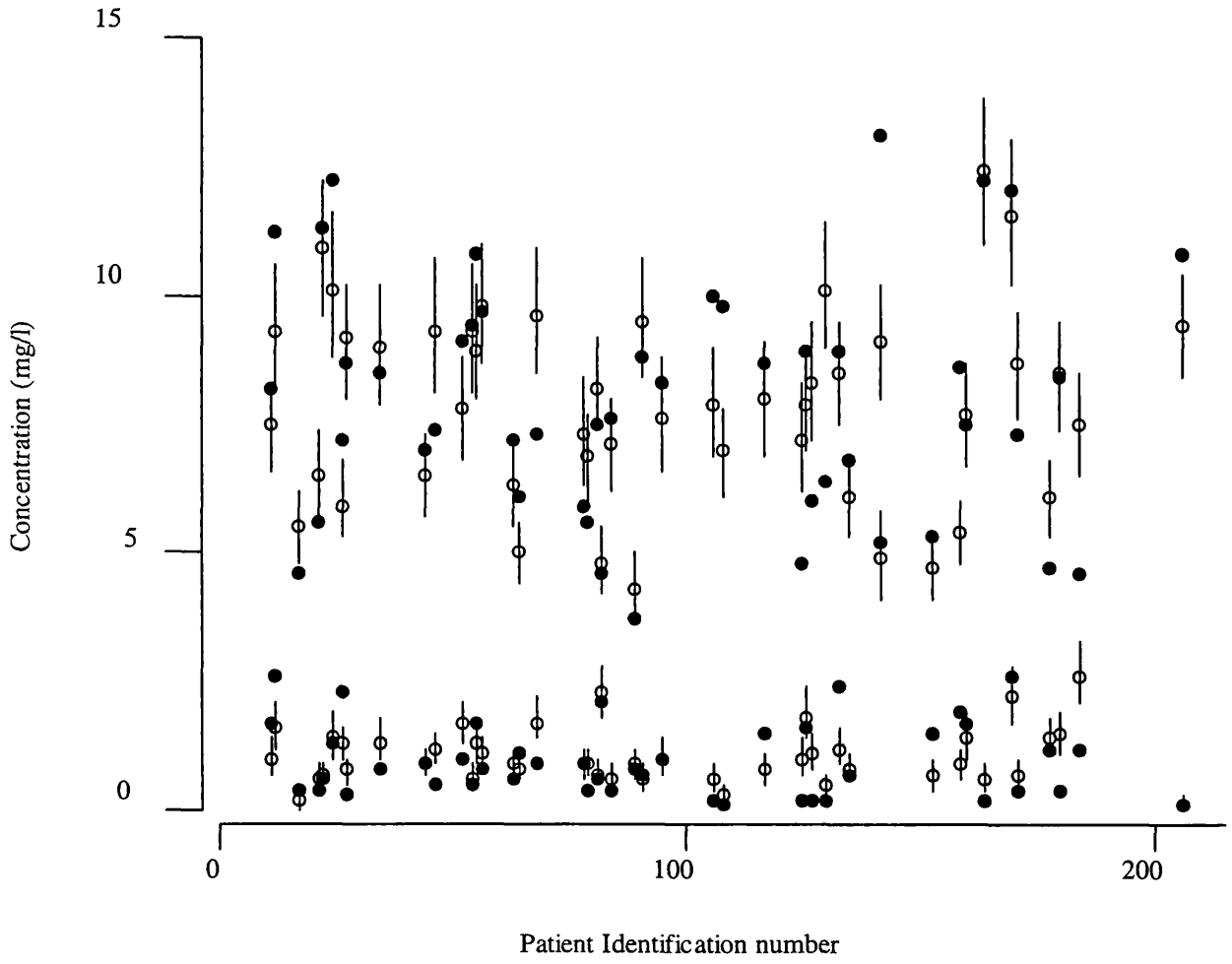

Key: Measured concentration - solid circles; Predicted concentration - open circles; line is the 2.5 -97.5 percentile range of 1000 concentrations

Figure 2.5.5 Simulated mean and 50 per cent interquartile range of the concentration-time profile obtained using the best model with two different nomograms

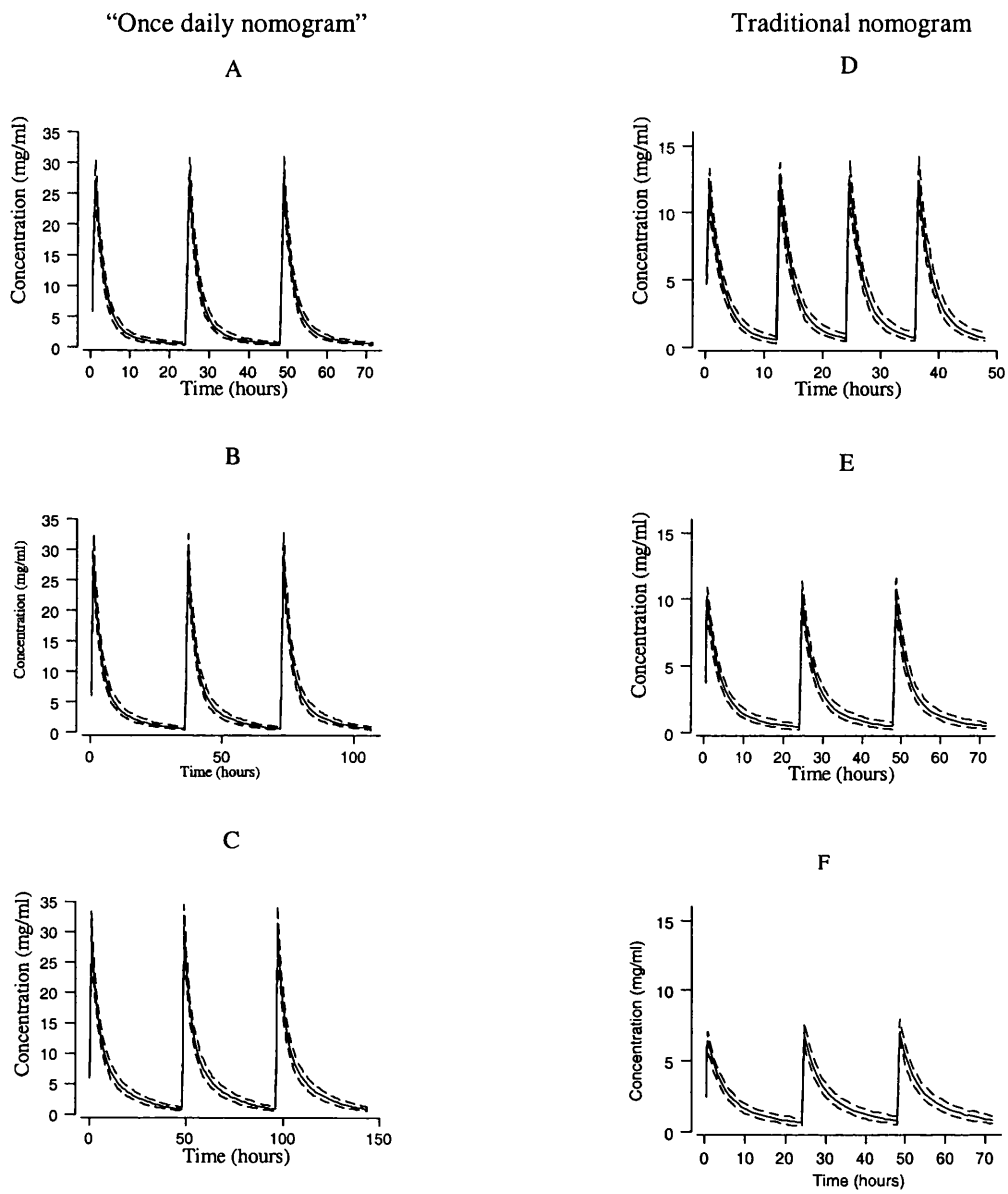

Creatinine Clearance	Panel	Dosage for Extended Interval	Panel	Dosage for Traditional nomogram
105 ml min^{-1}	A	490 mg/24h	D	200 mg/12h
65 ml min^{-1}	B	490 mg/36h	E	160 mg/24h
25 ml min^{-1}	C	490 mg/48h	F	100 mg/24h

Table 2.5.5 Summary of results of parameter estimates from the two best models using the combined data set (N=210)

		$CL = \theta_1 (1 + \theta_5 * Clcr)$ *cut off 60 μmol L^{-1}* $V_1 = \theta_2 * BSA (alb/34)^{\theta 6}$				$CL = \theta_1 * (Cr/71)^{\theta 5} * (Age/46)^{\theta 6} * BSA$ *cut off 70μmol L^{-1}* $V_1 = \theta_2 * BSA (alb/34)^{\theta 7}$	
		Estimate	SE (%)			Estimate	SE (%)
CL	θ1	0.88	19.2	CL	θ1	2.46	3.1
	θ5	0.043	24.4		θ5	- 0.78	9.2
					θ6	- 0.33	14.5
V_1	θ2	8.59	3.8	V_1	θ2	8.52	3.9
	θ6	- 0.39	30.0		θ7	- 0.40	28.5
Q	θ3	1.30	23.4	Q	θ3	1.34	24.2
V_2	θ4	9.79	28.5	V_2	θ4	9.05	20.6
Intersubject Variability							
ω_{CL} (CV%)		18.5	18.1			19.6	17.4
ω_{V1} (CV%)		indeterminate				indeterminate	
ω_Q (CV%)		28.2	189.2			30.1	174.4
ω_{V2} (CV%)		indeterminate				indeterminate	
Residual Variability							
σ *at 1 mgL^{-1}* (%)		36.4	17.9			35.6	20.8
at 8 mgL^{-1} (%)		16.5	24.6			16.3	27.4
Derived Parameters							
$T_{1/2\alpha}$ (h)		1.8	-			1.7	-
$T_{1/2\beta}$ (h)		8.0	-			7.5	-
Vss (L kg^{-1})		0.38	-			0.38	-

Key: Clcr - Creatinine clearance; alb - Albumin; Cr - Creatinine concentration; BSA - Body surface area; CL - Clearance; V_1 - Central volume of distribution; V_2 - Peripheral volume of distribution; ω^2 - Variance of intersubject variability; σ^2 - Variance of residual variability; $T_{1/2}$ - Half life.

2.6 DISCUSSION

Despite the fact that the pharmacokinetics of the aminoglycoside antibiotic gentamicin have been extensively studied, only limited and conflicting data have been published on the most appropriate pharmacokinetic model. For instance, a one-compartment model is usually assumed in clinical settings but several studies have found that gentamicin pharmacokinetics are better described by a two- or three-compartment model (Schentag et al., 1977; Laskin et al., 1983; MacGowan et al., 1994). Furthermore, with particular respect to patients with cancer, there are conflicting reports about the magnitude of the volume of distribution. In this study, the pharmacokinetics of gentamicin in patients with cancer have been investigated and characterised using a population approach applied to data collected during routine therapeutic drug monitoring.

The population mean clearance estimate was 4.2 L h^{-1}, and is consistent with 4.6 L h^{-1} /1.73m^2 reported by Bertino et al. (1991). As expected, estimated creatinine clearance and serum creatinine concentration were the covariates that had the strongest influence on gentamicin clearance. However, the relatively high intercept obtained is probably because few patients showed creatinine clearance estimates < 30 ml min^{-1}. It is therefore important that these results are not extrapolated to patients with very poor renal function in whom gentamicin clearance might be overestimated. The use of estimated creatinine clearance as a measure of renal function has some limitations, especially with low serum creatinine concentrations. In order to overcome this problem, some authors have recommended the use of a creatinine concentration corrected to 88.4 μmol L^{-1} (1 mg dL^{-1}) for concentrations less than or equal to 88.4 μmol L^{-1} (Winter, 1988; Robert et al., 1991). Nonetheless, other authors feel this might lead to underdosing of some patients (Bertino, 1993; Smythe et al., 1994). It has been noted (Duffull et al., 1997) that a better prediction of clearance was obtained when all serum creatinine values below 60 μmol L^{-1} were set at 60 μmol L^{-1}. In the institution where this research took place, values of creatinine concentration less than 60 μmol L^{-1} are set at 60 μmol L^{-1} (the lower limit of the reference range) for estimating gentamicin clearance and calculating dosage recommendations. The present study investigated the

consequences of setting low creatinine concentrations at 60 μmol L^{-1}, 70 μmol L^{-1} or 88.4 μmol L^{-1}. There was little difference using creatinine concentrations set at 60 μmol L^{-1} or 70 μmol L^{-1} when the creatinine clearance model was applied (model 8), whereas for the model including clinical values (model 27) the best fit was obtained when low creatinine concentrations were set at 70 μmol L^{-1} (Table 2.5.3.a). With both models the value 88.4 μmol L^{-1} was too high, but better than using the measured creatinine concentration.

The influence of gender on gentamicin clearance remains unclear. Cockcroft and Gault (1976) suggested a correction factor of 0.85 for women, having this value been chosen arbitrarily. Phillips et al. (1988) suggested that adjustment for gender was not necessary. In the present study, gender was included as a single covariate and associated with a significant influence in clearance but in the final clinical factors model the influence of gender was not significant. One possible explanation is that any gender difference in clearance is already taken into account via the differences in body surface area.

Gentamicin volume of distribution in oncology patients remains the subject of debate. It is often reported to range between 0.25 and 0.31 L kg^{-1} in adults from a general population (Zaske, 1992; Sande and Mandell, 1996) whereas in patients with cancer an increased volume of distribution in the range 0.38 L kg^{-1} to 0.43 L kg^{-1} has been reported (Phillips et al., 1988; Zeitany et al., 1990; Davis et al., 1991). In contrast, however, a study carried out on 880 cancer patients found a mean volume of distribution of 0.35 L kg^{-1} compared to 0.34 L kg^{-1} for the control group (Bertino et al., 1991). These authors concluded that the volume of distribution of gentamicin was not increased in patients with cancer. More recently, MacGowan et al. (1994) reported a volume of distribution of 24.5 L in patients with haematological malignancies. In this study, the value of 0.38 L kg^{-1}, equivalent to 24.6 L, is consistent with the values reported by both Bertino et al. (1991) and MacGowan et al. (1994) in similar patients. However the differences in volume of distribution in the published literature may simply

reflect different sampling protocols and the application of different pharmacokinetic models.

Significant relationships were found between the volume of the central compartment (V_1), and measures of body size (IBW, LBM, Wt and BSA) and serum albumin concentration. A relationship between low serum albumin and volume of distribution was also reported by Etzel et al. (1992) and, in a study of amikacin in patients with cancer, Davis et al. (1991) detected a significant influence of albumin on the volume of distribution. In contrast, Phillips et al. (1988) found no influence of albumin on volume of distribution but they did not report the range of albumin concentrations in their study. Since low serum albumin concentrations have been shown to alter intra- and extra-cellular fluid distributions, leading to an expanded extracellular fluid volume, the wide range of values in the present study may have favoured the identification of the influence of albumin on the volume of distribution. In this analysis, the volume of distribution ranged from 0.55 to 0.35 L kg^{-1} with albumin concentrations of 17 g L^{-1} to 53 g L^{-1}.

Gentamicin concentration-time profiles are frequently characterised by two-compartment models and in the present study the half-life of the initial phase was 1.7 hours (range 0.8-3.8), which is similar to previous observations (Wenk et al., 1979; Laskin et al., 1983; Aarons et al., 1989; MacGowan et al., 1994). However, the half-life of the late phase was found to be 8.0 hours (range 3.7-17.8) which is significantly shorter than in other reports. Laskin (1983), for instance, identified a terminal elimination half-life of 94 hours, although this only became dominant 12 hours after administration of gentamicin. In contrast, Aarons et al. (1989) reported a much shorter terminal half-life of 26.6 hours for the related aminoglycoside tobramycin but, according to these authors, limitations of their study design prevented identification of the long terminal elimination phase. A similar limitation probably applies to the results presented here: a long terminal half-life was not identified because 71% of the concentrations were measured in the first 12 hours post-dose and only two patients had concentrations taken more than 24 hours after gentamicin administration. The data were

collected during the first few days of routine monitoring, tissue accumulation would have been incomplete and the protracted elimination phase would not have been appropriately characterised. Lack of data at later times post dose probably also contributed to the inability to estimate intersubject variability on Q and V_2. The large residual error corresponding to a standard deviation of about 0.36 mg L^{-1} at low concentration values (1 mg L^{-1}) contrasts with the lower relative residual error with a standard deviation of 1.32 mg L^{-1} obtained at high concentrations (8 mg L^{-1}). Large residual errors may reflect poor assay performance and precision at low concentrations (White et al., 1994) although the assay standard deviation in this case was only 0.06 mg L^{-1} at 1 mg L^{-1}. Examination of the data identified a few patients in whom trough concentrations were unexpectedly higher or lower than predicted by the model and it is likely that these data points contributed to the high variability observed.

It has been shown that high gentamicin peak concentrations are associated with a better outcome and that target peak serum gentamicin concentrations should ideally be above 7 mg L^{-1} (Sculier and Klastersky, 1984; Moore et al., 1987). The dosage regimen recommended using the traditional nomogram (Thomson et al., 1996) yielded serum gentamicin concentrations within the target range (peak greater than 7 mg L^{-1} and trough less than 2 mg L^{-1}) for patients with normal renal function (Figure 2.5.5, panel D and E). However, in renal impairment, the mean peak concentration obtained from dosage regimens derived from the traditional nomogram (Thomson et al., 1996) was slightly lower than ideal (between 6-7 mg L^{-1} as shown in Figure 2.5.5 panel F). Target concentrations for the high dose regimen have not yet been established but very high peaks and low troughs should be obtained in patients with both normal and impaired renal function (Figure 2.5.5 panels A, B and C).

The use of multiple linear regression as an preliminary analysis for covariate model building in NONMEM has been advocated (Mandema et al., 1992), along with plots of the POSTHOC parameter estimates versus covariates (Ette and Ludden, 1995), for the decision which covariate to include in the model. The use of the plots can be misleading as false relationships can be exhibited due to correlation between covariates.

In this study, linear regression selected the same covariates as NONMEM (Table 2.5.2.b and Table 2.5.2.d). However, when the relationship was not linear, linear regression did not perform well and the plots were examined to suggest a suitable relationship. This was the case for creatinine concentration. NONMEM selected this as the second most influencial covariate while linear regression selected it as the fourth. Similar results were observed with albumin on volume.

In conclusion, this NONMEM analysis has shown that creatinine clearance estimated from creatinine concentrations was associated with a better fit when low values were set at 60 or 70 $\mu mol\ L^{-1}$ rather than using the measured creatinine concentration. Volume of distribution was similar to values estimated by other authors and was influenced by body surface area and serum albumin concentration. Examination of the results in the context of published nomograms has indicated that both the traditional approach and the new, "once daily" approach should usually achieve satisfactory concentrations in this patient group. Nevertheless, due to the high interpatient and residual variabilities, serum concentration monitoring is required to confirm optimal dosing in individual patients.

CHAPTER 3 A PHARMACOKINETIC-PHARMACODYNAMIC COMPARISON OF MIBEFRADIL, DILTIAZEM AND VERAPAMIL

3.1 SUMMARY

In this chapter the pharmacokinetic and pharmacodynamic characteristics of mibefradil, verapamil and diltiazem were determined after a single dose. The pharmacodynamics were measured with regard to diastolic blood pressure, heart rate and changes in PQ interval. In addition concentration-effect relationships for diastolic blood pressure, heart rate and changes in PQ interval for mibefradil and verapamil after both single and multiple doses were characterised and compared.

3.2 INTRODUCTION

3.2.1 CALCIUM CHANNELS

Calcium ions (Ca^{2+}) play an important role in biochemical reactions and participate in various intracellular messenger systems and processes. Changes in intracellular calcium concentration provoke the release of neurotransmitters and hormones, and the subsequent cellular responses to these substances. In the cardiovascular system, an increase in Ca^{2+} activates the actin-myosin interaction, causing myocardial contraction. Calcium is also implicated in the pacemaker activity of sinus node cells and in the conduction through the atrio-ventricular node.

Maintenance of intracellular calcium concentration is of pivotal importance. To achieve this, different proteins located in the cell membrane act as pathways or channels: In recent years, at least six different types of Ca^{2+} channel have been identified in mammalian cells. However, only two types can be found in heart and in vascular muscles: the long-lasting, L-type; and the transient, T-type. These voltage-operated Ca^{2+} channels play a crucial role in the cardiovascular system and it is recognised that they differ in some aspects such as threshold, entrance and expression within various cardiovascular tissues. The L-type Ca^{2+} channels initiate cardiac and vascular muscle contraction. The T-type Ca^{2+} channels take part in the pacemaker activity of the heart and in the regulation of hormone secretion (Katz, 1996). In the vascular muscle cells,

both the L-type and T-type channels are present and may also be important for vascular muscle contraction, but in neurohormonal cells T-type channels predominate. In the heart, the two types of channels are not equally distributed: the sinus node cells, responsible for the pacemaker, are rich in T-type, whereas the myocardial cells contain predominantly L-type channels.

3.2.2 CALCIUM CHANNEL BLOCKERS

Calcium antagonist drugs (calcium channel blockers) were introduced into the market in the 1960s. Since then they have been used in the treatment of cardiovascular diseases, particularly hypertension and angina pectoris.

3.2.2.1 Chemistry

Calcium channel blockers are conventionally sub-divided into three main chemical categories: 1,4-dihydropyridines, phenylalkylamines and benzothiazepines: the prototypes of these classes are respectively, nifedipine, verapamil and diltiazem. Recently, a new and distinct chemical class was identified through the prototype drug, mibefradil, a tetralol derivative. Representative chemical structures of the 'heart rate limiting' calcium blockers, mibefradil, verapamil and diltiazem are shown in Figure 3.2.2.

3.2.2.2 Mechanism of Action

The 1,4-dihydropyridines, phenylalkylamines and benzothiazepines are characterised by their shared ability to inhibit the inward flux of calcium ions across the cell membrane via the L-type calcium channels (long-lasting high voltage activated). At therapeutic concentrations, these agents have no effects on T-type calcium channels. In contrast, mibefradil preferentially blocks the T-type (transient low voltage activated) calcium channels as well as partially affecting the L-type channels (25-70%) (Mishra and Hermsmeyer, 1994).

Figure 3.2.2. Chemical structures of mibefradil, verapamil and diltiazem

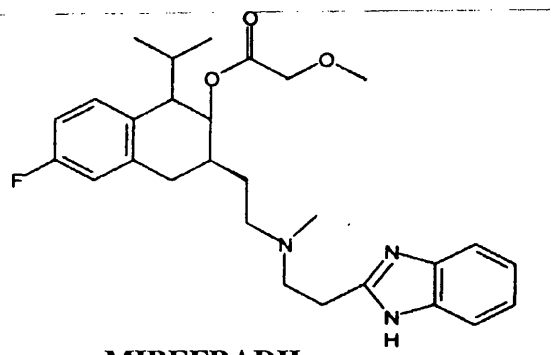

MIBEFRADIL

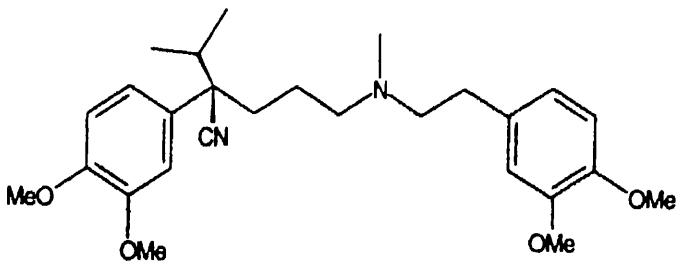

VERAPAMIL

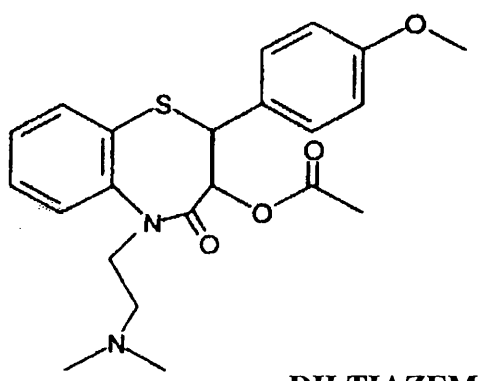

DILTIAZEM

3.2.2.3 Pharmacological Action

Differences in pharmacological action follow differences in mechanism of action. In vascular smooth muscle cells, the L- and T-type calcium channel blockers cause vasodilatation by a lowering of peripheral vascular resistance with a consequent lowering of blood pressure.

Additionally, the action of calcium channel blockers in the sinus node cells slows the rate of cardiac conduction to produce a reduction in the heart rate.

3.2.2.4 Pharmacokinetics

Mibefradil is rapidly absorbed after oral administration with peak plasma concentrations being reached after 1-2 hours (Welker, 1998). Mibefradil bioavailability is high with a low proportion of drug metabolised before reaching the systemic circulation (Clozel et al., 1991). A single 80 mg oral dose gives an absolute bioavailability of 70 % but with chronic dosing of 50 mg, the bioavailability of mibefradil approaches 90 % due to saturation of first-pass metabolism (Brogden and Marklam, 1997). Diltiazem is also rapidly and completely absorbed after oral administration with peak plasma concentrations reached within 1.5 hours after oral administration of a normal release formulation (Buckley et al., 1990). Verapamil is rapidly and almost completely absorbed ($\geq$ 90%) after oral administration, of a normal release formulation. A modified slow-release form of verapamil is more slowly absorbed and has an onset of action of 6 hours and duration of about 14 hours. However, because of extensive first-pass hepatic metabolism, only approximately 20 % of the drug reaches the circulation. The peak antihypertensive effect following intravenous administration occurs in 5 minutes, and by 10 to 20 minutes the effect is dissipated (Hamann et al., 1984).

The high volume of distribution of mibefradil (Vss 130-220 L) indicates that it is widely distributed in body tissues (Welker et al., 1989). At therapeutic concentrations, it is highly ($\geq$ 95%) bound to α_1 – acid glycoprotein in the plasma. Verapamil mean volume of distribution ranges from 310 to 406 L (Hamann et al., 1984) and it is highly protein

bound (80 to 90%). The absolute bioavailability in healthy individuals is 35 to 40% (Kirsten et al., 1998). The mean volume of distribution is 209 L (Buckley et al., 1990).

Verapamil exhibits a bi-exponential decline after a single dose of both oral and intravenous administration, with an initial distribution phase lasting from 18 to 35 minutes and a much slower elimination phase with a half-life varying from 3 to 7 hours. Seventy per cent of an oral or intravenous dose is excreted by the kidney and 15 % is eliminated via the gastrointestinal route. Only 3 to 4 % is excreted unchanged in the urine. The terminal elimination half-life for verapamil ranges from 2.7 to 4.8 hours and the systemic clearance is reported to be 875 ml min^{-1} (Hamann et al., 1984). Several metabolites are produced by hepatic metabolism. It is unclear to what extent these metabolites contribute to the drug's therapeutic effects. Diltiazem is metabolised by the liver (65%) with the remainder being excreted by the kidneys. The elimination half-life after oral administration ranges from 2 to 11 hours (Buckley et al., 1990).

Mibefradil is a lipophilic compound that is extensively metabolised by the liver and less than 3 per cent of an oral dose is excreted unchanged in urine. Its metabolism is mediated by two competing pathways: a) cytochrome P_{450}-catalysed oxidative reactions, including hydroxylation and dealkylation, and b) hydrolysis of the ester side-chain to give the major circulating metabolite, Ro-5966. Activity of the cytochrome P_{450} isoenzymes (CYP3A4, CYP1A2 and CYP2D6) is competitively inhibited by mibefradil. At steady state, the cytochrome P_{450}-catalyzed reactions become saturated and hydrolysis then becomes the more efficient of the two pathways. The inhibition of the first pathway of metabolism combined with low activity of the hepatic esterase is responsible for decrease in clearance after multiple dosing resulting in a prolongation of half-life. The elimination half-life ($t_{1/2\beta}$) after single oral administration is 12 to 14 hours and 23.7 hours at steady state with a dose of 100 mg daily. This increases further with higher doses (> 160 mg). One explanation for that phenomenon is that at low doses, plasma concentrations of mibefradil may not be sufficient to inhibit oxidative metabolism, but with multiple doses, increased drug concentrations may be sufficient to inhibit it. That is confirmed by the decrease in clearance values (CL/F) at steady state.

Clearance varies between 15.6 and 21.0 L h^{-1} after intravenous administration (Welker et al., 1989). After oral administration it is reported to be 7.6 L h^{-1} at steady state after the administration of 100 mg per day, as opposed to 13.1 L h^{-1} after the administration of 100 mg as single dose (Welker et al., 1998). Preclinical trials on Ro 40-5966, the major metabolite of mibefradil, have demonstrated that its pharmacodynamic activity is only about 10 % that of the parent compound. Thus, it is unlikely to affect mibefradil's overall pharmacological profile (Brogden and Marklam, 1997).

3.2.3 SELECTION OF THE PHARMACODYNAMIC MODEL

The description of the linear and Emax model has been given elsewhere (Chapter 1). Substituting the Emax parameter in the Emax model equation by the parameter representing the maximum velocity of the reaction (Vmax) and EC50 by the parameter representing the concentration at which half of the maximum velocity occurs (Km), the Michaelis-Menten model is obtained. Similarities of these two models arise from the fact that both equations were derived from the law of mass receptor theory as proposed by Ariens et al. (1964). The Michaelis Menten equation was first applied to enzymatic reactions. Later, it was adapted to pharmacokinetic modelling. It has been reported that problems may be encountered in parameter estimation with the Michaelis-Menten equation (Godfrey and Fitch, 1984). Estimates of Vmax and Km were associated with a high correlation. This is due to the fact that the parameters appear in the equation as a ratio and therefore changes in the estimates of Vmax may be compensated for by changes in Km. Parameters estimation is hampered by a high correlation between estimates of Vmax and Km as occurs when concentrations are below the Km. These investigators proposed an approximation to this model by linearization. Similar problems were encountered by Ratkowsky (1986) when using the Michaelis-Menten model for simple enzymatic reactions. They have suggested a reparameterization of this model, in which the two parameters appear in the denominator of the equation. Two new parameters were derived given by 1/Vmax and Km/Vmax.

In vivo, studies that achieve high plasma concentrations are limited by the occurrence of side effects. This can prevent the Emax effect being reached and thus the Emax curve is

not defined. This is a situation similar to that described for the Michaelis-Menten model. The variance-covariance matrix showed that Emax and EC50 were very highly correlated. The parameters estimated with a wide variability, rendering the conclusion meaningless. Holford et al (1982) proposed the use of a linear model, which is often useful in practice but is also limited by how close the data are to a straight line. Linear models can be useful when drug concentrations are very low but as plasma concentrations increase and the effect reaches Emax, the sigmoid curve became more defined and therefore data deviates more from linearity. Under these circumstances, fitting a straight line will force the data to fit a line but the slope will depend on the curvature and will vary from patient to patient according to the fraction of Emax attained by each patient.

Recently, Della Paschoa et al. (1998) proposed the use of an exponential equation derived from the sigmoid Emax model to describe the concentration-anticonvulsant effect relationship of phenytoin when the Emax values were not reached within acceptable electric stimulation levels. Another re-parameterization of the sigmoid Emax model was suggested by Bachman et al. (1998). These investigators claimed that the re-parameterized equation yielded a more precise and accurate parameter estimates than the standard sigmoid Emax model.

More recently, a different re-parameterization of the Emax model has been proposed by Schoemaker et al. (1998). The reparameterization consists of introducing an alternative parameter, S0, equal to Emax/EC50, into the Emax model. After mathematical re-arrangement, it yields the following equation for the concentration-effect relationship:

$$E = \frac{E\,max * S0 * Y}{E\,max + S0 * Y} \qquad \text{Eq. 3.1}$$

where S0 is a measure of potency of the drug and is equal to the slope of the tangent to the Emax curve at zero concentrations and Y is the drug concentration, either predicted or measured. The S0 model can be used to relate the effect site concentration (Y_e) to the effect, i.e.

$$E = \frac{Emax * S0 * Y_e}{Emax + S0 * Y_e} \qquad \text{Eq. 3.2}$$

where Y_e is the concentration predicted at the effect site.

3.3 AIMS OF THE ANALYSIS

This study had two primary aims:

i) Characterisation of the single-dose pharmacokinetics and pharmacodynamics of mibefradil relative to verapamil and diltiazem;

ii) Characterisation of the concentration-effect relationships of single and multiple doses of mibefradil and verapamil in hypertensive patients.

3.4 PATIENTS AND METHODS

3.4.1 STUDY DESIGN

The study was carried out in two centres: one in Glasgow (Western Infirmary) and the other in Berkshire (Chiltern International Ltd, UK). The protocol was approved by the ethics review committees of each centre and all patients gave written informed consent before any screening procedures were performed. Patients were withdrawn from previous unsatisfactory antihypertensive treatment to enter a 4-week single-blind placebo run-in period (Period I). The principal inclusion criterion was a sitting diastolic blood pressure of 95-114 mmHg (inclusive) on days 21 and 28 of the placebo run-in, prior to drug intake. Patients were required to be in a satisfactory healthy state, as assessed by medical history, physical examination and clinical laboratory determination.

Patients were excluded if they had severe or malignant hypertension (WHO stage III) secondary hypertension, or had had a myocardial infarction within the last 6 months, or with current or prior evidence of heart failure. Patients with haemodynamically relevant rhythm disturbances, 1st degree AV-block (PQ-interval above 200 msec) or higher

degree AV-block were not enrolled in the study. Patients taking drugs that might affect blood pressure or which were known to interact with the effects of calcium channel blockers, such as anti-arrhythmics, sympathomimetic drugs, oral contraceptives, psychotropic medications, non steroidal anti-inflammatory drugs, were not incorporated in the study.

Patients who fulfilled the inclusion criteria were then enrolled in a single-dose, double blind, crossover study (Period II) of four different treatments, including placebo. Over a four-week period, patients reported at weekly intervals to receive capsules containing mibefradil 150 mg, verapamil 240 mg, and diltiazem 240 mg or matching placebo. Treatments were administered with 100 ml of tap water and the blood sampling and the pharmacodynamic measurements were timed according to the time of the administration of the drugs.

After a further washout period of one week, patients entered a second steady-state (Period III). They were randomly allocated to receive either mibefradil 100 mg or verapamil 240 mg (slow release) once daily for 4 weeks. Pharmacodynamic and drug concentration measurements were made on a fifth occasion, the last day of the steady-state period.

3.4.2 PATIENTS

Twenty-three patients aged 18-70 years were entered into this study. Only 20 of the 23 recruited patients met the inclusion criteria at the end of the placebo period and 18 completed the single-dose study (Period II). Table 3.4.2 lists the demographic characteristics and the clinical status of the patients involved in the single dose study.

Table 3.4.2 Demographic characteristics and clinical status of the patients included in the single-dose study (Period II)

ID	Height (cm)	Weight (kg)	Sex	Smoking status	Age (years)	Baseline DBP (mmHg)	Baseline HR (bpm)
1	173	81	M	1	60	95	65
2	146	52	F	1	58	98	86
3	169	75	M	1	46	93	74
4	163	93	M	0	30	105	92
6	165	74	M	0	50	98	84
7	150	77	F	0	67	92	67
8	157	72	F	0	68	99	71
9	173	107	M	1	61	107	101
11	166	78	F	0	60	96	78
13	173	62	M	1	53	94	70
14	164	76	F	0	69	104	96
16	158	68	F	0	58	94	69
17	178	108	M	0	50	87	71
18	165	77	F	0	59	110	106
19	183	98	M	1	57	99	103
20	169	77	M	0	55	102	94
22	168	79	M	0	60	101	64
23	166	88	M	0	66	97	80
MEAN	166	80			57	98	82
SD	9	14			9	6	14

Key: F - female; M - male; DBP - Diastolic blood pressure; HR - Heart rate. 0 - non-smoker; 1 - smoker; bpm - beats per minute.

Of those 18 patients, seventeen underwent the steady-state study (Period III), 10 receiving mibefradil and 7 receiving verapamil. The ten patients from the mibefradil group had a mean age of 59 years and a mean weight of 85 kg. Three were females and seven were males, their entry diastolic blood pressure was 98 mmHg and heart rate was 81 beats per minute (bpm). The verapamil group included three females and four males with a mean age of 54 years and a mean weight of 77 kg and the entry diastolic blood pressure was 99 mmHg and the heart rate was 82 bpm.

3.4.3 DRUG ASSAY

Venous blood samples were taken at 0, 0.5, 1, 1.5, 2, 3, 4, 6, 8, 10, 24 and 48 hours after the dose, then separated immediately into serum (mibefradil, placebo) or plasma (verapamil, diltiazem) and stored at -20° C. Verapamil and norverapamil and diltiazem plasma concentrations were measured using liquid/liquid extraction followed by reverse-phase high performance liquid chromatography with ultraviolet detection (mean coefficients of variation 7.1, 8.9 and 4.7%, respectively) (Dube et al., 1988). Mibefradil concentrations were measured using a high performance liquid chromatography-fluorescence method (mean coefficients of variation 6.3 and 6.2%, respectively) (Eggers et al., 1990). Drug assay of verapamil and diltiazem were performed in Glasgow and mibefradil in Roche, Basel.

3.4.4 PHARMACODYNAMIC MEASUREMENTS

Pharmacodynamic endpoints were changes in diastolic blood pressure (DBP), heart rate (HR) and electrocardiographic PQ interval. The times of drug administration were defined as time zero and haemodynamic measurements were made at 0.5, 1, 1.5, 2, 3, 4, 6, 8, 10, and 24 hours for study Period II. The same schedule was followed for the last day of the steady-state study (Period III) for mibefradil. For verapamil, PD measurements were performed only until 10 hours of the last dose of the steady-state study.

Blood pressure and the heart rate were measured with a Dinamap Critikon (Tampa, Florida, USA) semi-automatic sphygmomanometer. Baseline measurements were recorded after a 60-minute period of rest in a supine position. Blood pressure and heart rate were measured supine (after not less than 10 minutes rest) and standing (after 2 and 4 minutes). Mean values for supine and standing blood pressure were calculated for each time point.

PQ intervals were calculated as the mean of five consecutive readings from a conventional electrocardiogram (ECG) rhythm strip at 50 mm/s (lead II where available). An independent, blind observer measured these using customised software with a supergrid 20 x 20 SPGTT Digitizer (Summagraphics, Fairfield, Connecticut, USA).

3.4.5 PHARMACOKINETIC DATA ANALYSIS

All calculations in this section were performed on an Opus personal computer, with a Pentium 120 MHZ processor under MSWindows version 3.11, using the software WinNonlin (1996a).

A hierarchy of pharmacokinetic models was fitted to the individual concentration-time profiles for mibefradil, diltiazem and verapamil by nonlinear regression analysis. The equations used are described in Appendix I. Drug concentrations below the limit of

quantification were removed from the analysis, except when they were at the beginning of the concentration-time profile (for a single dose). In this case they were set to zero.

The pharmacokinetic model was fitted to the data with and without a weighting scheme. The weighting (W_i) was set to the reciprocal of the concentration predicted from the pharmacokinetic model as:

$$W_i = \frac{1}{\hat{Y}_j^{\,n}}$$

where $\hat{Y}_j$ represents the predicted concentration at the jth time. Several values of n were tested.

Individual pharmacokinetic parameters were estimated by the least squares method using the Gauss-Newton (Levenbergh and Hartley) search algorithm. Initial pharmacokinetic parameter estimates for a one-compartment model were calculated by the curve stripping method (Gibaldi and Perrier, 1982). Parameters were constrained by arbitrary setting of upper and lower boundaries on the initial parameter estimates.

For the single-dose studies with each drug, the following pharmacokinetic models were fitted to the concentration-time data set of each individual. The same approach was applied to the steady state mibefradil data but parameters for steady state verapamil were not estimated because a modified release formulation was used and the data could not be modelled. The models were parameterised as shown:

Mono-exponential; first-order absorption	(V/F, k01, k10)
Mono-exponential; first-order absorption; tlag	(V/F, k01, k10, tlag)
Bi-exponential; first-order absorption	(V/F, k01, k10, k12, k21)
Bi-exponential; first-order absorption; tlag	(V/F, k01, k10, k12, k21, tlag)
Mono-exponential; zero-order absorption	(V/F, Tmax, k10)
Bi-exponential; zero-order absorption	(V/F, Tmax, k12, k21, k10)
Bi-exponential; zero-order absorption; tlag	(V/F, Tmax, k12, k21, k10, tlag)

where k01 is the first-order absorption rate constant of drug into compartment 1, k10 is the first-order elimination rate constant from compartment 1; V is the volume of distribution of the central compartment, F is the bioavailability and k12 and k21 represent the first-order rate constants associated with the transfer of drug between compartments 1 and 2.

The first four models were selected from compiled models included in the WinNonlin pharmacokinetic model library. The last three models were written in ASCII code. Examples of relevant model commands are shown in Appendix II. Secondary parameters from these models, AUC and clearance, were derived using the equations shown in Appendix I. For the mono-exponential decline model, half-life was calculated from k10, as shown in Appendix I. In the case of the two-compartment model the relationships between the disposition rate constants, λ_1 and λ_2, and the microconstants were calculated as follows:

$$\lambda_1, \lambda_2 = \frac{1}{2}\left[(k_{12} + k_{21} + k_{10}) \pm \sqrt{(k_{12} + k_{21} + k_{10})^2 - 4\,k_{21}\,k_{10}}\right]$$

and the terminal half-life was:

$T_{1/2\,\lambda 2} = 0.693/\lambda_2$

3.4.6 PHARMACODYNAMIC RESPONSES

Diastolic blood pressure and heart rate were measured as described previously. For modelling the haemodynamic effects, the effect profiles derived on each study day were subjected to 3-point smoothing and then at each time the response of patient on placebo was subtracted from the responses measured during active treatment.

The normal cardiac cycle is triggered by an electrical impulse originating in the sinoatrial (SA) node. The electrical impulse is then transmitted to the AV node where it is delayed before being rapidly propagated through the 'Bundle of His'. It then divides in the septum between the ventricles into the right and left (bundle) branches of the 'Purkinje System'. The electrical changes associated with contraction of the heart can

be recorded in an electrocardiogram (ECG). The sinus rhythm cycle begins with a 'P' wave which corresponds to the contraction of the atria. Following an isoelectrical period (PR segment) the ventricles contract causing a large deflection of the ECG and this is called the 'QRS' complex. The 'T' wave of the ECG is caused by the return of the ventricular mass to the resting electrical state (repolarisation). Figure 3.4.6 represents a cycle from the electrocardiogram.

PQ interval - Segments and intervals between waves (P, Q, R, S, T, U) can be calculated. The PQ segment is measured from the end of the P wave to the onset of QRS, while the PQ interval includes beginning of P to the onset of Q. It corresponds to the activation of the atria. The placebo data was corrected in the same manner as described for blood pressure and heart rate.

3.4.7 PHARMACOKINETIC/PHARMACODYNAMIC RELATIONSHIPS

To take account of diurnal variations and background changes, pharmacodynamic responses were determined after subtraction of the measured responses following active drug treatment (both single dose and steady state) from the responses obtained after (single dose) placebo.

Predicted concentrations derived from the pharmacokinetic analysis were used when fitting the pharmacodynamic model, except for verapamil at steady state where the measured concentrations were used. Pharmacodynamic analyses were carried out with the weighting scheme set at 1.

Several models were assessed for relating drug concentrations to measured effects. The linear model was used when the pharmacological effect showed a direct proportionality with predicted/measured concentrations. The Emax model was used when the time course of action was characterised by a hyperbolic shape. Alternatively, the sigmoidal Emax model was used to fit to the data and the concentration-effect relationship. Detailed description of those models was given in Chapter 1 Section 1.5.2. In addition,

Figure 3.4.6 Representation of an electrocardiogram cycle

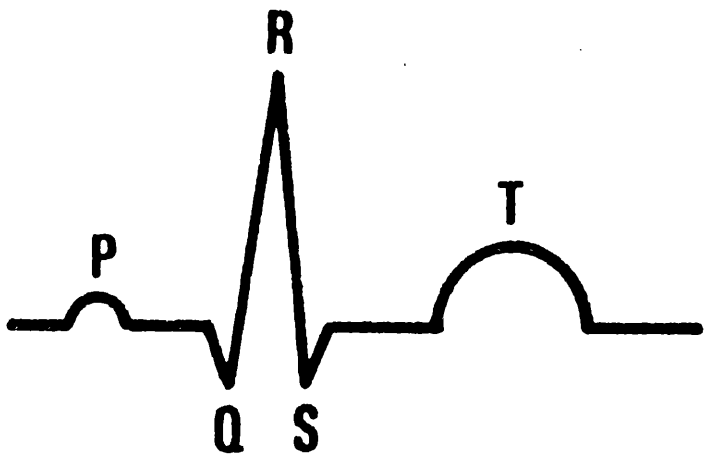

the alternative parameterization of the Emax model, proposed by Schoemaker (Schoemaker et al., 1998), was used in this analysis.

Plots of pharmacological effect against plasma concentration, with points connected in time order were used to identify hysteresis. Hysteresis was removed by incorporating a hypothetical effect compartment to the pharmacokinetic/ pharmacodynamic model. Equations describing the predicted concentration at the effect site, Y_e, are listed in Appendix I and examples of the command files used are presented in Appendix II.

The population values of pharmacokinetic and pharmacodynamic parameters were obtained by calculating the mean values and the standard deviation of the individual parameter estimates.

3.4.8 MODEL SELECTION

The criteria used to assess the adequacy of a model in describing the data included the ability of WinNonlin to produce estimates for all parameters (including standard errors and their magnitudes) and analysis of residual plots. Whenever appropriate, the goodness of fit was complemented by statistical tests, such as the general linear test or the Aikaike Information Criterion (AIC).

The precision of parameter estimates was used in the assessment of goodness of fit (Boxenbaum et al., 1974). The standard errors (SE) and the confidence intervals (CI) of the parameter estimates were used as a tool to assess the parameter estimate precision. The precision of parameter estimates was expressed in terms of coefficient of variation (cv) defined as follows:

$$CV\ (\%) = 100 * \frac{SE}{\hat{\theta}}$$

where $\hat{\theta}$ represents the parameter estimates.

WinNonlin calculates confidence intervals by two different methods, univariate and by planar limits. The confidence interval for the planar method takes into account the correlation between model parameters and was calculated by:

$$\hat{\theta} \pm \sqrt{F^{*}_{(\alpha, NP, df)} * NP * (SE)^2}$$

whereas the univariate method calculates the confidence interval without taking into consideration the correlation between parameters and was obtained from the equation:

$$\hat{\theta} \pm (t_{\alpha}, df)\ (SE)$$

where $\hat{\theta}$ represents the parameter estimate, t is the Student t-statistic, α is the probability level, p is the number of parameters, df is the degrees of freedom and F is derived from an F distribution table. DF are degrees of freedom calculated by:

$DF = N - p$

N represents the number of data points.

Correlation between parameters is an indication that there may be insufficient information in the concentration-time data to be able to determine both parameters accurately and precisely. High correlation may also manifest itself in large standard deviations and CI. The matrix of correlation coefficients provided in the WinNonlin output was inspected.

The condition number from the WinNonlin output is defined as the square root of the ratio of the largest to the smallest eigenvalue, and was used as an indication of the stability of the parameter estimates. The smaller the condition number the better the fit.

The general linear test (Boxenbaum et al., 1974) was used to evaluate the statistical significance of the change of the residual sum of squares obtained by fitting a hierarchical model with an additional parameter. The test entails calculating the ratio of the model variance F, by:

$$F = \frac{WSS_r - WSS_f}{WSS_f} * \frac{DF_f}{DF_r - DF_f}$$

where WSS_r is the weighted sums of squared deviations obtained from the model with a reduced number of parameters, WSS_f is the weighted sum of squared deviations obtained from the model with an extra parameter. The subscripts r and f represent the reduced and the full model, respectively ($DF_r > DF_f$). The significance level was set to $p < 0.05$. The calculated F was compared to the critical value derived from an F distribution table, where the numerator had ΔDF (differences in degrees of freedom between the two models) and the denominator had DF_f (degrees of freedom with the full model). If the calculated F value was less than the value from the table, the weighted sums of squared deviation from the reduced and full model were not significantly different and therefore the reduced model was selected.

The model selection process was also based upon another statistical test, the Akaike Information Criterion (AIC) (Yamaoka et al., 1978) calculated as follows:

$AIC = N \ln WSS + 2p$

where N is the number of data points, p is the number of estimated parameters, WSS is the weighted sum of squared residuals. The Schwarz Criterion (SC) can similarly be used in model selection and was calculated as follows (Schwarz, 1978):

$SC = N \ln WSS + p \ln N$

The model which best described the data was the one corresponding to the lowest values of the AIC and SC criteria. The AIC and SC were used to compare models with the same number of parameters.

The choice of the weighting scheme was based on the inspection of plots of residuals (weighted or unweighted) against fitted concentrations. The weighting which produced a random, homogeneous scatter of the residuals/weighted residuals about the abscissa axis was selected.

Parameters for the competing pharmacodynamic models were estimated for each individual. The choice between a linear and an Emax-model was made for each patient based on the precision of parameter estimates and the reduction in the sum of squared deviations. The choice between an Emax model with or without an intercept was made

for each patient using the general linear test (Ludden et al., 1994). The statistical significance of the incorporation of an effect compartment in the pharmacodynamic model was evaluated by the general linear test (Ludden et al., 1994).

3.4.9 STATISTICS

A comparison of individual pharmacokinetic/pharmacodynamic parameters was used to assess differences between treatments. Individual parameter estimates obtained for each treatment were compared with each other by parametric or non-parametric t-statistics. Paired tests were used in the case of the single-dose study as all patients received the three drugs. Unpaired tests were used for the steady state study as not all patients received each drug at steady state. For mibefradil, pharmacokinetic and pharmacodynamic parameters obtained at steady state and after a single dose were compared by a paired t-test. Only patients participating in both studies were included. Two-sided p values less than 0.05 were considered statistically significant. Statistical analyses were carried out using the statistical software, Minitab (1996b).

3.5 RESULTS I

3.5.1 PHARMACOKINETICS: SINGLE-DOSE STUDY

3.5.1.1 Mibefradil

The data set comprised 195 concentrations from 18 patients with measurements ranging from 14.5 to 1727.0 ng ml^{-1}. According to the protocol, all patients in this treatment group should have had blood samples taken up to 48 hours post-dose, but patients 4 and 6 only had blood samples collected up to 24 hours after the dose and one concentration at 3 hours for patient 3 was not available. Patient 17 had the lowest range of plasma concentrations whereas patient 11 had the widest range of measured plasma concentrations.

A mono-exponential open model with first-order input, elimination from the central compartment and a weighting scheme of $W_i = \frac{1}{\hat{Y}^2}$ best described the concentration-time data after the administration of a single dose of 150 mg of mibefradil. Secondary parameters such as time to peak (Tmax), maximum concentration (Cmax), area under the concentration-time curve (AUC), half-life ($T_{1/2}$) and clearance (CL) were derived from the equations shown in Appendix I . Table 3.5.1.a shows the individual pharmacokinetic parameters estimated from this model and Figure 3.5.1.a presents the predicted and measured concentrations against time for each individual.

The lowest estimate of V/F was 96.1 L for patient 11 which reflected a high Cmax of 1727 ng ml^{-1} measured plasma concentration. In contrast, for patient 17 the V/F estimate of 530 L corresponded to low measured plasma concentrations (Cmax 267 ng ml^{-1}). This range of volume of distribution estimates might reflect variability in both F and volume of distribution.

Figure 3.5.1.a Measured (●) and predicted (○) concentrations against time for mibefradil (single-dose study) for patients 1 to 13.

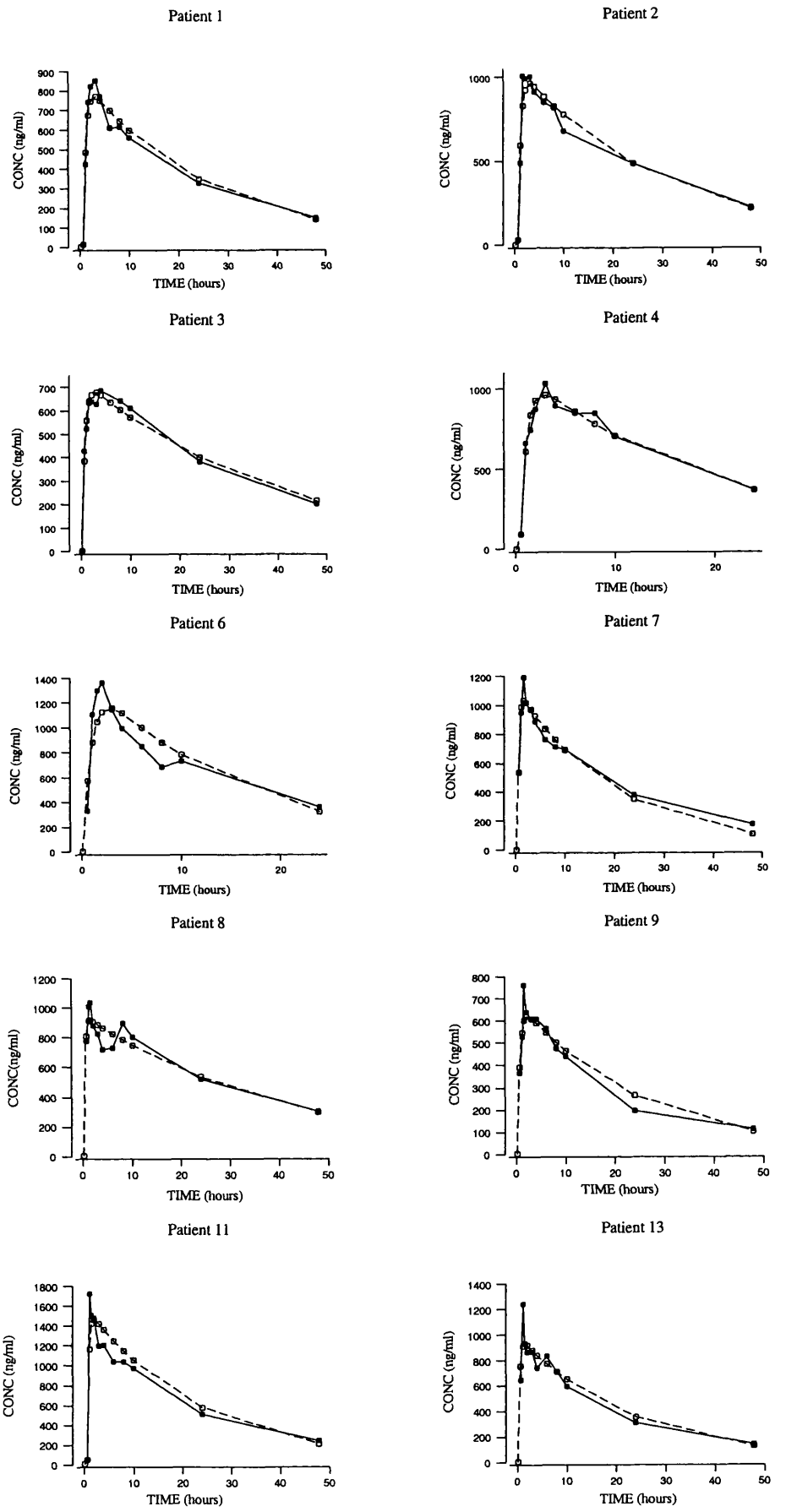

Figure 3.5.1.a (cont.) Measured (•) and predicted (○) concentrations against time for mibefradil (single-dose study) for patients 14 to 23.

Patient 14

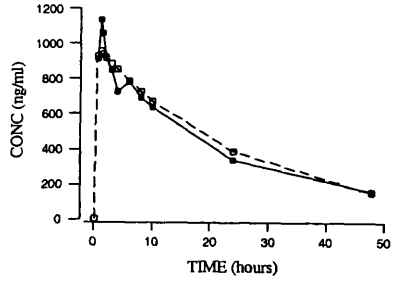

Patient 20

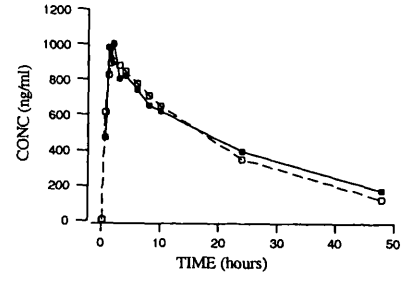

Patient 16

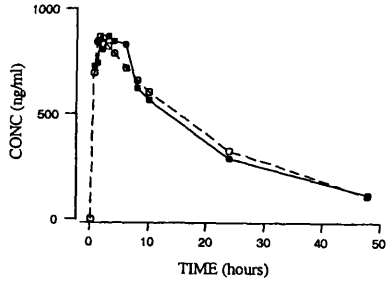

Patient 22

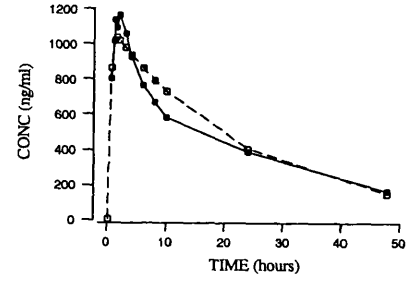

Patient 17

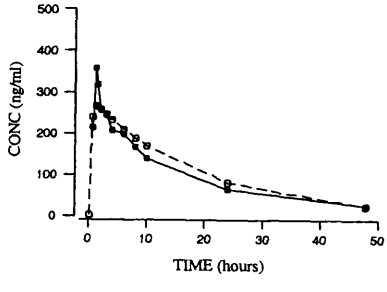

Patient 23

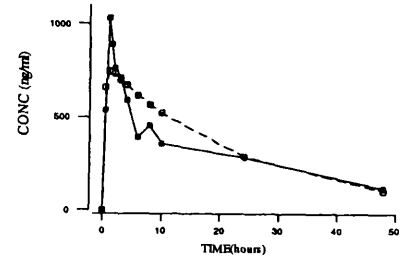

Patient 18

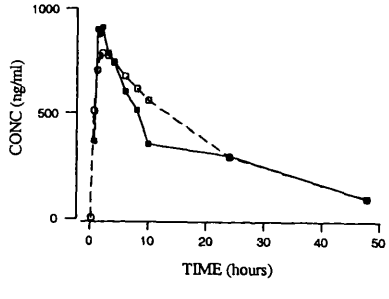

Patient 19

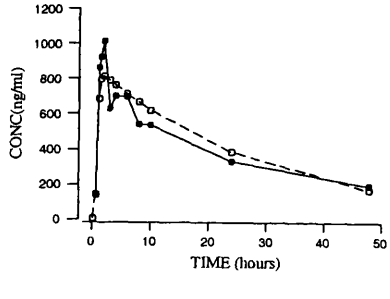

Table 3.5.1 a Individual pharmacokinetic parameter estimates of mibefradil, 150 mg (single-dose study)

ID	Model [a]	V/F (L)	cv %	k (h^{-1})	cv %	Tlag (h)	cv %	$T_{1/2}$ (h)	cv %	Tmax (h)	cv %	Cmax ($ngml^{-1}$)	cv %	R^2
1	2	179	5.1	0.0384	6.9	0.49	0.4	18.1	6.8	2.77	10.4	769	4.2	0.84
2	2	144	5.9	0.0336	9.1	0.48	0.7	20.7	9.1	2.88	12.2	960	4.9	0.82
3	1	205	3.5	0.0271	6.4			26.0	6.3	2.59	8.2	681	2.9	0.78
4	2	139	4.8	0.0469	10.1	0.44	2.1	14.8	10.1	2.80	6.3	963	3.5	0.76
6	1	109	15.1	0.0626	24.1			11.1	24.1	2.77	22.1	1155	10.2	0.68
7	2	145	4.3	0.0388	6.1	0.34	44.0	17.9	6.1	1.37	46.8	993	4.1	0.77
8	1	156	4.6	0.0248	10.6			28.0	10.5	1.33	29.3	930	4.1	0.61
9	1	221	6.4	0.0403	8.6			17.2	8.6	2.20	30.9	621	5.3	0.77
11	2	96.1	10.1	0.0433	12.6	0.49	1.0	16.0	12.6	2.01	30.5	1462	8.7	0.79
13	1	152	6.7	0.0437	8.7			15.9	8.7	1.43	66.3	929	5.9	0.75
14	1	151	4.3	0.0398	6.4			17.4	6.4	0.81	17.1	961	4.2	0.76
16	1	162	4.0	0.0446	5.1			15.6	5.0	1.48	46.8	869	3.5	0.76
17	1	530	7.4	0.0534	8.1			13.0	8.0	1.12	46.8	267	6.7	0.79
18	1	172	9.6	0.0468	11.1			14.8	11.1	2.08	25.8	793	7.9	0.77
19	2	175	9.2	0.0348	14.2	0.44	8.5	19.9	14.2	1.94	36.1	814	7.9	0.77
20	1	152	6.6	0.0372	22.0			15.5	22.0	1.96	18.2	906	4.7	0.74
22	1	137	5.4	0.0031	7.3			16.4	7.3	1.37	26.7	1037	4.7	0.77
23	1	190	10.4	0.0423	14.1			16.4	14.1	1.19	64.3	749	9.2	0.72
Mean		179		0.0390				17.4		1.89		881		
SD		93.0		0.0125				4.1		0.66		243		

Key: F represents the bioavailability; Tlag the lag time; V is the volume of distribution; $T_{1/2}$ is the elimination half-life; k the elimination rate constant; cv is the coefficient of variation; T max is the time to reach the Cmax and Cmax is the maximum concentration, R^2 coefficient of determination

[a] mono-exponential decline model with first order absorption, with or without tlag.

Mibefradil was rapidly absorbed and peak concentrations were attained at 1.9 ± 0.7 hours post dose. It was noted that points collected during the absorption phase were scarce. The inclusion of a lag time as an extra parameter in the model improved the fit for patients 1, 2, 4, 7, 11 and 19. The mean (SD) elimination rate constant was 0.0390 ± 0.0125 h^{-1}, the mean (SD) value for clearance/F was 7.4 (± 5.0) L h^{-1} and the average elimination half-life was 17.4 hours. Although the profiles suggested a bi-exponential decline for patients 18, 22 and 23, this model gave imprecise parameter estimates, with a wide cv therefore a mono-exponential decline model was chosen.

3.5.1.2 Verapamil

One hundred and eighty-seven verapamil concentrations were available from the single-dose study. Concentrations ranged from 8.9 to 1091.6 ng ml^{-1} and most patients were sampled up to 24 hours after the administration of the dose. Patients 3, 4 and 6 only had samples up to 10 hours and patients 11 and 14 had drug concentrations measured up to 48 hours after the dose.

The absorption of verapamil was rapid and best described by a zero-order process. For patients 4, 6, 7, 8, 11, 17 and 23, the first measured concentration coincided with Cmax, and it can be seen in Figure 3.5.1.b that for these individuals peak concentrations were attained within 0.5 hours after the dose, therefore no information during the absorption phase was available for modelling. The disposition followed a bi-exponential decline with elimination from the central compartment.

Predicted and measured concentrations from the best model were plotted against time and are shown in Figure 3.5.1.b. V_1/F varied within a wide range (from 168 to 823 L) with a mean value of 390 L, as shown in Table 3.5.1.b. Coefficients of variations of

Figure 3.5.1.b (cont.) Measured (•) and predicted (○) concentrations against time for verapamil (single-dose study) for patients 14 to 23

Patient 14

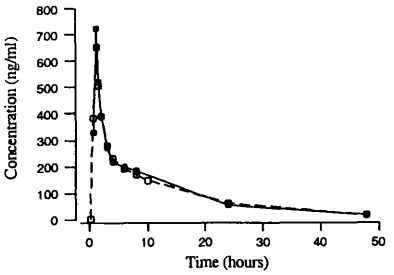

Patient 20

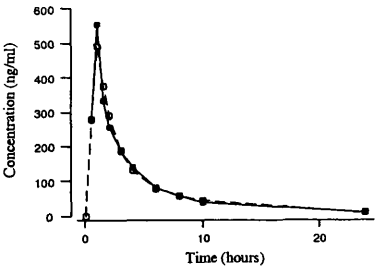

Patient 16

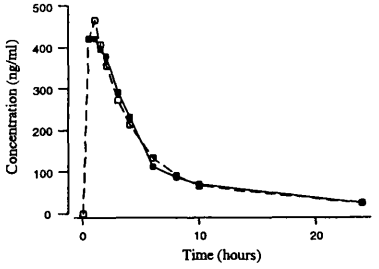

Patient 22

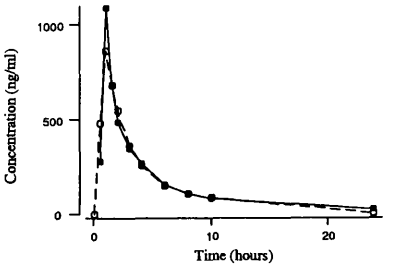

Patient 17

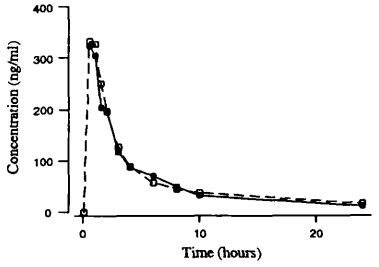

Patient 23

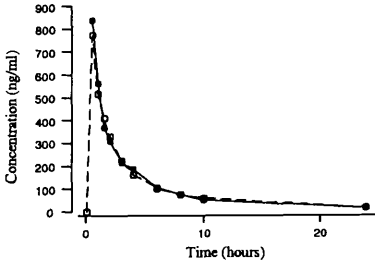

Patient 18

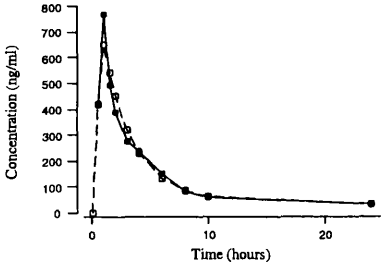

Patient 19

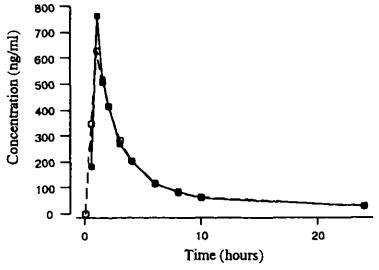

Table 3.5.1 b Individual pharmacokinetic parameter estimates of verapamil, 240 mg (single-dose study)

ID	V/F (L)	cv %	k (h^{-1})	cv %	Tabs (h)	cv %	Tlag (h)	cv %	$T_{1/2}$ (h)	R^2
1	168	4.2	0.270	4.1	0.761	4.7			7.45	0.86
2	227	41.8	0.274	25.5	1.06	33.0			9.83	0.80
3	621	24.3	0.250	280.6	1.99	31.7			10.0	0.85
4	214	*	0.492	*	0.463	*			3.24	0.93
6	341	*	0.328	*	0.325	*			4.29	0.91
7	775	*	0.250	*	0.232	*	0.29	*	11.7	0.88
8	175	*	0.260	*	0.586	*			10.5	0.84
9	446	18.4	0.191	18.2	1.00	26.5			15.0	0.83
11	823	*	0.161	*	0.141	*	0.39	*	39.4	0.89
13	500	16.4	0.220	30.9	1.00	16.7			9.3	0.85
14	250	19.6	0.191	26.7	1.04	10.8			10.9	0.84
16	427	6.8	0.173	8.5	0.634	11.4			19.5	0.82
17	500	21.1	0.276	14.8	0.632	17.6			11.9	0.94
18	301	9.8	0.191	13.8	0.874	14.6			26.1	0.85
19	313	17.9	0.238	14.5	1.00	24.3			13.9	0.86
20	376	18.5	0.337	17.2	1.00	10.1			6.47	0.88
22	221	18.2	0.285	14.3	1.00	25.3			8.99	0.86
23	337	*	0.250	*	0.231	*	0.31	*	12.3	0.90
Mean	390		0.258		0.77				12.8	
SD	194		0.076		0.44				8.48	

Key: F represents the bioavailability; Tlag the lag time; V is the volume of distribution; $T_{1/2}$ is the elimination half-life; k the elimination rate constant; cv is the coefficient of variation; and Tabs is the time taken for the drug to be absorbed.

** Not estimated*

the parameter estimates were not estimated for patients 4, 6, 7, 8, 11 and 23. However the addition of a Tlag to the model further improved the fit for patients 7, 11, and 23. The mean estimate for clearance/F for verapamil was 95.2 (± 41.9) L h^{-1}.

3.5.1.3 *Diltiazem*

Two hundred and one concentrations were available from the single-dose study for analysis of diltiazem. Drug concentrations ranged from 2.2 to 1371.0 ng ml^{-1} and were measured up to 48 hours in most patients, but patients 3, 4 and 19 had the last measurement taken at 24 hours post dose. Patient 8 had only nine samples available, the last being taken 10 hours post dose. The diltiazem disposition was similar to that of verapamil, and was most appropriately described by a model with a zero-order absorption process and bi-exponential elimination. The weighting scheme was $\frac{1}{\hat{Y}^2}$ as before. The pharmacokinetic parameter estimates for diltiazem are shown in Table 3.5.1.c and Figure 3.5.1.c shows the measured and predicted concentration-time profiles for each individual. Rapid absorption and lack of data points for patients 7, 20 and 23 led to peak drug concentrations being reached within 0.5 hours, therefore there was no information available to fully characterise the absorption phase. The average time taken to reach the maximum concentration (Tabs) was 1.08 ± 0.74 hours. For patient 16, the Tmax occurred 3 hours post dose. Although the zero-order absorption model was the best model, it was not always able to predict the peak plasma concentration.

The mean V_1/F estimate was 320 ± 154 L (620 L for patient 20 and 708 L for patient 23).

Figure 3.5.1.c Measured (•) and predicted (○) concentrations against time for diltiazem (single-dose study) for patients 1 to 13

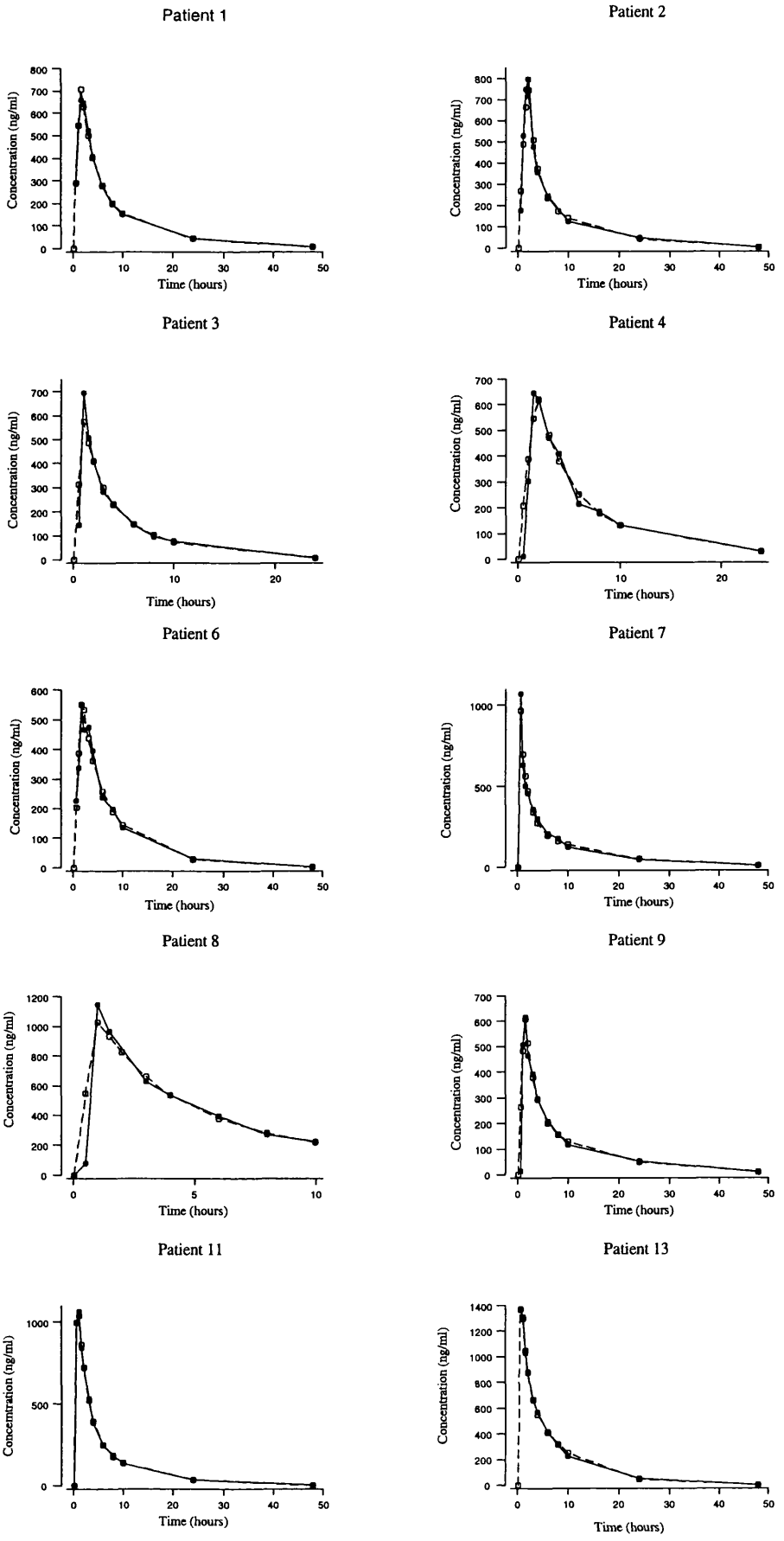

Figure 3.5.1.c (cont.) Measured (•) and predicted (o) concentrations against time for diltiazem (single-dose study) for patients 14 to 23

.

Patient 14

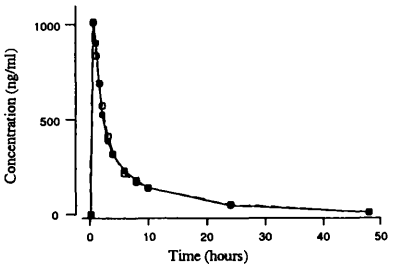

Patient 16

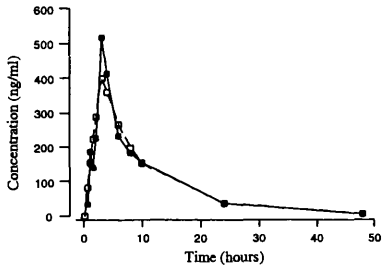

Patient 17

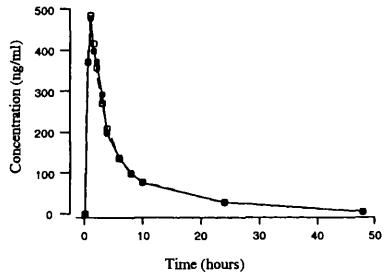

Patient 18

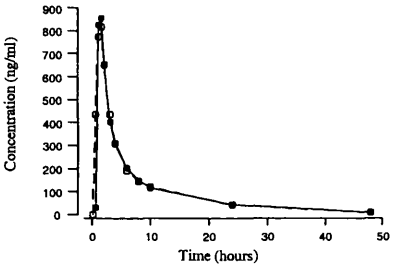

Patient 19

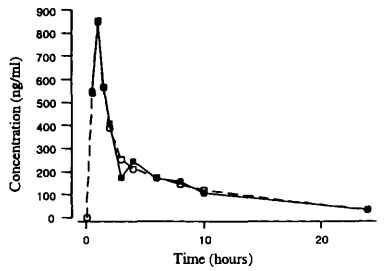

Patient 20

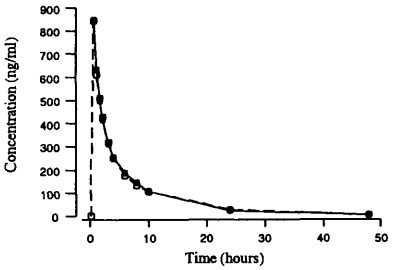

Patient 22

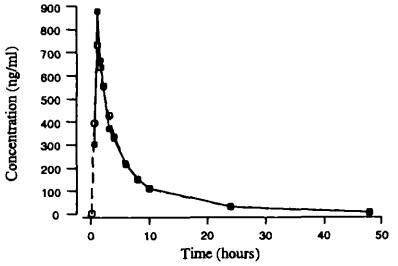

Patient 23

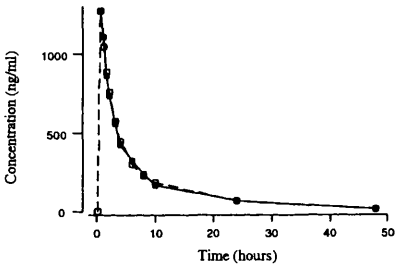

Table 3.5.1 c Individual pharmacokinetic parameter estimates of diltiazem, 240 mg (single-dose study)

ID	V/F (L)	cv %	k (h^{-1})	cv %	Tabs (h)	cv %	Tlag (h)	$T_{1/2}$ (h)	R^2
1	281	16.0	0.165	21.6	1.39	6.7		9.23	0.91
2	212	31.1	0.232	22.8	1.88	35.7		8.40	0.85
3	344	20.8	0.262	20.3	1.01	27.6		4.58	0.84
4	296	47.6	0.191	34.4	1.83	62.3		7.14	0.83
6	350	7.8	0.162	7.4	1.60	9.1		6.48	0.89
7	383	*	0.212	*	0.291	*	0.21	19.5	0.93
8	256	*	0.168	*	0.802	*	0.37	27.4	0.98
9	300	32.1	0.172	26.3	1.39	36.9		10.9	0.87
11	178	3.1	0.240	2.7	0.61	3.9		8.05	0.99
13	129	5.7	0.238	5.4	0.59	10.8		5.73	0.93
14	209	10.9	0.210	9.9	0.51	12.7		10.1	0.93
16	451	25.9	0.132	25.7	3.15	27.2		9.45	0.88
17	406	4.3	0.189	3.9	0.741	6.0		10.8	0.92
18	195	26.4	0.258	31.9	1.25	31.5		9.59	0.87
19	156	28.6	0.397	17.9	1.06	17.4		7.50	0.87
20	620	*	0.234	*	0.21	*	0.29	7.26	0.94
22	286	10.2	0.199	8.6	0.994	12.9		9.24	0.92
23	708	*	0.201	*	0.12	*	0.43	10.2	0.93
Mean	320		0.215		1.08			10.1	
SD	154		0.058		0.74			5.34	

Key: F represents the bioavailability; Tlag the lag time; V is the volume of distribution; $T_{1/2}$ is the elimination half-life; k the elimination rate constant; cv is the coefficient of variation, and Tabs is the time taken for the drug to be absorbed.

** Not estimated*

3.5.2 PHARMACOKINETICS: STEADY-STATE STUDY

3.5.2.1 Mibefradil

One hundred and thirteen steady-state mibefradil concentrations were available for analysis. The range of drug concentrations was 61.9 ng ml^{-1} to 1421.0 ng ml^{-1}. Patient 17 had the lowest range of plasma concentrations after steady- state dose.
The pharmacokinetics of mibefradil at steady state were best described by a mono-exponential decline with first-order absorption and the weighting scheme was the same as described for the single-dose study. Table 3.5.2 contains the individual pharmacokinetic parameter estimates obtained from this model. The mean V/F estimate was 259 ± 94 L and ranged from 148 L to 438 L. The mean elimination rate constant was 0.0282 ± 0.0127 h^{-1}, which is smaller than after the single dose. At steady state the mibefradil elimination half-life was 28.1 hours, which is longer than after the single dose (17.4 hours). Plots of predicted and measured concentrations against time are shown in Figure 3.5.2.a.

3.5.2.2 Verapamil

After multiple doses of verapamil SR 240 mg, plasma concentrations ranged from 16.1 to 1015.5 ng ml^{-1}. Seventy-eighty concentrations were available. Individual plots of measured concentration against time are shown in Figure 3.5.2.b and showed a slow absorption. As these profiles were difficult to model, the measured concentrations were used in the pharmacodynamic model.

Figure 3.5.2.a Measured (•) and predicted (o) concentrations against time for mibefradil (steady-state study)

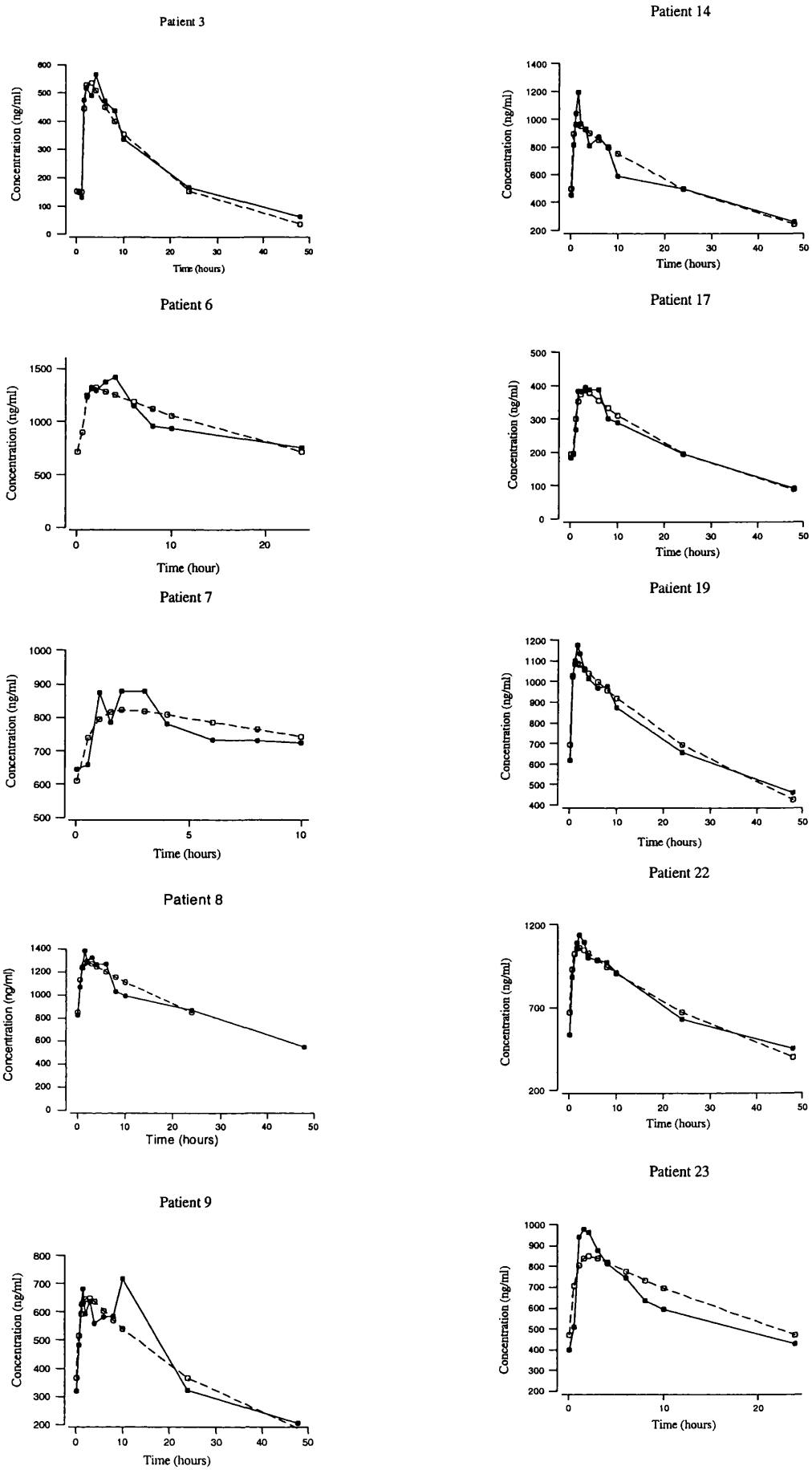

Figure 3.5.2.b Measured concentrations against time for verapamil (steady-state study)

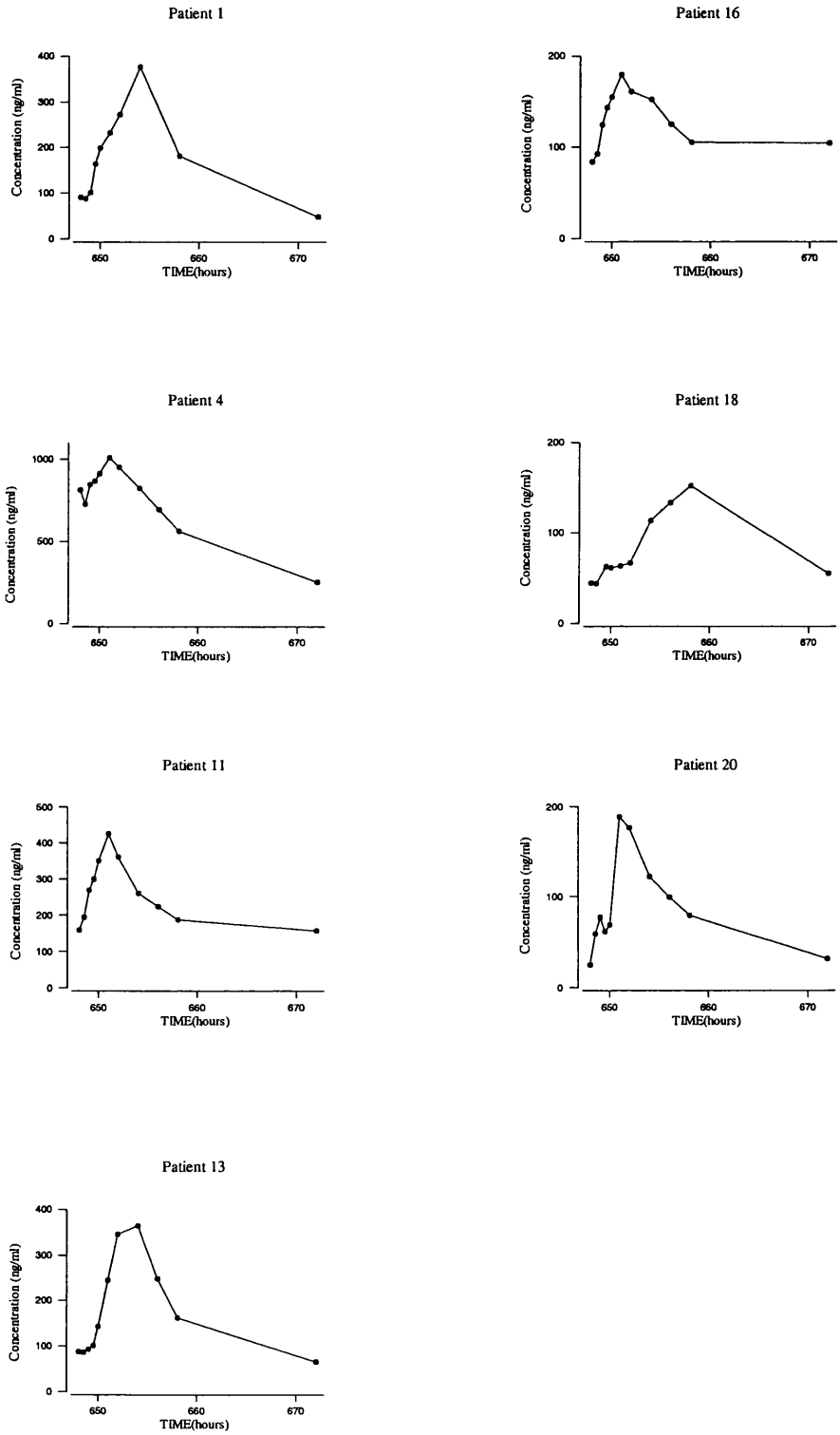

Table 3.5.2 Individual pharmacokinetic parameter estimates of mibefradil, 100 mg (multiple-dose study)

ID	MODEL[a]	V/F (L)	cv %	K (h^{-1})	cv %	Tlag (h)	cv %	$T_{1/2}$ (h)	cv %	Tmax (h)	cv %	Cmax ($ngml^{-1}$)	cv %
3	2	220	19.7	0.0603	20.5	0.99	6.8	11.5	20.5	2.63	30.4	412	16.4
6	2	148	22.5	0.0281	22.4	0.38	*	24.6	22.4	2.03	133.1	646	17.9
7	1	407	29.0	0.0142	30.5			48.7	30.5	2.95	47.1	235	27.5
8	1	203	8.9	0.0190	8.2			36.1	8.2	2.57	30.3	469	8.0
9	1	290	20.8	0.0282	22.1			24.5	22.0	3.13	36.3	316	18.3
14	1	197	10.7	0.0295	9.6			23.5	9.6	1.47	57.4	516	14.3
17	2	438	7.2	0.0331	6.0	0.49	11.2	20.9	6.0	3.33	16.5	207	6.1
19	1	233	7.1	0.0202	6.8			34.4	6.8	1.58	38.6	416	6.6
22	1	225	11.0	0.0214	10.1			32.3	10.1	2.45	43.1	415	10.2
23	1	228	15.9	0.0277	14.0			25.0	13.9	2.56	49.9	406	13.9
MEAN		**259**		**0.0282**				**28.1**		**2.47**		**404**	
SD		**94**		**0.0127**				**10.2**		**0.62**		**129**	

Key: F represents the bioavailability; Tlag the lag time; V is the volume of distribution; $T_{1/2}$ is the elimination half-life; k the elimination rate constant; cv is the coefficient of variation; Tmax is the time taken to reach Cmax; Cmax is the maximum concentration.

*Not estimated

[a] mono-exponential decline model with first-order absorption, with (1) or without tlag (2)...

3.6 RESULTS II

The mean values for changes of peaks and troughs in diastolic blood pressure, heart rate and PQ interval for mibefradil, verapamil and diltiazem are shown in Table 3.6.

3.6.1 PHARMACODYNAMICS: SINGLE-DOSE STUDY

The mean values for changes in diastolic blood pressure, heart rate and PQ interval with time after single doses of mibefradil, verapamil and diltiazem are represented in Figures 3.6.1a and 3.6.1.b and 3.6.1.c, respectively.

3.6.1.1 Mibefradil

Pharmacodynamic data available for analysis after the administration of a single dose of mibefradil 150 mg comprised data from 18 patients and contained 198 measurements (11 per patient) for each pharmacodynamic endpoint. Typical examples of the time-course of action for the placebo-subtracted changes in diastolic blood pressure (DBP), heart rate (HR) and PQ interval are illustrated in Figure 3.6.1.d.

Blood Pressure - The DBP decreased by 10-19 mmHg with the maximum effect occurring between 1.5 to 3 hours post dose. In patients 8 and 23 the peak effect occurred earlier, at 1 hour post dose. In patient 3 the peak effect was delayed to 3 hours after the dose and was associated with a drop in blood pressure of only 10 mmHg. The most accentuated drop in DBP, 19 mmHg, occurred in patient 18. Twenty-four hours after the dose, the DBP measurements had not returned to the placebo values.

Figure 3.6.1.a Mean values (SD) for changes in DBP, HR and PQ interval after a single dose of mibefradil (150 mg)

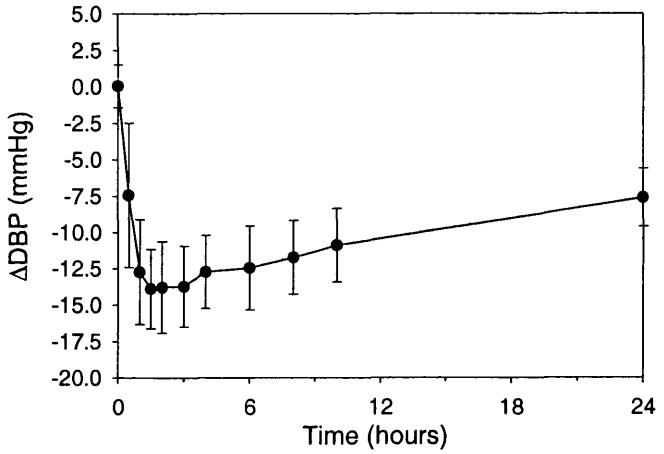

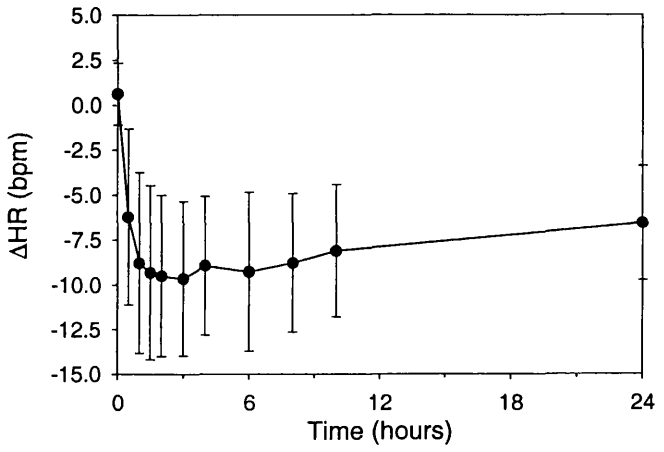

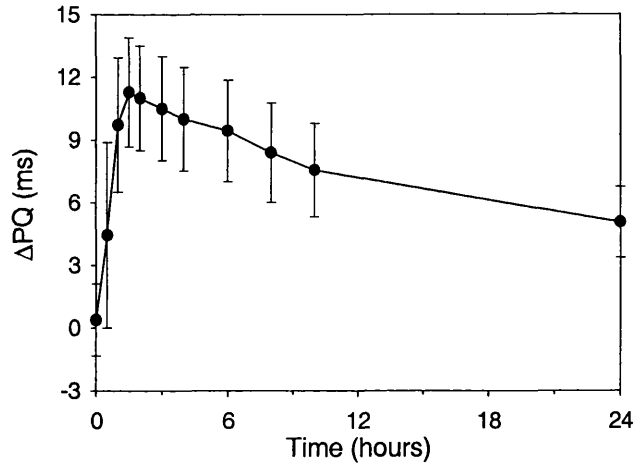

Figure 3.6.1.b Mean values (and SD) for changes in DBP, HR and PQ interval after a single dose of verapamil (240 mg)

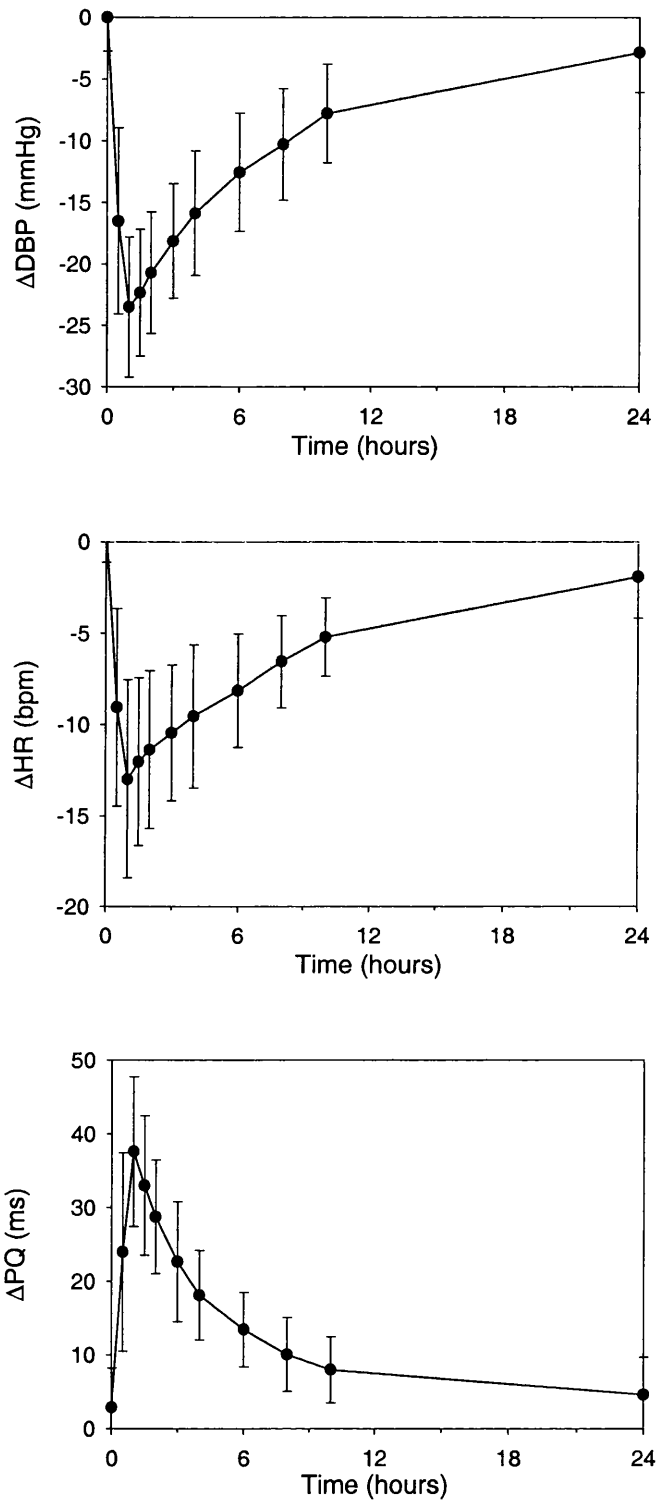

Figure 3.6.1.c Mean values (SD) for changes in DBP, HR and PQ interval after a single dose of diltiazem (240 mg)

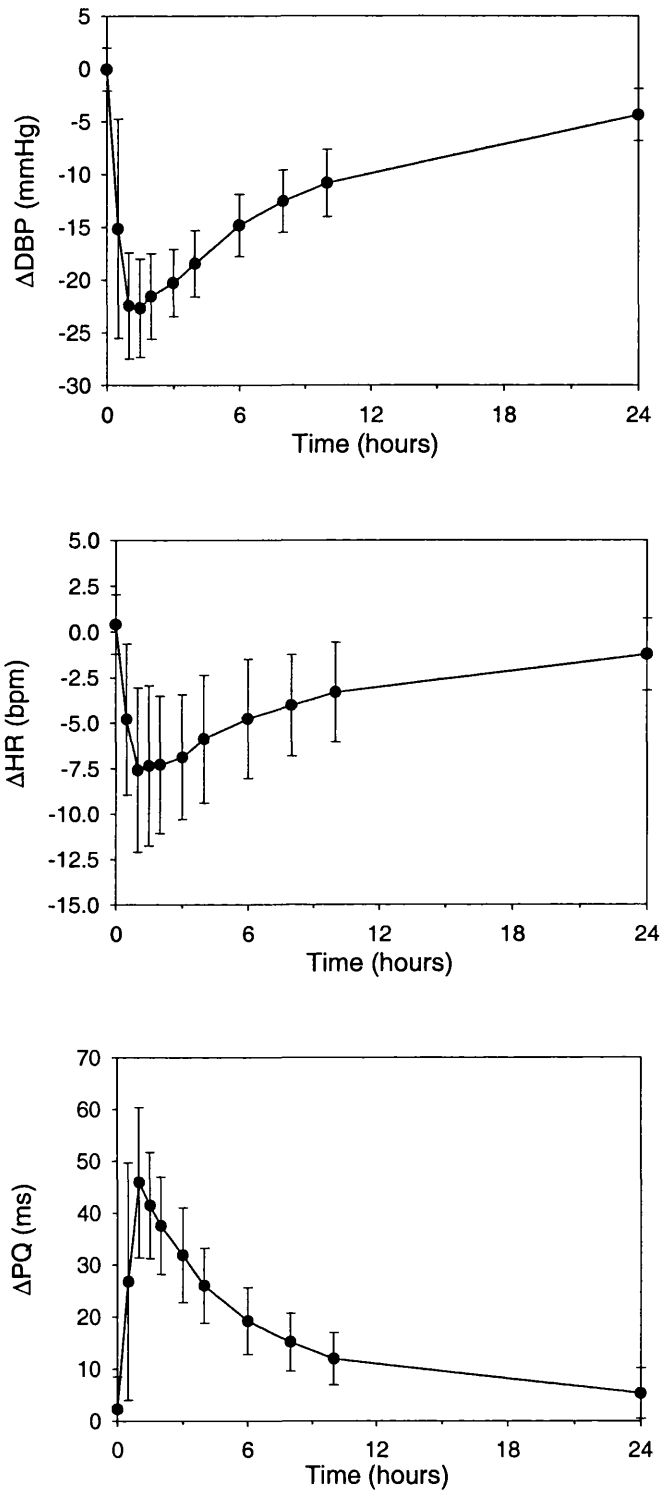

Figure 3.6.1.d Typical examples of the time-course of action for DBP (solid line and close circles), HR (broken line and open circles) and PQ interval after a single dose of mibefradil (150 mg)

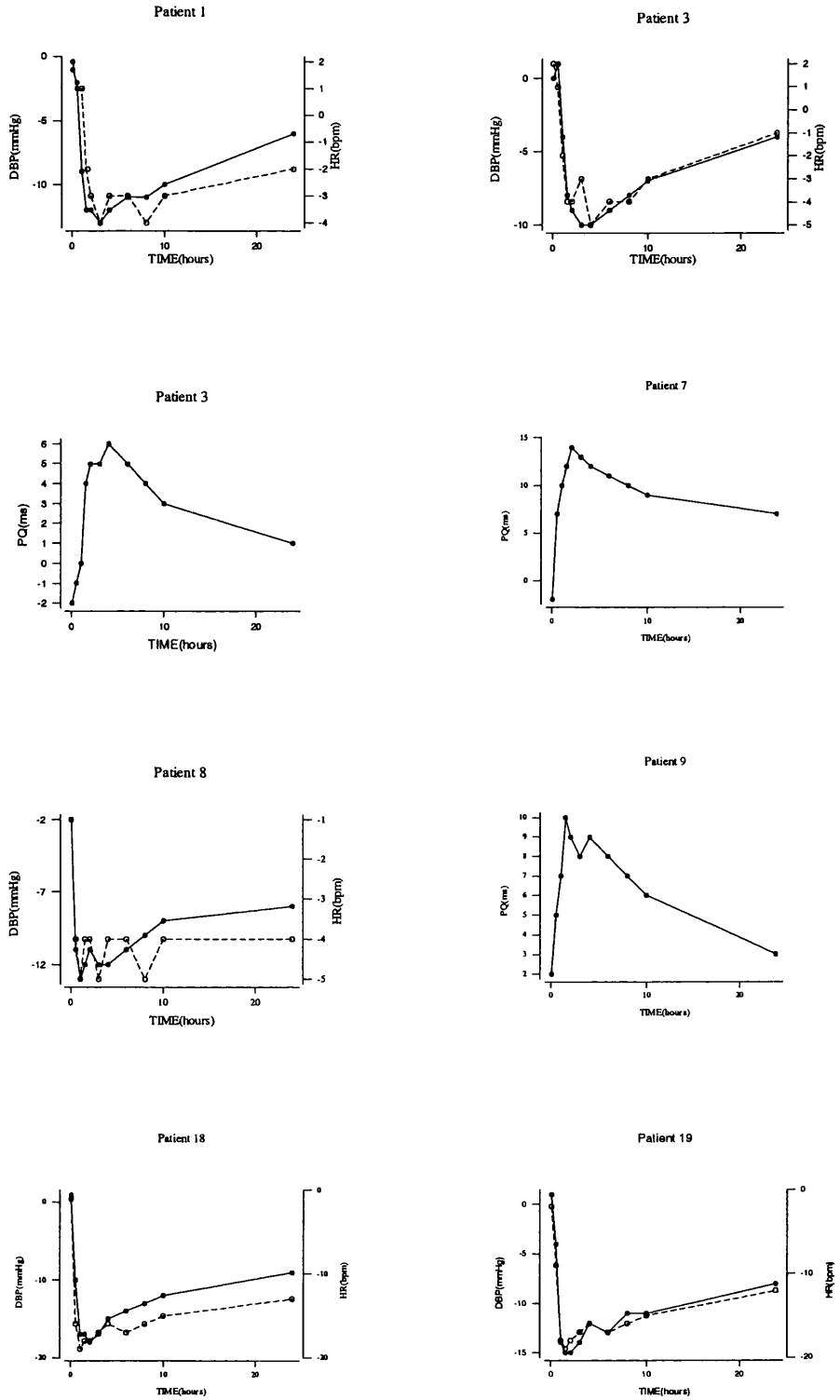

Table 3.6 The mean placebo corrected effects of mibefradil, verapamil and diltiazem after single dose and at steady state

	MIBEFRADIL		VERAPAMIL		DILTIAZEM	
	Peak	**Trough**	**Peak**	**Trough**	**Peak**	**Trough**
Single dose	(n=18)		(n=18)		(n=18)	
DBP (mmHg)	-15 ± 3	-8 ± 2	-26 ± 5	-3 ± 3	-27 ± 3	-4 ± 2
HR (bpm)	-11 ± 4	-7 ± 3	-15 ± 5	-2 ± 2	-9 ± 4	-1 ± 2
PQ interval (msec)	12 ± 2	5 ± 2	42 ± 8	4 ± 5	52 ± 10	5 ±5
Steady state	(n=10)		(n=7)			
DBP (mmHg)	-15 ± 3	-11 ± 3	-21 ± 4	-10 ± 3		
HR (bpm)	-11 ± 5	-8 ± 4	-14 ± 4	-7 ± 3		
PQ interval (msec)	11 ± 2	7 ± 2	25 ± 10	9 ± 4		

Data are mean values ± SD

Key:DBP represents diastolic blood pressure and HR represents heart rate

Heart Rate - It can be seen from Figure 3.6.1.d, that the changes in HR were small and therefore the profile was nearly flat. Patients 1 and 8 had more than one peak effect. The maximum effect occurred between 1 to 3 hours after the dose. Patients 18 and 19 had the greatest fall in heart rate, of 17 bpm. Heart rate started to return to normal values 8-10 hours after the dose, but by 24 hours post dose it had not yet returned to placebo values.

PQ interval - The PQ interval increased during the first hours after dosing, with the maximum effect occurring between 1.5 and 4 hours. The increase in PQ interval ranged from 8 msec for patients 3 and 9 to 16 msec for patient 7. After the peak effect, the extent of the PQ prolongation started to decrease slowly, although again it was sustained for more than 24 hours.

3.6.1.2 Verapamil

The data set contained information collected from 18 patients who had received verapamil 240 mg. Each patient had 11 measurements for each pharmacodynamic endpoint. Typical profiles for the time-course of action for the placebo-subtracted changes in DBP, HR, and PQ interval are represented in Figure 3.6.1.e.

Blood Pressure – The peak effect of verapamil on DBP occurred 1 hour after the administration of the dose for most patients, although it occurred at 2 hours in patient 3, as shown in Figure 3.6.1.e. The fall in DBP ranged from 22 (patient 7) to 37 mmHg (patient 6). Twenty-four hours post-dose the DBP values were close to placebo values for all patients.

Heart Rate - The change in HR was pronounced (Figure 3.6.1.e) with the maximum effect ranging from 7 bpm (for patient 1) to 26 bpm (for patients 9 and 18). The peak effect was generally achieved between 0.5 to 1 hours. Only patient 3 had the maximum effect delayed to 2 hours post dose. Twenty-four hours after the dose the heart rate values were similar to placebo values.

Figure 3.6.1.e Typical examples of the time-course of action for DBP (solid line and close circles), HR (broken line and open circles) and PQ interval after a single dose of verapamil (240 mg)

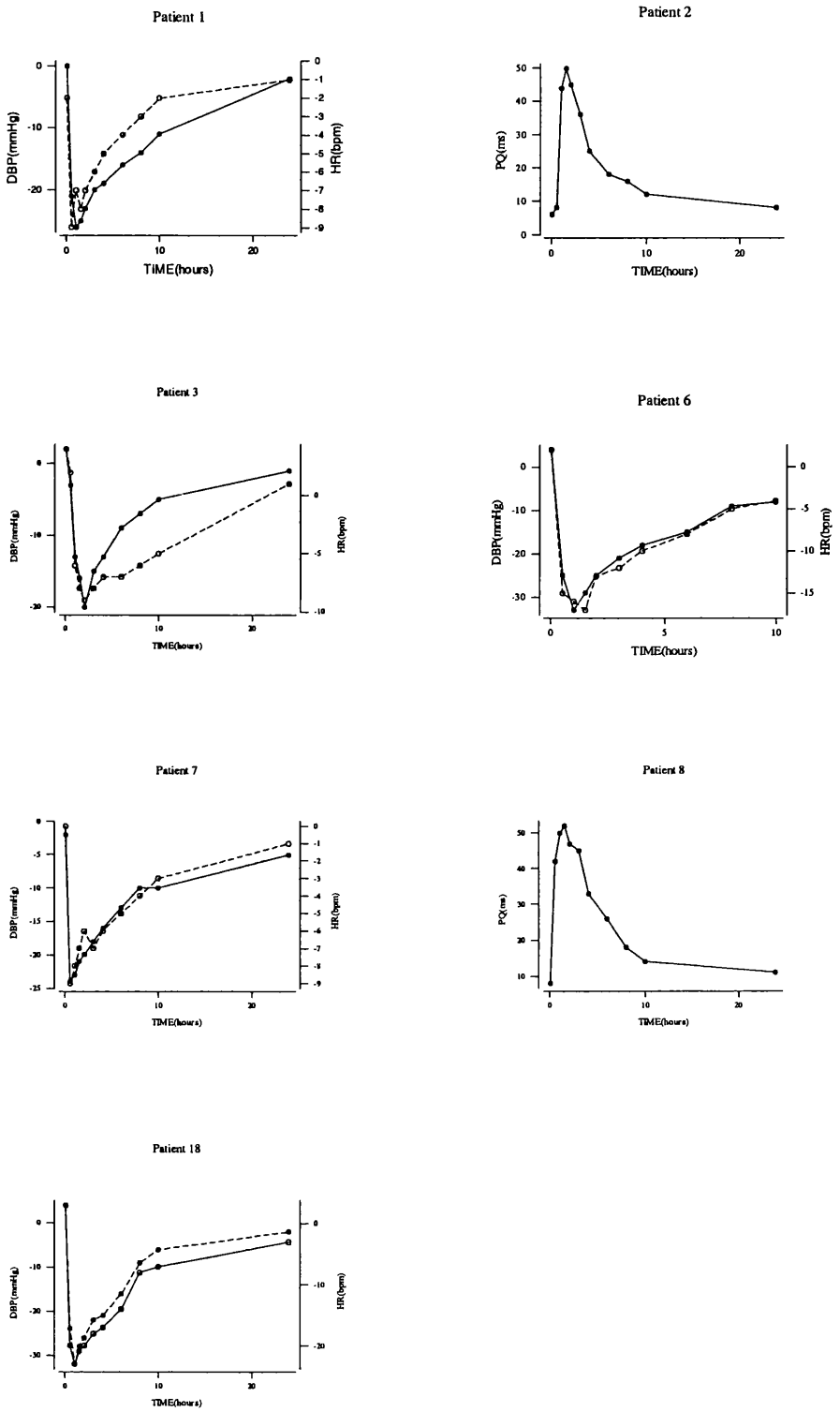

PQ interval - The maximum effect for PQ interval was attained between 0.5 and 1 hour in most patients. For patients 2 and 8 the maximum effect occurred 1.5 hours after the dose and for patient 3 at 2 hours after the dose. The PQ changes varied from 24 msec to 52 msec.

3.6.1.3 Diltiazem

Eighteen patients received 240 mg of diltiazem and each had 11 measurements for analysis. Figure 3.6.1.f shows typical effect-time profiles for DBP, HR and PQ interval.

Blood Pressure – The maximum decrease in DBP was reached at 1.5 – 2 hours after the dose, apart from patient 16 in whom the maximum effect occurred 3 hours after the dose. The reduction in DBP varied from 20 (for patient 17) to 31 mmHg (for patient 14). The DBP values had returned to the placebo values by 24 hours post dose.

Heart Rate - The reduction in heart rate ranged from 5 bpm to 17 bpm. Maximum changes in HR occurred 1-2 hours post dose, except for patient 16 in whom the peak was delayed and occurred 3 hours post dose. After 24 hours HR had returned to placebo values.

PQ interval - For most patients the maximum effect or PQ interval occurred within 1 to 2 hours, apart from patients 2 and 16 who had the peak effect at 3 hours after the dose. The increases were marked and ranged from 33 to 66 msec, as shown in Figure 3.6.1.f.

Figure 3.6.1.f Time-course of action for DBP (solid line and close circles), HR (broken line and open circles) and PQ interval after a single dose of diltiazem (240mg)

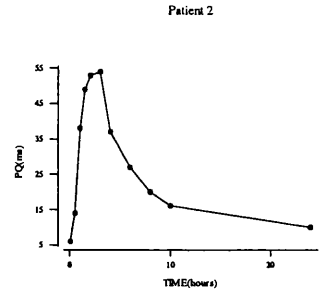

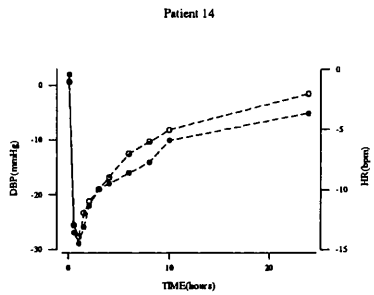

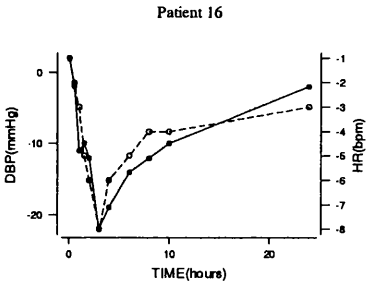

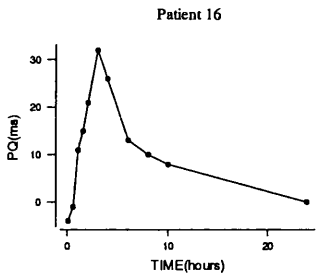

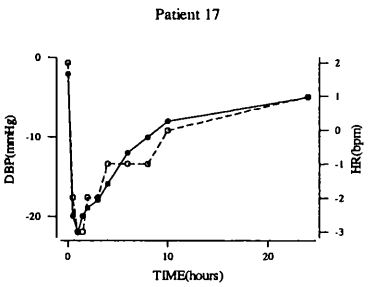

3.6.2 PHARMACODYNAMICS: STEADY-STATE STUDY

The mean values for changes in DBP, HR and PQ interval after multiple doses of mibefradil (100 mg) and verapamil SR (240 mg) are represented in Figure 3.6.2.a and Figure 3.6.2.b, respectively.

3.6.2.1 Mibefradil

One hundred and ten measurements for each pharmacodynamic endpoint were available from 10 patients who had multiple doses of 100 mg mibefradil. Figure 3.6.2.c shows the time-course of action of DBP, HR and PQ interval.

Blood Pressure - For DBP the peak effect was reached after 1.5 to 2 hours, with the exception of patient 17 in whom the peak effect was reached 6 hours after the dose. The peak effect was not marked, with a fall in DBP of only 3-6 mmHg. DBP at time 0 ranged between -3 to -2. After 48 hours it ranged from -11 to -4 mmHg.

Heart Rate - The peak effect for changes in heart rate occurred within 1 to 2 hours after the dose. For all patients the time course of action was sustained with changes of 6 bpm, and the profile was relatively flat, as shown in Figure 3.6.2.d. The placebo-subtracted values of HR at time 0 varied between –2 to 2 bpm whereas at 48 hours it ranged from –13 to –2 bpm.

PQ interval - PQ interval was prolonged for 3 to 5 msec and the peak effect occurred 1.5 to 3 hours after the dose. At time 0 the placebo subtracted PQ interval values ranged from -3 to 20 msec and after 48h were between 1 and 7 msec.

Figure 3.6.2.a Mean values (and SD) for changes in DBP, HR and PQ interval after multiple doses of mibefradil (100 mg)

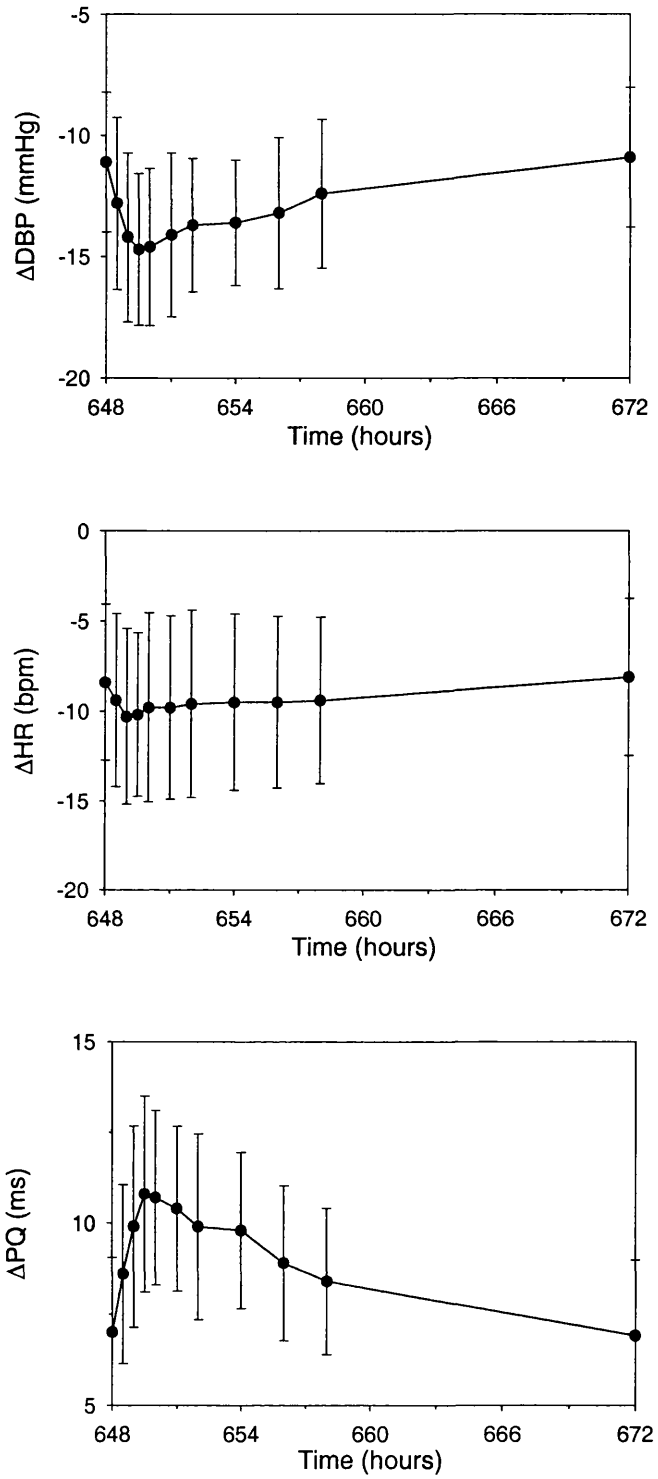

Figure 3.6.2.b Mean values (and SD) for changes in DBP, HR and PQ interval after multiple doses of verapamil (240 mg)

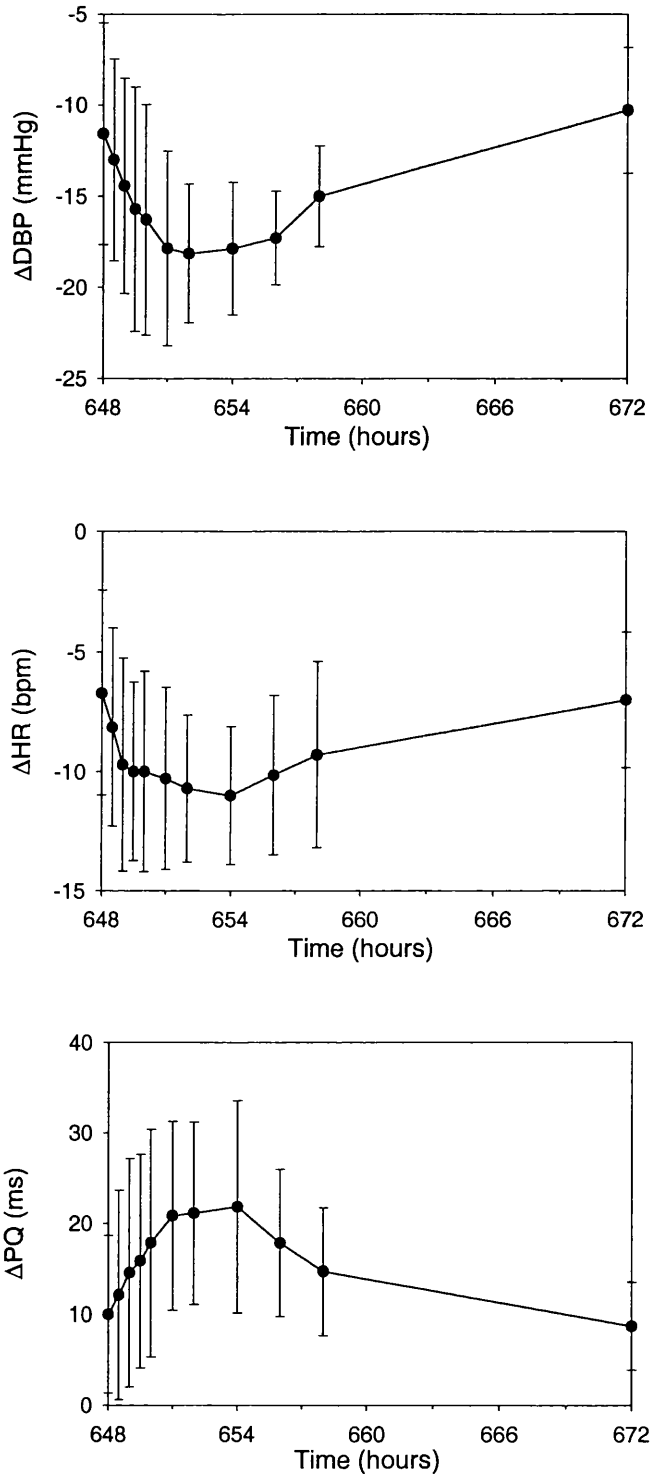

Figure 3.6.2.c Time-course of action for changes in DBP (solid line, close circles), HR (broken line, open circles) and PQ interval after multiple doses of mibefradil (100 mg)

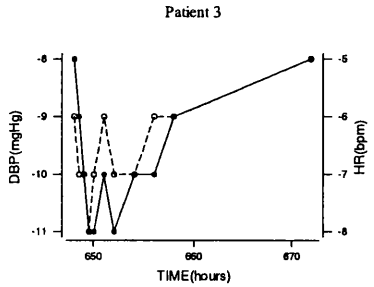

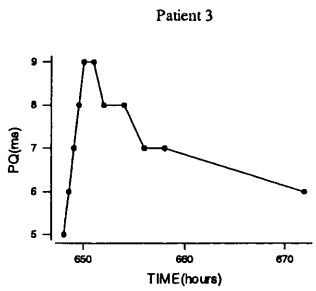

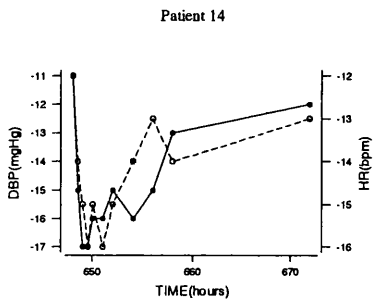

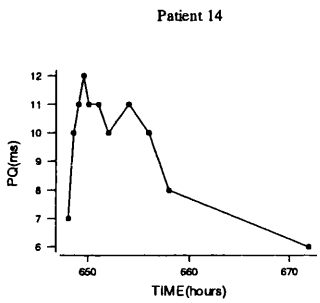

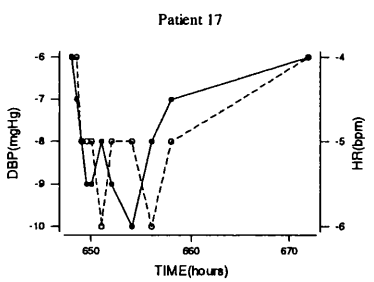

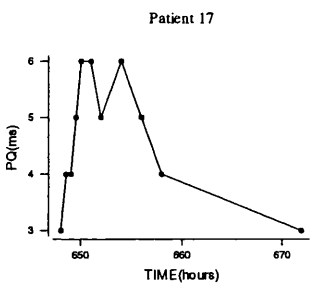

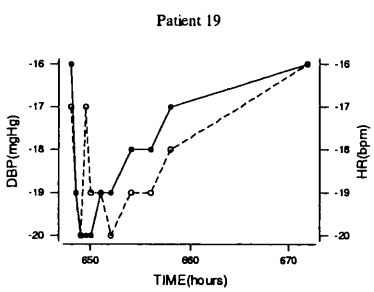

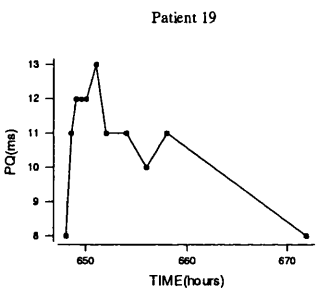

Figure 3.6.2.d Time-course of action for changes in DBP (solid line, close circles), HR (broken line, open circles) and PQ interval after multiple doses of verapamil SR (240 mg)

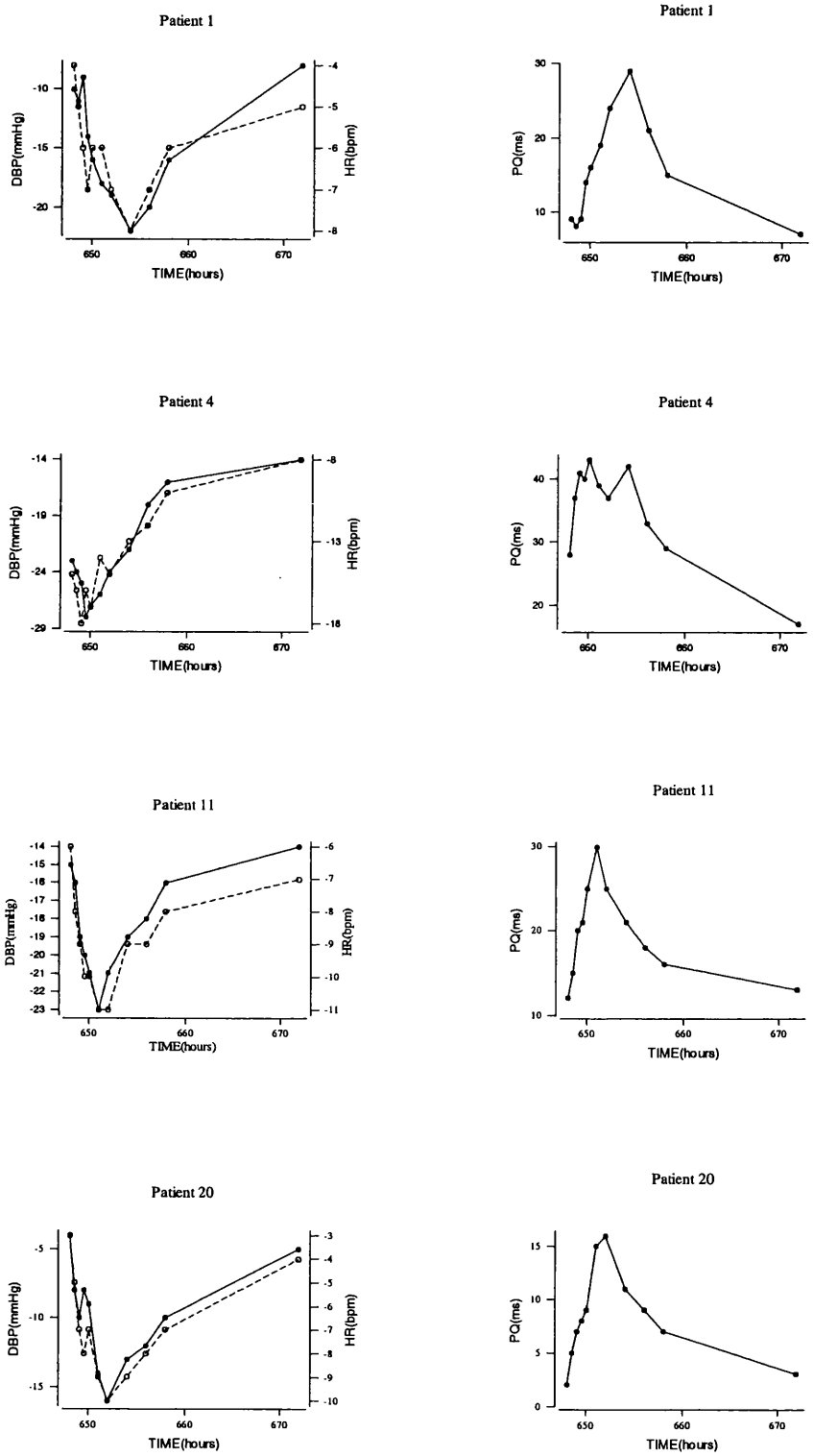

3.6.2.2 Verapamil

Each of the 7 patients who were enrolled in the study had 11 measurements recorded for each pharmacodynamic endpoint after the administration of multiple doses of verapamil SR 240 mg. Figure 3.6.2.d shows the time-course of action for changes in DBP, HR and PQ interval.

Blood Pressure - At steady state the peak changes in DBP varied from 5 (patient 4) to 12 mmHg (patients 1 and 20). The peak effect generally occurred between 3 and 10 hours after the last dose but occurred 1.5 hours after the last dose in patient 4. At time zero the placebo-corrected values of blood pressure varied from –23 to –4 mmHg but 10 hours later they ranged from –19 to –10 mmHg.

Heart Rate - The maximum reduction in HR for verapamil varied from 3 hours (patient 4) to 10 hours (patient 18) post dose. The peak effect for patient 4 occurred at 1 hour after the dose, for the remaining patients it occurred from 3 to 10 hours after the dose. The values of HR at time 0 was –15 to –3 bpm 10 hours later they ranged from –17 to –7 bpm.

PQ interval - PQ interval was prolonged by 6 msec for patient 16; in contrast, for patient 1 it was prolonged by 20 msec. The peak occurred between 3 to 6 hours, except for patient 4. The placebo corrected PQ interval at time 0 varied from 2 to 28 msec and at 10 hours it ranged from 7-29 msec.

3.7 RESULTS III

3.7.1 PHARMACOKINETIC/PHARMACODYNAMIC RELATIONSHIPS: SINGLE-DOSE STUDY

3.7.1.1 Mibefradil

Blood Pressure - The existence of hysteresis was checked by inspection of the plots of the reductions in DBP against predicted concentrations in individual patients and is shown in Figure 3.7.1.a. Visual inspection of curves showed that hysteresis could be excluded and the data from most subjects appeared to correspond to Emax-type behaviour. There were no consistent indications of a sigmoidal Emax-type concentration-effect relationship and this was ultimately confirmed by the fact that the n values were not statistically different from 1. The suitability of the linear and Emax models was compared and the results are shown in Table 3.7.1.a. Aikaike information criterion (AIC) values obtained from the Emax model were smaller for most patients than the ones obtained from linear model, although the difference was negligible. The Emax model was considered superior to the linear model. The Emax model re-parameterized in terms of S0 parameter was used to avoid correlation between Emax and EC50. The coefficient of variation for EC50 from the model from patient 9 was 89.7%, whereas the S0 parameter was associated with a cv of 34.8%.

As illustrated, only patient 17 had a very high decrease of AIC and therefore an effect compartment was included in the pharmacodynamic model of this patient. Figure 3.7.1.b shows the predicted and measured effects against time obtained with the S0 model (or S0 model with effect compartment).

Figure 3.7.1.a Decrease in diastolic blood pressure against predicted concentrations of mibefradil (single-dose study) for patients 1 to 13

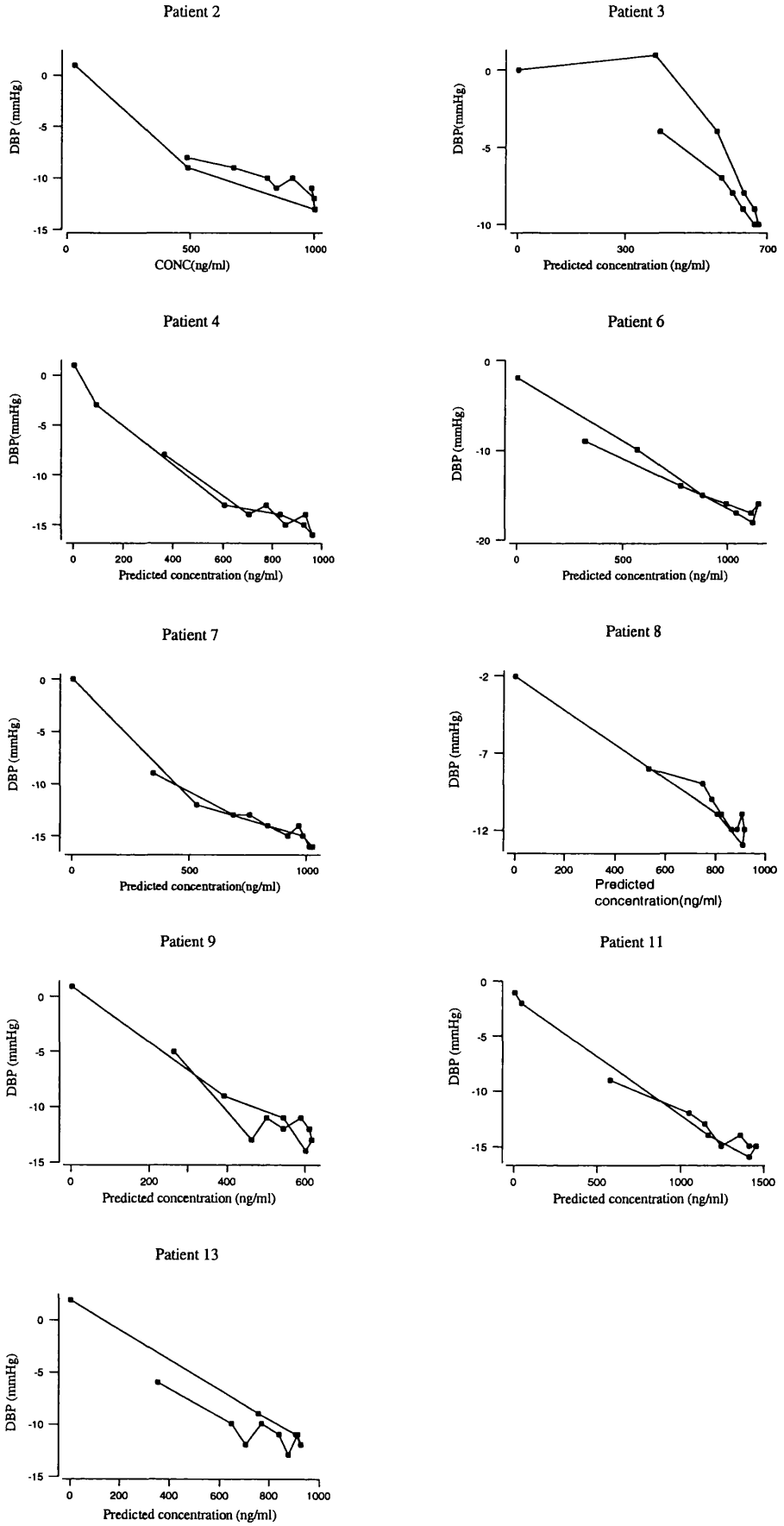

Figure 3.7.1.a (cont.) Decrease in diastolic blood pressure against predicted concentrations of mibefradil (single-dose study) for patients 14 to 23

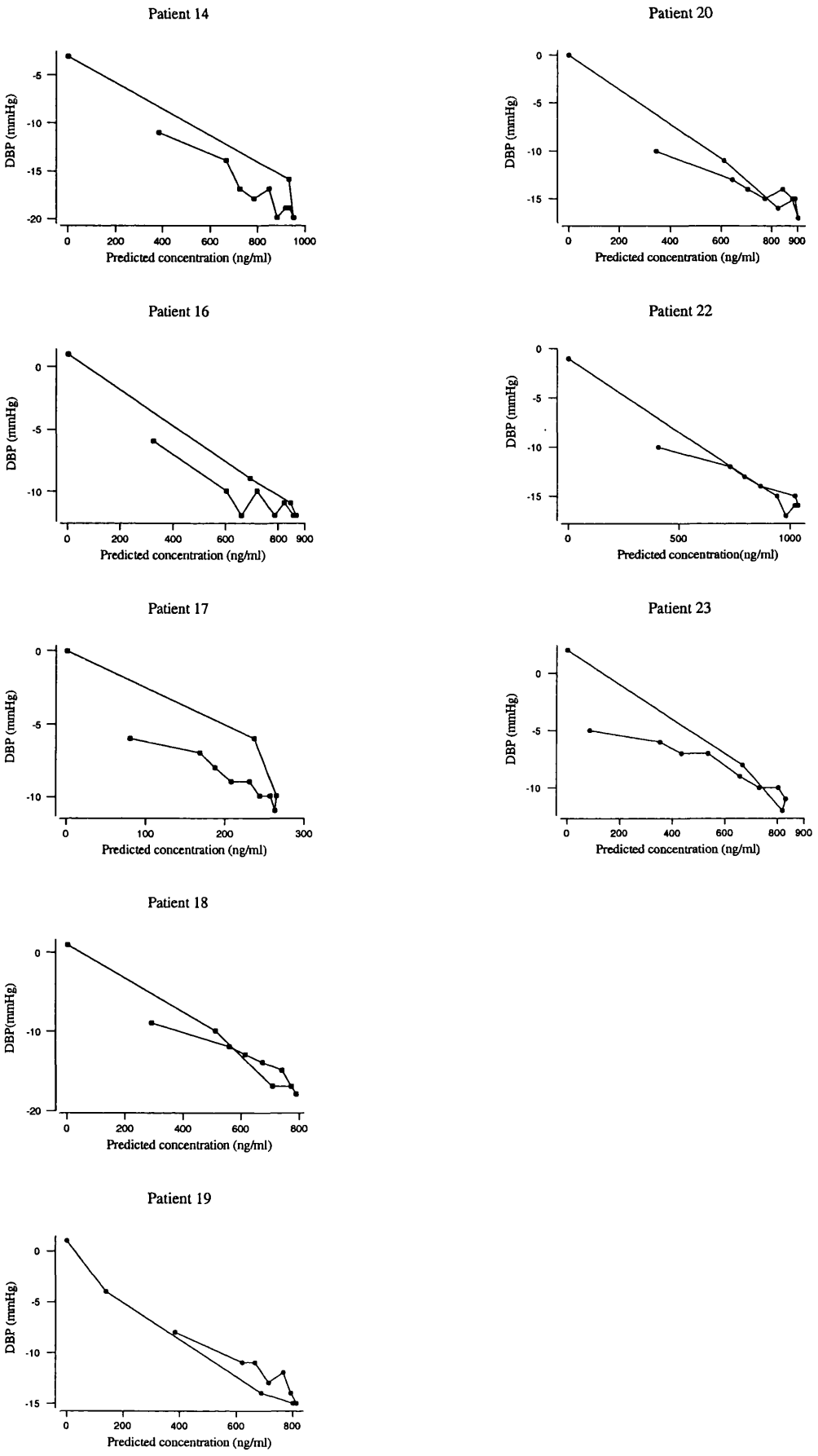

Figure 3.7.1.b Time-course of response (Δ DBP) to a single dose of mibefradil using the S0 model, for patients 1 to 13 (● measured data; ○ predicted response)

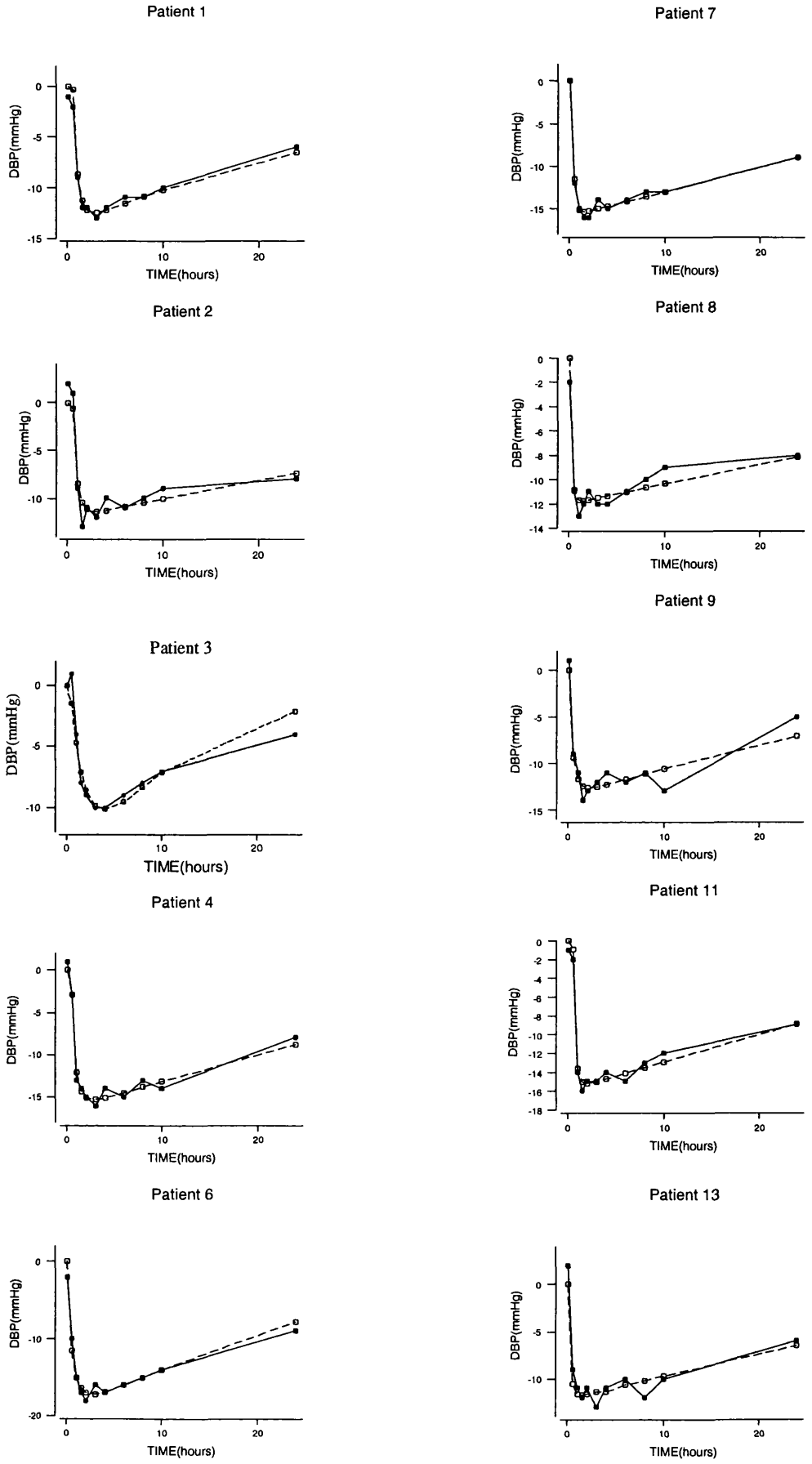

Figure 3.7.1.b (Cont.) Time course of response (Δ DBP) to a single dose of mibefradil using the S0 model, for patients 14 to 23 (● measured data; ○ predicted response)

Patient 14

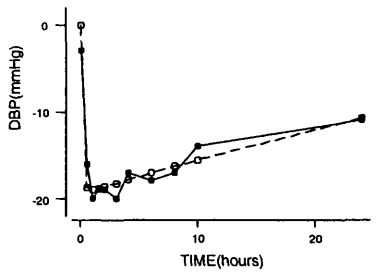

Patient 16

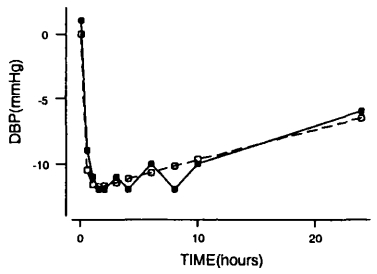

Patient 17
with effect compartment

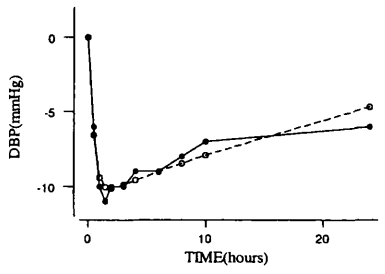

Patient 18

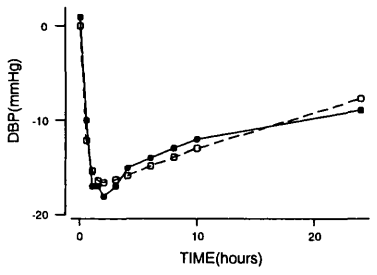

Patient 19

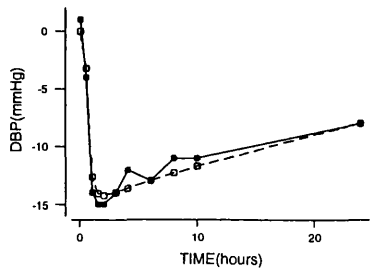

Patient 20

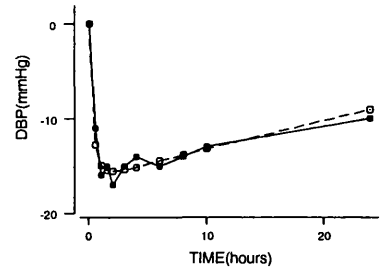

Patient 22

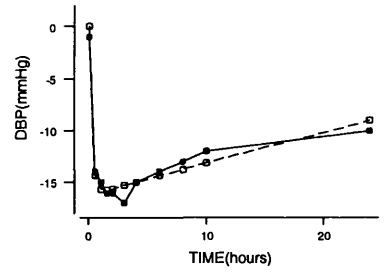

Patient 23

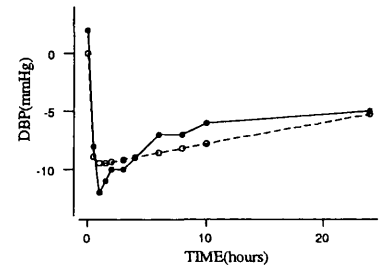

Table 3.7.1.a Parameter estimates from the Emax, linear and S0 models for changes in blood pressure after a single dose of mibefradil (150 mg)

	EMAX MODEL[a]						LINEAR MODEL[b]				S0 MODEL[c]					
ID	**Emax**	**cv%**	**EC50**	**cv%**	**AIC**	**R^2**	**m**	**cv%**	**AIC**	**R^2**	**Emax**	**cv%**	**S0**	**cv%**	**AIC**	**R^2**
1	-44.8	59.0	2001	78.7	23.03	0.99	-0.0167	2.5	22.6	0.99	-50.5	67.0	-0.0216	19.3	22.9	0.99
2	-23.0	48.9	988	89.4	33.02	0.98	-0.0126	4.5	34.6	0.96	-25.7	56.9	-0.0210	39.3	33.3	0.98
3	*	*	*	*	*	*	-0.1230	9.8	45.1	0.85	-16.0	177	-0.0212	139	39.8	0.76
4	-28.3	17.0	816	33.2	23.64	0.99	-0.0172	3.6	35.7	0.97	-28.3	17.0	-0.0346	16.5	23.6	0.99
6	-31.7	19.6	979	38.3	30.26	0.98	-0.0160	3.7	39.4	0.98	-32.6	20.4	-0.0314	18.7	30.2	0.98
7	-24.1	8.2	583	19.7	14.91	0.99	-0.0160	4.1	39.8	0.95	-24.1	8.2	-0.0413	11.7	14.9	0.99
8	-34.5	75.3	1762	111.0	27.89	0.96	-0.0132	2.6	25.2	0.98	-30.0	65.2	-0.0211	38.3	28.3	0.96
9	-30.0	55.2	854	89.7	34.87	0.96	-0.0214	3.7	33.1	0.95	-30.0	55.1	-0.0350	34.8	34.9	0.96
11	-28.1	19.2	1234	38.4	23.14	0.99	-0.0112	3.1	32.7	0.99	-28.1	19.3	-0.0220	19.4	23.1	0.99
13	-22.4	40.3	847	78.0	33.02	0.97	-0.0134	4.2	34.9	0.94	-22.8	41.2	-0.0250	37.7	33.0	0.97
14	-36.4	34.3	885	66.4	39.66	0.96	-0.0209	3.6	42.4	0.96	-39.4	38.2	-0.0383	31.1	39.6	0.96
16	-20.9	28.7	690	59.2	27.92	0.97	-0.0143	3.7	31.7	0.95	-22.6	31.7	-0.0280	29.5	27.7	0.97
17	-20.6	54.9	294	97.1	34.18	0.92	-0.0390	5.4	35.7	0.90	-15.2	33.7	-0.0960	47.3	33.7	0.92
18	-45.9	51.1	1412	75.7	35.00	0.97	-0.0218	2.6	31.4	0.97	-50.0	55.7	-0.0312	24.0	34.6	0.97
19	-46.8	58.7	1866	81.2	29.29	0.98	-0.0180	2.9	29.3	0.97	-48.3	6.0	-0.0247	6.4	29.3	0.98
20	-28.1	22.0	729	45.0	28.61	0.98	-0.0180	3.4	36.4	0.96	-28.3	22.2	-0.0383	23.1	28.6	0.98
22	-24.7	17.5	617	42.2	27.29	0.98	-0.0160	2.9	33.5	0.97	-30.0	22.0	-0.0319	21.1	26.1	0.98
23	-18.4	40.5	649	81.4	36.96	0.93	-0.0130	4.3	31.2	0.96	-19.0	67.3	-0.0250	58.2	37.9	0.95

[a] Equation 1.18, Chapter 1; [b] Equation 1.17; Chapter 1; [c] Equations 3.1, Chapter 3.

* Not estimated

Key: Emax is the maximum effect; EC50 is the concentration that produces half of the Emax effect; m is the slope of linear model; S0 is Emax/EC50; AIC represents the Akaike Information Criterion and R^2 is the coefficient of determination

Table 3.7.1.b Parameter estimates from the S0 model with a link model for changes in blood pressure after single dose of mibefradil (150 mg)

	LINK MODEL[a]								
ID	**Emax**	**cv%**	**S0**	**cv%**	**Ke0**	**cv%**	**AIC**	**ΔAIC**	**R^2**
1	-89.7	151.4	-0.0119	22.7	2.22	25.1	27.5	4.6	0.97
2	-45.6	186.2	-0.0211	59.1	1.72	59.2	46.3	13.0	0.93
3	-27.0	60.2	-0.0858	30.3	0.472	20.8	32.7	-7.2	0.96
4	-37.4	44.6	-0.0280	28.6	1.95	32.5	36.6	13.0	0.98
6	-89.4	17.5	-0.0350	20.8	7.77	63.9	29.1	-1.1	0.99
7	-25.0	9.6	-0.0390	12.8	3.56	18.7	16.1	1.2	0.99
8	-80.1	233.5	-0.0151	37.8	50.2	814.4	30.1	1.8	0.97
9	-52.0	117.3	-0.0270	3.32	46.9	720.8	36.1	1.2	0.96
11	-50.0	98.4	-0.0157	39.8	1.68	36.9	44.0	20.9	0.94
13	*	*	*	*	*	*	*		-
14	-50.0	44.4	-0.0330	24.9	4.35	34.8	37.0	-2.6	0.98
16	-27.9	37.6	-0.0240	25.0	6.10	48.3	25.6	-2.2	0.98
17	-25.1	38.7	-0.0650	23.0	2.85	27.2	23.2	-10.5	0.97
18	-59.8	67.7	-0.0300	23.9	9.83	82.2	34.7	0.1	0.98
19	-40.0	99.3	-0.0258	47.4	2.42	48.0	42.0	12.7	0.96
20	-29.5	22.3	-0.0360	22.2	8.39	62.3	26.6	-2.0	0.98
22	-33.1	26.8	-0.0290	21.4	18.4	181.5	27.5	1.4	0.98
23	-15.1	19.7	-0.129	32.5	18.2	292.7	35.6	-2.3	0.95

[a] Equation 3.2, Chapter 3.
* Not estimated

Key: Emax is the maximum effect; S0 is Emax/EC50; Keo is the constant rate for drug loss from the effect compartment; AIC represents the Akaike Information Criterion; R^2 coefficient of determination and ΔAIC is the difference in AIC between S0 modeol with and without effect compartment.

Heart Rate - The existence of hysteresis was inspected from the plot of individual changes of HR against predicted concentration. Close examination of these shows that the amplitudes of the heart rate reductions were very small and the profile was nearly flat so that an Emax shape was not well defined (Figure 3.7.1.c). Both models were tried and the parameter estimates and the AIC values obtained. The choice between the linear and Emax models was not clear. For patient 1 the search algorithm did not converge with the Emax model. Inclusion of an intercept parameter and the power parameter in the sigmoidal Emax model were not justified.

Results from the Emax, reparameterized as S0 models and linear model are shown in Table 3.7.1.c. The S0 model performed better than the linear model as judged by the coefficient of determination and AIC. The S0 model was further evaluated.

The inclusion of an effect compartment in the S0 model was also tested. From the plots it can be seen that patients 3, 13 and 17 required an effect compartment. This was confirmed by the results shown in Table 3.7.1.d. Figure 3.7.1.d shows the predicted values of the responses from the S0 model and the measured heart rate responses against time for mibefradil; it is apparent that the model predicted effects were in close agreement with those measured.

Figure 3.7.1.c Decrease in HR against predicted concentrations of mibefradil (single-dose study) for patients 1 to 13

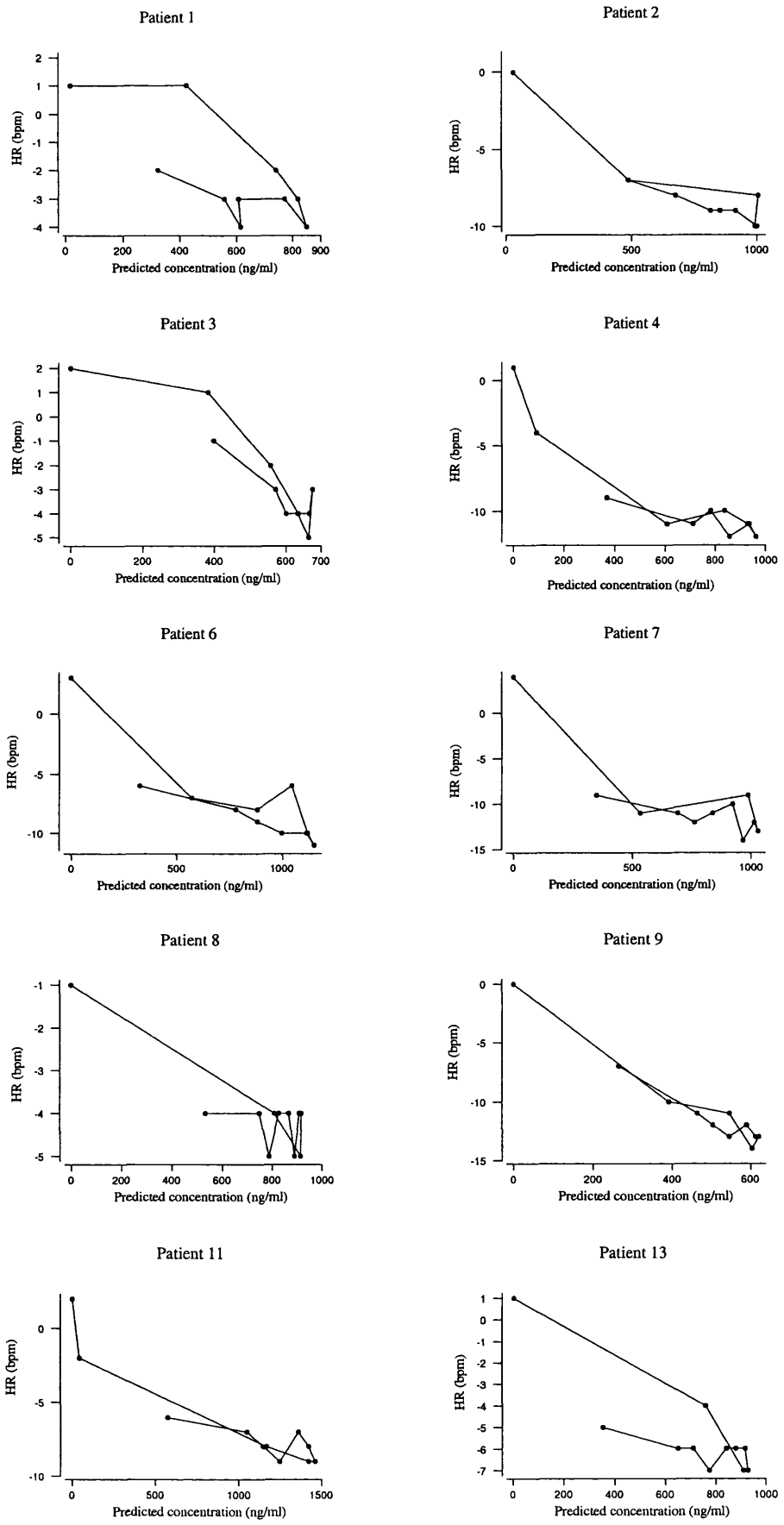

Figure 3.7.1.c (cont.) Decrease in heart rate against predicted concentrations of mibefradil (single dose study) for patients 14 to 23

Patient 14

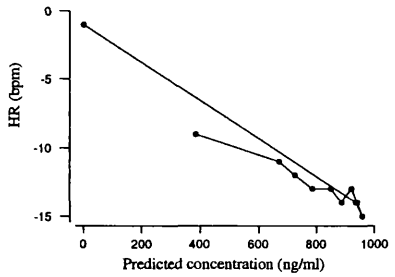

Patient 20

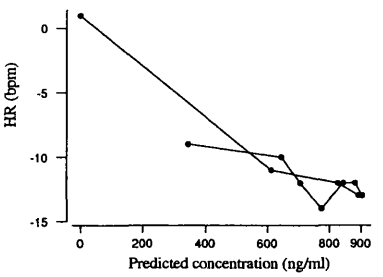

Patient 16

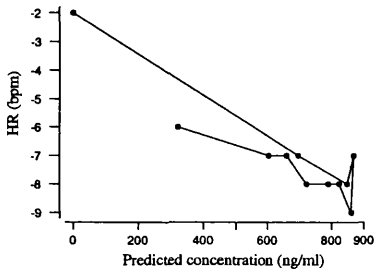

Patient 22

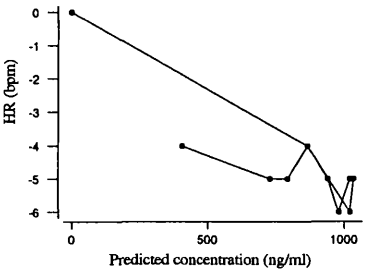

Patient 17

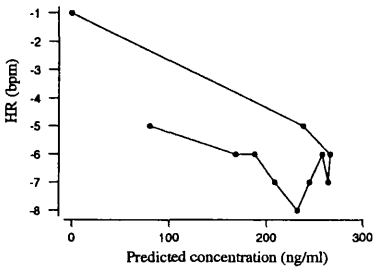

Patient 23

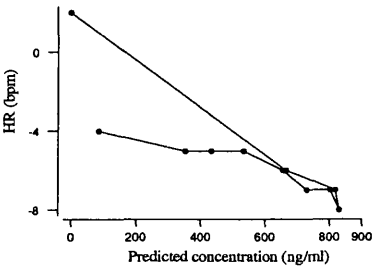

Patient 18

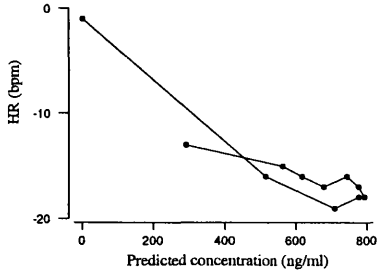

Patient 19

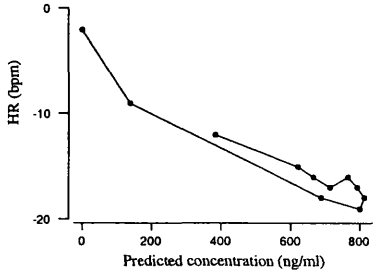

Figure 3.7.1.d Time-course of response (Δ HR) to a single dose of mibefradil using the S0 model, for patients 1 to 13 (● measured data; ○ predicted response)

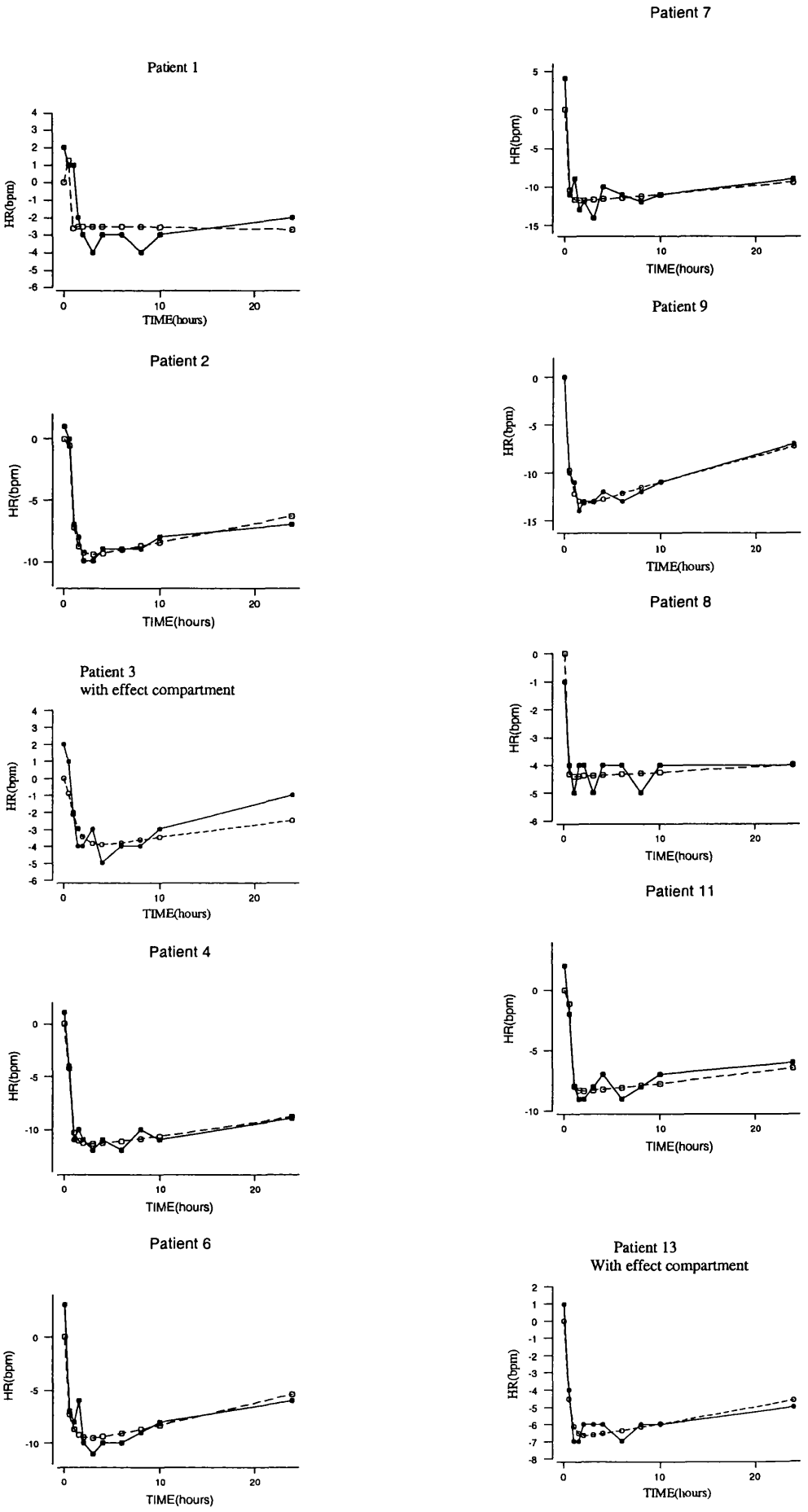

Figure 3.7.1.d (Cont.) Time-course of response (Δ HR) to a single dose of mibefradil using the S0 model, for patients 14 to 23 (● measured data; ○ predicted response).

Patient 14

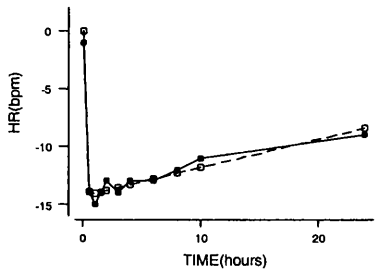

Patient 16

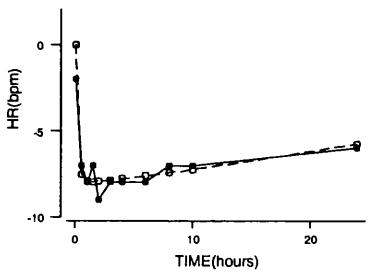

Patient 17
with effect compartment

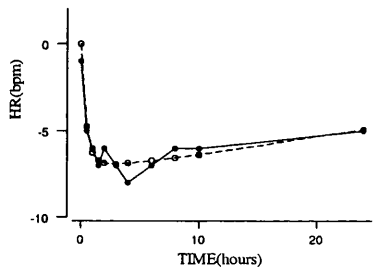

Patient 18

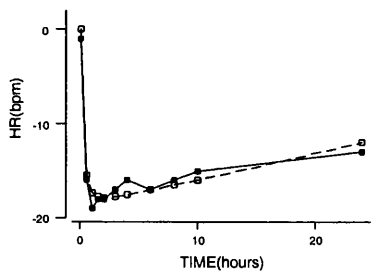

Patient 19

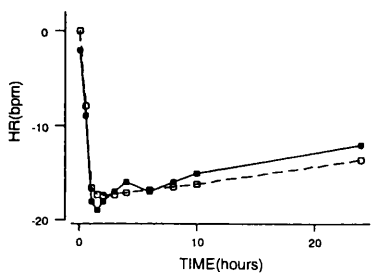

Patient 20

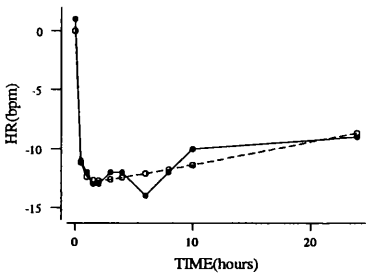

Patient 22

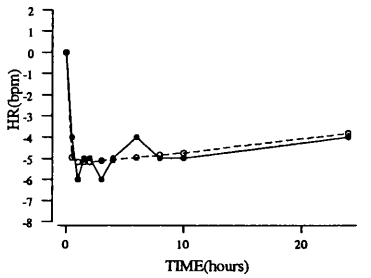

Patient 23

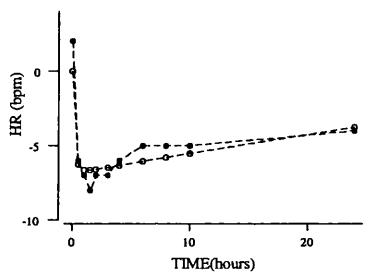

Table 3.7.1.c Parameter estimates from the linear and S0 models for changes in heart rate after a single dose of mibefradil (150 mg)

	LINEAR MODEL[a]				S0 MODEL[b]					
ID	**m**	**cv%**	**AIC**	**R^2**	**Emax**	**cv%**	**S0**	**cv%**	**AIC**	**R^2**
1	-0.0041	16.6	17.8	0.86	-2.38	20.8	-0.056	86.2	38.5	0.71
2	-0.010	3.3	23.4	0.97	-19.1	29.2	-0.019	24.8	18.1	0.99
3	-0.0052	14.2	34.7	0.91	-5.00	180.7	-0.011	252.4	39.8	0.82
4	-0.013	6.5	43.3	0.89	-13.8	6.9	-0.066	23.0	21.7	0.99
6	-0.0091	7.1	41.6	0.87	-13.5	32.0	-0.027	58.9	39.1	0.94
7	-0.013	8.3	50.7	0.81	-13.6	19.9	-0.086	95.6	42.8	0.96
8	-0.005	5.3	19.9	0.87	-5.10	31.3	-0.034	168.8	16.0	0.91
9	-0.022	2.5	25.9	0.98	-33.4	28.8	-0.035	16.4	19.7	0.99
11	-0.006	5.8	34.1	0.92	-10.3	17.5	-0.029	58.2	28.1	0.96
13	-0.0074	6.3	30.9	0.86	-7.82	23.4	-0.035	79.0	25.8	0.94
14	-0.016	2.9	31.1	0.98	-25.5	16.5	-0.033	17.6	19.1	0.99
16	-0.010	5.5	32.9	0.93	-10.3	19.5	-0.040	54.8	25.2	0.95
17	-0.028	7.4	35.5	0.81	-7.54	15.2	-0.194	77.9	25.6	0.90
18	-0.024	4.9	47.8	0.92	-25.0	11.9	-0.078	24.2	28.8	0.98
19	-0.024	4.8	46.6	0.96	-23.0	10.8	-0.087	26.4	34.4	0.98
20	-0.015	4.5	38.7	0.92	-17.8	15.6	-0.048	31.5	26.3	0.98
22	-0.0055	5.5	23.5	0.88	-6.71	22.4	-0.021	62.0	17.8	0.93
23	-0.0095	4.6	24.5	0.96	-13.0	57.5	-0.018	52.4	27.6	0.97

[a] Equation 1.78; Chapter 1; [b] Equation 3.1, Chapter 3.

* Not estimated.

Key: Emax is the maximum effect; m is the slope of linear model; S0 is Emax/EC50; AIC is the Akaike Information Criterion and R^2 represents the coefficient of determination.

Table 3.7.1.d Parameter estimates from the S0 model with a link model for changes in heart rate after a single dose of mibefradil (150 mg)

	LINK MODEL[a]								
ID	Emax	cv%	S0	cv%	Ke0	cv%	AIC	ΔAIC	R^2
1	*	*	*	*	*	*	*		-
2	-22.0	62.6	-0.0239	45.5	0.58	41.7	34.7	16.7	0.96
3	-15.0	360.8	-0.00810	118.5	1.4	109.0	34.7	-5.2	0.94
4	-14.9	14.4	-0.0580	43.1	1.1	43.9	31.1	9.3	0.97
6	-13.1	32.9	-0.0302	71.3	5.9	171.6	40.6	1.5	0.94
7	-13.8	21.7	-0.0825	98.3	2.2	123.4	44.5	1.7	0.96
8	-5.5	43.1	-0.0250	164.4	6.0	226.2	17.8	1.8	0.92
9	-33.1	32.8	-0.0350	19.4	56	489.6	21.8	2.1	0.99
11	-10.0	29.8	-0.0312	109.0	0.8	96.7	38.5	10.4	0.95
13	-10.0	25.9	-0.0217	44.4	2.4	50.0	21.2	-4.7	0.97
14	-25.4	18.0	-0.0329	19.3	53	1703.8	21.2	2.1	0.99
16	-11.0	24.1	-0.0344	55.4	6.7	132.0	26.6	1.4	0.96
17	-8.98	15.5	-0.122	42.7	1.4	42.5	20.5	-5.1	0.96
18	-22.0	9.2	-0.110	28.9	100	1898.5	29.5	0.7	0.98
19	-40.0	43.6	-0.0390	31.7	2.9	34.9	36.9	2.4	0.97
20	-19.0	19.8	-0.0420	34.3	54.4	954.4	28.2	1.9	0.98
22	-7.36	24.5	-0.01800	52.8	3.7	74.4	17.4	-0.4	0.95
23	-47.5	270.6	-0.0100	42.1	17	278.9	28.2	0.6	0.96

[a] Equation 3.2, Chapter 3.

* Not estimated.

Key: Emax is the maximum effect; S0 is Emax/EC50; Keo is the constant rate for drug loss from the effect compartment; AIC is the Akaike Information Criterion; R^2 is the coefficient of determination and ΔAIC is the difference in AIC between S0 model with and without effect compartment

Figure 3.7.1.e Changes in PQ interval against predicted concentrations of mibefradil (single-dose study) for patients 1 to 13.

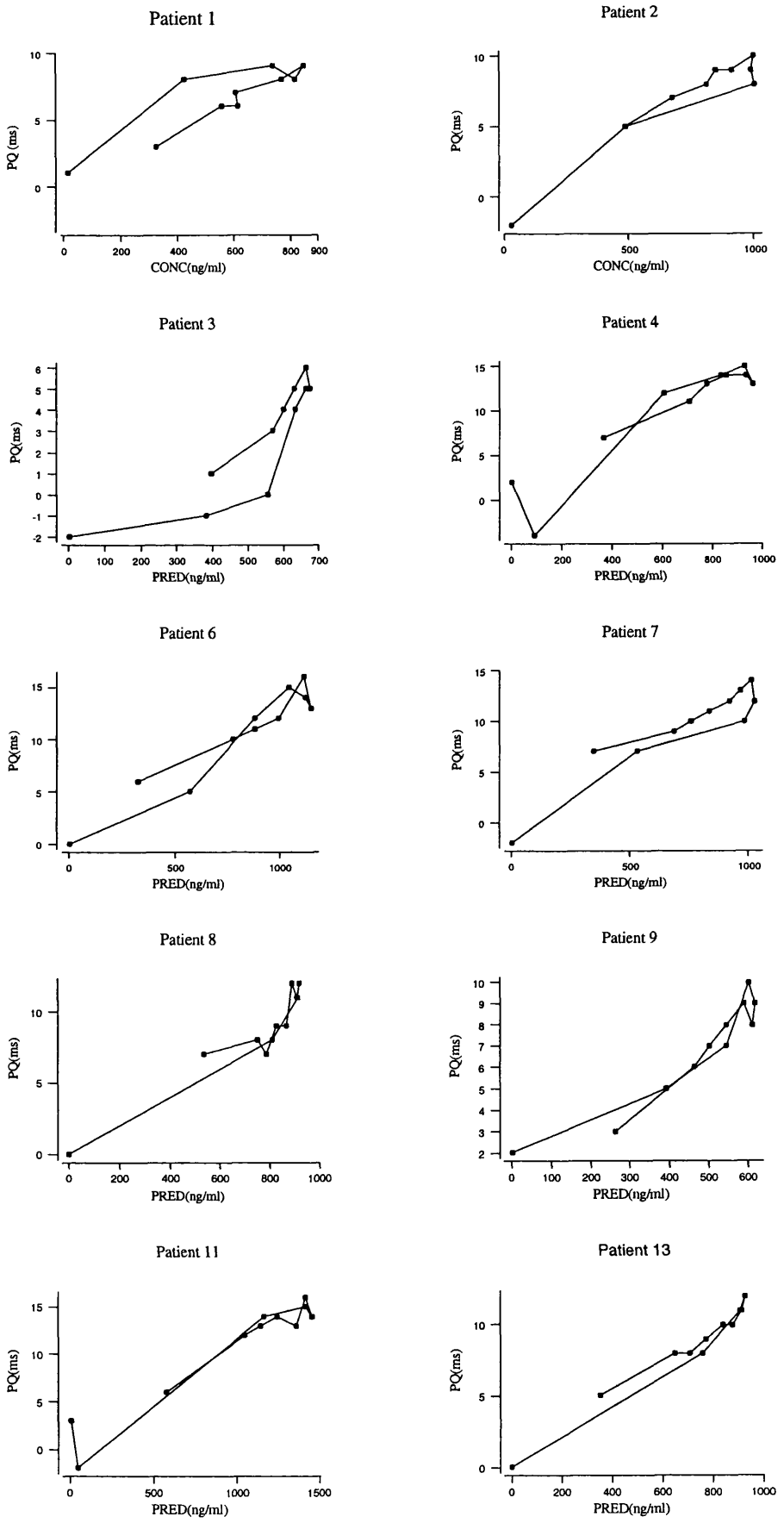

Figure 3.7.1.e (cont.) Changes in PQ interval against predicted concentrations of mibefradil (single-dose study) for patients 14 to 23.

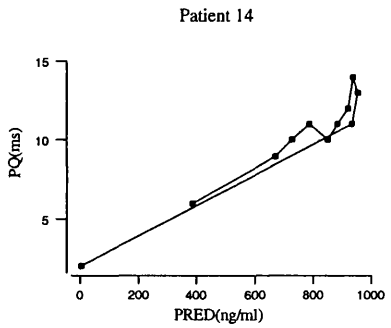

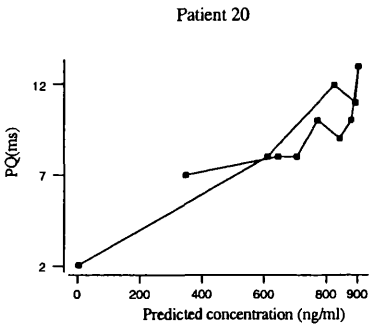

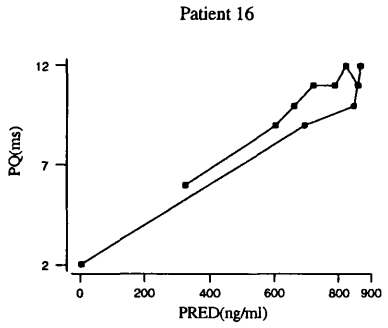

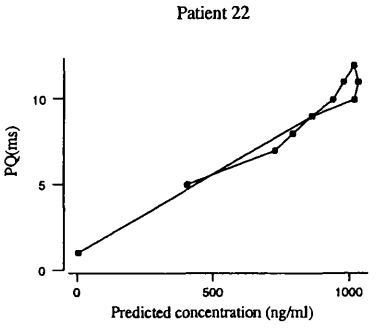

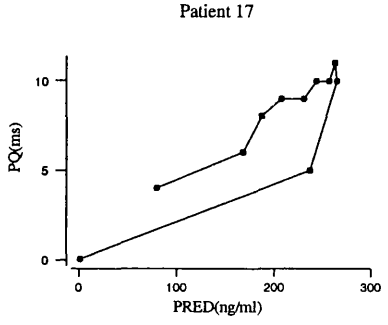

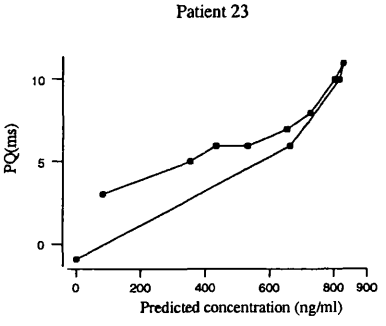

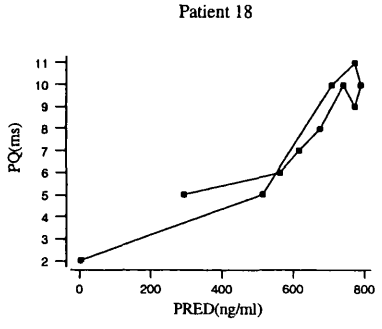

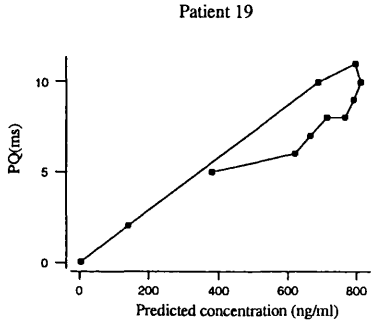

Figure 3.7.1.f Time-course of response (Δ PQ interval) to a single dose of mibefradil using the linear model, for patients 1 to 13 (● measured data; ○ predicted response)

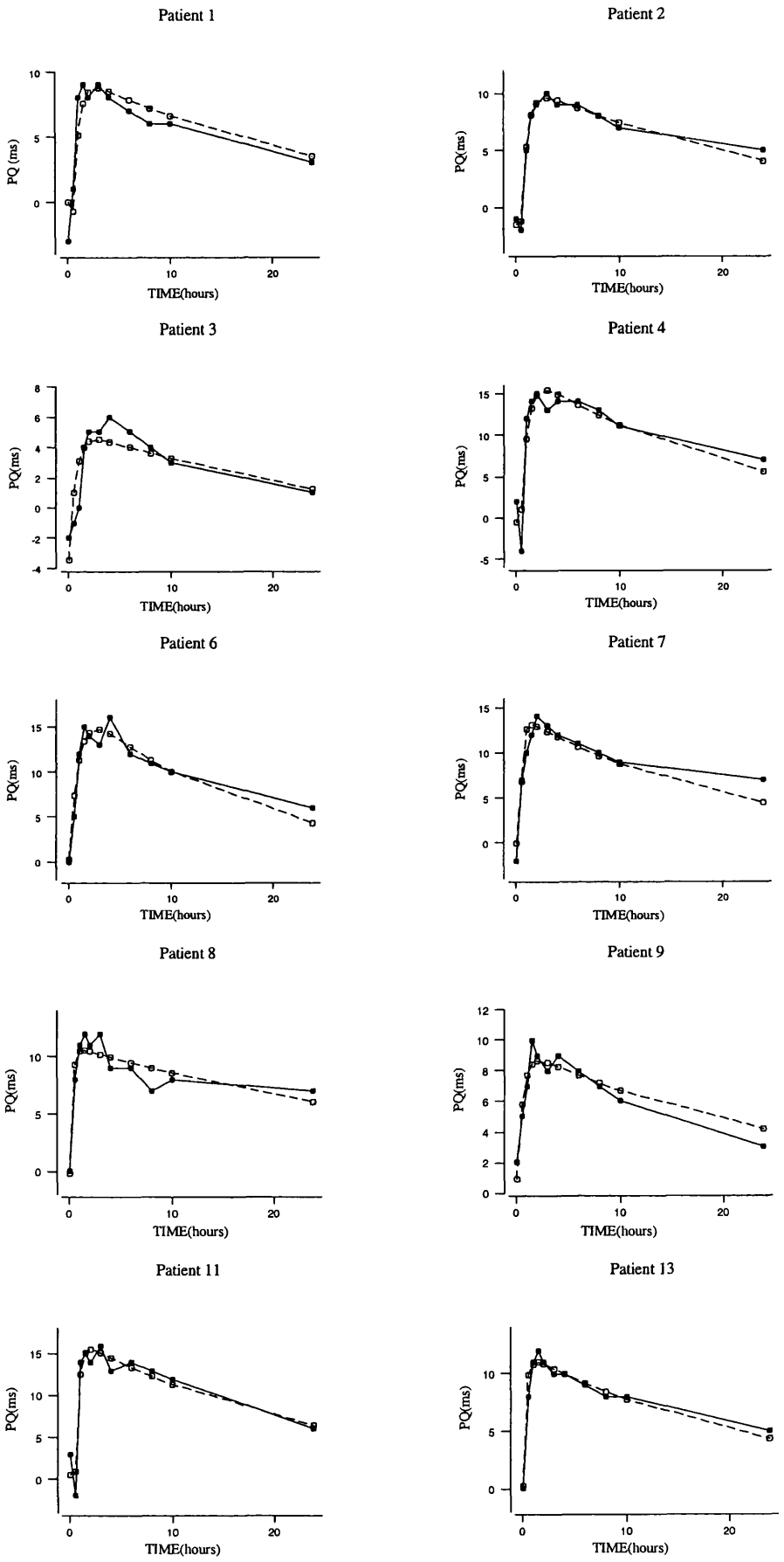

Figure 3.7.1.f (Cont.) Time-course of response (Δ PQ interval) to single dose of mibefradil using the linear model, for patients 14 to 23 (● measured data; ○ predicted response)

Patient 14

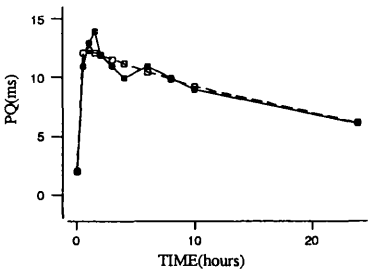

Patient 20

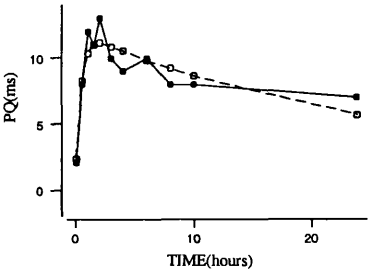

Patient 16

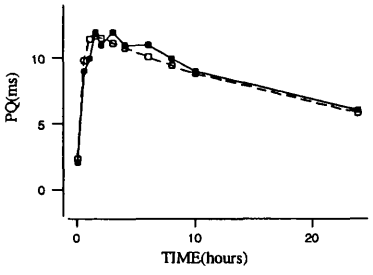

Patient 22

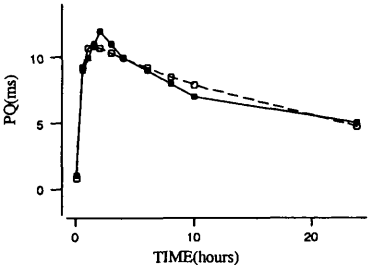

Patient 17

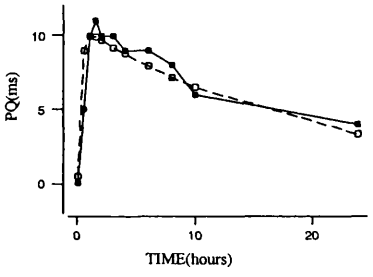

Patient 23

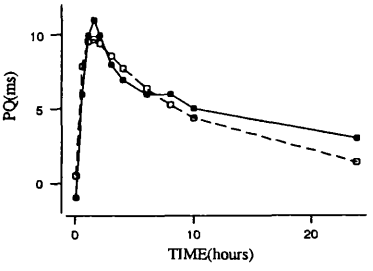

Patient 18

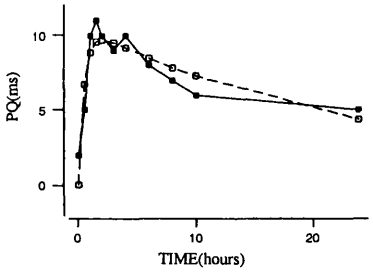

Patient 19

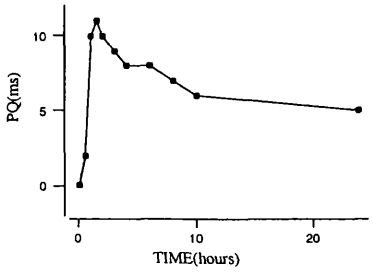

Figure 3.7.1.g Decrease in DBP against predicted concentrations of verapamil (single-dose study) for patients 1 to 13

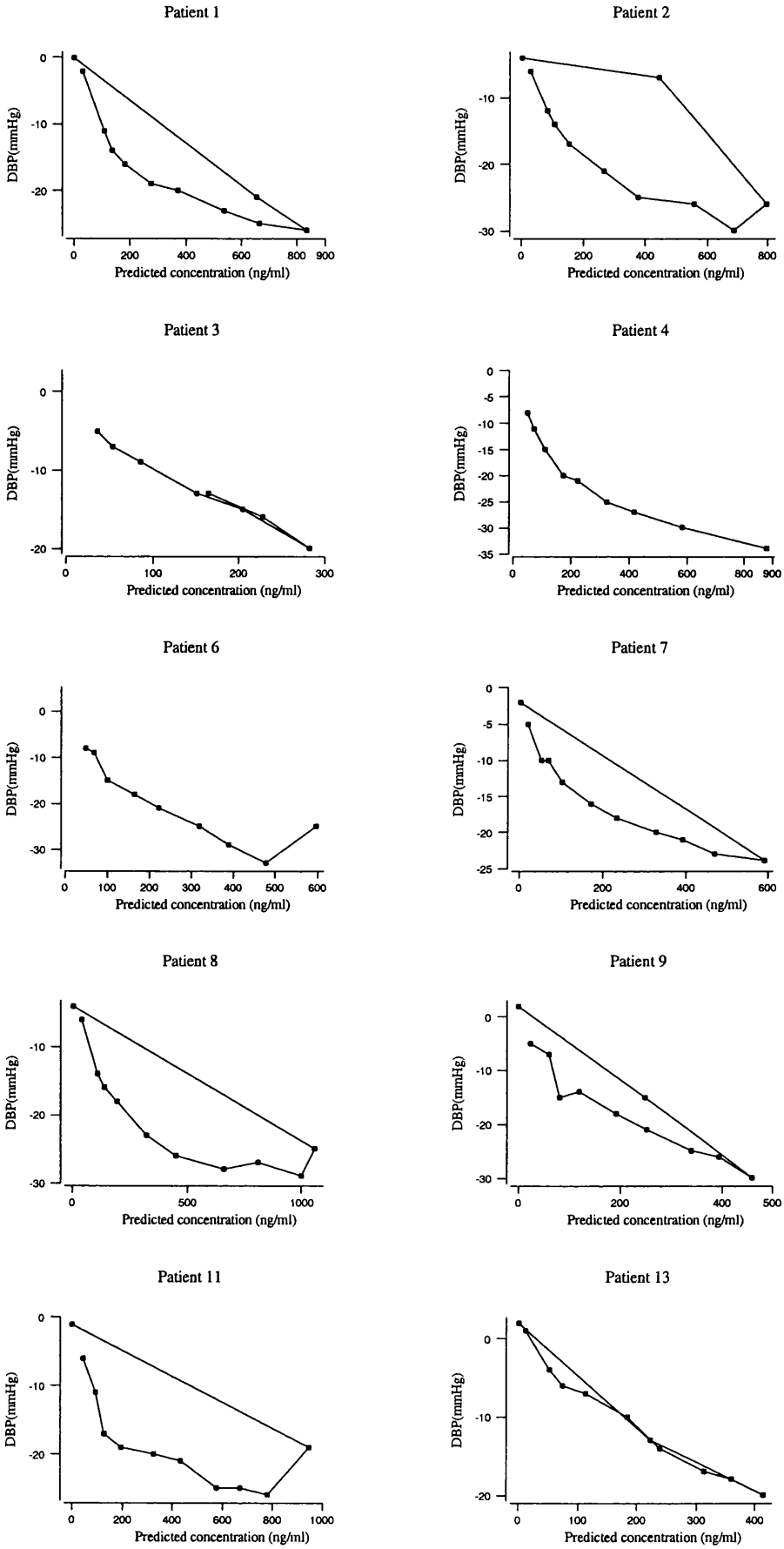

Figure 3.7.1.g (cont.) Decrease in DBP against predicted concentrations of verapamil (single-dose study) for patients 14 to 23

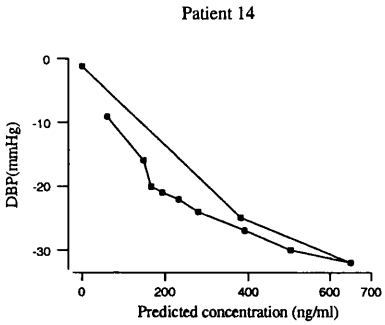

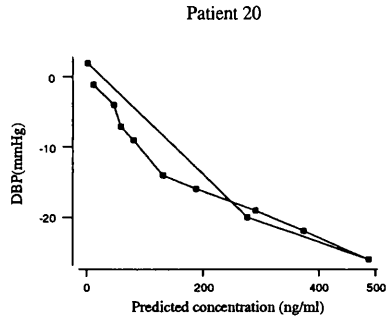

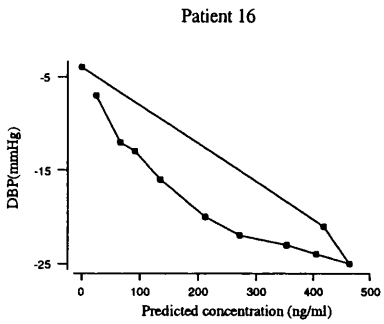

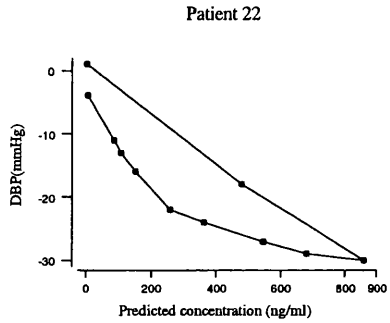

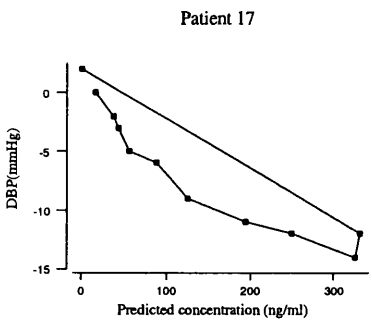

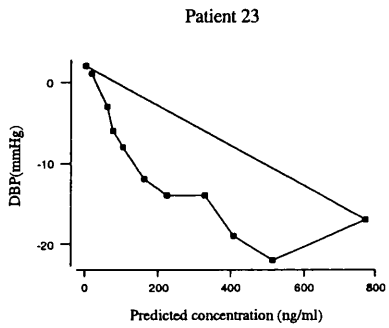

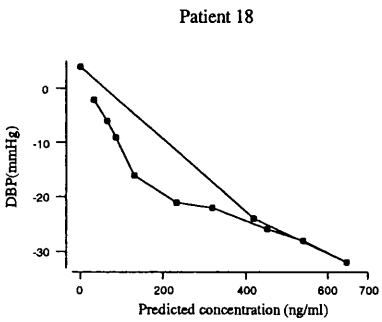

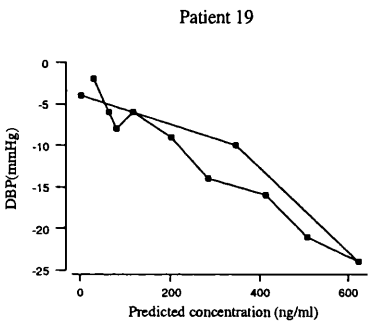

Figure 3.7.1.h Time-course of response (Δ DBP) to a single dose of verapamil using the S0 model, for patients 1 to 13 (● measured data; ○ predicted response)

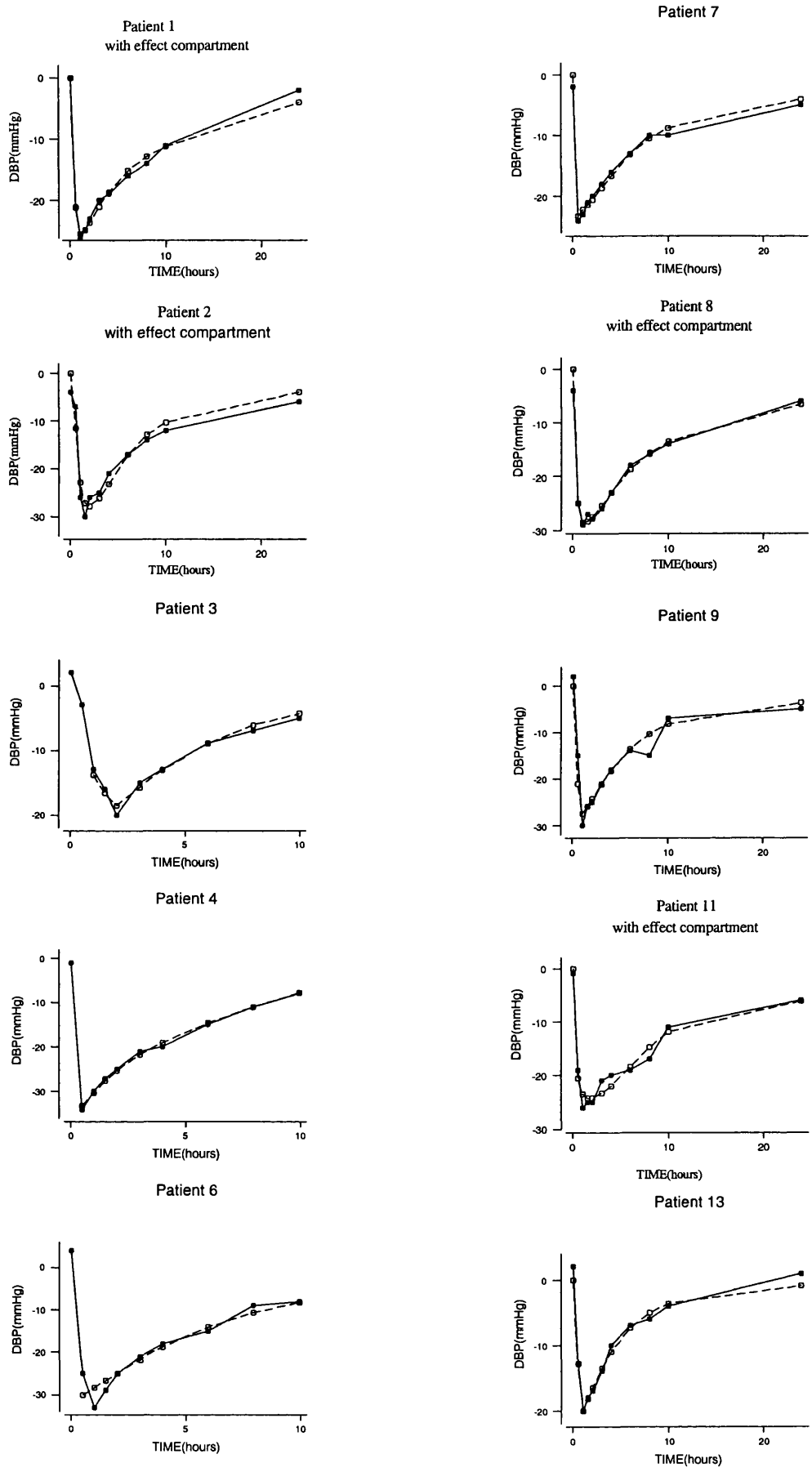

Figure 3.7.1.h (Cont.) Time course of response (Δ DBP) to a single dose of verapamil using the S0 model, for patients14 to 23 (● measured data; ❍ predicted response).

Patient 14

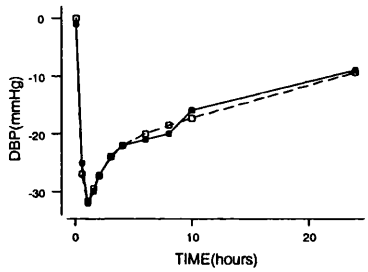

Patient 20

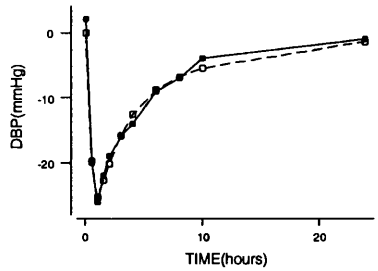

Patient 16

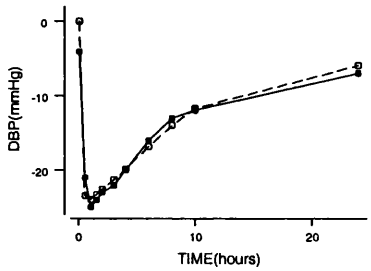

Patient 22
with effect compartment

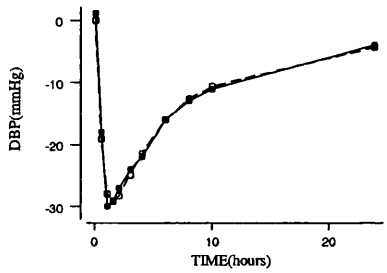

Patient 17

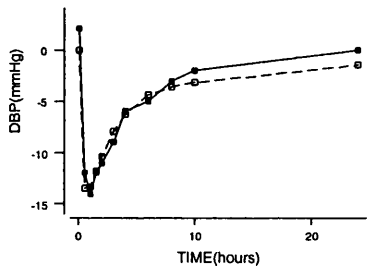

Patient 23
with effect compartment

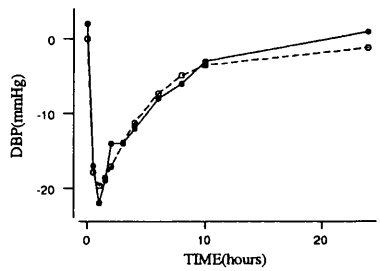

Patient 18

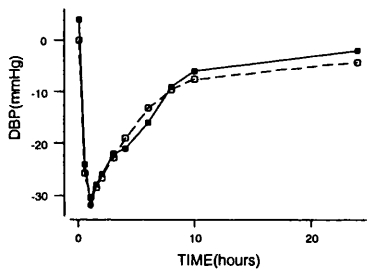

Patient 19

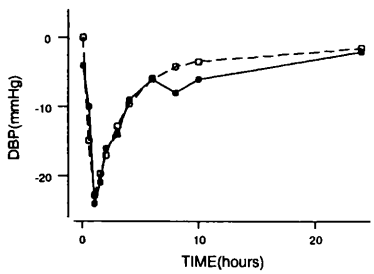

PQ interval - Figure 3.7.1.e shows the changes in PQ interval along with the predicted concentrations. The relationship was close to a straight line and the linear model generally proved satisfactory (Table 3.7.1.e). The linear model produced a greater reduction in the residual sum of squares for all patients except patient 7. For this patient, the reduction in the residual sum of squares differed by only of 0.95 points (Table 3.7.1.e). Figure 3.7.1.f shows the measured and predicted effects from the linear model for PQ interval. The linear model satisfactory described the data and therefore was chosen. The estimation of EC50 for the Emax model was bounded.

3.7.1.2 Verapamil

Blood pressure - Analysis of the plots in Figure 3.7.1.g indicated the likelihood of hysteresis in patients 1, 2, 8, 11, 22 and 23. Examination of plots suggested that an Emax model might describe the relationship between DBP and the predicted concentration. This was confirmed by the AIC values which favoured the Emax model. Table 3.7.1.f shows the parameter estimates and AIC for the two competing models. The sigmoidal Emax model showed no improvements in the fit and an intercept was not necessary.

The S0 parameter estimated from S0 model had a smaller coefficient of variation than that of EC50 from the Emax model. The presence of hysteresis was tested (Table 3.7.1.g). Patients 1, 2, 8, 11, 22 and 23 had the highest decrease in AIC after the inclusion of effect compartment in the model. The effect predicted from the S0 model and the measured effects with time is shown in Figure 3.7.1.h.

Table 3.7.1.e Parameter estimates from the Emax and linear models for changes in PQ interval after a single dose of mibefradil (150 mg)

	EMAX MODEL[a]						LINEAR MODEL[b]			
ID	**Emax**	**cv%**	**EC50**	**cv%**	**AIC**	**R^2**	**m**	**cv%**	**AIC**	**R^2**
1	29.8	173.0	1977	231.5	38.1	0.93	0.0112	6.9	36.2	0.92
2	27.6	94.4	1999	133.9	29.9	0.99	0.0097	3.7	24.6	0.99
3	15.3	597.4	1997	738.4	44.3	0.82	0.00591	17.1	41.3	0.85
4	44.9	109.5	1999	154.5	46.4	0.94	0.0158	5.8	44.6	0.93
6	38.2	65.1	1999	96.5	39.0	0.95	0.0128	3.7	34.3	0.96
7	30.9	51.0	1534	79.7	34.3	0.96	0.0127	4.3	35.3	0.95
8	32.6	133.0	1999	188.7	35.0	0.92	0.0115	3.9	31.0	0.94
9	36.0	140.0	1999	178.2	30.7	0.91	0.0142	4.0	25.9	0.94
11	45.9	83.5	2998	118.8	38.9	0.96	0.0107	4.0	37.3	0.96
13	45.4	68.1	2999	86.7	19.0	0.98	0.0119	1.9	14.5	0.98
14	50.8	98.2	2986	126.3	30.7	0.96	0.0132	3.2	29.2	0.97
16	25.3	40.6	1060	69.3	27.7	0.96	0.0138	3.5	30.2	0.97
17	41.0	160.6	848.6	204.7	37.2	0.90	0.0378	5.5	35.4	0.90
18	46.3	162.1	2998	199.7	33.9	0.91	0.0120	4.4	30.6	0.93
19	44.2	147.1	2999	182.6	30.6	0.95	0.0118	4.1	27.8	0.95
20	28.2	74.5	1422	115.3	36.2	0.91	0.0127	4.7	35.5	0.92
22	41.6	78.0	2999	101.8	23.8	0.97	0.0106	2.3	19.1	0.98
23	42.8	241.0	2997	294.5	37.2	0.93	0.0117	5.5	33.2	0.94

[a] Equation 1.18, Chapter 1; [b] Equation 1.17, Chapter 1.

Key: Emax is the maximum effect; EC50 is the concentration that produces half of Emax effect; m is the slope of linear model; AIC Akaike Information Criterion and R^2 coefficient of determination

Table 3.7.1.f Parameter estimates from the linear and S0 models for changes in blood pressure after a single dose of verapamil (240 mg)

	LINEAR MODEL[a]				S0 MODEL[b]					
ID	**m**	**cv%**	**AIC**	**R^2**	**Emax**	**cv%**	**S0**	**cv%**	**AIC**	**R^2**
1	-0.0389	10.7	67.1	0.88	-30.4	5.7	-0.168	12.5	35.5	0.99
2	-0.0423	14.4	74.0	0.77	-28.6	19.9	-0.238	54.1	67.1	0.80
3	-0.0756	5.4	28.6	0.78	-34.8	15.6	-0.140	12.2	17.2	0.58
4	-0.0522	13.8	59.9	0.82	-40.2	2.4	-0.212	4.3	14.0	0.67
6	-0.0645	12.0	57.0	0.79	-38.7	12.1	-0.223	21.0	40.3	0.65
7	-0.0528	11.1	65.4	0.92	-27.5	4.3	-0.249	9.8	28.8	0.99
8	-0.0341	14.2	76.1	0.83	-32.0	5.3	-0.233	15.6	42.9	0.98
9	-0.0724	7.3	59.5	0.94	-42.5	20.2	-0.168	22.7	51.3	0.96
11	-0.0348	15.1	74.5	0.76	-26.9	7.4	-0.263	24.1	48.1	0.96
13	-0.0526	3.8	36.2	0.98	-56.8	28.6	-0.074	11.5	29.7	0.99
14	-0.0650	9.2	68.7	0.91	-41.7	4.9	-0.298	7.6	29.6	0.99
16	-0.0634	10.0	65.9	0.93	-28.8	6.8	-0.298	17.2	40.4	0.98
17	-0.0455	7.6	43.1	0.94	-23.1	18.4	-0.097	17.6	31.6	0.99
18	-0.0570	7.3	61.4	0.94	-45.6	12.7	-0.142	15.8	45.2	0.99
19	-0.0398	6.7	49.9	0.96	-64.9	66.8	-0.056	25.9	50.3	0.95
20	-0.0630	6.9	54.2	0.95	-40.0	9.2	-0.142	9.4	30.3	0.99
22	-0.0447	11.1	69.9	0.89	-34.3	10.5	-0.199	22.9	51.0	0.96
23	-0.0350	13.1	63.2	0.83	-27.1	16.6	-0.112	24.4	47.6	0.97

[a] Equation 1.17; Chapter 1; [b] Equation 3.1, Chapter 3.

Key: Emax is the maximum effect; m is the slope of linear model; S0 is Emax/EC50; AIC is the Akaike Information Criterion and R^2 is the coefficient of determination

Table 3.7.1.g Parameter estimates from the S0 model with a link model for changes in blood pressure after a single dose of verapamil (240 mg)

	LINK MODEL[a]								
ID	**Emax**	**cv%**	**S0**	**cv%**	**Ke0**	**cv%**	**AIC**	**ΔAIC**	**R^2**
1	-31.8	4.6	-0.122	8.8	4.61	28.7	28.8	-6.7	0.99
2	-42.7	19.0	-0.140	22.6	1.17	27.3	53.1	-14.0	0.96
3	-45.8	37.6	-0.120	19.2	4.22	43.0	39.5	22.3	0.98
4	-40.2	7.9	-0.212	9.4	99.9	4695.1	26.3	12.3	0.99
6	-49.8	21.4	-0.157	21.4	2.52	34.6	49.9	10.0	0.99
7	-27.4	9.8	-0.531	26.2	99.8	15052.0	32.1	3.4	0.99
8	-33.8	5.3	-0.194	14.3	2.71	35.4	38.8	-4.1	0.99
9	-45.1	18.5	-0.165	19.0	5.47	51.1	48.7	-2.6	0.97
11	-31.3	10.1	-0.615	20.2	1.04	28.0	42.1	-6.0	0.98
13	-58.1	31.6	-0.073	12.2	99.5	519.0	31.7	2.1	0.99
14	-42.2	4.4	-0.199	6.6	10.5	40.4	27.2	-2.4	0.99
16	-30.2	7.2	-0.270	15.6	4.89	54.8	39.1	-1.3	0.99
17	-25.9	20.5	-0.089	16.0	7.16	48.3	29.8	-1.8	0.99
18	-47.3	13.6	-0.134	15.6	14.8	120.3	46.2	1.0	0.99
19	-69.8	69.4	-0.057	24.7	7.18	66.1	49.7	-0.6	0.96
20	-39.7	10.2	-0.141	10.3	100	591.2	32.5	2.3	0.99
22	-39.1	4.9	-0.161	7.8	2.84	15.8	30.9	-20.1	0.99
23	-42.0	36.5	-0.068	23.5	3.10	37.7	42.3	-5.3	0.98

[a] Equation 3.2, Chapter 3.

Key: Emax is the maximum effect; S0 is Emax/EC50 and AIC is the Akaike Information Criterion; Keo is the constant rate for drug loss from the effect compartment; R^2 coefficient of determination and ΔAIC is the difference in AIC between S0 model with and without effect compartment.

Heart Rate - The relationship between HR and predicted concentration is shown in Figure 3.7.1.i. Patients 2, 13, 19, and 22 showed signs of hysteresis (Table 3.7.1.i). The relationship between heart rate and predicted concentrations agreed well with an Emax response. Table 3.7.1.h shows the values of AIC for the linear and S0 models. For the S0 model, the AIC values were smaller than with the linear model, and accordingly, the S0 model was further evaluated. Figure 3.7.1.j shows the responses predicted from the S0 model and the measured responses following single-dose verapamil.

PQ interval - The changes in PQ interval with the predicted concentrations are shown in Figure 3.7.1.l. The Emax model did not converge for patients 3 and 4. Results obtained from fitting the linear and Emax model are listed in Table 3.7.1.j. Figure 3.7.1.m shows the time-course of the PQ interval responses following verapamil. The linear model was chosen..

Figure 3.7.1.i Decrease in HR against predicted concentrations of verapamil (single-dose study) for patients 1 to 13

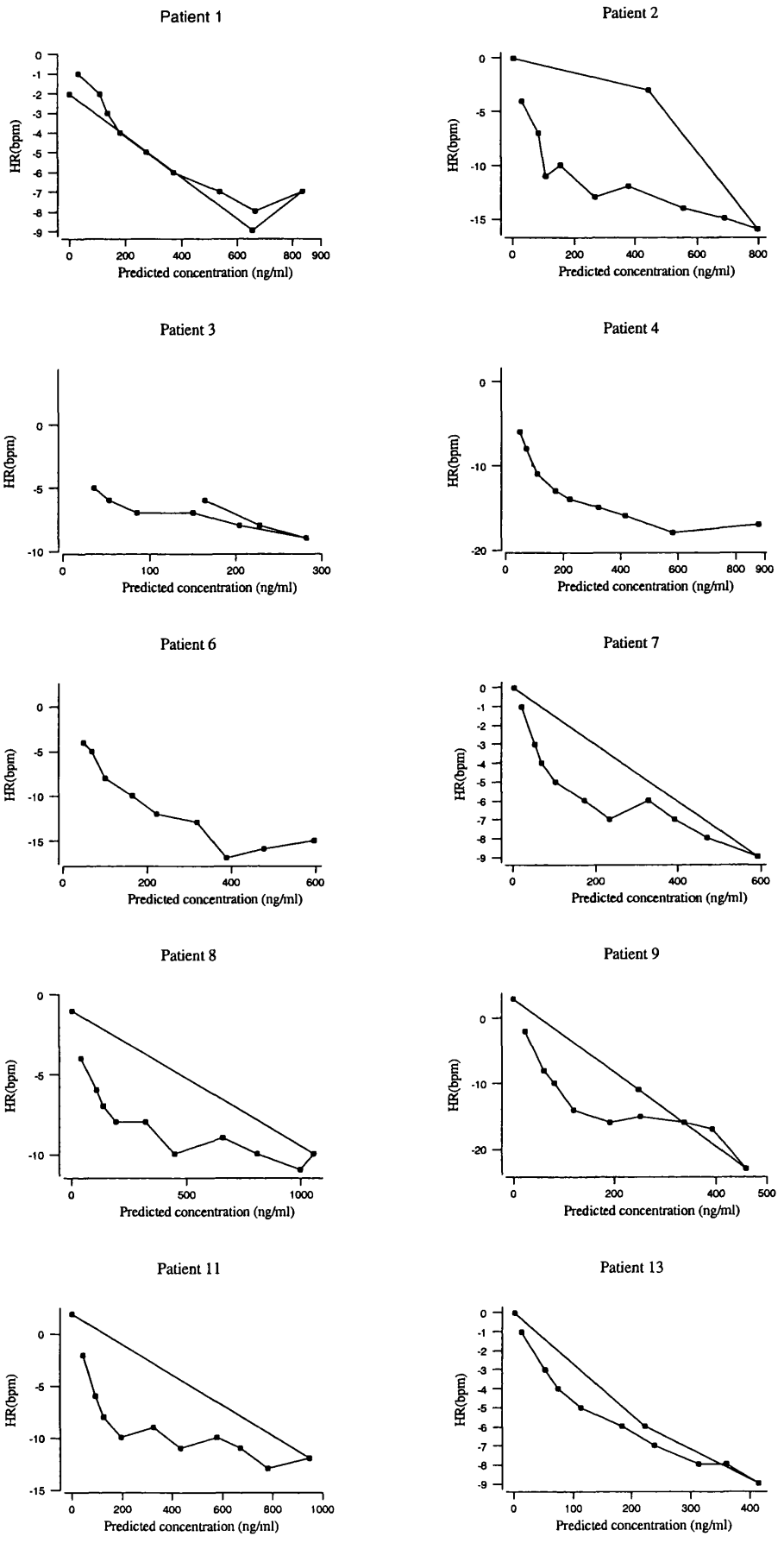

Figure 3.7.1.i (cont.) Decrease in HR against predicted concentrations of verapamil (single-dose study) for patients 14 to 23

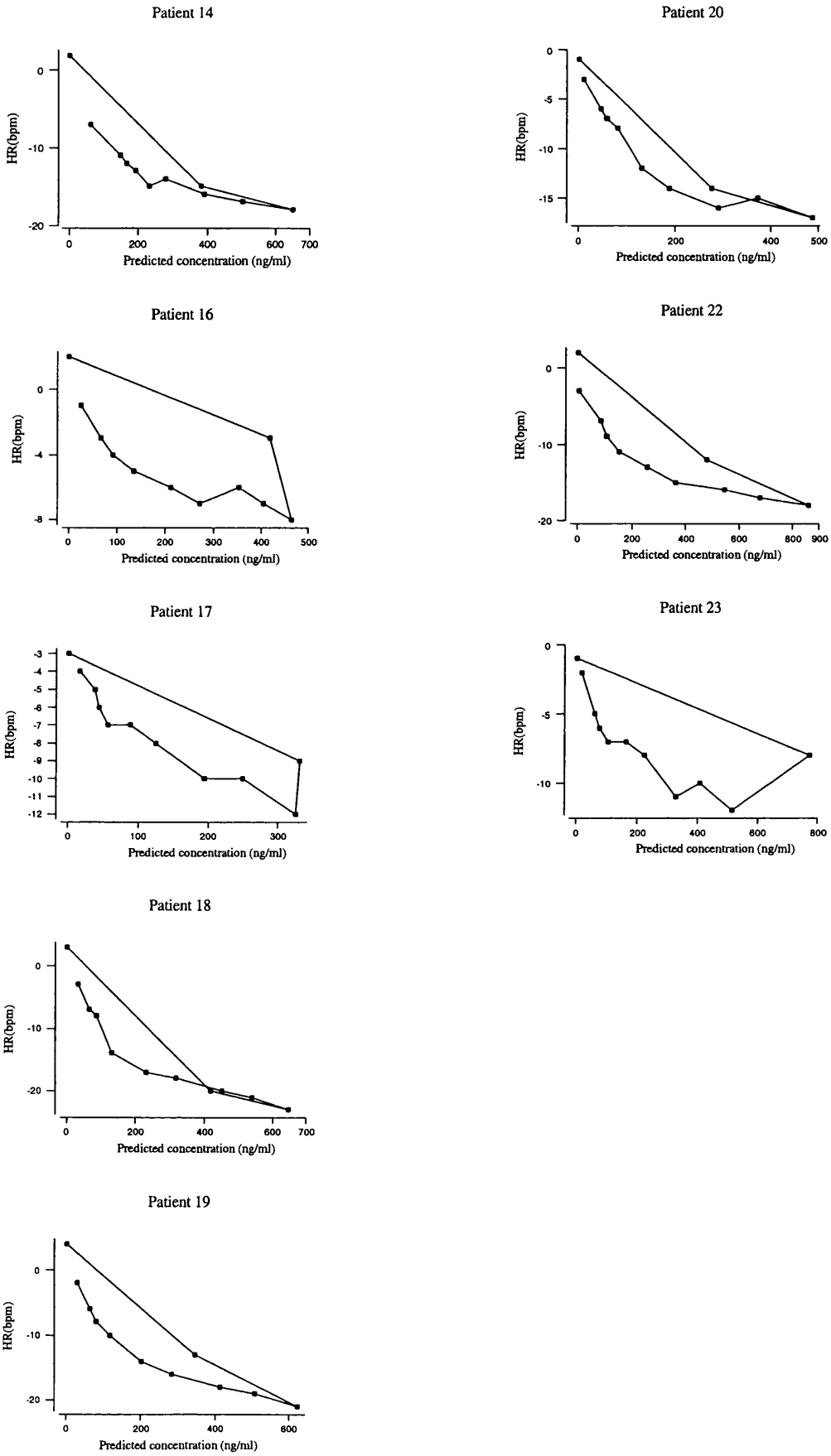

Figure 3.7.1.j Time-course of response (Δ HR) to a single dose of verapamil for patients 1 to 13 (● measured data; ○ predicted response) using the S0 model

Patient 1

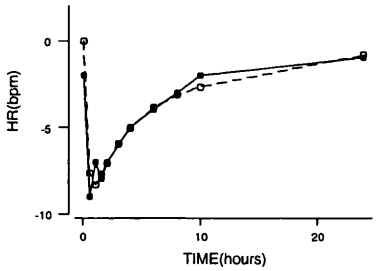

Patient 7

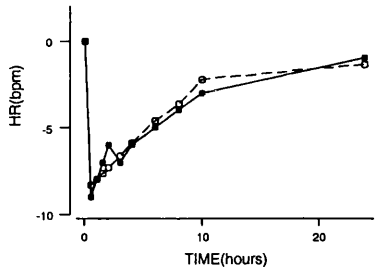

Patient 2
with effect compartment

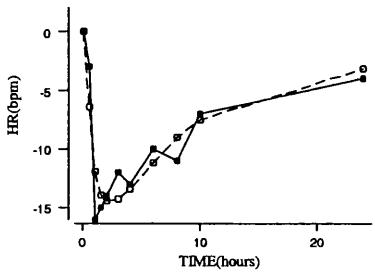

Patient 8

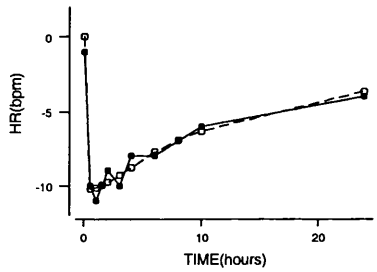

Patient 3

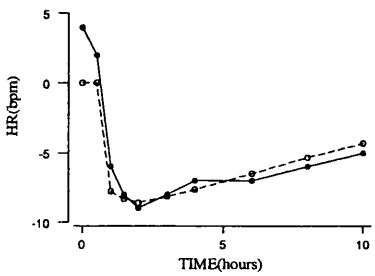

Patient 9

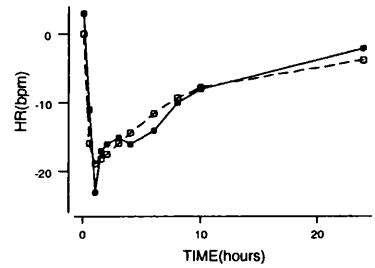

Patient 4

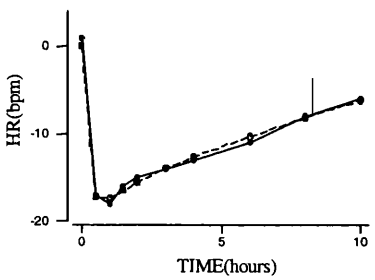

Patient 11

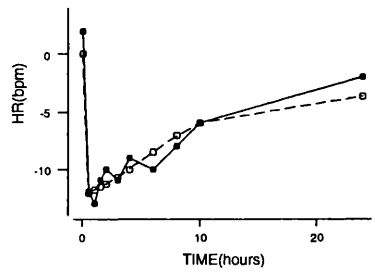

Patient 6

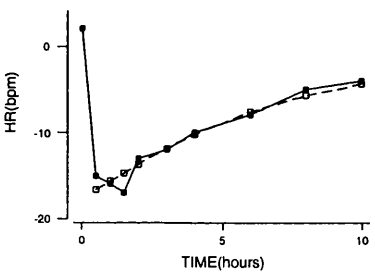

Patient 13
with effect compartment

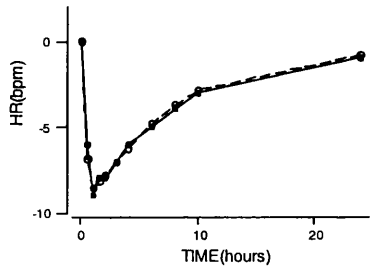

Figure 3.7.1.j (Cont.) Time-course of response (Δ HR) to a single dose of verapamil for patients 14 to 23 (● measured data; ○ predicted response) using the S0 model

Patient 14

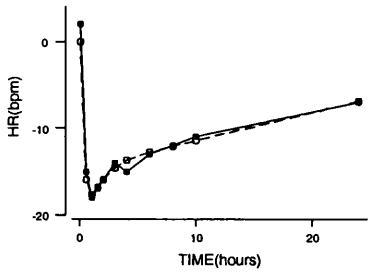

Patient 20

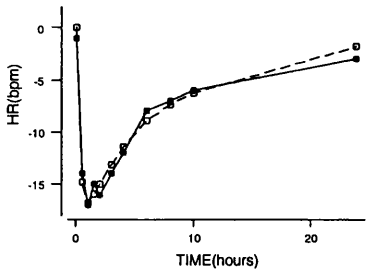

Patient 16

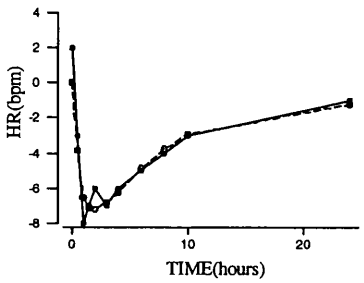

Patient 22
with effect compartment

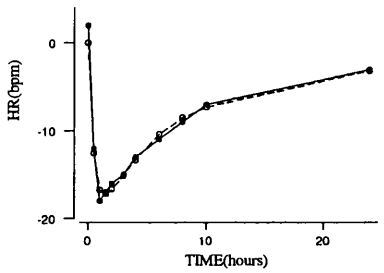

Patient 17

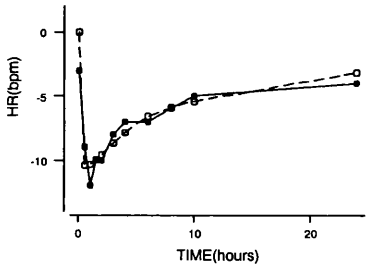

Patient 23

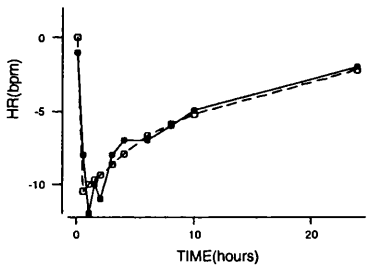

Patient 18

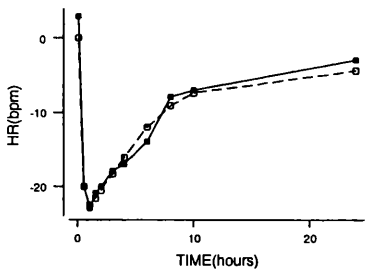

Patient 19
with effect compartment

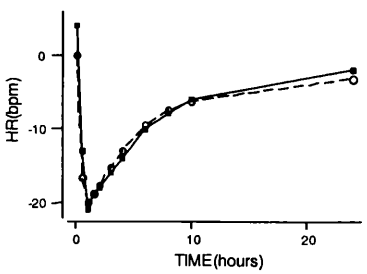

Figure 3.7.1.1 Change in PQ interval against predicted concentrations of verapamil (single-dose study) for patients 1 to 13

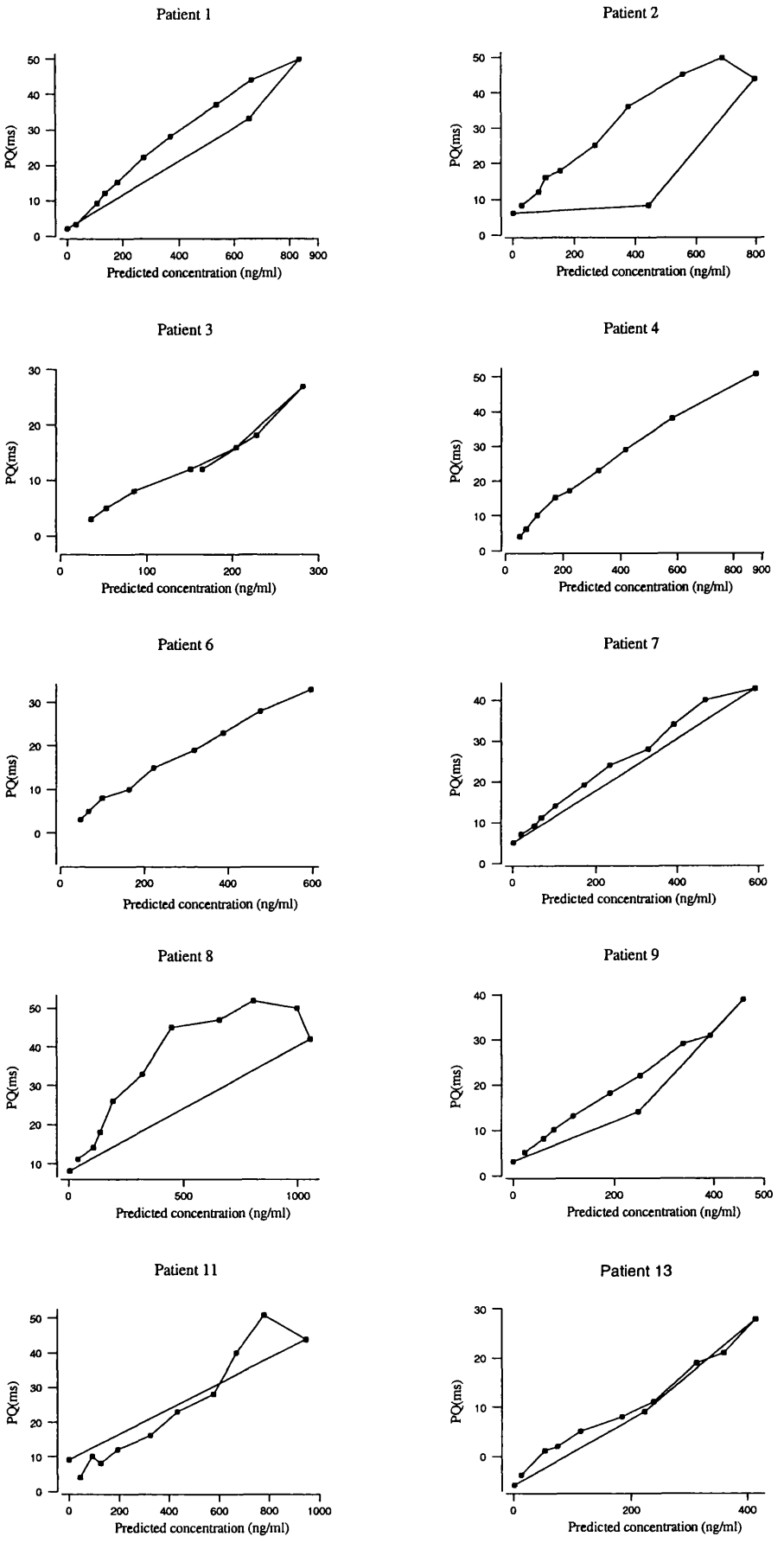

Figure 3.7.1.1 (cont.) Change in PQ interval against predicted concentrations of verapamil (single-dose study) for patients 14 to 23

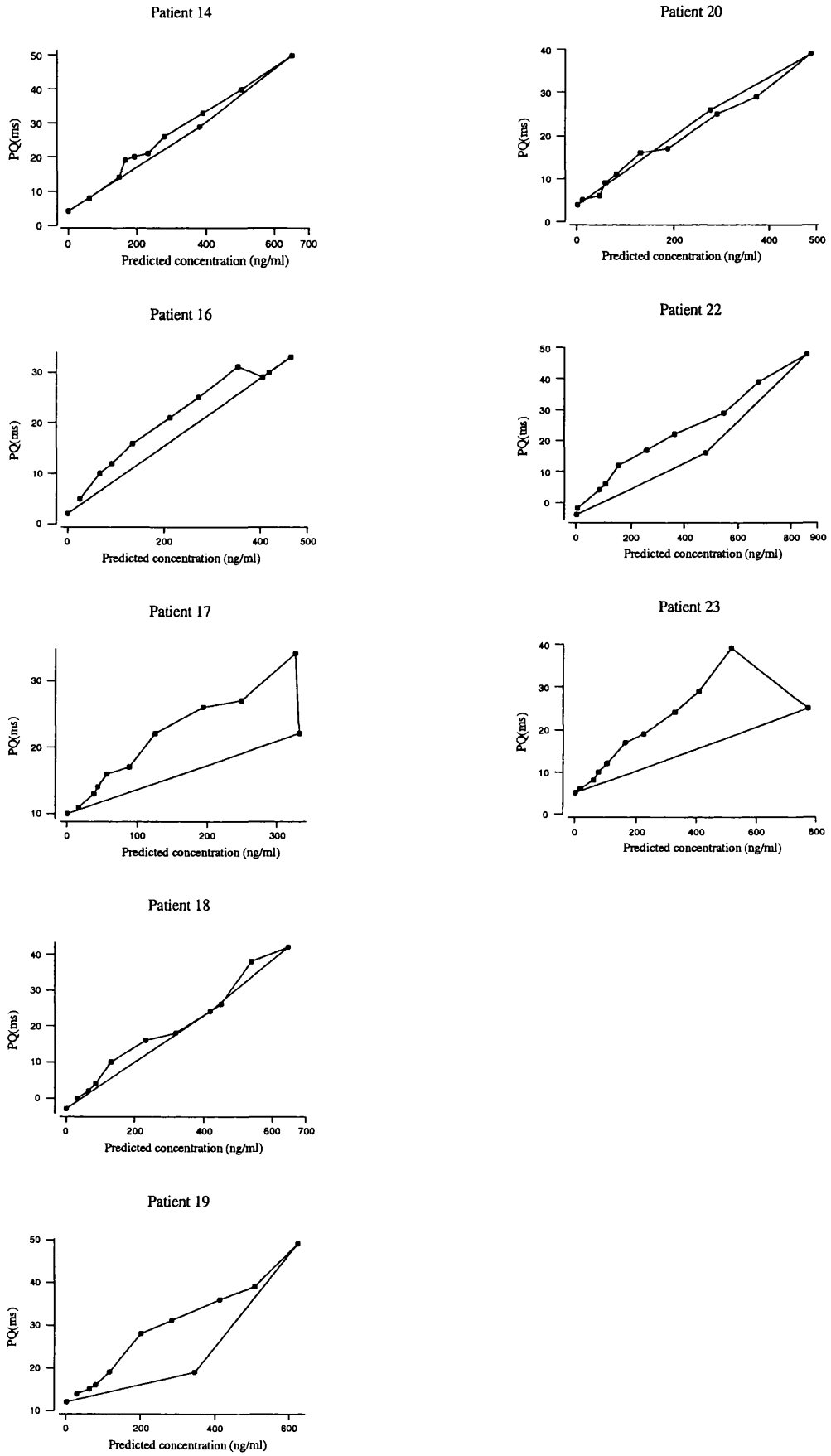

Figure 3.7.1.m Time-course of response (Δ PQ interval) to a single dose of verapamil using the linear model, for patients 1 to 13 (● measured data; ○ predicted response)

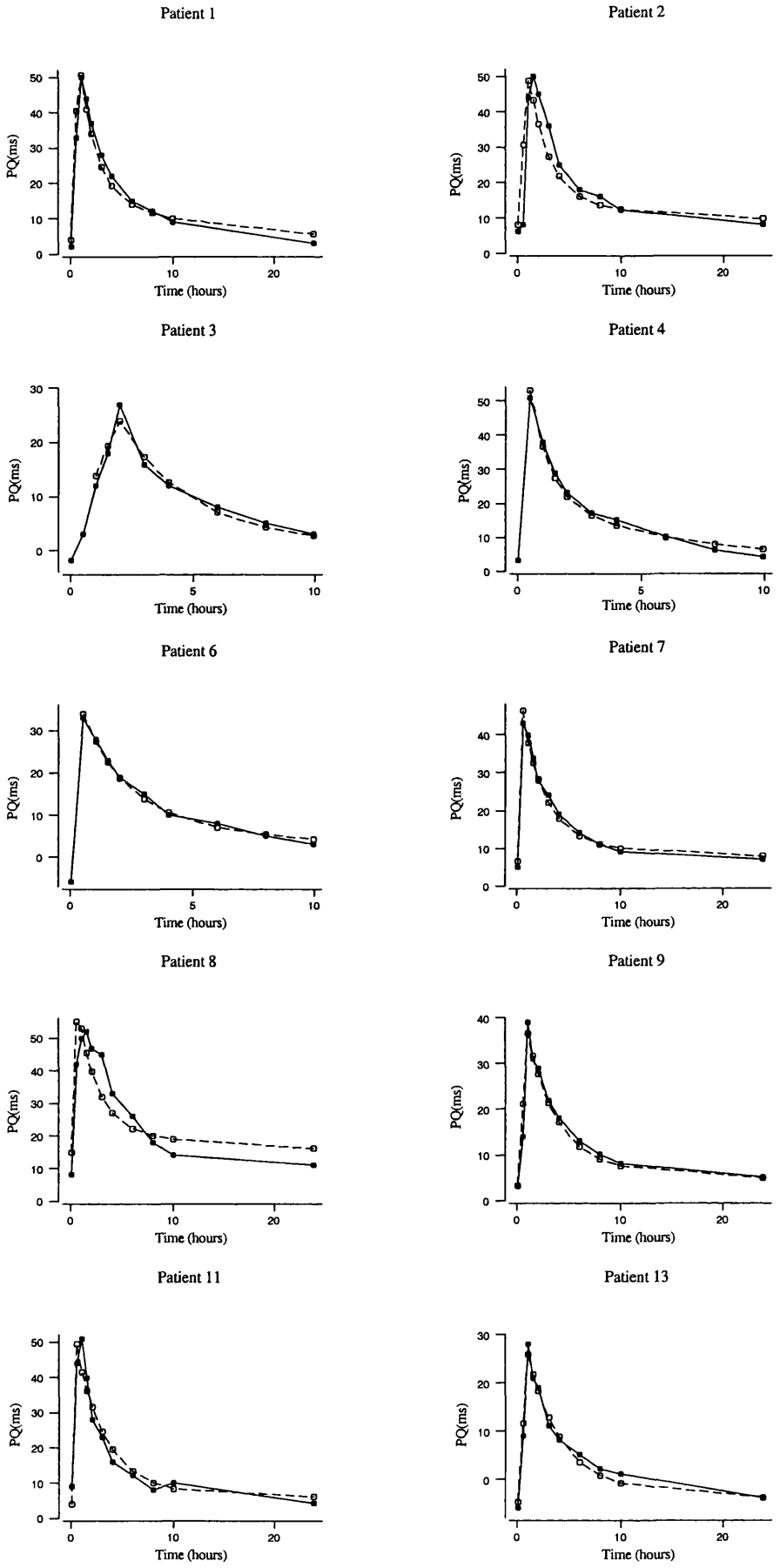

Figure 3.7.1.m (Cont.) Time-course of response (Δ PQ interval) to a single dose of verapamil using the linear model, for patients 14 to 23 (● measured data; ○ predicted response)

Patient 14

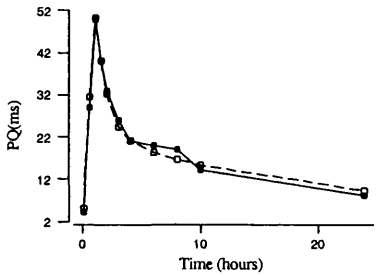

Patient 20

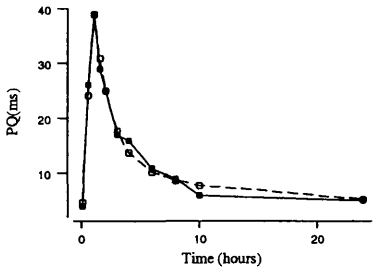

Patient 16

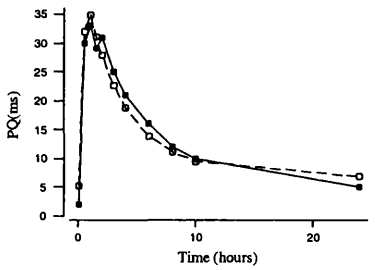

Patient 22

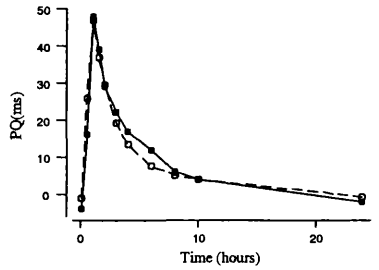

Patient 17

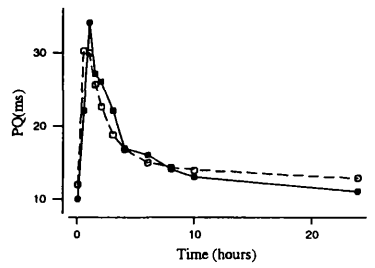

Patient 23

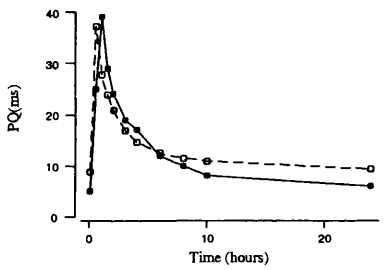

Patient 18

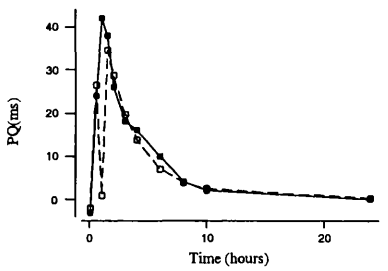

Patient 19

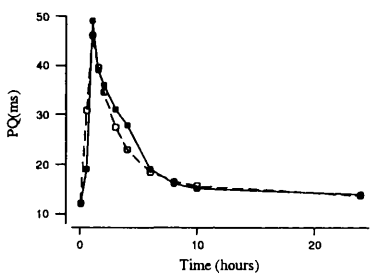

Table 3.7.1.h Parameter estimates from the linear and S0 models for changes in heart rate after a single dose of verapamil (240 mg)

	LINEAR MODEL[a]				S0 MODEL[b]					
ID	**m**	**cv%**	**AIC**	**R^2**	**Emax**	**cv%**	**S0**	**cv%**	**AIC**	**R^2**
1	-0.0121	9.2	38.0	0.92	-12.3	19.2	-0.0311	24.4	27.1	0.95
2	-0.0232	16.3	63.6	0.79	-14.1	17.7	-0.216	67.9	55.7	0.78
3	-0.0388	14.0	33.1	0.88	-10.0	10.6	-0.217	30.9	17.1	0.87
4	-0.0298	18.5	55.0	0.78	-19.8	2.9	-0.207	7.9	12.3	0.76
6	-0.0354	11.4	45.6	0.90	-21.7	9.3	-0.117	15.5	24.2	0.86
7	-0.0186	11.3	43.0	0.89	-10.0	7.3	-0.083	15.9	17.0	0.98
8	-0.0128	15.6	56.6	0.81	-11.0	4.0	-0.138	15.9	18.6	0.98
9	-0.0527	10.0	59.6	0.91	-24.2	17.7	-0.184	32.7	50.2	0.94
11	-0.0174	13.6	56.9	0.84	-13.5	8.0	-0.118	24.5	33.3	0.97
13	-0.0253	7.2	34.3	0.95	-12.0	6.8	-0.071	10.0	6.4	0.99
14	-0.0384	11.2	61.5	0.88	-21.0	5.5	-0.172	12.9	25.6	0.99
16	-0.0173	14.1	44.9	0.83	-10.0	31.4	-0.0546	50.3	38.7	0.86
17	-0.0399	14.6	54.5	0.82	-11.7	10.0	-0.265	27.7	34.5	0.93
18	-0.0442	9.4	61.3	0.92	-29.0	7.6	-0.156	13.9	35.9	0.99
19	-0.0408	9.3	57.6	0.92	-26.9	13.5	-0.125	20.9	42.6	0.97
20	-0.0463	11.4	58.4	0.88	-20.3	5.6	-0.198	11.8	25.6	0.99
22	-0.0272	12.1	61.0	0.87	-19.5	8.8	-0.147	23.1	38.8	0.97
23	-0.0198	18.8	58.6	0.74	-11.5	9.6	-0.157	28.6	33.8	0.94

[a] Equation 1.17; Chapter 1; [b] Equation 3.1, Chapter 3.

Key: Emax is the maximum effect; m is the slope of linear model; S0 is Emax/EC50; AIC is the Akaike Information Criterion and R^2 coefficient of determination

Table 3.7.1.i Parameter estimates from the S0 model with a link model for changes in heart rate after a single dose of verapamil (240 mg)

	LINK MODEL[a]								
ID	**Emax**	**cv%**	**S0**	**cv%**	**KEO**	**cv%**	**AIC**	**ΔAIC**	**R^2**
1	-12.2	20.8	-0.0245	26.6	99.9	1780.3	29.4	2.2	0.95
2	-19.2	19.7	-0.117	34.5	0.81	38.2	46.8	-8.9	0.92
3	-12.9	46.6	-0.132	60.0	0.84	60.6	47.5	30.5	0.94
4	-20.3	7.5	-0.1845	20.4	4.74	108.2	35.4	23.1	0.99
6	-24.6	14.8	-0.0956	18.2	3.16	38.8	32.5	8.4	0.99
7	-9.59	15.1	-0.191	40.8	51.4	12084.9	19.0	2.0	0.98
8	-11.0	4.4	-0.130	17.8	10.6	327.6	20.4	1.8	0.98
9	-25.3	18.0	-0.180	30.3	4.19	76.8	50.1	-0.1	0.95
11	-13.6	8.9	-0.397	30.4	5.42	336.7	35.1	1.8	0.97
13	-12.2	6.2	-0.070	8.7	10.6	46.1	4.16	-2.2	0.99
14	-21.2	5.8	-0.170	13.1	10.3	92.1	26.6	1.0	0.99
16	-11.5	27.5	-0.052	31.1	1.28	37.3	29.6	-9.1	0.96
17	-12.0	11.2	-0.247	29.5	4.27	135.1	35.6	1.1	0.94
18	-29.6	8.4	-0.147	14.8	78.5	896.3	38.0	2.1	0.99
19	-28.1	12.3	-0.124	17.3	4.52	45.1	40.0	-2.7	0.99
20	-20.6	6.0	-0.193	11.8	9.90	80.1	26.3	0.7	0.99
22	-21.3	5.9	-0.124	12.0	3.13	28.2	27.9	-10.9	0.99
23	-12.3	14.2	-0.115	34.2	1.84	76.5	33.9	0.1	0.95

[a] Equation 3.2, Chapter 3.

Key: Emax is the maximum effect; S0 is Emax/EC50; Keo is the constant rate for drug loss from the effect compartment; and AIC is the Akaike Information criterion; R^2 coefficient of determination. and ΔAIC is the difference in AIC between S0 model with and without effect compartment

Table 3.7.1.j Parameter estimates from the Emax and linear models for changes in PQ interval after a single dose of verapamil (240 mg)

	EMAX MODEL						LINEAR MODEL			
ID	**Emax**	**cv%**	**EC50**	**cv%**	**AIC**	**R^2**	**m**	**cv%**	**AIC**	**R^2**
1	100	23.3	966	36.9	52.9	0.98	0.0629	4.5	58.4	0.98
2	78.0	53.2	585	98.5	78.5	0.83	0.0661	11.3	78.5	0.85
3	*	*	*	*	*	*	0.0844	3.9	25.1	0.72
4	*	*	*	*	*	*	0.0635	4.0	41.0	0.84
6	100	17.1	1266	22.8	19.0	0.99	0.0580	2.4	26.3	0.88
7	77.4	17.3	488	30.3	49.7	0.99	0.838	5.9	61.6	0.99
8	63.3	10.7	274	30.5	63.7	0.96	0.0579	11.7	83.4	0.88
9	100	54.6	868	74.9	55.5	0.96	0.0828	4.7	52.9	0.97
11	100	49.8	1164	77.2	66.9	0.94	0.0544	5.9	63.6	0.96
13	100	185.4	1480	224.	59.3	0.98	0.0568	8.0	54.2	0.98
14	100	20.5	781	31.0	49.2	0.98	0.0819	3.7	53.8	0.99
16	53.4	8.4	307	16.9	33.9	0.99	0.0792	5.5	57.8	0.97
17	32.5	14.3	56.4	46.7	62.1	0.88	0.105	14.3	75.5	0.89
18	100	55.8	1125	78.5	57.8	0.98	0.0633	3.4	46.5	0.99
19	54.3	25.2	211	62.6	72.3	0.86	0.0839	10.5	76.1	0.93
20	81.7	27.0	605	41.1	48.3	0.98	0.0849	5.2	54.3	0.99
22	*	*	*	*	*	*	0.0539	5.2	57.7	0.97
23	41.7	19.4	221	47.4	62.1	0.92	0.0557	14.1	74.9	0.83

[a] Equation 1.18, Chapter ; [b] Equation 1.17, Chapter 1.

* Not estimated

Key: Emax is the maximum effect; EC50 is the concentration that produces half of Emax effect; m is the slope of linear model; AIC is the Akaike Information Criterion.and R^2 coefficient of determination

3.7.1.3 Diltiazem

Blood Pressure - The plots for DBP against the predicted concentration for patient 16 failed to show signs of hysteresis, as illustrated in Figure 3.7.1.n. These plots show that an S0 model could satisfactorily describe the decrease in DBP and the parameter estimates are shown in Table 3.7.1.l. The S0 model was fitted to the data and the results were compared with the linear model (Table 3.7.1.l). The link model was used for patients 3, 4, 6, 11, 16 and 18, Table 3.7.1.m. Plots for the time course of action for the decrease in blood pressure are shown in Figure 3.7.1.o. The DBP measured at 10 hours after the dose in patient 18 was unexpectedly low and was not predicted by the model (Figure 3.7.1.o).

Heart Rate - The profile of the decrease in heart rate with predicted concentration is shown in Figure 3.7.1.p and was best described using the S0 model (Table 3.7.1.n). The existence of hysteresis could not clearly be identified in the plots although the link model was necessary for patients 2, 4 and 18 (Table 3.7.1.o). Figure 3.7.1.q shows the predicted and measured time course of effect for each patient. The fall in HR for patient 17 was very small, causing problems in the convergence of the algorithm for the S0 model.

PQ interval – The changes in PQ interval (Figure 3.7.1.r) were best described by a linear model and the results from this model are shown in Table 3.7.1.p.

Figure 3.7.1.n Decrease in DBP against predicted concentrations of diltiazem (single-dose study) for patients 1 to 13

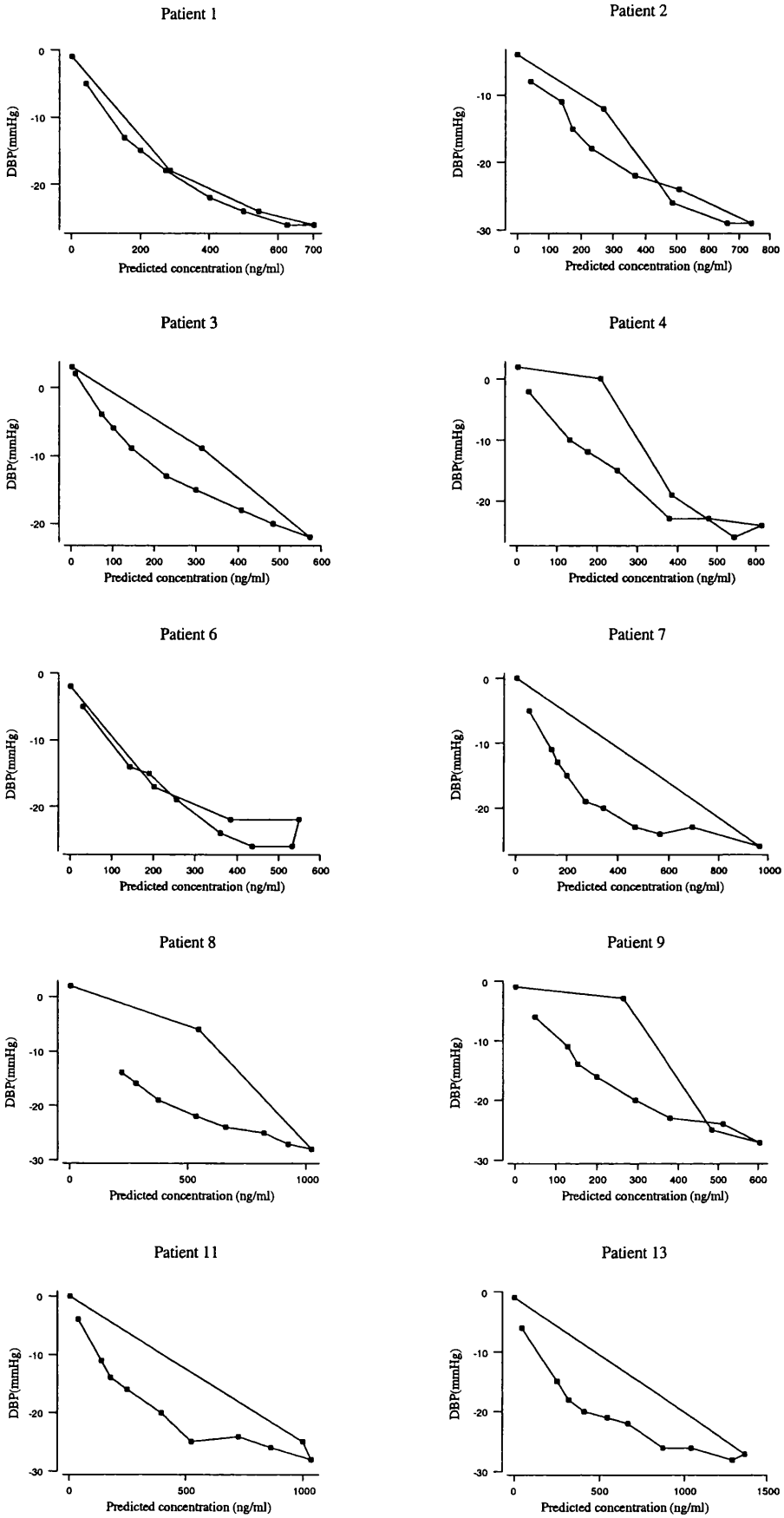

Figure 3.7.1.n (Cont.) Decrease in DBP against predicted concentrations of diltiazem (single-dose study) for patients 14 to 23

Patient 14

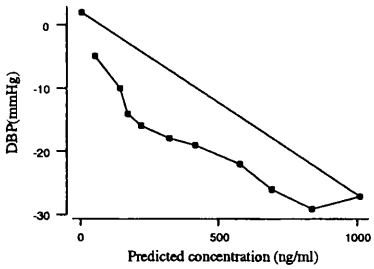

Patient 20

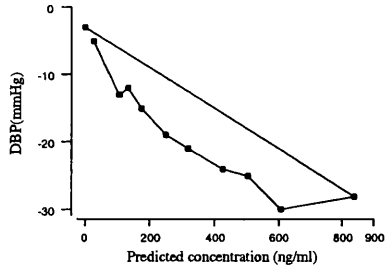

Patient 16

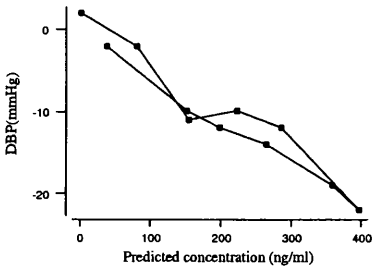

Patient 22

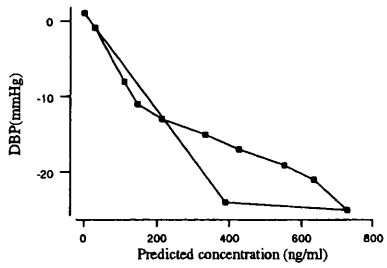

Patient 17

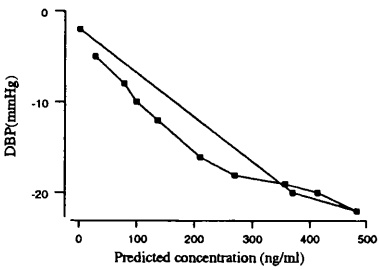

Patient 23

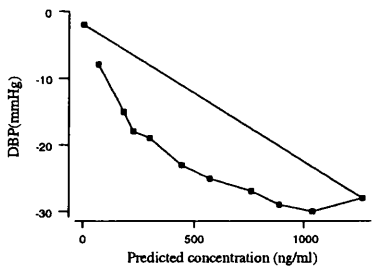

Patient 18

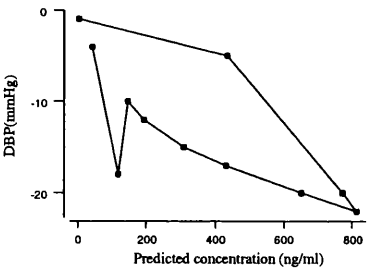

Patient 19

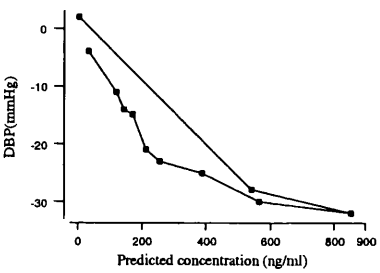

Figure 3.7.1.o Time-course of response (Δ DBP) to a single dose of diltiazem using the S0 model for patients 1 to 13 (● measured data; ○ predicted response) .

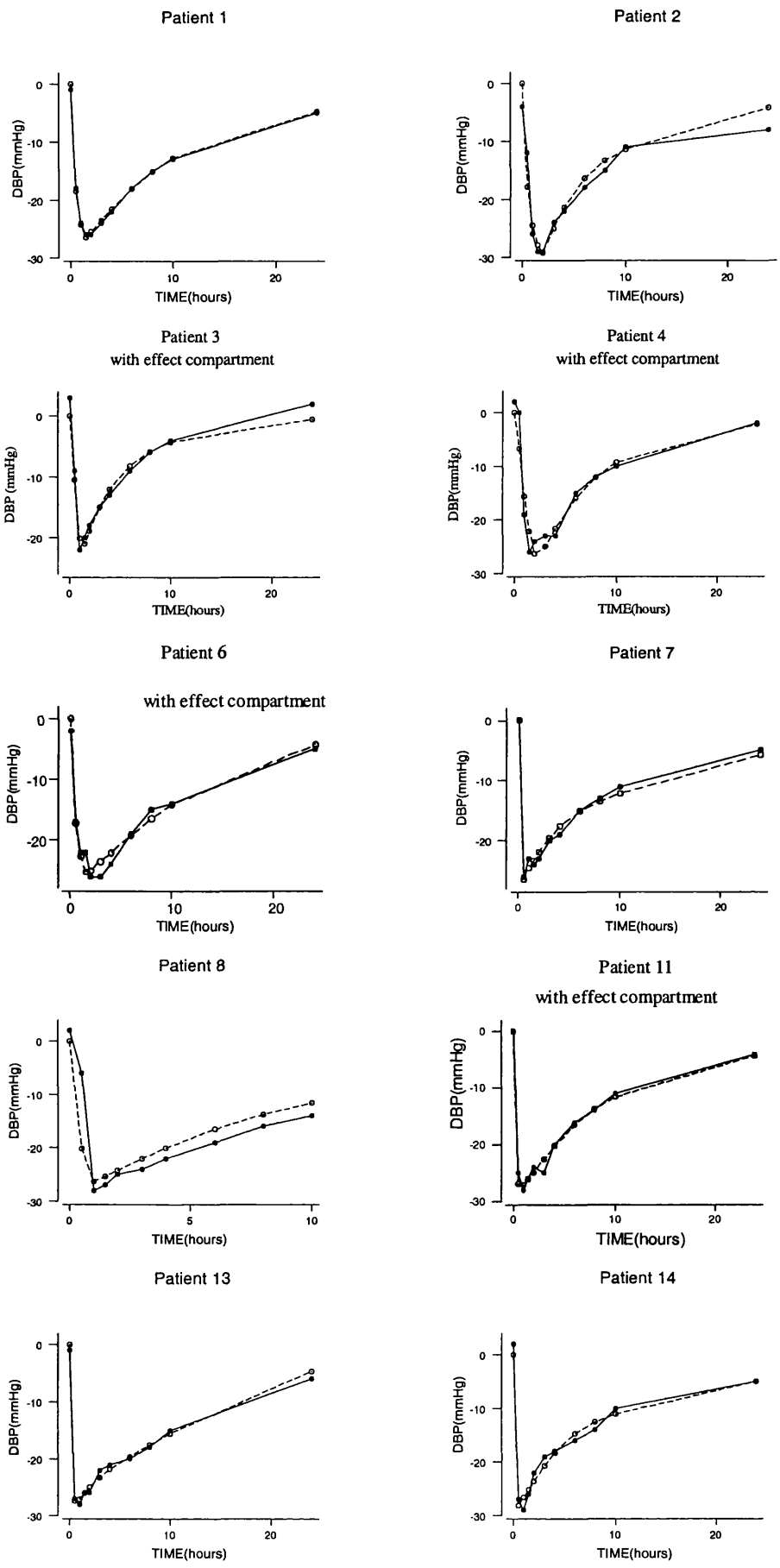

Figure 3.7.1.o (Cont.) Time-course of response (Δ DBP) to a single dose of diltiazem using the S0 model, for patients 16 to 23 (● measured data; ❍ predicted response)..

Patient 16
with effect compartment

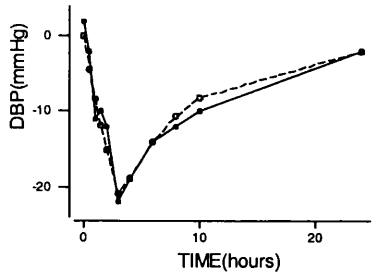

Patient 17

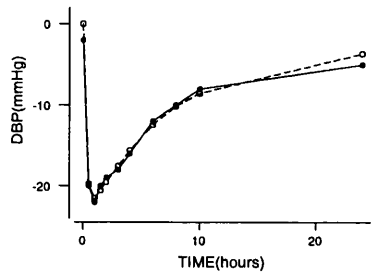

Patient 18
with effect compartment

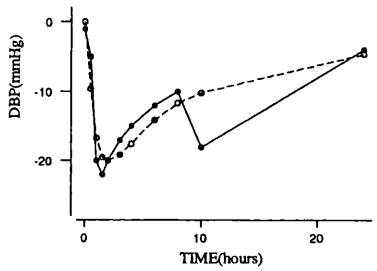

Patient 19

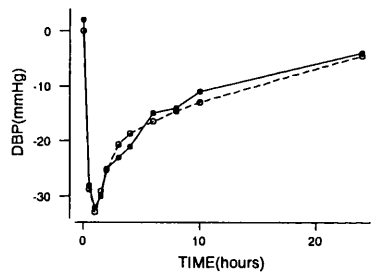

Patient 20

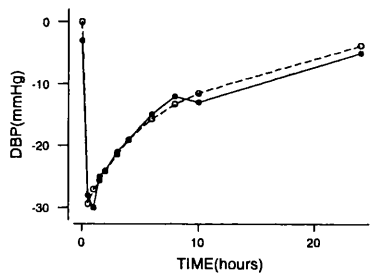

Patient 22

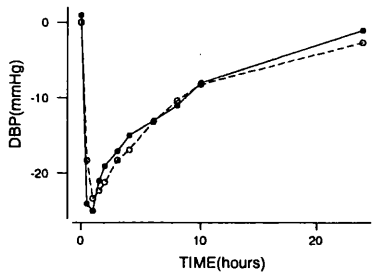

Patient 23

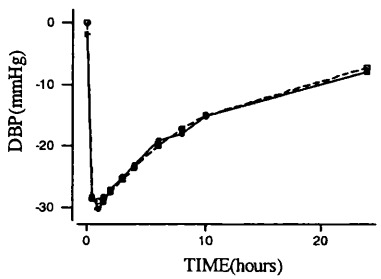

Figure 3.7.1.p Decrease in HR against predicted concentrations of diltiazem (single-dose study) for patients 1 to 13

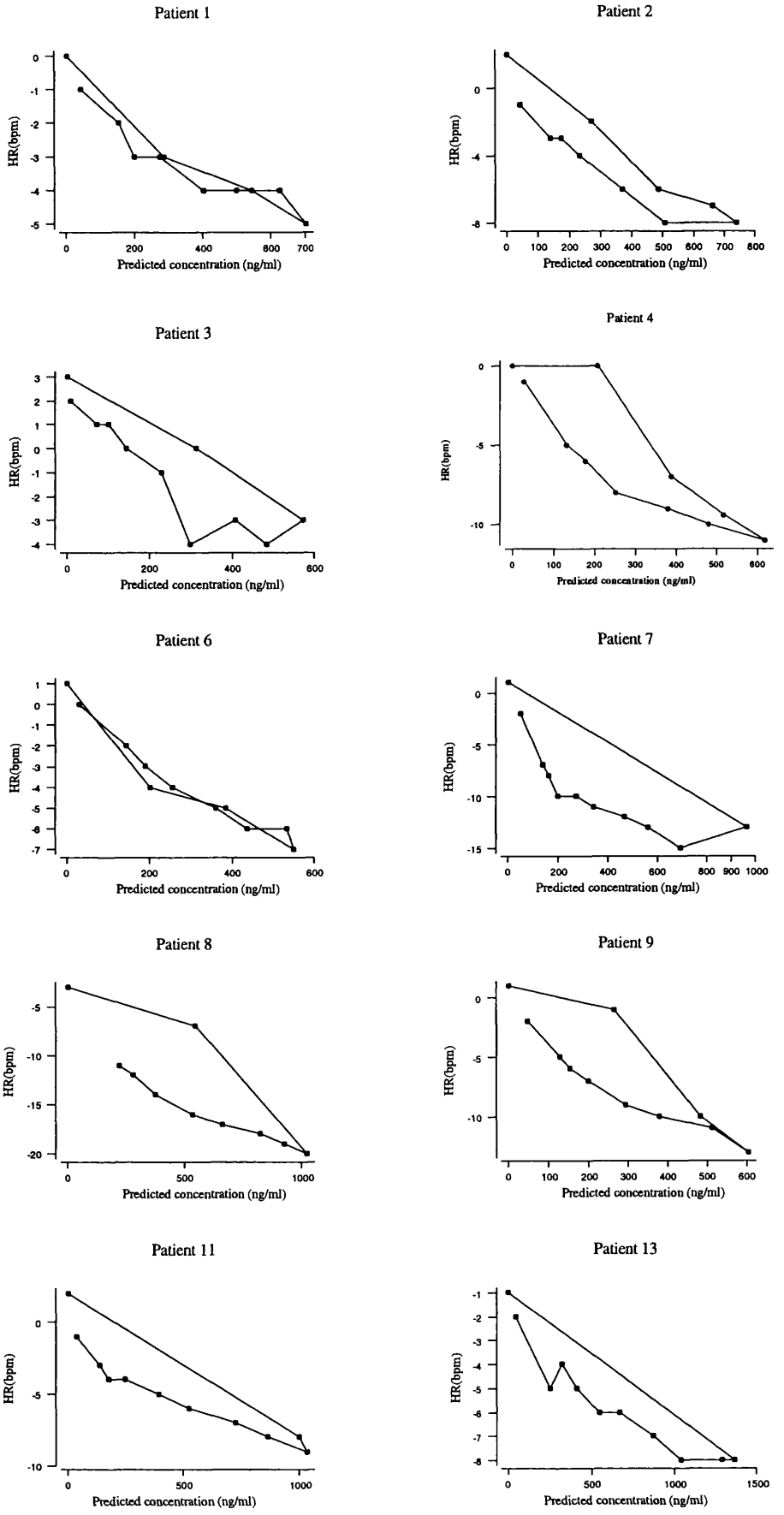

Figure 3.7.1.p (Cont.) Decrease in heart rate against predicted concentrations of diltiazem (single-dose study) for patients 14 to 23

Patient 14

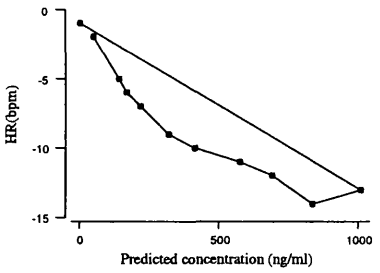

Patient 20

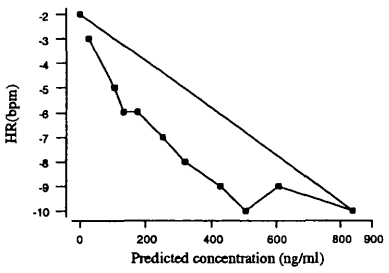

Patient 16

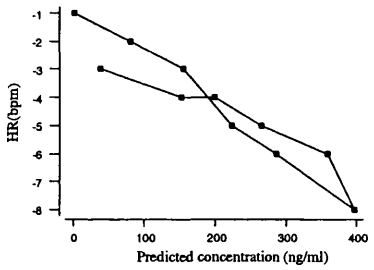

Patient 22

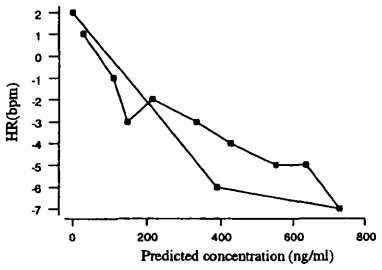

Patient 17

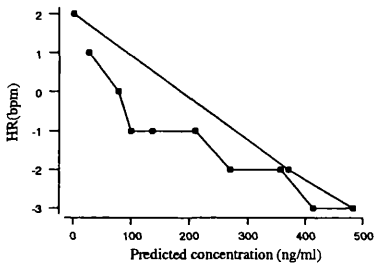

Patient 23

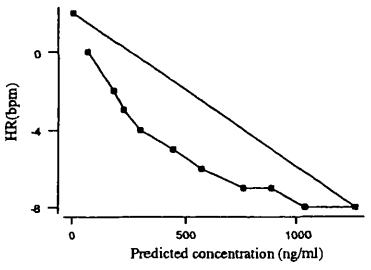

Patient 18

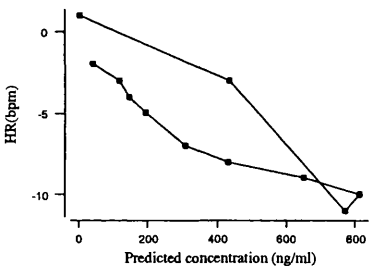

Patient 19

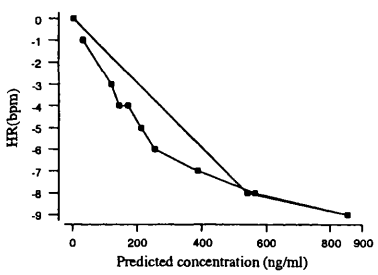

Figure 3.7.1.q Time-course of response (Δ HR) to a single dose of diltiazem using the S0 model, for patients 1 to 14 (● measured data; ○ predicted response)

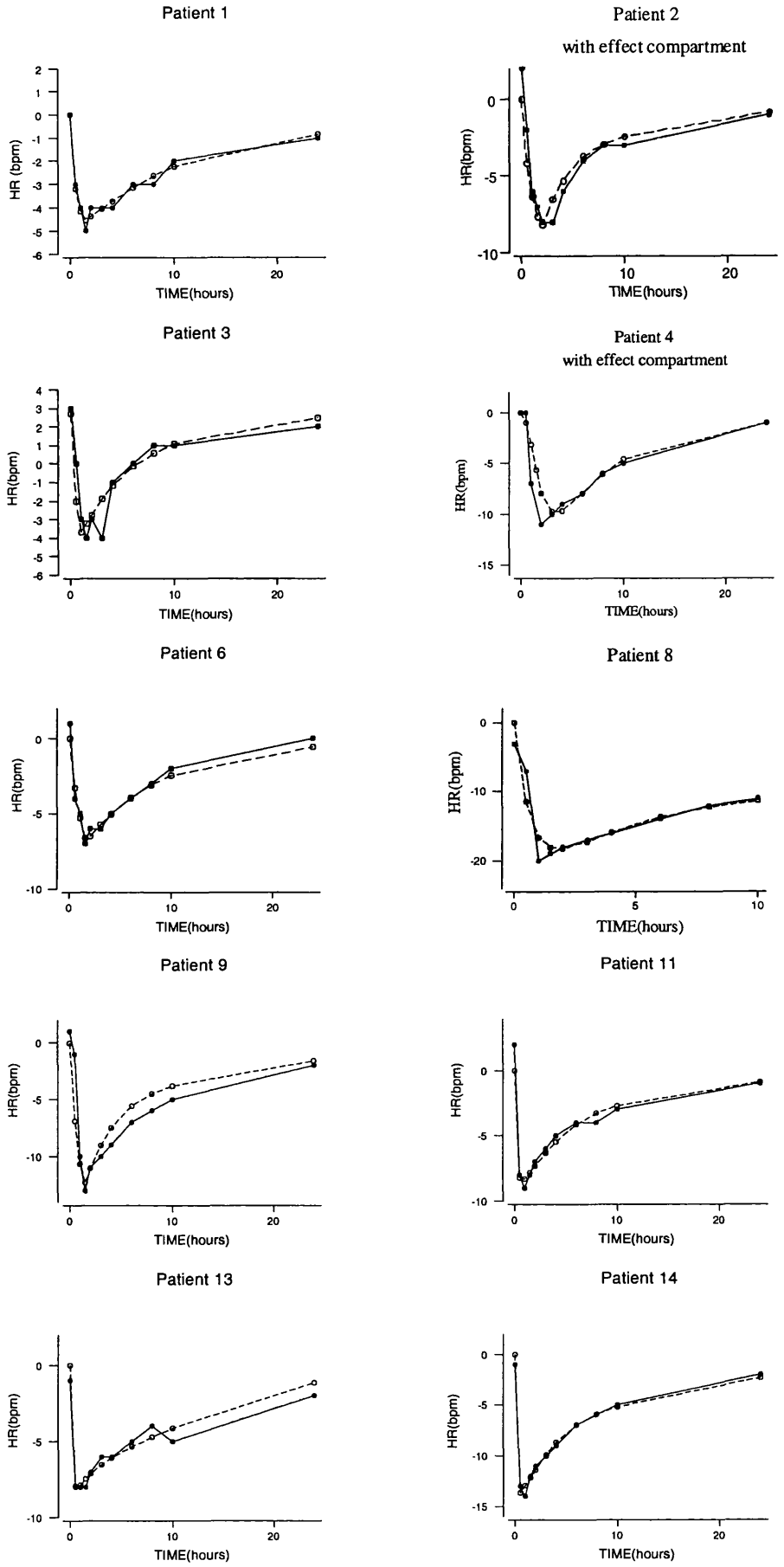

Figure 3.7.1.q (Cont.) Time-course of response (Δ HR) to a single dose of diltiazem using the S0 model, for patients 16 to 23 (● measured data; ○ predicted response)

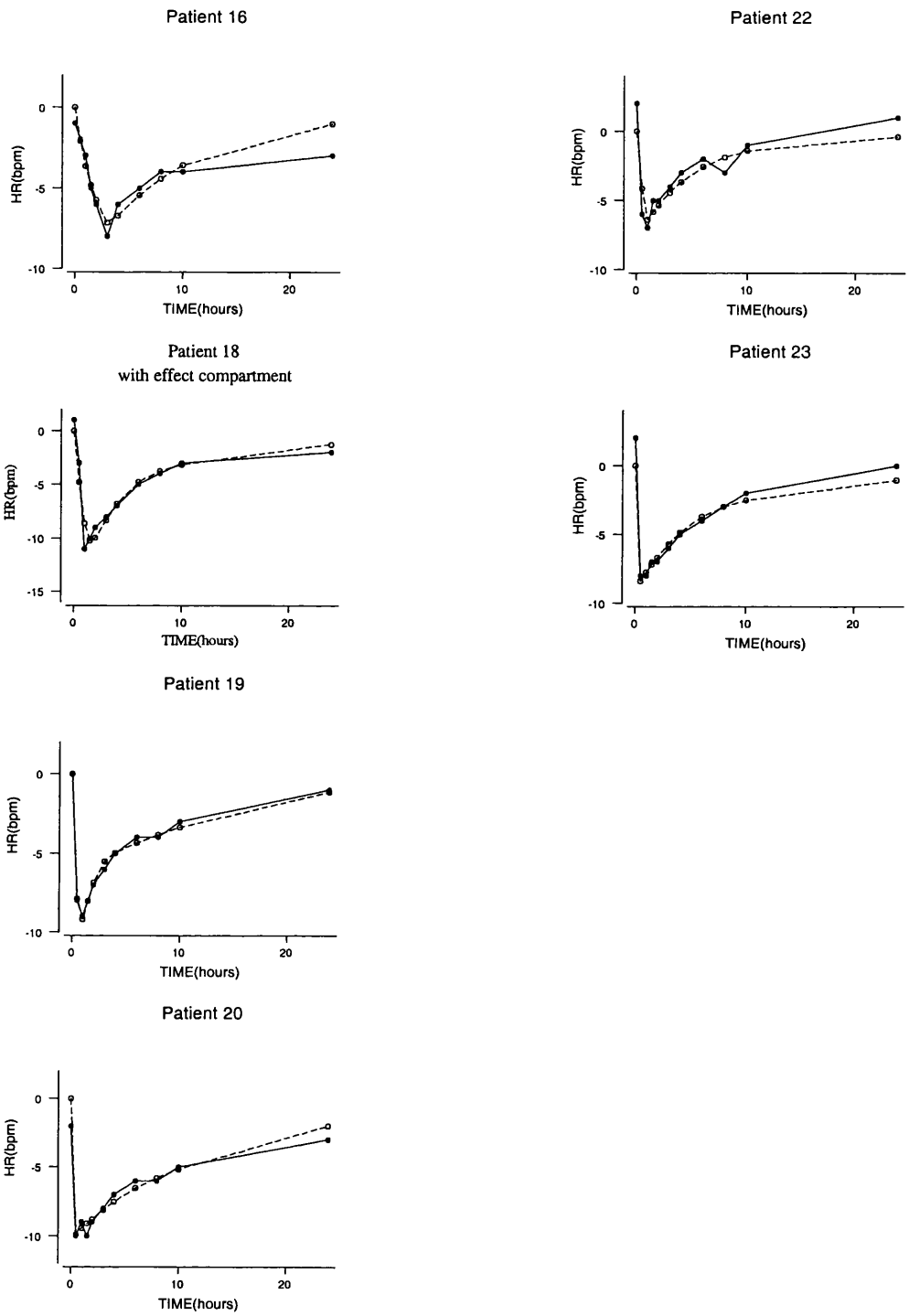

Figure 3.7.1.r Changes in PQ interval against predicted concentrations of diltiazem (single-dose study) for patients 1 to 13

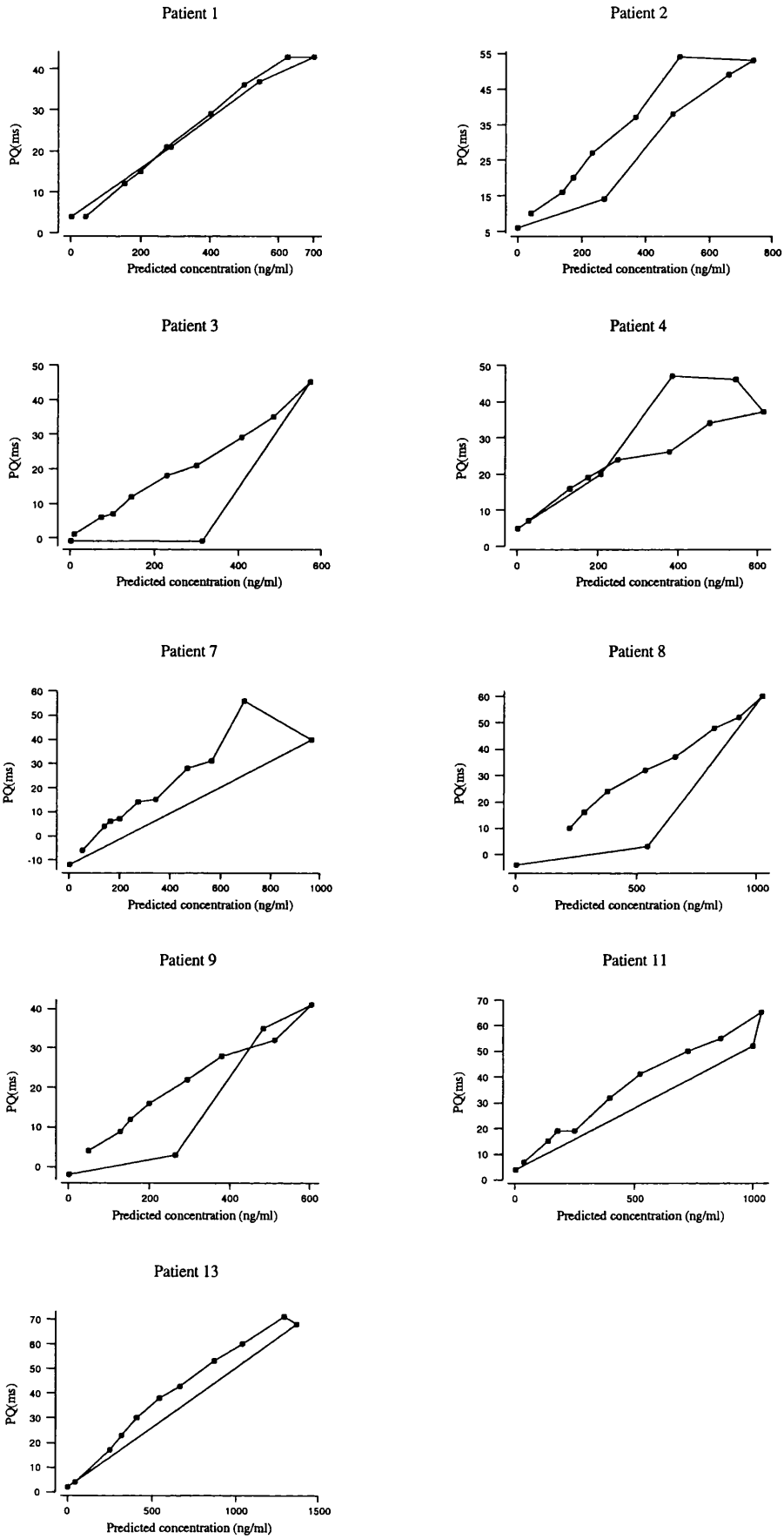

Figure 3.7.1.r (Cont.) Changes in PQ interval against predicted concentrations of diltiazem (single-dose study) for patients 14 to 23

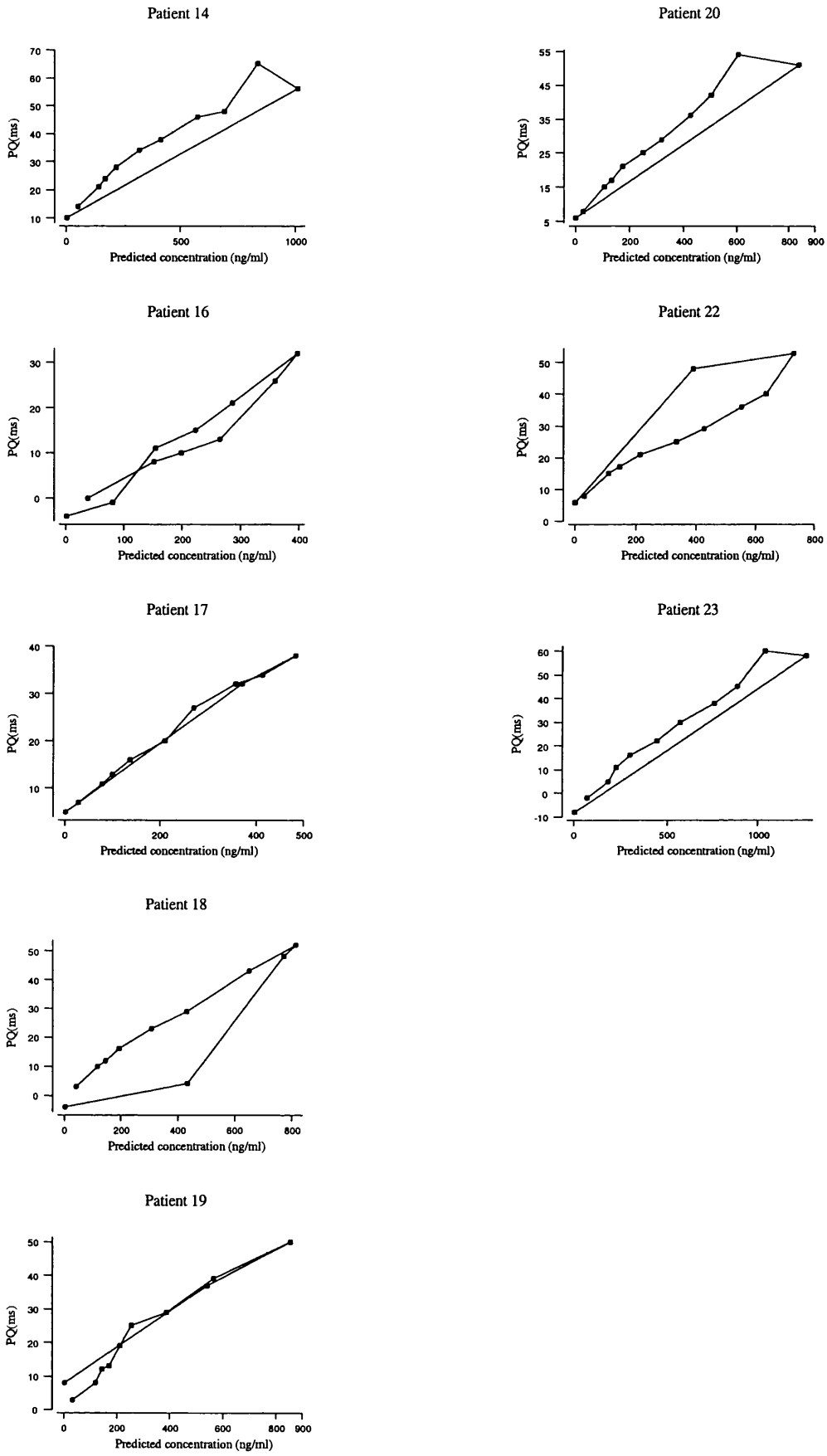

Table 3.7.1.1 Parameter estimates from the linear and S0 models for changes in blood pressure after a single dose of diltiazem (240 mg)

	LINEAR MODEL[a]				S0 MODEL[b]					
ID	**m**	**cv%**	**AIC**	**R^2**	**Emax**	**cv%**	**S0**	**cv%**	**AIC**	**R^2**
1	-0.0461	7.1	59.9	0.95	-37.6	3.1	-0.127	4.4	13.0	0.99
2	-0.0476	7.7	62.2	0.96	-45.5	19.0	-0.109	20.9	51.5	0.96
3	-0.0417	6.2	48.2	0.95	-57.1	53.3	-0.061	23.4	47.2	0.97
4	-0.0467	8.0	59.7	0.91	-89.6	105.6	-0.062	33.8	60.8	0.91
6	-0.0555	7.8	61.8	0.92	-35.0	10.9	-0.165	17.6	40.8	0.98
7	-0.0378	11.6	68.7	0.86	-32.9	4.5	-0.139	8.0	27.9	0.99
8	-0.0308	10.1	60.3	0.81	-40.2	40.4	-0.074	49.3	58.6	0.73
9	-0.0507	9.2	63.7	0.87	-52.3	53.3	-0.089	37.3	63.0	0.87
11	-0.0310	10.0	67.5	0.90	-33.8	4.5	-0.129	9.5	31.2	0.99
13	-0.0258	10.4	69.5	0.89	-33.0	3.5	-0.119	8.6	26.5	0.99
14	-0.0355	9.4	65.5	0.91	-37.2	7.3	-0.112	11.6	37.8	0.99
16*	**-0.0528**	**4.8**	**41.8**	**0.96**	**-611**	**5.8**	**-0.054**	**10.7**	**43.8**	**0.96**
17	-0.0543	7.3	55.6	0.96	-30.3	6.3	-0.154	9.5	26.1	0.99
18	-0.0298	14.5	68.4	0.73	-20.8	21.8	-0.182	65.0	63.2	0.76
19	-0.0512	10.5	70.0	0.89	-43.7	7.0	-0.154	9.9	38.4	0.99
20	-0.0470	10.3	68.1	0.92	-38.0	7.7	-0.155	12.5	39.9	0.99
22	-0.0390	8.13	59.0	0.91	-34.4	18.4	-0.099	23.7	47.9	0.96
23	-0.0316	11.5	72.8	0.88	-35.3	3.7	-0.151	8.7	30.6	0.99

[a] Equation 1.17; Chapter 1; [b] Equation 3.1 Chapter 3 * inrrealistic parameter estimates.

Key: Emax is the maximum effect; m is the slope of linear model. S0 is from Emax/EC50; AIC is the Akaike Information Criterion. Patient 16 in bold because unrealistic parameters estimates were obtained and R^2 coefficient of determination

Table 3.7.1.m Parameter estimates from the S0 model with a link model for changes in blood pressure after a single dose of diltiazem (240 mg)

	LINK MODEL[a]								
ID	**Emax**	**cv%**	**S0**	**cv%**	**Ke0**	**cv%**	**AIC**	**ΔAIC**	**R^2**
1	-34.3	7.1	-0.252	11.9	0.78	12.2	31.5	18.4	0.99
2	-79.9	58.1	-0.0829	23.2	0.67	18.7	52.5	1.0	0.97
3	-65.6	46.7	-0.0606	17.3	5.18	37.3	41.4	-5.8	0.99
4	-64.6	51.9	-0.0780	27.0	2.75	46.2	55.3	-5.4	0.96
6	-33.3	8.1	-0.179	15.6	12.7	103.5	38.6	-2.3	0.99
7	-39.3	19.8	-0.285	21.1	1.39	33.1	47.8	20.0	0.97
8	-60.0	86.6	-0.284	42.4	0.45	32.8	61.0	2.4	0.94
9	-30.0	70.0	-0.381	89.4	0.51	82.4	69.0	6.0	0.82
11	-34.9	4.3	-0.120	8.3	6.89	40.2	28.3	-3.0	0.99
13	-33.1	3.9	-0.117	9.5	16.5	144.5	28.2	20.5	0.99
14	-38.4	8.7	-0.107	12.7	12.4	110.8	39.0	1.2	0.99
16	-17.6	62.6	-0.0297	31.9	98.7	2065.4	27.6	-16.2	0.93
17	-30.1	6.6	-0.157	9.9	99.2	699.3	27.8	1.7	0.99
18	-26.1	23.3	-0.131	41.3	1.25	56.6	58.6	-4.6	0.87
19	-44.5	7.5	-0.157	10.1	15.2	100.7	39.1	0.7	0.99
20	-38.9	9.2	-0.334	14.6	6.17	98.5	40.7	0.9	0.99
22	-34.4	19.8	-0.0990	25.3	99.4	1515.3	50.1	2.2	0.96
23	-35.5	3.8	-0.617	9.1	3.27	40.7	29.3	10.0	0.99

[a]Equation 3.2, Chapter 3.

Key: Emax is the maximum effect; S0 is Emax/EC50 and Keo is the constant rate for drug loss from the effect compartment; AIC is the Akaike Information Criterion; R^2 represents the coefficient of determination and ΔAIC is the difference in AIC between S0 model with and without effect compartment

Table 3.7.1.n Parameter estimates from the linear and S0 models for changes in heart rate after a single dose of diltiazem (240 mg)

	LINEAR MODEL[a]				S0 MODEL[b]					
ID	**m**	**cv%**	**AIC**	**R^2**	**Emax**	**cv%**	**S0**	**cv%**	**AIC**	**R^2**
1	-0.0079	7.4	22.1	0.93	-6.38	10.0	-0.022	14.8	0.64	0.98
2	-0.0123	8.0	33.4	0.91	-17.4	48.6	-0.020	29.3	31.7	0.94
3	-0.0061	28	38.9	0.88	-15.0	569.1	-0.0070	118	41.3	0.89
4	-0.0158	20.2	56.2	0.55	-10.5	65.3	-0.049	110	56.2	0.61
6	-0.013	19.2	52.3	0.92	-16.7	34.5	-0.020	17.0	14.6	0.99
7	-0.0209	13.0	58.2	0.81	-17.3	7.7	-0.089	15.6	28.5	0.98
8	-0.0226	9.7	53.3	0.76	-25.2	27.0	-0.068	45.5	48.3	0.77
9	-0.0225	9.1	45.6	0.87	-30.0	75.8	-0.034	37.2	46.2	0.87
11	-0.0074	7.8	35.4	0.92	-12.2	14.7	-0.025	20.3	23.0	0.97
13	-0.0171	9.6	40.3	0.93	-10.0	9.6	-0.028	19.6	18.6	0.98
14	-0.0199	9.1	48.9	0.93	-18.5	5.9	-0.051	8.70	15.9	0.99
16	-0.0062	6.2	26.2	0.95	-17.8	18.1	-0.029	17.2	25.6	0.93
17	-0.0141	14.1	22.2	0.93	*	*	*	*	*	-
18	-0.0141	9.1	41.6	0.89	-16.6	34.8	-0.030	34.1	39.1	0.91
19	-0.0169	9.5	39.5	0.92	-12.8	4.3	-0.038	5.50	-2.28	0.99
20	-0.0169	12.9	50.7	0.90	-11.5	8.3	-0.089	20.8	24.9	0.98
22	-0.0096	9.4	31.5	0.91	-16.74	89.4	-0.014	40.0	32.2	0.94
23	-0.0080	7.8	34.0	0.92	-13.9	20.9	-0.017	20.1	23.6	0.99

[a] Equation 1.17; Chapter 1; [b] Equation 3.1 Chapter 3.

* Not estimated

Key: Emax is the maximum effect; m is the slope of linear model. S0 is Emax/EC50; AIC represents the Akaike Information Criterion and R^2 coefficient of determination.

Table 3.7.1.o Parameter estimates from the S0 model with a link model for changes in heart rate after a single dose of diltiazem (240 mg)

	LINK MODEL[a]								
ID	**Emax**	**cv%**	**S0**	**cv%**	**Ke0**	**cv%**	**AIC**	**ΔAIC**	**R^2**
1	-5.81	13.5	-0.0451	23.2	-0.73	22.8	7.0	6.4	0.97
2	-40.0	173.4	-0.0183	30.5	0.60	22.3	29.6	-2.1	0.97
3	-78.4	2872.6	-0.0072	105.9	2.71	136.2	41.4	0.2	0.96
4	-35.4	194.6	-0.0310	59.2	0.68	49.5	50.6	-5.6	0.83
6	-12.7	26.6	-0.0226	20.7	99.9	1113.0	18.0	3.4	0.98
7	-22.3	22.9	-0.161	23.6	1.27	35.0	37.3	8.9	0.96
8	-48.0	67.5	-0.205	29.7	0.43	22.5	46.9	-1.4	0.93
9	-30.0	149.2	-0.102	53.8	-0.46	41.5	47.5	1.3	0.92
11	-12.49	17.1	-0.0245	22.4	20.7	284.6	25.0	2.0	0.98
13	-10.0	10.8	-0.0280	22.3	58.4	1252.3	20.7	2.1	0.98
14	-19.34	6.5	-0.0487	8.7	9.92	54.3	15.0	-0.9	0.99
16	-15.7	68.4	-0.0319	38.8	0.77	31.2	29.8	4.1	0.92
17	*	*	*	*	*	*	*	*	-
18	-17.5	25.3	-0.0312	23.3	2.73	41.3	32.9	-6.3	0.96
19	-12.8	4.7	-0.0443	5.9	99.4	450.3	-0.77	1.5	0.99
20	-11.5	38.4	-0.201	42.6	32.3	16989.5	27.3	2.1	0.97
22	-16.0	91.2	-0.0102	43.3	49.9	969.3	34.6	2.3	0.93
23	-14.7	28.5	-0.0701	24.1	4.26	74.8	24.6	1.1	0.99

[a] Equation 3.2, Chapter 3.

* Not estimated

Key: Emax is the maximum effect; S0 is Emax/EC50 and Keo is the rate constant for drug loss from the effect compartment; AIC is the Akaike Information Criterion; R^2 represents the coefficient of determination and ΔAIC is the difference in AIC between S0 model with and without effect compartment

Table 3.7.1.p Parameter estimates from the Emax and linear models for changes in PQ interval after a single dose of diltiazem (240 mg)

	EMAX MODEL[a]						LINEAR MODEL[b]			
ID	**Emax**	**cv%**	**EC50**	**cv%**	**AIC**	**R^2**	**m**	**cv%**	**AIC**	**R^2**
1	100	21.2	951	32.1	46.5	0.98	0.0680	2.7	47.0	0.99
2	100	36.2	684	61.3	70.1	0.93	0.0820	6.7	71.4	0.94
3	99.9	145.3	1120	197.5	75.7	0.85	0.0670	11.0	71.5	0.88
4	74.6	37.1	477	68.0	68.5	0.91	0.0790	8.2	72.0	0.89
6	78.1	24.8	417	46.7	61.5	0.97	0.0929	6.5	69.0	0.98
7	100	86.1	1250	126.7	78.0	0.95	0.0530	10.9	75.0	0.92
8	*	*	*	*	*	*	0.0530	8.8	68.6	0.84
9	100	84.3	1092	116.8	67.8	0.93	0.0661	6.8	62.9	0.94
11	100	15.1	761	28.9	58.3	0.98	0.0637	5.1	67.9	0.98
13	100	15.5	803	31.7	63.8	0.98	0.0567	3.6	63.6	0.99
14	84.8	14.6	446	32.1	64.9	0.97	0.0720	8.6	79.5	0.96
16	100	152.7	1200	189.3	61.9	0.97	0.0680	7.1	56.0	0.97
17	75.7	18.5	4500	30.8	45.2	0.99	0.0872	4.7	56.2	0.99
18	*	*	*	*	*	*	0.0605	8.6	72.3	0.91
19	100	22.9	913	35.6	54.7	0.98	0.0667	5.5	61.4	0.98
20	93.9	18.2	620	32.1	58.1	0.98	0.0604	7.1	71.0	0.93
22	84.8	38.2	592	68.4	70.3	0.92	0.0747	8.0	72.8	0.92
23	*	*	*	*	*	*	0.0504	4.1	60.6	0.98

[a] Equation 1.18, Chapter ; [b] Equation 1.17, Chapter 1.

* Not estimated

Key: Emax is the maximum effect; EC50 is the concentration that produces half of the Emax effect; m is the slope of linear model; AIC is the Akaike Information Criterion and R^2 coefficient of determination

The linear model produced predictions that were close to the measured effects, as shown in Figure 3.7.1.s.

3.7.1.4 Summary of Final Results: Single-Dose Study

After a single dose of mibefradil and for DBP the mean value of EC50 estimate obtained from the Emax model was (1012.1 ± 484.7 ng ml^{-1}). For verapamil was 320.4 ± 238.4 ng ml^{-1} and for diltiazem was 421.7 ± 292.3 ng ml^{-1}. The mean Emax values and the mean S0 values estimates for each drug are presented in Table 3.7.1q.

For heart rate, the EC50 estimate for mibefradil was 423.2 ± 202 ng ml^{-1}, for verapamil was 228.0 ± 87.4 ng ml^{-1} and for diltiazem was 567.1 ± 420.6 ng ml^{-1}. Table 3.7.1.q shows the result from the S0 model, Emax and S0 paramters estimates.

For mibefradil the EC50 estimates obtained from the Emax model, for changes in PQ interval was 2212.0 ± 724.0 ng ml^{-1}. Smaller values of EC50 were obtained for verapamil (693.3 ± 440.3 ng ml^{-1}) and diltiazem (788.6 ± 286.0 ng ml^{-1}). The results obtained for changes in PQ interval from the linear model are shown in Table 3.7.1.q

Figure 3.7.1.s Time-course of response (Δ PQ interval) to a single dose study of diltiazem using the linear model, for patients 1 to 13 (● measured data; ○ predicted response)

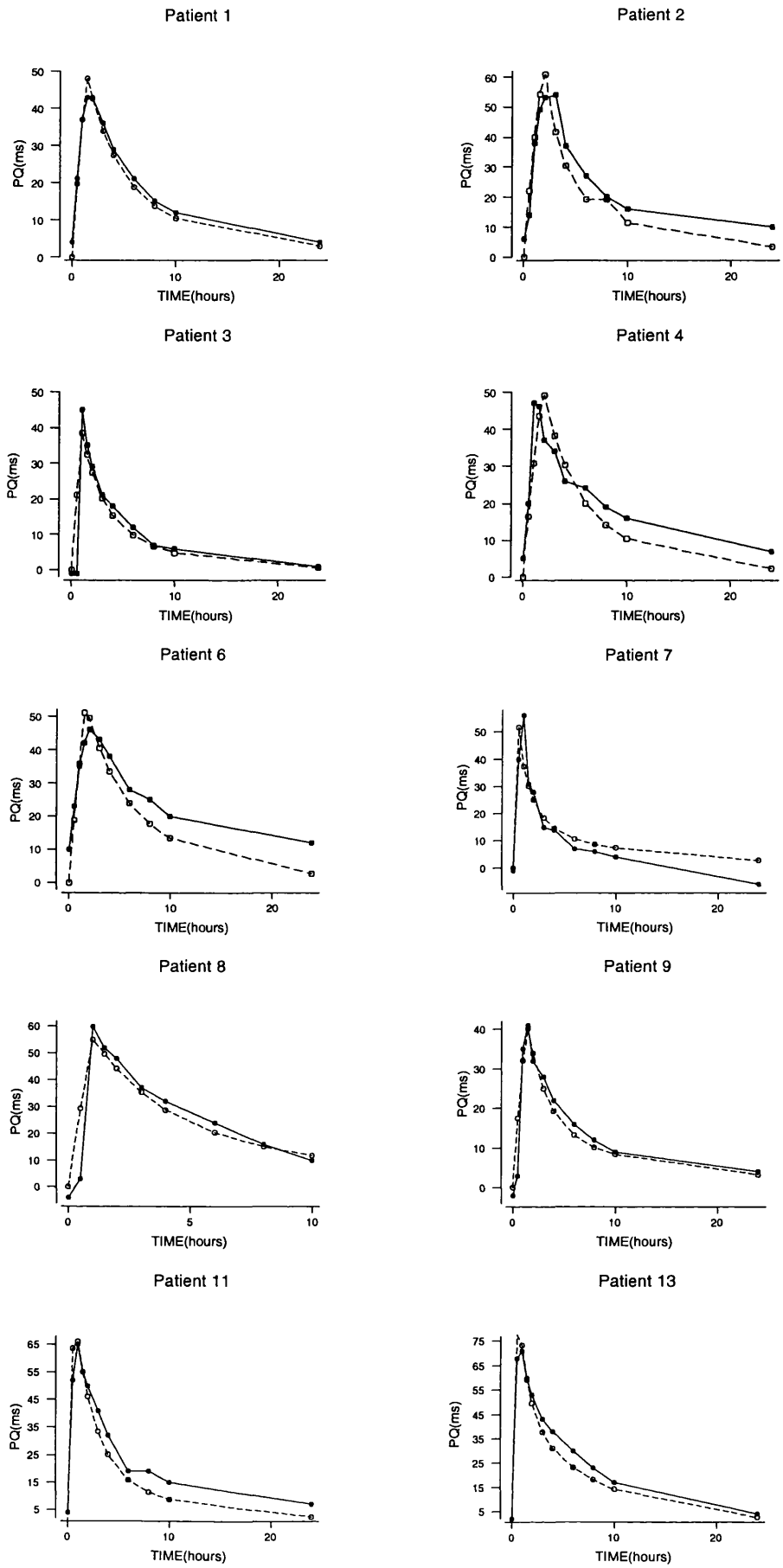

Figure 3.7.1.s (Cont.) Time-course of response (Δ PQ interval) to a single dose study of diltiazem using linear model, for patients 14 to 23 (● measured data; ○ predicted response)

Patient 14

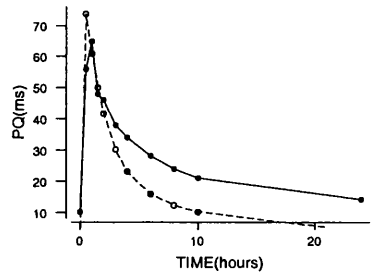

Patient 20

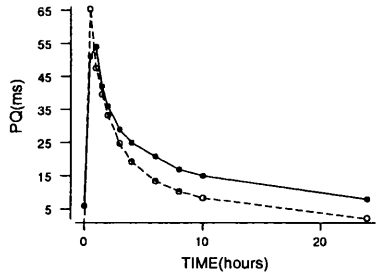

Patient 16

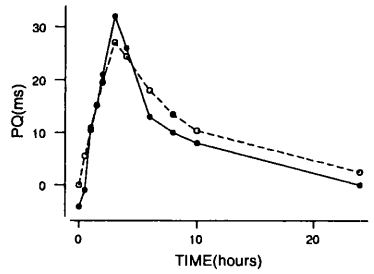

Patient 22

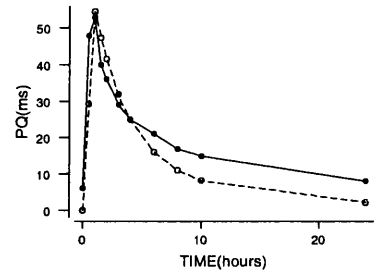

Patient 17

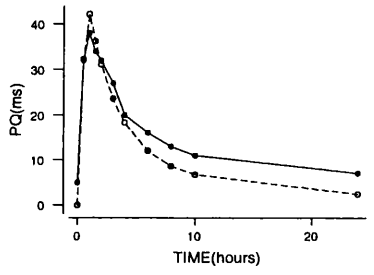

Patient 23

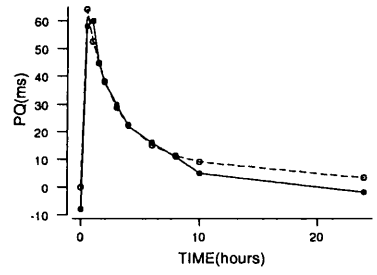

Patient 18

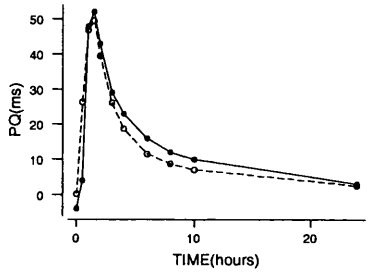

Patient 19

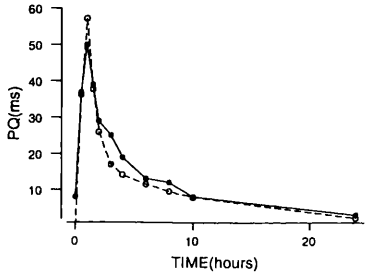

Table 3.7.1.q Mean values of parameter estimates from the best model for the single-dose study

		MIBEFRADIL	VERAPAMIL	DILTIAZEM
DBP (mmHg)	Emax	-31.2 ± 9.6	-39.2 ± 10.1	-40.3 ± 11.1
	S0	-0.033 ± 0.017	-0.183 ± 0.1	-0.148 ± 0.13
HR (bpm)	Emax	-14.8 ± 8.0	-17.1 ± 6.2	-18.6 ± 10.2
	S0	-0.039 ± 0.039	-0.139 ± 0.1	-0.0443 ± 0.05
PQ interval (msec)	m	0.013 ± 0.006	0.113 ± 0.2	0.108 ± 0.17

Values represent mean ± SD

Key: DBP represents the diastolic blood pressure; HR is the heart rate; Emax is the maximum effect and S0 is Emax/EC50.

3.7.2 PHARMACOKINETIC/PHARMACODYNAMIC RELATIONSHIPS: STEADY-STATE STUDY

3.7.2.1 Mibefradil

Blood Pressure - The pharmacokinetic/ pharmacodynamic relationship for mibefradil after multiple doses, was satisfactorily described by an Emax model without an intercept (Table 3.7.2.a). Better parameter estimates were obtained with the S0 model than with the Emax model and the link model provided no advantage. Figure 3.7.2.a shows the individual plots of measured and predicted values obtained from the S0 model for DBP against time and Figure 3.7.2.b shows the predicted response using S0 model.

Heart Rate - Inspection of the plots (Figure 3.7.2.c) and analysis of the results (Table 3.7.2.b) showed that the time course of action for the heart rate effect was best described by the Emax model. The magnitude of the decrease in heart rate was small, so the profile of the course of action was relatively flat (Figure 3.7.2.d). The S0 model proved to have advantages over the Emax model and the comparison of the results is shown in Table 3.7.2.b. The S0 model predicted an effect close to the measured one (Figure 3.7.2.d).

PQ interval - The superiority of the linear model over the Emax model was not marked, as shown in Table 3.7.2.c, and this was in agreement with the plots in Figure 3.7.2.e. Figure 3.7.2.f shows the predicted and measured effects with time. The plots for patients 6, 8, and 17 suggested that the linear model failed to describe the effect around 10 hours. However, the AIC values obtained from the linear and Emax models were similar suggesting that the Emax model offered no advantage for these patients. The estimation of EC50 from Emax model was bounded due to difficulties in converging.

Figure 3.7.2.a Decrease in DBP against predicted concentrations of mibefradil (steady-state study)

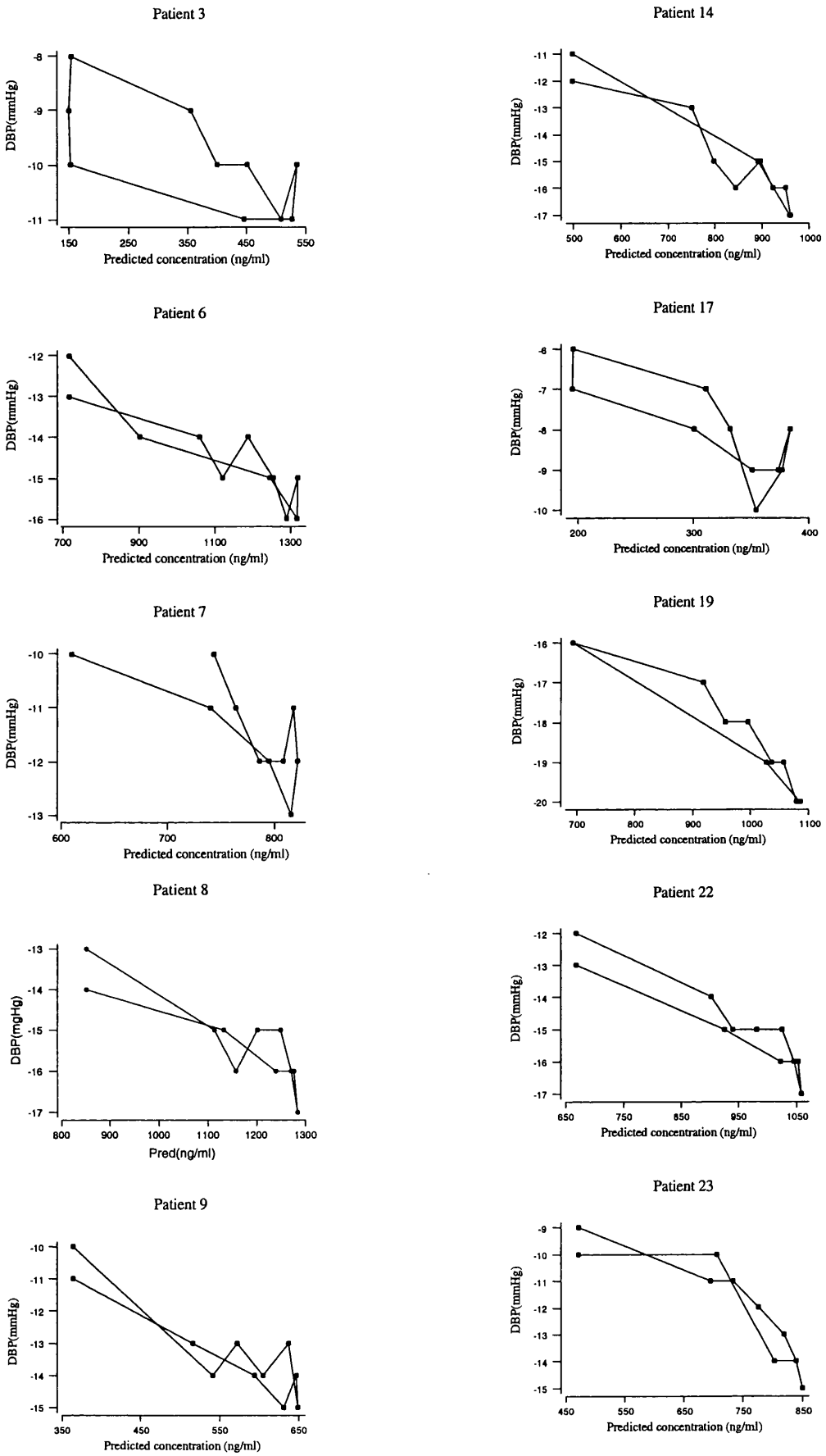

Figure 3.7.2.b Time course of response (Δ DBP) to multiple dose of mibefradil using the S0 model (● measured data; ○ predicted response)

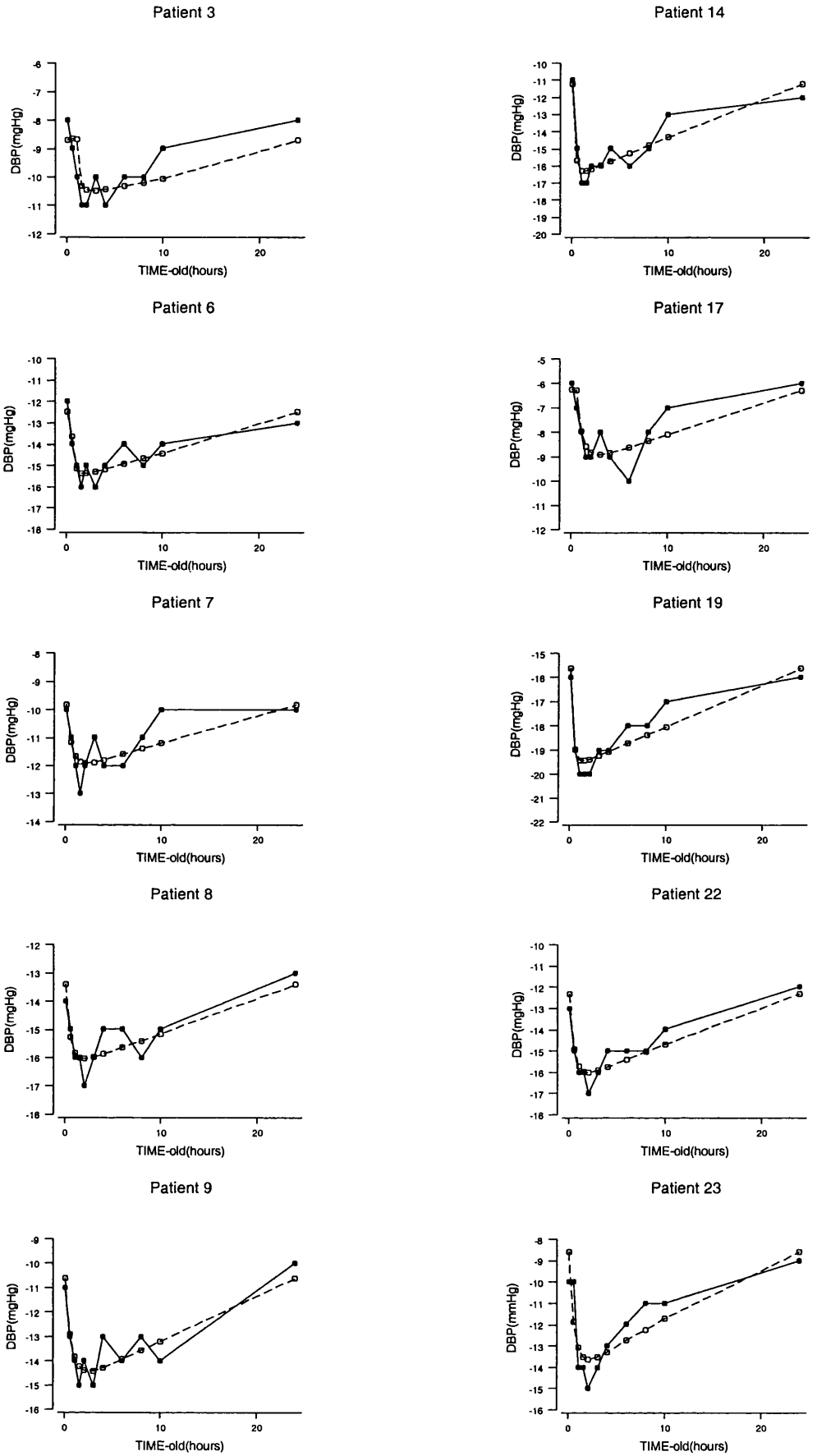

Figure 3.7.2.c Decrease in HR against predicted concentrations of mibefradil (steady-state study)

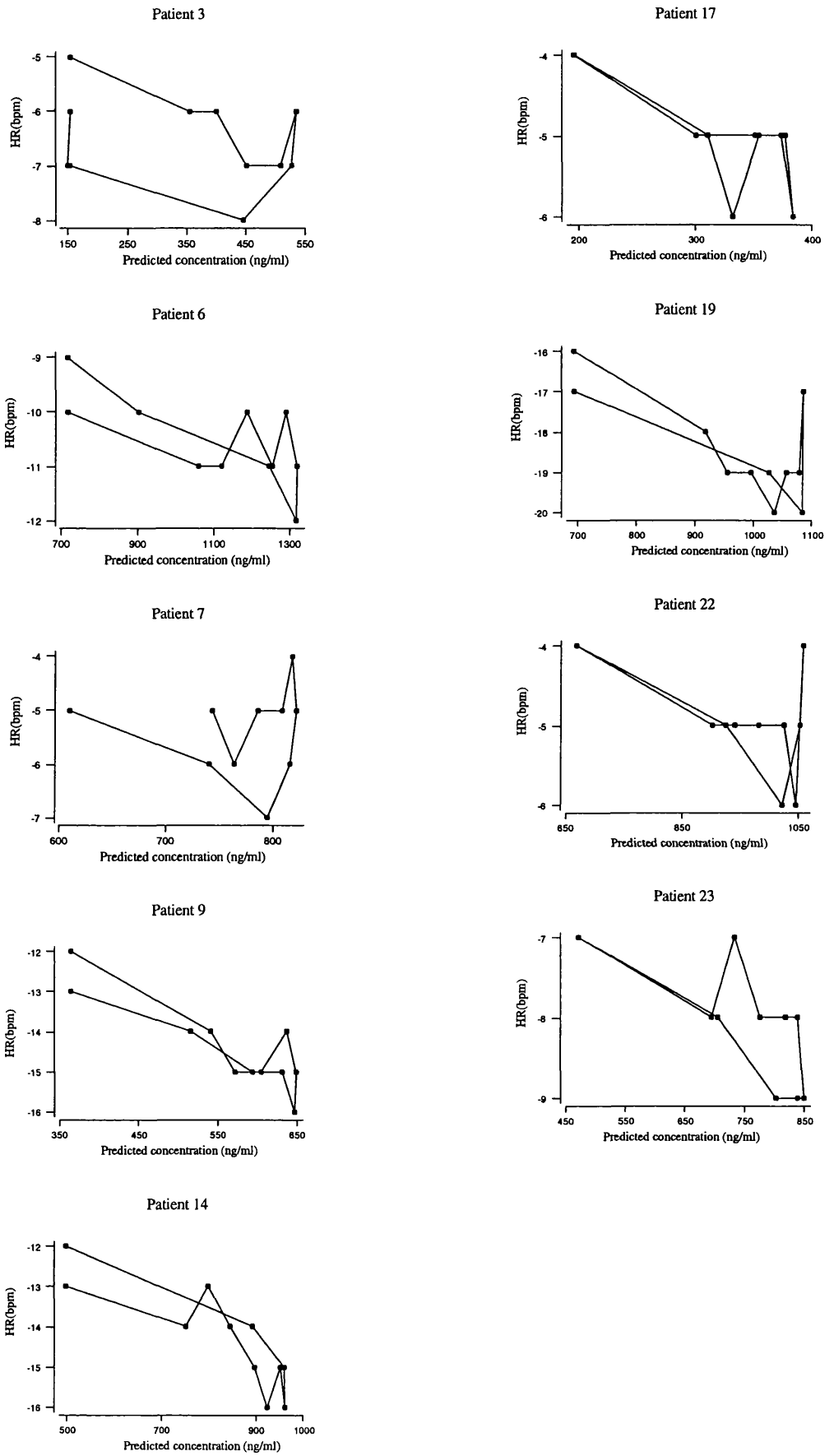

Figure 3.7.2.d Time course of response (Δ HR) to multiple dose of mibefradil using the S0 model (● measured data; ○ predicted response)

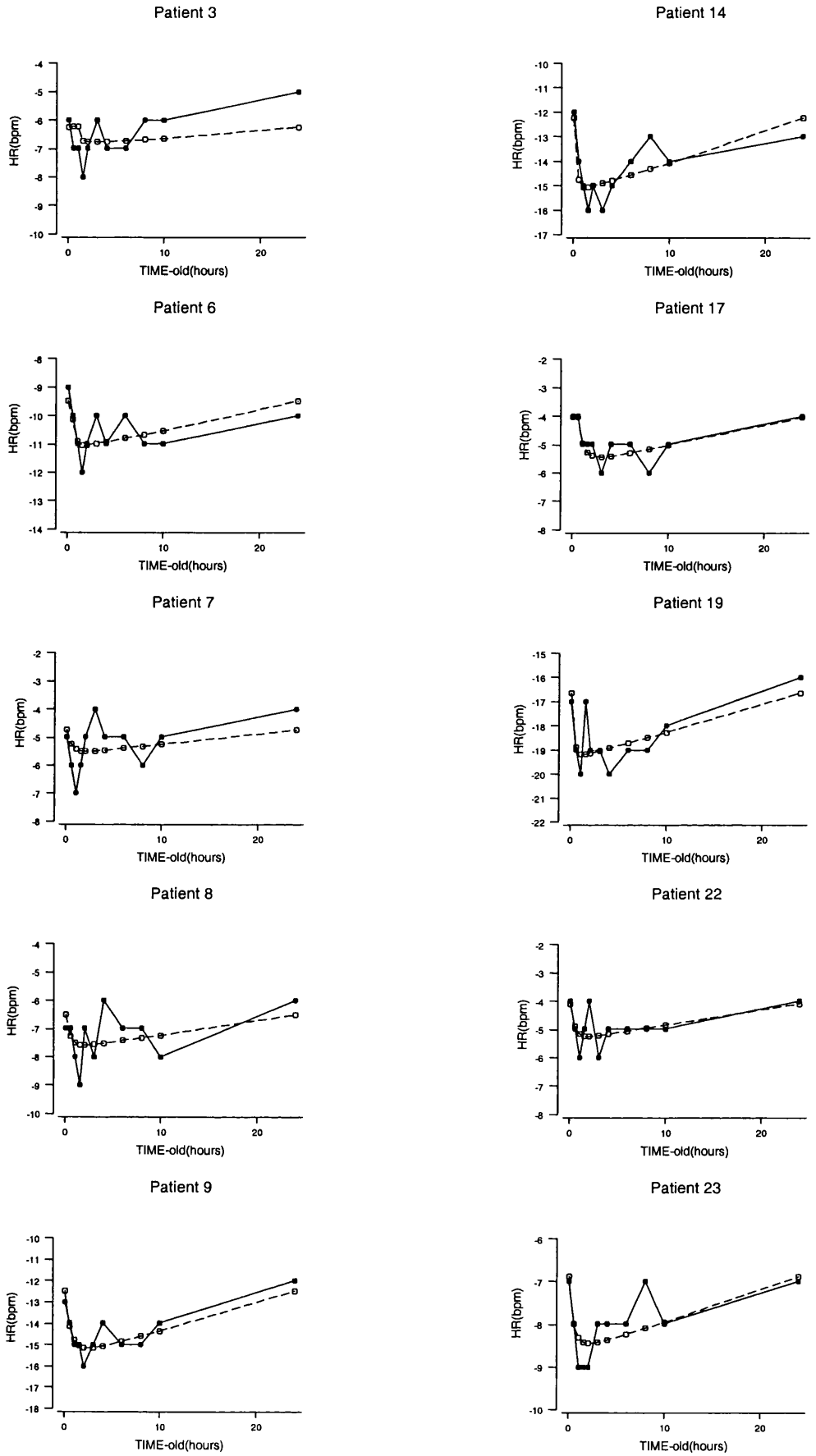

Figure 3.7.2.f Time course of response (Δ PQ) to multiple dose of mibefradil using the linear model (● measured data; ○ predicted response)

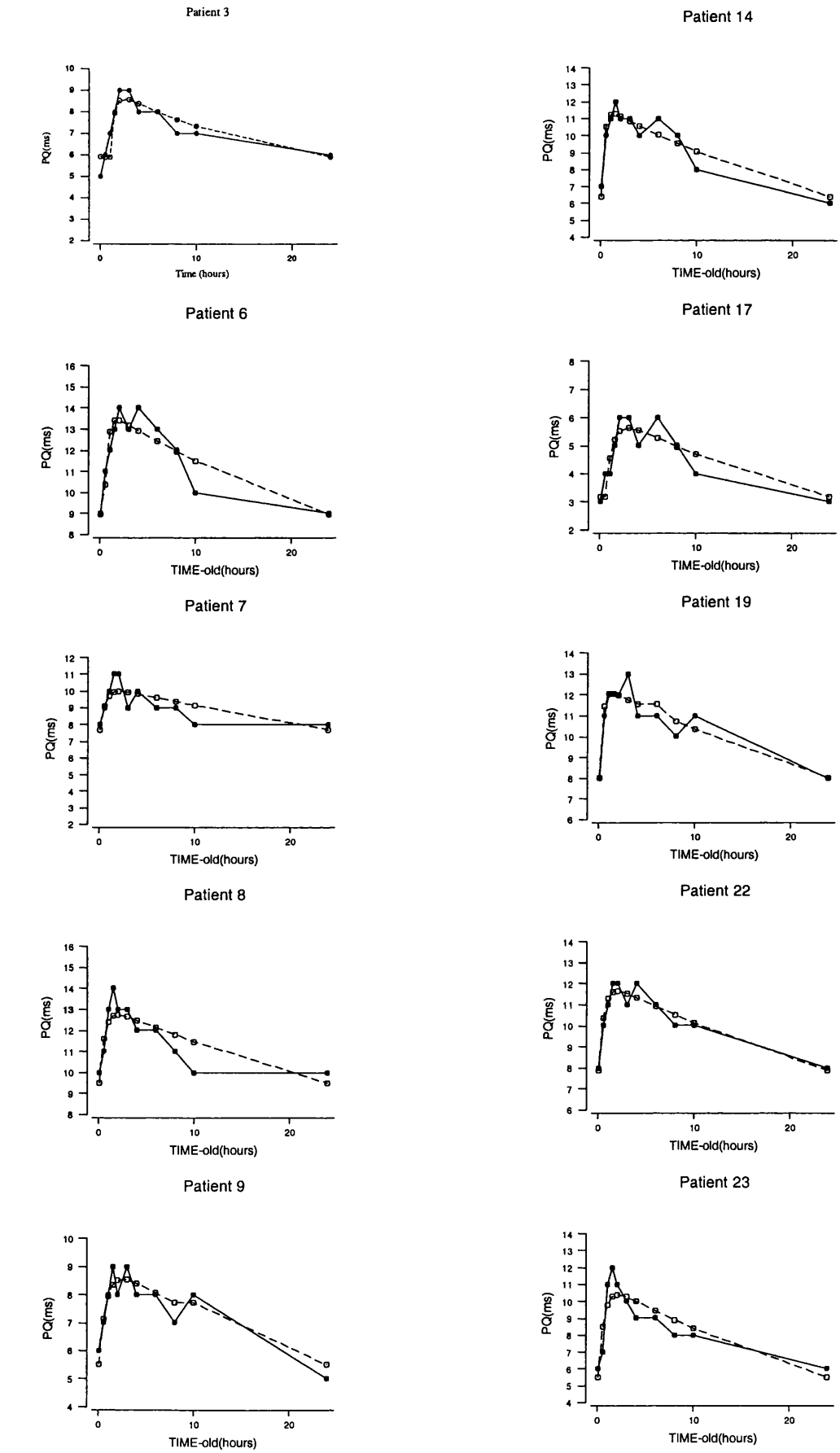

Table 3.7.2.a Parameter estimates from the linear and S0 models for changes in blood pressure after multiple doses of mibefradil (100 mg)

	LINEAR MODEL[a]				S0 MODEL[b]					
ID	**m**	**cv%**	**AIC**	**R^2**	**Emax**	**cv%**	**S0**	**cv%**	**AIC**	**R^2**
3	-0.00519	11.4	54.8	0.60	-11.4	5.5	-0.2440	31.8	22.7	0.77
6	-0.0478	4.07	41.9	0.81	-21.2	8.1	-0.0427	17.9	15.5	0.89
7	-0.0101	1.95	20.4	0.61	-25.0	41.6	-0.0273	34.6	19.7	0.77
8	-0.00608	2.48	32.4	0.76	-26.0	14.6	-0.0325	21.1	16.4	0.86
9	-0.0134	2.89	32.7	0.81	-26.4	17.6	-0.0487	18.5	20.1	0.91
14	-0.0110	2.79	34.4	0.89	-31.6	17.1	-0.0338	15.8	22.0	0.93
17	-0.0144	4.17	29.4	0.71	-15.9	24.3	-0.0528	25.5	21.7	0.84
19	-0.00978	2.32	34.9	0.90	-34.0	12.2	-0.0418	14.6	16.2	0.93
22	-0.00948	2.10	28.2	0.88	-32.6	17.5	-0.0290	15.1	15.5	0.93
23	-0.0127	2.83	30.3	0.75	-36.1	52.1	-0.0252	27.58	31.1	0.84

[a] Equation 1.17; Chapter 1; [b] Equation 3.1, Chapter 3.

* Not estimated

Key: Emax is the maximum effect; m is the slope of linear model; S0 is the Emax/EC50; AIC represents the Akaike Information Criterion and R^2 coefficient of determination

Table 3.7.2.b Parameter estimates from the linear and S0 models for changes in heart rate after multiple doses of mibefradil (100 mg)

	LINEAR MODEL[a]				S0 MODEL[b]					
ID	**m**	**cv%**	**AIC**	**R^2**	**Emax**	**cv%**	**S0**	**cv%**	**AIC**	**R^2**
3	-0.0159	10942	69.9	0.85	-8.30	12.3	-0.0999	44.2	29.2	0.70
6	-0.0093	5980	80.4	0.98	-13.6	10.4	-0.0436	35.7	17.5	0.70
7	-0.0069	4481	65.4	0.97	-10.0	98.8	-0.0140	111.3	25.9	0.78
8	-0.00627	4033	599.3	0.98	-11.2	39.7	-0.0183	74.3	24.7	0.86
9	-0.0235	16135	87.1	0.99	-20.8	8.7	-0.0854	19.8	15.3	0.91
14	-0.0171	10920	87.0	0.98	-20.0	10.3	-0.0630	26.2	22.7	0.93
17	-0.0156	9979	63.7	0.98	-8.47	17.7	-0.0395	25.7	8.5	0.83
19	-0.0188	12015	92.6	0.99	-26.2	13.7	-0.0650	33.1	26.2	0.93
22	-0.0052	3343.0	63.8	0.98	-10.0	50.4	-0.0100	49.8	16.2	0.92
23	-0.0108	0.00	0.00	0.98	-11.8	15.5	-0.0350	33.5	14.9	0.84

[a] Equation 1.17; Chapter 1; [b] Equation 3.1, Chapter 3.

Key: Emax is the maximum effect; m is the slope of linear model; S0 is Emax/EC50; AIC represents the Akaike Information Criterion and R^2 coefficient of determination

Table 3.7.2.c Parameter estimates from the Emax and linear models for changes in PQ interval after multiple doses of mibefradil (100 mg)

	EMAX MODEL[a]						LINEAR MODEL[b]			
ID	**Emax**	**cv%**	**EC50**	**cv%**	**AIC**	**R^2**	**m**	**cv%**	**AIC**	**R^2**
3	9.87	7.6	102	30.1	20.3	0.85	0.0185	9.3	44.4	0.89
6	33.0	30.8	1945	48.8	23.2	0.91	0.0106	2.7	28.6	0.91
7	46.0	136.0	2983	171.0	22.3	0.75	0.0123	2.4	20.4	0.76
8	40.8	63.8	2833	90.1	24.8	0.82	0.0102	2.3	24.8	0.84
9	28.7	51.0	1546	70.1	14.1	0.91	0.0135	2.3	15.5	0.91
14	45.9	60.7	2998	78.2	20.0	0.94	0.0119	2.1	18.8	0.94
17	34.1	138.3	1939	162.0	15.7	0.87	0.0150	3.5	14.2	0.88
19	44.7	55.9	2999	74.4	17.8	0.93	0.0112	1.6	14.7	0.93
22	44.2	42.2	2999	55.8	10.6	0.96	0.0111	1.3	9.61	0.96
23	45.7	131.7	2999	165.1	31.1	0.86	0.0121	3.4	27.4	0.87

[a] Equation 1.18, Chapter ; [b] Equation 1.17, Chapter 1.

Key: Emax is the maximum effect; EC50 is the concentration that produces half of the Emax effect; m is the slope of linear model; AIC represents the Akaike Information Criterion and R^2 coefficient of determination

3.7.2.2 Verapamil

Blood Pressure - Decreases in blood pressure with measured concentrations were best described by the S0 model. Individual results are shown in Table 3.7.2.d. Figure 3.7.2.g shows the decrease in blood pressure along with the predicted concentration for verapamil after multiple-dose administration and the effect against time profile is shown in Figure 3.7.2.h.

Heart Rate – Figure 3.7.2.i represents the changes in heart rate against predicted concentration. The S0 model gave the best fit to the changes in heart rate with measured concentration. The parameter estimates from the Emax and linear models are shown in table Table 3.7.2.e. The predicted course of action for S0 model is represented in Figure 3.7.2.j.

PQ interval – Changes in the PQ interval were adequately described by the linear model. In Table 3.7.2.f are listed the parameter estimates from both models. Figure 3.7.2.l shows the change in PQ interval against predicted concentration and Figure 3.7.2.m shows the measured and predicted time-course of action.

Figure 3.7.2.g Decrease in DBP against predicted concentrations of verapamil (steady-state study)

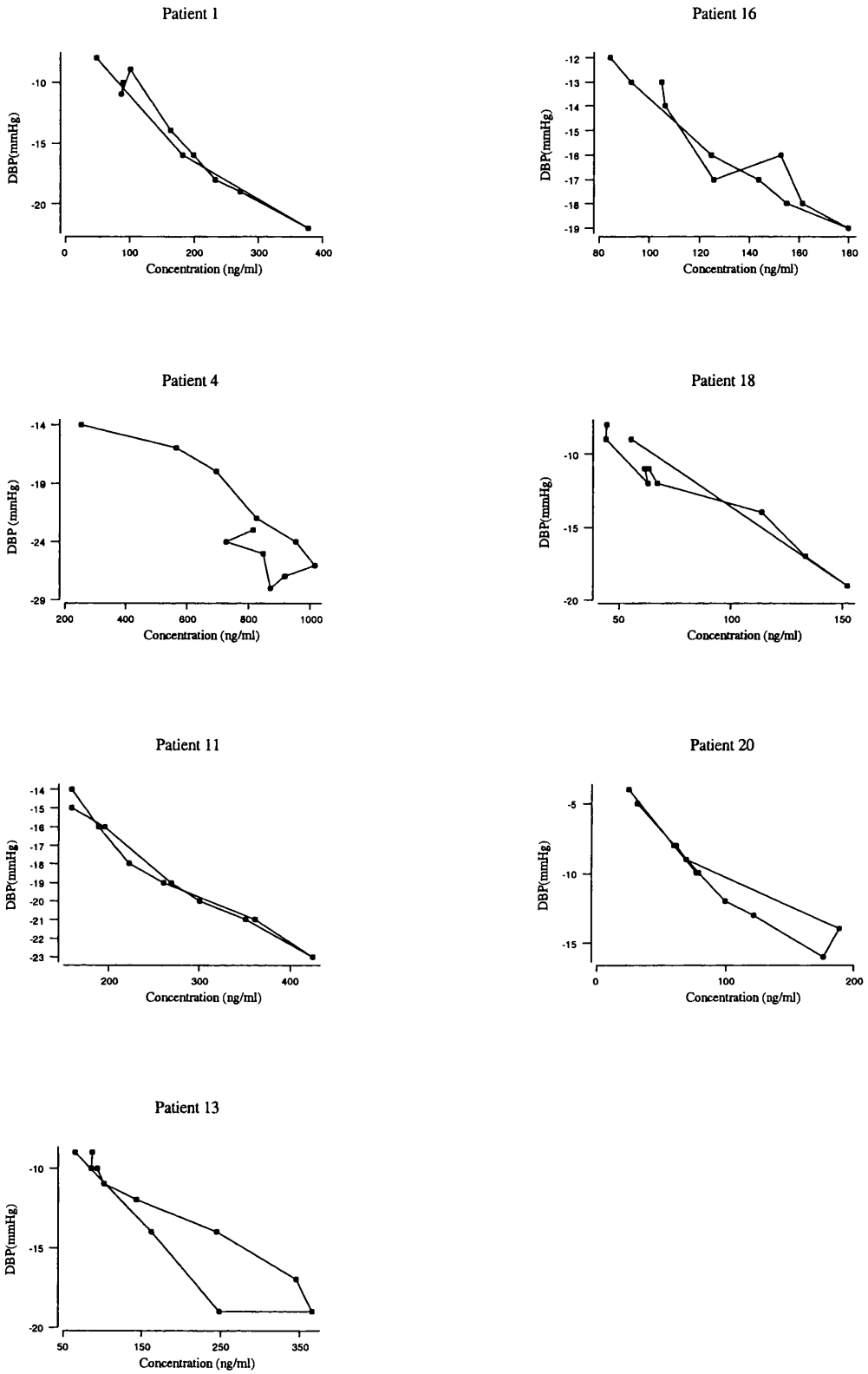

Figure 3.7.2.h Time-course of response (Δ DBP) to multiple dose of verapamil using the S0 model (● measured data; ○ predicted response)

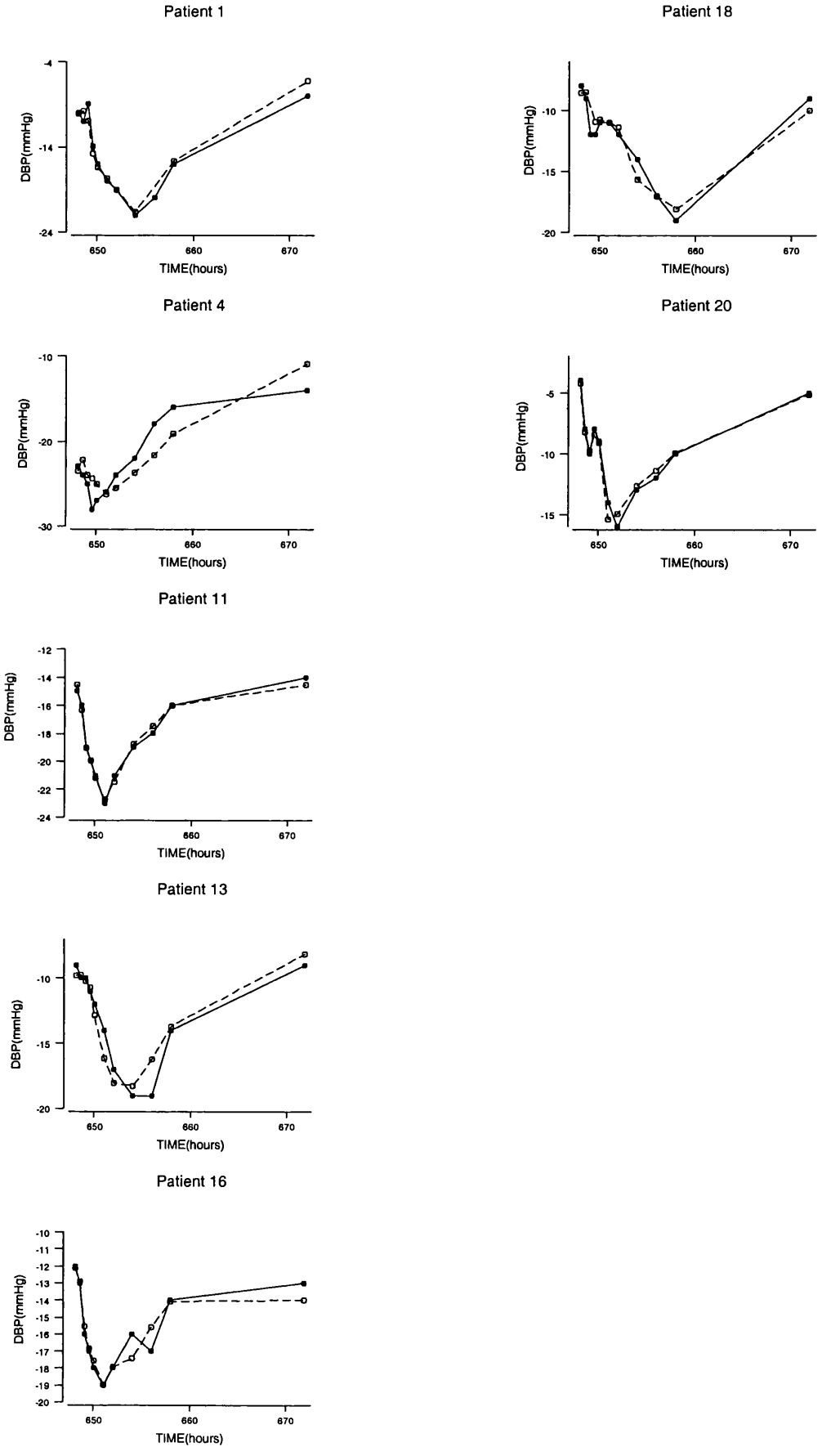

Figure 3.7.2.i Decrease in HR against predicted concentrations of verapamil (steady-state study)

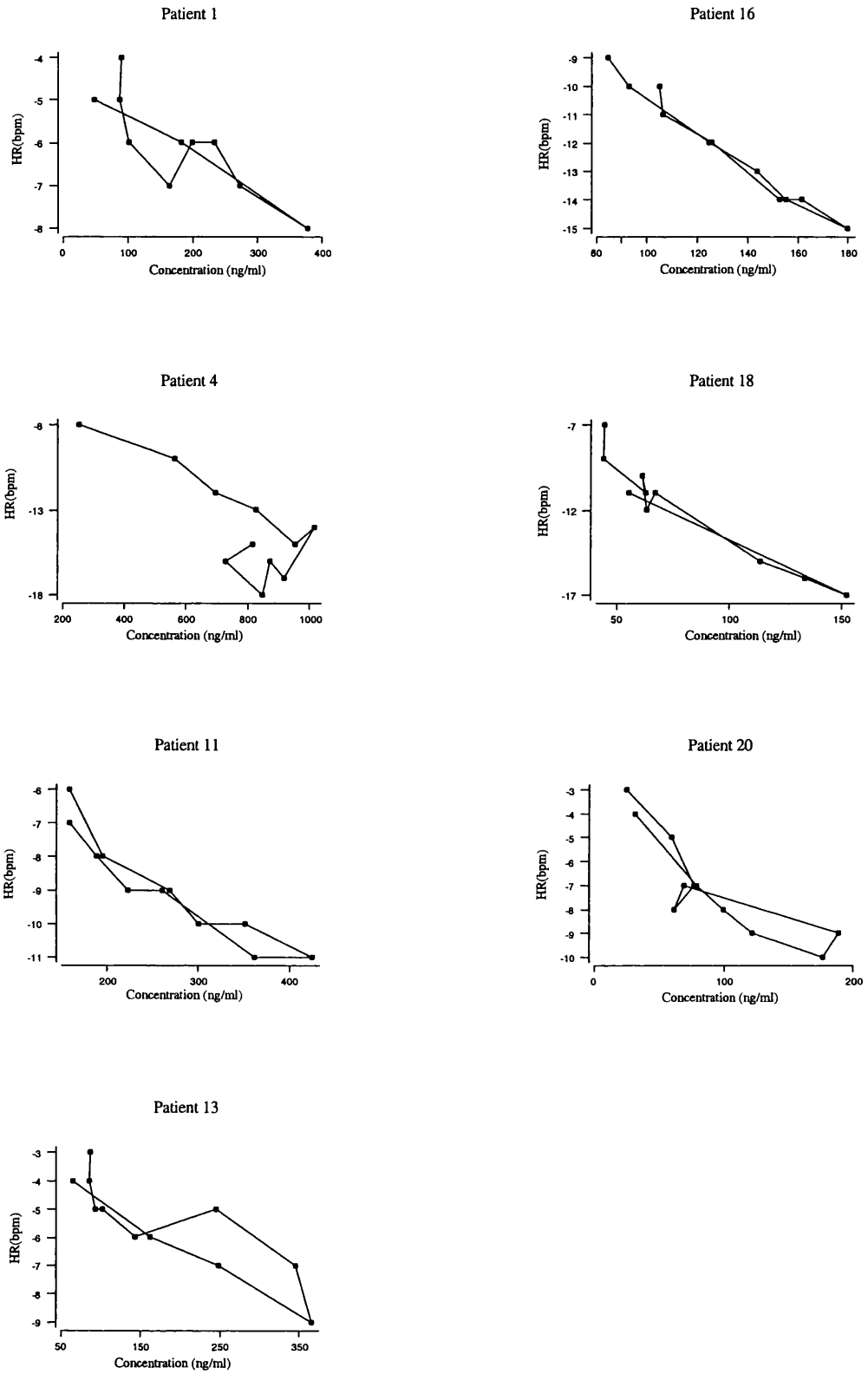

Figure 3.7.2.j Time course of response (Δ HR) to multiple doses of verapamil using the S0 model (● measured data; ○ predicted response)

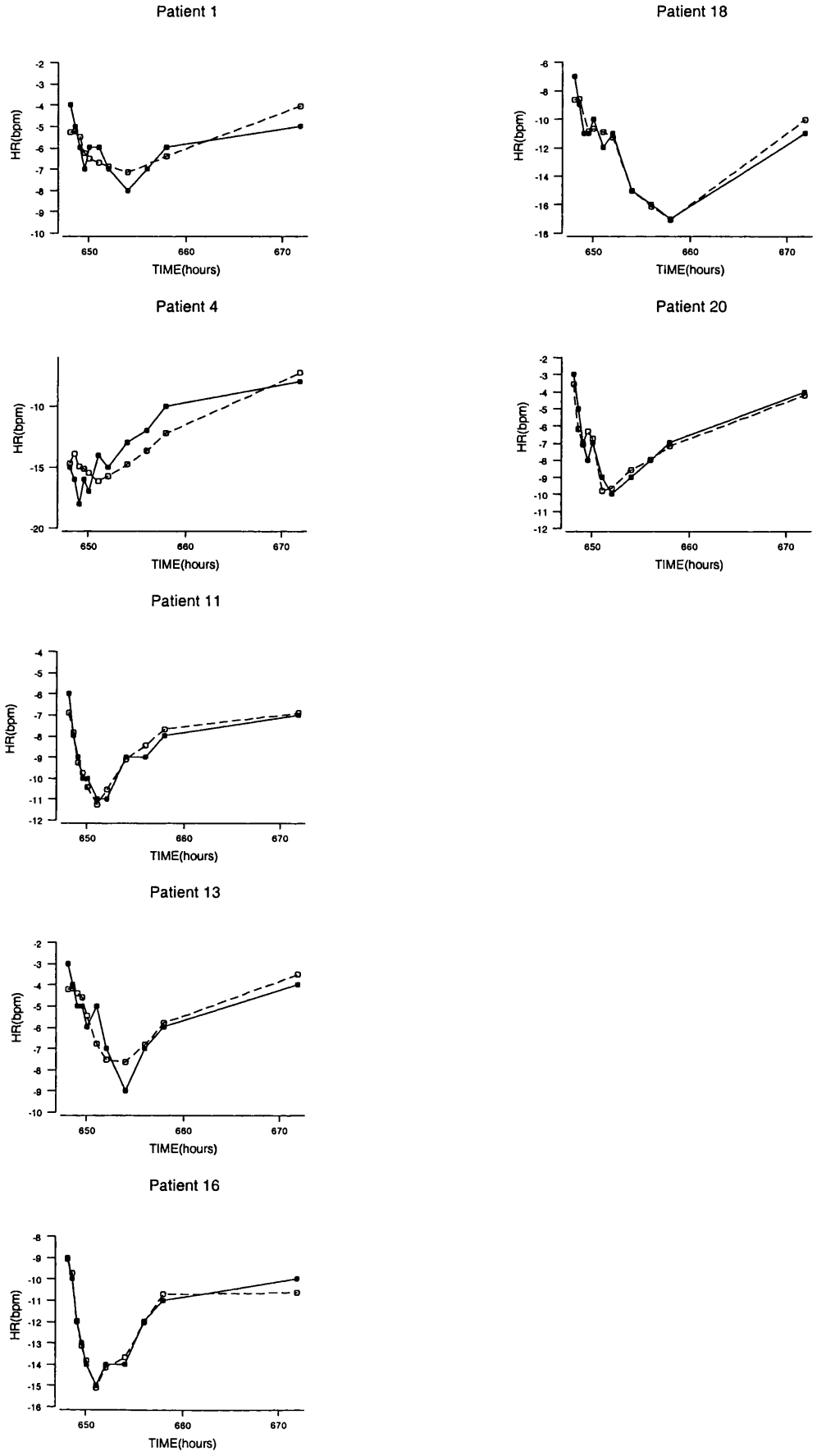

Figure 3.7.2.1 Changes in PQ interval against predicted concentrations of verapamil (steady-state study)

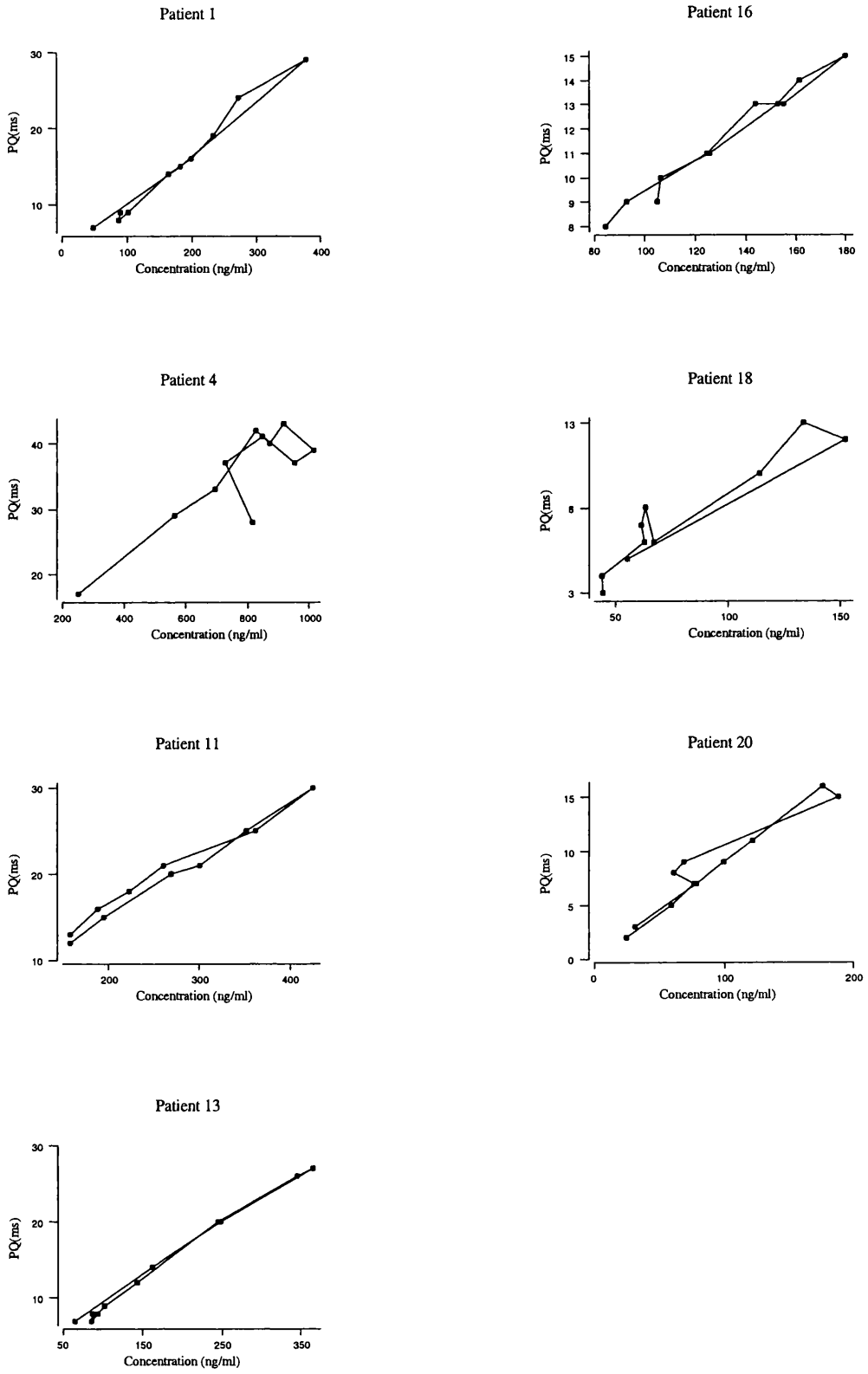

Figure 3.7.2.m Time-course of response (Δ PQ) to multiple doses of verapamil, using the linear model (● measured data; O predicted response).

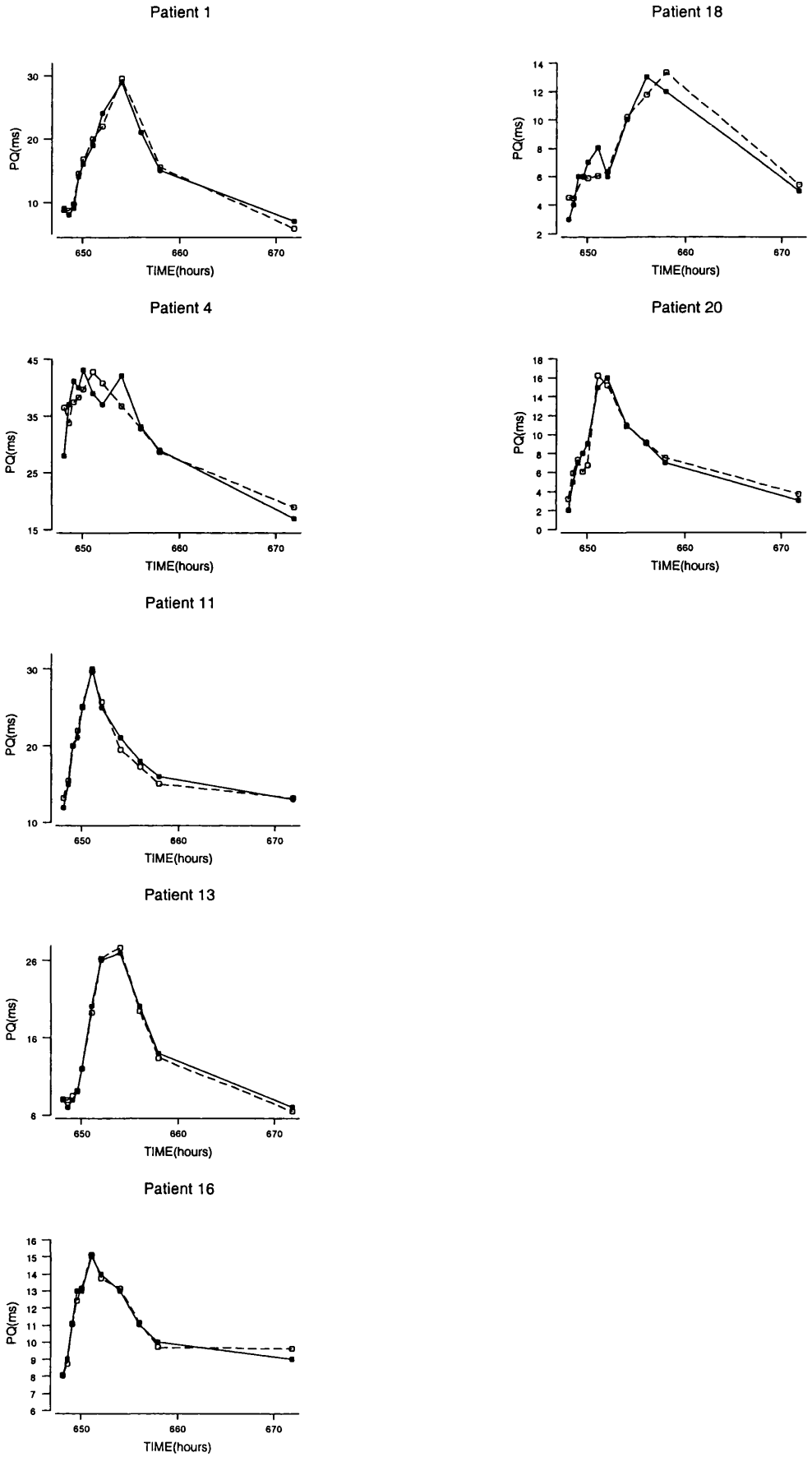

Table 3.7.2.d Parameter estimates from the linear and S0 models for changes in blood pressure after multiple doses of verapamil SR (240 mg)

	LINEAR MODEL[a]				S0 MODEL[b]					
ID	**m**	**cv%**	**AIC**	**R^2**	**Emax**	**cv%**	**S0**	**cv%**	**AIC**	**R^2**
1	-0.0733	49996	79.2	0.95	-33.7	10.5	-0.160	10.5	26.4	0.70
4	-0.0284	18166	97.3	0.98	-48.5	33.0	-0.0562	31.2	48.9	0.85
11	-0.0662	42523	92.7	0.97	-33.8	3.5	-0.161	4.6	6.8	0.99
13	-0.0635	0.00	85.8	0.92	-25.1	9.9	-0.184	14.0	34.72	0.94
16	-0.118	*	*	0.99	-37.9	15.9	-0.211	12.0	22.6	0.95
18	-0.142	0.00	75.8	0.96	-33.5	13.2	-0.259	9.6	23.2	0.65
20	-0.0991	20379	61.2	0.95	-25.5	8.8	-0.206	7.9	18.9	0.98

[a] Equation 1.17; Chapter 1; [b] Equation 3.1 Chapter 3.
* Not estimated

Key: Emax is the maximum effect; m is the slope of linear model; S0 is Emax/EC50 and AIC represents the Akaike Information.; R^2 coefficient of determination

Table 3.7.2.e Parameter estimates from the linear and S0 models for changes in heart rate after multiple doses of verapamil SR (240 mg)

	LINEAR MODEL[a]				S0 MODEL[b]					
ID	**m**	**cv%**	**AIC**	**R^2**	**Emax**	**cv%**	**S0**	**cv%**	**AIC**	**R^2**
1	-0.0286	20379	61.2	0.87	-8.06	10.4	-0.169	33.1	20.1	0.70
4	-0.0177	11365	87.0	0.97	-27.0	33.1	-0.039	39.2	42.5	0.85
11	-0.0323	*	*	0.92	-17.8	9.6	-0.072	10.6	11.1	0.80
13	-0.0268	0.00	67.0	0.90	-10.2	15.9	-0.082	23.9	26.8	0.96
16	-0.0921	58440	83.7	0.99	-36.8	9.7	-0.142	5.2	1.0	0.85
18	-0.137	93141	75.2	0.96	-28.3	10.9	-0.280	9.8	21.3	0.99
20	-0.0674	44707	72.1	0.91	-13.3	11.7	-0.196	16.7	23.1	0.77

[a] Equation 1.17; Chapter 1; [b] Equation 3.1 Chapter 3.
* Not estimated

Key: Emax is the maximum effect; m is the slope of linear model; S0 is Emax/EC50 and AIC represents the Akaike Information Criterion; R^2 coefficient of determination.

Table 3.7.2.f Parameter estimates from the Emax and linear models for changes in PQ interval after multiple doses of verapamil SR (240 mg)

	EMAX MODEL[a]						LINEAR MODEL[b]			
ID	**Emax**	**cv%**	**EC50**	**cv%**	**AIC**	**R^2**	**m**	**cv%**	**AIC**	**R^2**
1	100	31.3	955	39.3	29.5	0.98	0.0824	2.9	32.1	0.83
4	76.0	33.7	862	65.4	59.3	0.86	0.0446	4.3	63.0	0.85
11	100	21.0	1052	26.9	25.6	0.98	0.0735	2.1	34.6	0.98
13	100	12.3	999	15.5	14.0	0.99	0.0780	2.2	30.9	0.99
16	67.8	24.6	635	30.0	4.8	0.98	0.0873	1.4	14.1	0.99
18	55.8	67.4	504	81.5	27.0	0.95	0.0907	4.7	27.4	0.77
20	56.4	44.6	490	56.3	31.3	0.96	0.0897	4.4	33.9	0.96

[a] Equation 1.18, Chapter ; [b] Equation 1.17, Chapter 1.

Key: Emax is the maximum effect; EC50 is the concentration that produces half of the Emax effect; m is the slope of linear model and AIC represents the Akaike Information Criterion; R^2 coefficient of determination

3.7.2.3 Summary of Final Results: Steady-State Study

At steady state the mean EC50 value for DBP estimated from the Emax model was 731.3 ± 340.2 ng ml^{-1} for mibefradil. That contrast with the value obtained for verapamil, 391.2 ± 215.2 ng ml^{-1}.

For changes in heart rate, after multiple doses the mean value of EC50 estimate was 421.4 ± 137.3 ng ml^{-1} for mibefradil and 337.2 ± 204.6 ng ml^{-1} for verapamil.

The mean values for DBP and HR obtained from the S0 model are presented in Table 3.7.2.g.

The Emax model for changes in PQ interval produced an estimate of EC50 of 2334.5 ± 963.2 ng ml^{-1} for mibefradil and 785.2 ± 238.3 ng ml^{-1} for verapamil. The results obtained from the linear model are shown in Table 3.7.2.g.

Table 3.7.2.g Mean values of parameter estimates from the best model for the multiple-dose study

		MIBEFRADIL	VERAPAMIL
DBP (mmHg)	Emax	-26.0 ± 8.0	-34.0 ± 7.9
	S0	-0.058 ± 0.066	-0.176± 0.06
HR (bpm)	Emax	-14.0 ± 6.1	-20.2 ± 10.7
	S0	-0.047 ± 0.03	-0.140 ± 0.084
PQ interval (msec)	m	0.013 ± 0.003	0.078 ± 0.016

Values represent mean ± SD.

Key: DBP represents the diastolic blood pressure; HR is the heart rate; Emax is the maximum effect and S0 is Emax/EC50.

3.7.3 STATISTICAL ANALYSIS

The pharmacodynamic parameters obtained from DBP, HR, and PQ interval, after the administration of a single dose of mibefradil were compared. The results from 10 patients included in the analysis are presented in Table 3.7.3.a. For blood pressure and heart rate, the Emax was higher after a single dose than at steady state, whereas the S0 parameter was higher at steady state for both PD endpoints. For PQ interval there was an increase in potency, measured by the S0 parameter, at steady state.

The differences between the parameters were not statistically significant but on the basis of the 95% confidence level it cannot be concluded that the two sets of figures are in close agreement. Thus it is not possible to make any definitive conclusions regarding change in sensitivity (or lack of it) during the translation from single dose to steady state treatment. This can be explained, in part by the small number of patients.

The pharmacodynamic parameters obtained after the administration of a single dose of verapamil and at steady state, for 7 patients, are shown in Table 3.7.3.b. For blood pressure the mean Emax and S0 values were lower at steady state than after a single dose. In contrast, for heart rate the mean values of those parameters were higher at steady state than after single dose. For PQ interval a higher value of the parameter m was obtained at steady state, indicating an increase in potency. As for mibefradil, the difference between the parameters after single dose and at steady state was not statistically significant.

For both drugs the parameter estimates after single dose and at steady state were poorly correlated (Figure 3.7.3). A larger study population would have been necessary to assess the differences.

Figure 3.7.3 Pharmacodynamic parameter estimates after the administration of a single dose of mibefradil against the parameter estimates at steady state

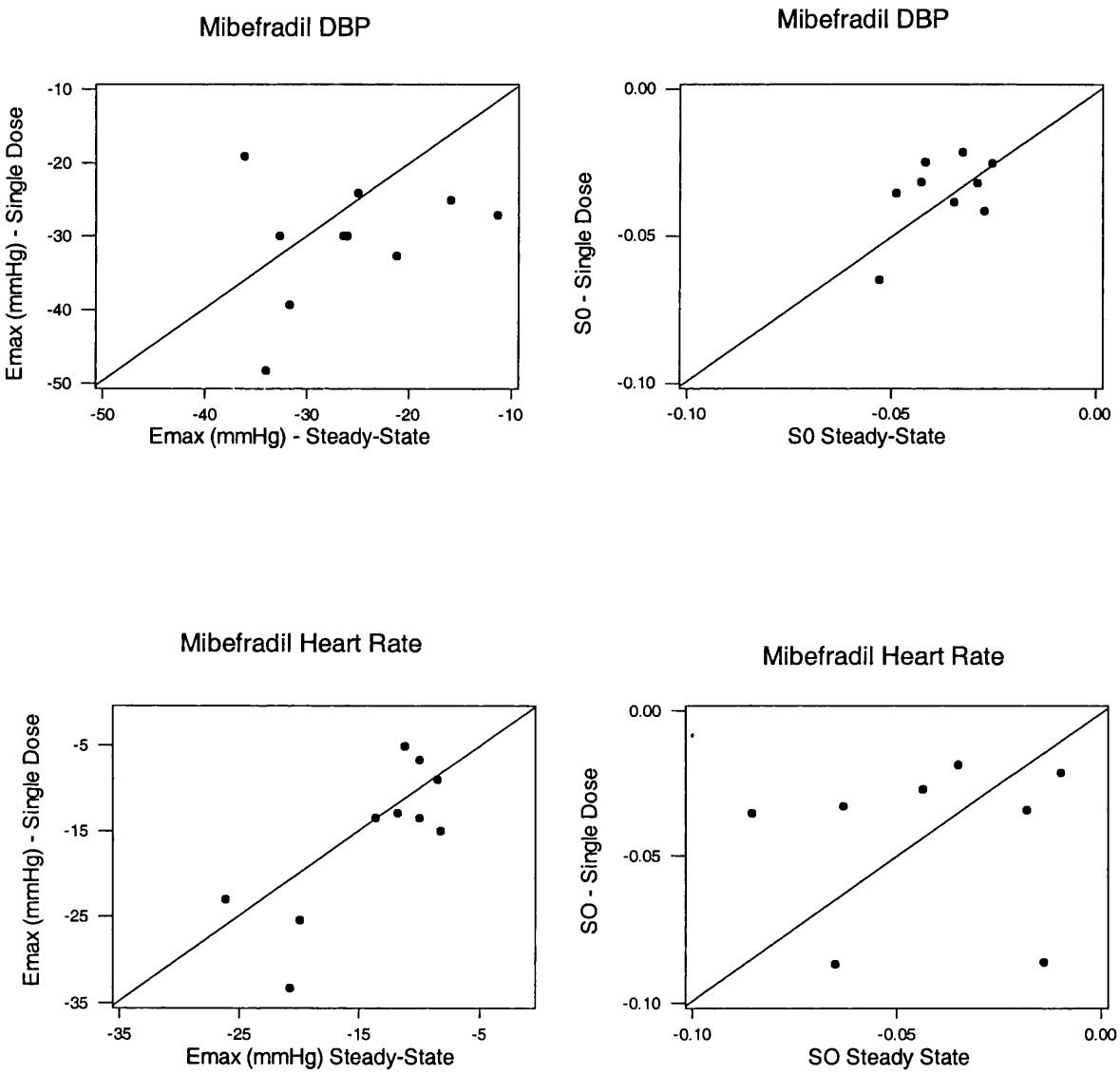

Table 3.7.3.a Pharmacodynamic parameters obtained after the administration of a single dose of mibefradil and at steady state (N=10)

	Diastolic Blood Pressure				**Heart Rate**				**PQ interval**	
	Emax		**S0**		**Emax**		**S0**		**m**	
	SD	**SS**	**SD**	**SS**	**SD**	**SS**	**SD**	**SS**	**SD**	**SS**
3	-27.03	-11.38	-0.0858	-0.2440	-15.0	-8.30	-0.0081	-0.0999	0.0059	0.0185
6	-32.61	-21.15	-0.0314	-0.0427	-13.51	-13.64	-0.0270	-0.0436	0.0128	0.0106
7	-24.05	-24.99	-0.0413	-0.0273	-13.56	-10.00	-0.0864	-0.0140	0.0127	0.0123
8	-30.00	-26.03	-0.0211	-0.0325	-5.10	-11.21	-0.0341	-0.0183	0.0115	0.0102
9	-29.99	-26.41	-0.0350	-0.0487	-33.37	-20.81	-0.0350	-0.0854	0.0142	0.1346
14	-39.38	-31.64	-0.0383	-0.0348	-25.47	-20.00	-0.0327	-0.0630	0.0132	0.0119
17	-25.08	-15.94	-0.0650	-0.528	-8.98	-8.47	-0.1215	-0.0395	0.0378	0.0150
19	-48.34	-34.01	-0.0247	-0.0418	-23.01	-26.18	-0.0870	-0.0650	0.0118	0.0112
22	-29.95	-32.62	0.0319	-0.0290	-6.71	-10.00	-0.0210	-0.0100	0.0106	0.0111
23	-18.99	-36.10	-0.0250	-0.0253	-13.00	-11.77	-0.0183	-0.0350	0.0117	0.0121
Mean	**-30.54**	**-26.03**	**-0.040**	**-0.0579**	**-15.77**	**-14.04**	**-0.0471**	**-0.0474**	**0.0142**	**0.0247**
Δ mean	**-4.52**		**0.0179**		**-1.73**		**0.0003**		**-0.0105**	
95% CI	**-11.5 ; 2.44**		**-0.0182 ; 0.0540**		**-5.69 ; 2.22**		**-0.0376 ; 0.0382**		**-0.0388 ; 0.0178**	

Key: Δ represents difference between mean values; SD is single dose; SS is the steady state; Emax is the maximum effect and S0 is defined by Emax/EC50.

Table 3.7.3.b Pharmacodynamic parameters obtained after the administration of a single dose of verapamil and at steady state (N=7)

	Diastolic Blood Pressure				Heart Rate				PQ interval	
	Emax		S0		Emax		S0		m	
	SD	SS	SD	SS	SD	SS	SD	SS	SD	SS
	-31.8	-33.7	-0.122	-0.1600	-12.3	-20.5	-0.0311	-0.169	0.0629	0.0824
	-40.2	-48.5	-0.212	-0.0562	-20.3	-27.0	-0.1845	-0.039	0.0635	0.0446
	-31.3	-33.8	-0.615	-0.1610	-13.5	-17.8	-0.1177	-0.072	0.0544	0.0735
	-56.8	-25.1	-0.074	-0.1840	-12.0	-10.2	-0.0710	-0.082	0.0568	0.0780
	-28.8	-37.9	-0.298	-0.2110	-11.5	-36.8	-0.0518	-0.142	0.0792	0.0873
	-45.6	-33.5	-0.142	-0.2590	-29.0	-28.3	-0.1557	-0.280	0.0633	0.0907
	-40.0	-25.5	-0.142	-0.2060	-20.3	-13.3	-0.1984	-0.196	0.0539	0.0897
Mean	**-39.2**	**-34.0**	**-0.233**	**-0.18**	**-17.0**	**-22.0**	**-0.1157**	**-0.1400**	**0.062**	**0.07803**
Δ mean	**-5.21**		**-0.0523**		**5.0**		**0.0243**		**0.016**	
95% CI	**-19.00 ; 8.57**		**-0.2414 ; 0.1363**		**-4.62 ; 14.62**		**0.069 ; 0.118**		**-0.0323 ; 0.00022**	

Key: Δ represents difference between mean values; SD is single dose; SS is the steady state; Emax is the maximum effect and S0 is defined by Emax/EC50.

3.8 DISCUSSION

This study was designed to evaluate and compare the antihypertensive efficacy of mibefradil, verapamil and diltiazem when administered as a single dose or as multiple doses to mildly hypertensive patients. The effect of these drugs on heart rate and on atrio-ventricular conduction was also studied.

Pharmacokinetics – Mibefradil, verapamil and diltiazem were all rapidly absorbed after oral administration of a single dose. For verapamil and diltiazem, the fast absorption led to difficulties in model selection. For some patients the first concentration, sampled at 0.5 hours after the dose, corresponded to the peak concentration and therefore for these patients, information on absorption was not available. In the case of verapamil, 9 out of 18 patients had a similar problem whereas for diltiazem it occurred in only 5 patients. For diltiazem, patient 16 had the peak concentration at 3 hours after the dose administration. The unusual profile observed in this patient (see Figure 3.5.1.c) created problems with pharmacokinetic/ pharmacodynamic modelling. The delay can be caused by problems with absorption. For patient 3 the incorporation of a time lag was justified, as the concentration measured at 0.5 hours was not available. The inclusion of a lag time, as an extra parameter in the model, was necessary for some patients. The lag time was incorporated in the cases that sampling information was missing at 0.5 hours or the drug concentration at that point was very low (e.g. patients 1, 2, 4, 7, 11, 19 of mibefradil).

The model selected to describe the absorption process, the zero-order model, was the model, which more closely described the observed profiles. For verapamil and diltiazem the absorption process was not well characterised due to the lack of early data points. Mibefradil had a slower absorption than the other two drugs, with an estimated time to peak (Tmax) of 1.9 ± 0.7 hours after a single dose and 2.5 ± 0.6 hours at steady state. Welker et al. (1998) reported similar values. A first-order absorption model was used to characterise the data.

Results from mibefradil revealed that it possesses particular pharmacokinetic features, which were shared neither by verapamil nor by diltiazem. Mibefradil half-life after a single dose of 150 mg (17.4 ± 4.1 hours) and at steady state on 100 mg daily (28.1 ± 10.2 hours) were in agreement with what has been published, 15.1 ± 4.4 and 23.7 ± 7.8 hours, respectively (Welker et al., 1989; Welker et al., 1998). This increase in elimination half-life after multiple doses can be a result of the self-inhibition of one metabolic pathway, CYP3A4-mediated oxidative metabolism. For verapamil and diltiazem the estimated terminal half-life was higher than previously reported (Hamann et al., 1984; Buckley et al., 1990) at 12.8 hours and 10.1 hours, respectively. However, these values were estimated with imprecision, as they were defined only by one point, sampled at 24 hours. For some patients the coefficient of variation of parameter estimates were not obtained (see Table 3.5.1.b and Table 3.5.1.c). The verapamil half-life ranged from 3.2 to 39.4 hours and diltiazem ranged from 4.6 to 27.4 hours. These points were low concentrations and therefore high assay error was associated with them.

For mibefradil the volume of distribution (V/F) was increased compared with the single dose and could be another factor contributing to the long half-life along with the decrease in clearance (CL/F). An investigator reported that clearance (CL/F) is reduced with increasing dose indicating that bioavailability (F) increases as doses increase (Welker, 1998). This finding is mostly likely to be due to a reduction in first-pass metabolism. This can in part explain differences in volume of distribution (V/F) after single dose and at steady state. Values of CL/F obtained after a single dose of mibefradil were lower than expected, 7.2±5.6 L h^{-1}. Welker reported a clearance of 14.0 ± 9.3 L h^{-1} after a single dose of 150 mg of mibefradil (Welker, 1998). Differences in bioavailability could also explain the discrepancies in the results.

The mono-exponential decline model best described the disposition of mibefradil for all patients. Although the profiles suggested a bi-exponential decline for patients 18, 22 and 23, this model gave imprecise parameter estimates, with a wide coefficient of variation and therefore a mono-exponential decline model was chosen. More data points beyond 48 hours would have been necessary to fully characterise the terminal

elimination as only one measurement was available to characterise the second compartment. A bi-exponential decline model was selected for verapamil and diltiazem, but for some patients the coefficient of variation of pharmacokinetic parameters could not be estimated. For verapamil, patient 1 had pharmacokinetic parameters estimated with great precision, contrasting with patients 4, 6, and 7 in whom parameters had a wider coefficient of variation. In both cases the model provided a good fit of the data as judged by coefficient of determination and residual plots.

Pharmacodynamics - The findings of the study showed that mibefradil in doses of 150 mg smoothly lowered the diastolic blood pressure (DBP) during a 24-hour period. The effect on DBP was more sustained than after single doses, with a more marked effect 24 hours after administration, which was similar to verapamil SR 240 mg. Verapamil 240 mg and diltiazem 240 mg, after single doses, had a more pronounced effect on DBP than mibefradil but the effect was less sustained after 24-hours. Mibefradil 100mg and Verapamil SR 240 mg at steady state had a more attenuated effect on DBP than after single doses (Table 3.7.3.b).

Following single dose, the three drugs produced a decrease in heart rate with the greatest effect being observed after verapamil and the least effect with diltiazem. At steady state verapamil SR showed a more marked (Table 3.7.3.a and Table 3.7.3.b) and sustained decrease up to 24 hours than mibefradil.

Mibefradil and verapamil showed a greater PQ prolongation at steady state than after a single dose (Table 3.7.3.a). Verapamil and diltiazem had a more marked effect on the PQ interval than mibefradil. Studies with diltiazem suggested that the effect on atrio-ventricular conduction might be dependent on the pharmaceutical formulation used. Rapidly absorbed formulations led to high drug concentrations, causing a greater prolongation of the PQ interval.

Pharmacokinetic/Pharmacodynamic relationships – The Emax model, parameterised as the S0 model was selected as appropriate to describe the time-course of action of blood

pressure of mibefradil. The results of mibefradil presented in table 3.7.1.a show that at concentrations ranging from 61.9-1421.0 ng ml^{-1}, marked reductions in DBP could be expected. This was reflected by a relatively low estimated value of EC50 of 1012.1 ng ml^{-1} for the blood pressure lowering effect. The Emax values could be estimated precisely as is evident by the relatively narrow coefficient of variation. Furthermore, there was less interindividual variability for Emax than for EC50. The EC50 values revealed wide interindividual variability. Individual variation in pharmacokinetics has long been recognised. Pharmacokinetic variability may be pronounced in drugs such as the other calcium antagonists, which undergo extensive CYP-mediated metabolism. The reduction in DBP, after a single dose administration, caused by verapamil and diltiazem was associated with a much lower EC50 concentration (320.4 ± 238.4 ng ml^{-1} and 421.7 ± 292.3 ng ml^{-1}, respectively) than mibefradil (1012.1 ± 484.7 ng ml^{-1}). The interindividual variability in EC50 for mibefradil was wider than with verapamil and diltiazem.

For mibefradil the concentration-effect relationship for HR was difficult to model as the changes in HR were small, conferring a nearly flat profile. This contrasted with verapamil.

As with verapamil and diltiazem, mibefradil increases the PQ interval, and caution should be taken when treating patients who are susceptible to drugs that affect atrio ventricular conduction. However, with mibefradil the atrio-ventricular nodal conduction times were minimally affected at the therapeutic doses, as shown by much higher concentrations needed to induce changes in the PQ interval, and the EC50 value was 3-fold higher than the one for the DBP. The EC50 for changes in PQ interval was smaller with verapamil (693.4 ng ml^{-1}) than with diltiazem (789.6 ng ml^{-1}) or with mibefradil (2212.0 ng ml^{-1}). The same conclusions were reached by other investigators (Rosenquist et al., 1997). For changes in PQ interval a linear model was more appropriate for all drugs. The Emax model estimated an EC50 for DBP (2212.0 ng ml^{-1}) outside the range of plasma concentrations obtained after a single dose of mibefradil, rendering the linear model more appropriate. For the other two calcium antagonists, the

EC50 estimates from the Emax model were lower. For verapamil at steady state the prolongation in PQ interval could have been fitted with an Emax model, since similar values of the Akaike Information Criteria were obtained with both models. In this analysis the changes in PQ interval were fairly described by a linear model. Although the conclusions drawn from the Emax and linear were similar, the variability with the linear model was smaller.

An interesting issue was identifying the drug concentration-effect relationships. The concentration-effect relationship for DBP and HR were best described by an Emax type model for the three drugs, either after single dose or multiple doses. Although the linear model yielded precise parameter estimates, the Akaike information criterion favoured the Emax model. For some patients (e.g. patient 3, mibefradil single doses DBP, Table 3.7.1.a) the algorithm did not converge. The EC50 estimates were imprecisely estimated. This occurred because the drug concentrations were not high enough to fully characterise the Emax effect, generating correlation between the model's parameters during the estimation process. After a single dose of mibefradil the estimated EC50 for DBP was 1012.1 ± 484.7 ng ml^{-1} and the mibefradil plasma concentrations ranged between 14.5 and 1727.0 ng ml^{-1}. This correlation caused problems during the estimation of EC50, but not Emax. The correlation matrix between Emax and EC50 was very high. To overcome this problem, the Emax model was re-parameterized in order to remove EC50 as a parameter from the model. The new parameter, S0, was better estimated than EC50, as it avoided the correlation. This contrasted with the Emax estimates that were obtained similarly in both models. The S0 parameter can also be used as a measure of potency (Schoemaker et al., 1998) to compare the action of drugs. Plasma concentrations of verapamil and diltiazem were higher relative to EC50 estimates for DBP and therefore the problem of parameter correlation was less noticeable.

The use of Emax model, when effect-concentration relationships are linear can cause problems in parameter estimation due to over parameterization. The routine use of the Emax model should be recommended. In pratice, the linear concentration-effect

relationships are only obtained in a very narrow range of concentrations. As the concentration increases the effect approaches the Emax effect and deviates from linear. At very low concentrations the measurement error is high, deflecting the data from linearity and therefore the use of linear model is not appropriate. The lowest concentration the slope estimates from linear model are less variable than the corresponding S0 estimates from the S0 model. Problems in parameter estimates can arise when the concentrations are not high enough to define the Emax model that prompted Schoemaker et al. (1998) to recommend the routine use of S0 model. In this study the parameterization proposed for the Emax model proved to have advantages over the traditional Emax model.

For DBP and after a single dose, hysteresis was observed in some patients, indicating a delay between the concentration of the drug and its concentration at the effect site. For the PQ interval, hysteresis was not observed. For verapamil more patients showed hysteresis than for diltiazem. No hysteresis was observed at steady state, therefore DBP, HR and changes in PQ interval were directly correlated to drug concentrations.

From the comparative analysis between single dose and steady state of the pharmacodynamic parameters in the individual patients it was concluded that the parameters were not correlated. That contrasts with the results published by some investigators (Donnelly et al., 1994), as they reported that responsiveness to the first dose correlates with parameters obtained after 4 to 6 weeks of treatment with calcium antagonists. The discrepancies found in the results can be explained by either the insufficient statistical power of the study or by a change in responsiveness as seen with one of the verapamil parameters. This could only be addressed by a larger study population.

In conclusion, the findings of this study indicate that a once-daily administration of mibefradil 100 mg was associated with reductions in diastolic blood pressure. This long half-life renders mibefradil suitable for once daily administration without the need for a modified formulation. Mibefradil has long-lasting and potent

CHAPTER 4 COMBINING PHARMACOKINETIC AND PHARMACODYNAMIC DATA DURING POPULATION ANALYSIS

4.1 SUMMARY

In this chapter the mixed effect modelling approach was utilised in the assessment of the influence of covariates on pharmacokinetic and pharmacodynamic parameter estimates. In addition, four different approaches of combining pharmacokinetic/ pharmacodynamic data were explored and compared.

4.2 INTRODUCTION

Sheiner and co-workers (1977) proposed carrying out a covariate analysis by iteratively incorporating the covariates in the model, using NONMEM. However, several alternative strategies have been suggested in the literature to deal with the incorporation of covariates into a population model (Mallet et al., 1988; Maitre et al., 1991; Mandema et al., 1992; Mentre and Mallet, 1994). The first was a three-step approach (Maitre et al., 1991) integrating the individual Bayes parameter estimates (POSTHOC) with graphical exploratory analysis. This approach consisted of plotting the POSTHOC parameter estimates obtained from the best structural model against each covariate in order to identify and describe possible relationships. Only the covariates showing an influence were used in further NONMEM runs. This approach has some drawbacks: the influence of POSTHOC parameter estimates and covariates is less obvious than the relationship between the true individual parameters, because POSTHOC parameter estimates are biased towards the typical population values. This is more noticeable in the case of sparse data with high variability. Another disadvantage is that the graphical method does not take into account the correlation among covariates.

A subsequent extension of this approach was proposed by Mandema (1992), who applied stepwise multiple linear regression analysis and a spline smoothing function in stepwise generalised additive modelling (GAM) to identify and describe the relationships between individual parameter estimates and covariates. Generalised additive modelling has the advantage of allowing non-linear relationships to be expressed (Hastie and Tibshirani, 1996). It is represented by the mathematical equation:

$$Pi=\alpha + \sum_{i=1}^{n} g_k(X_{ij})$$

where $g_k(X_{ij})$ repressents a function, such as natural splines, P_i is the POSTHOC parameters and α is an intercept.

One of the drawbacks of the GAM procedure is that it can be influenced by outlying individuals that can interfere with the expression of covariate-parameter relationships. It has been applied in population analysis of pharmacokinetic and pharmacodynamic data (Davidian and Gallant, 1992). An integrated approach to the selection of covariates comprising multiple linear regression, stepwise generalised additive modelling, tree-based modelling and linearisation of the non-linear mixed effect model was suggested by Ette et al. (1995). Jonsson et al. (1999) developed a program, Xpose® that performs plots and auxiliary analyses to assist in the covariate selection.

All of the approaches mentioned above were implemented using parametric methodology. Alternative strategies have been proposed using the semi-nonparametric (SNP) method (Davidian and Gallant, 1992) or the nonparametric method (Mentre and Mallet, 1994).

4.3 AIMS OF THE ANALYSIS

The data analysis was carried out to:

i) Determine the influence of covariates on the PK and PD parameter estimates obtained after the administration of single and multiple doses of mibefradil.

ii) Compare different approaches for combining pharmacokinetic/pharmacodynamic data during the modelling process using data obtained after a single dose of mibefradil.

4.4 METHODS

The data used in the present analysis were obtained from the study described in Chapter 3. For the single-dose study, 18 patients were included who were given 150 mg of mibefradil. Details of the demographic characteristics and clinical status were given in section 3.4.2 and presented in Table 3.4.2. In addition, steady-state data were obtained from 10 patients who were given 100 mg of mibefradil.

4.5 DATA ANALYSIS

The analysis was carried out on an Opus Personal Computer with a Pentium 120 MHZ processor. Data were analysed by a nonlinear mixed effects model using the NONMEM software package, version V, level 2 (Beal and Sheiner, 1998). Fortran Power-Station® (version 1.0a, Microsoft Corporation) was used as the compiler. Statistical analysis was carried out using the software Splus® (1998) installed on a Compaq Armada 7792 DMT, computer.

Data were first entered into an Excel® spreadsheet. The data set for single dose analysis contained information on time, dose, measured concentrations and measured pharmacodynamic variables. Models were implemented using either the PRED subroutine or the PREDPP library. The data item TYPE was included as a flag to distinguish between drug concentration and pharmacodynamic measurements. Items required by the PREDPP subroutine, such as Event Identification Data Item (EVID) and Compartment Data Item (CMT) were also included. From the full data set, two new data sets, one with the rows corresponding to drug measurements removed and the other with the PD measurements removed were produced. For the steady-state analysis, the data set included date, time, dose, measured observations, either concentration or pharmacodynamic variables, and TYPE. The additional items required by PREDPP were EVID, SS, II and CMT. SS indicates that the dose is a steady state dose and II is the dosing interval. Both data sets were checked for errors and outliers by the

"Checkout" option available in NONMEM. Exploratory analysis was carried out to identify possible outliers.

4.5.1 PHARMACOKINETIC DATA ANALYSIS

Structural Model - Mono- and bi-exponential decline models were fitted to the concentration-time data. Models were parameterised to give estimates of absorption rate constant (ka), for the first-order or duration of the absorption for the zero-order model, volumes of distribution of the central and peripheral compartments (V/F, V_1/F, V_2/F), clearance/bioavailability (CL/F), intercompartmental clearance (Q) and lag time (Tlag). The PREDPP subroutines ADVAN2/TRANS2 and ADVAN4/ TRANS4 were selected to run mono- and bi-exponential decline models, respectively. A data set without PD measurements was used to identify the pharmacokinetic structural model.

The mathematical equations used to model zero-order and first-order oral absorption processes after single-dose administration for mono- and bi-exponential declines are described in Gibaldi & Perrier (Gibaldi and Perrier, 1982). The elimination half-life was derived from the microscopic rate constants as described in section 2.4.3.

The interindividual variability was assumed to follow a logarithmic, Gaussian distribution. The models for residual variability, described in section 1.4.5, were fitted to the data and the selection was made as indicated from graphical analysis. Choice of estimation method was made between the FO (First Order Method) and FOCE (First Order Conditional Estimation Method). FOCE was used providing such an estimation method was warranted. Diagonal elements of the Ω-matrix were first estimated. In addition, once the structural pharmacokinetic model was finalised, covariance terms of the lower triangle of the Ω-matrix were estimated (full variance-covariance matrix) and retained providing successful completion of the NONMEM run. POSTHOC parameters were estimated from the "best" (basic model-without covariates) pharmacokinetic model.

Covariate Model - Covariates were incorporated into the pharmacokinetic model by a two step approach using individual 'POSTHOC' estimates. Linear and nonlinear relationships between individual pharmacokinetic parameter estimates and covariates were investigated graphically. A generalised additive model (GAM, available in the statistical package Splus (1998)) was used to investigate relationships between the POSTHOC estimates of individual parameters (from the basic model) with covariates. For each covariate a hierarchy of models such as: not included, linear and non-linear models (spline) were tried. The model selection for the GAM fitting was made based on the Akaike Information Criterion (AIC) and the models that produced the lowest AIC were selected. Plots of the AIC against each model were also produced to help in the model selection. The demographic characteristics and clinical status of the patients (Table 3.4.2) were used as covariates in the modelling process. If no covariates showed an influence on the primary pharmacokinetic parameter, the covariate submodel was omitted. Covariates selected through the GAM were then evaluated using NONMEM by testing each covariate individually on each parameter as described in Chapter 1 section 1.4.8 and model selection was based on the criteria described in Chapter 1 section 1.4.7. A reduction on objective function value of more than 7.9 points was considered statistically significant at 99.5 % confidence level.

4.5.2 PHARMACOKINETIC/PHARMACODYNAMIC DATA ANALYSIS

Structural Model – Once the best-fit pharmacokinetic population model was obtained the mean and variance estimates of the final population pharmacokinetic parameters were fixed during the subsequent pharmacodynamic modelling process. A full data set including PK and PD measurements was used in the analysis. Only one response variable was used for population pharmacodynamic modelling, the diastolic blood pressure. As a result of the previous analysis, the Emax pharmacodynamic model re-parameterised as proposed by Schoemaker (1998) and described in Chapter 3 was implemented. The interindividual variability on the pharmacodynamic parameters were assumed to follow a logarithmic, Gaussian distribution. The residual error on the

pharmacodynamic measurements was assumed to be homoscedastic and therefore the additive model was used.

Covariate Model - The influence of covariates was tested on the pharmacodynamic (Emax, and S0) parameter estimates. Covariate model building was carried out as described in section 4.5.1.

4.5.3 COMBINING PHARMACOKINETIC/PHARMACODYNAMIC DATA

Four different approaches were used to analyse the pharmacokinetic/pharmacodynamic relationships of mibefradil to changes in diastolic blood pressure after single-dose administration:

1. All pharmacokinetic parameters for each individual were fixed to the population averages previously obtained. Pharmacodynamic parameters were estimated (PD data set)
2. Pharmacokinetic parameters and their variances were fixed to the population estimates previously obtained and the pharmacodynamic parameters were estimated, but the pharmacokinetic data were left in the data set under DV (the dependent variable)
3. The pharmacokinetic and pharmacodynamic models were fitted simultaneously using the same NMTRAN subroutines as in 1).
4. The pharmacodynamic parameters were estimated using individual predicted concentrations (IPRED) obtained from the pharmacokinetic model fit. Individual predicted concentrations were included as an extra item in the data set and a PRED control file was written.

4.6 RESULTS

4.6.1 PHARMACOKINETIC MODEL

4.6.1.1 Single-Dose Study

Structural Model - One hundred and ninety-five concentrations, ranging from 14.5 to 1727.0 ng ml^{-1}, were available after a single oral dose of mibefradil. Eighty-three per cent of the patients had 11 measured concentrations each and the remainder had 10 concentrations each.

A comparison of mono- and bi-exponential decline models and zero- and first order absorption models showed that the pharmacokinetics of mibefradil were better described using an open model with first-order absorption and a bi-exponential decline. Details of this comparison are shown in Table 4.6.1.a. Comparing the mono- and bi-exponential decline models estimated under the FO method, the parameters were estimated with similar degree of confidence and there was a decrease in the proportional component of the residual error from 84.1 to 27.7%. Clearance was estimated with similar precision by both models. The oral absorption rate and lag time estimates were better estimated with a bi-exponential decline model than with a mono-exponential decline model. However, the variability in the peripheral compartment volume was poorly estimated with the two-compartment model. The value of the objective function was reduced by 49.5 points when the bi-exponential decline model was fitted to the data. Plots of weighted residuals against time after the dose obtained from both models are shown in Figure 4.6.1.a. The bi-exponential decline model yielded a more random scatter of weighted residuals around zero than the mono-exponential decline model, especially at later time points, and therefore was selected for further analysis.

The FO and FOCE methods estimated clearance to be 6.8 and 6.4 L h^{-1} respectively, with an error of 8.7 and 10.3%. Difficulties in estimating interpatient variance in CL/F, Q, V_1/F, Ka and Tlag were experienced with the FOCE approach, while interpatient variability in V_2 was poorly characterised by the FO method. In addition, residual error

Figure 4.6.1.a Weighted residuals versus time obtained from mono-exponential and bi-exponential decline models using the FO method with single dose mibefradil data

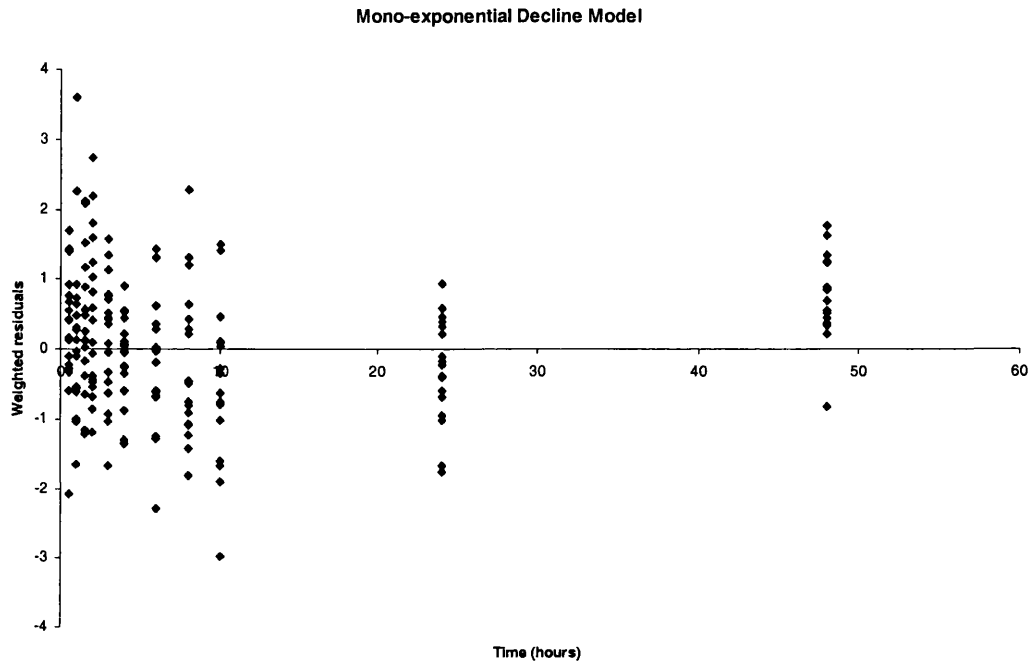

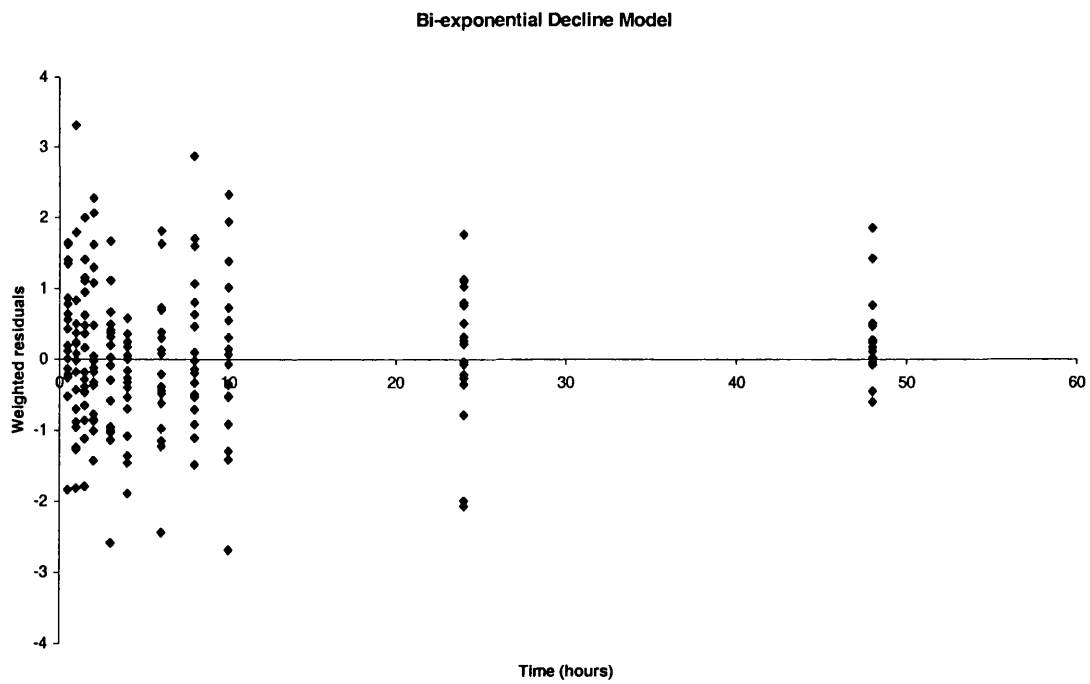

Table 4.6.1.a Pharmacokinetic parameter estimates with mono- and bi-exponential decline models after a single dose of mibefradil (150 mg)

	Mono-exponential		Bi-exponential	
Parameters	**FO**	**FOCE**	**FO**	**FOCE**
ka (h^{-1})	2.30	9.93	3.05	2.38
(% SE)	*21*	*20*	*13*	*22*
Variability ka (%)	114	101	92.0	42.5
(% SE)	*25*	*48*	*33*	*61*
CL/F (Lh^{-1})	6.60	7.10	6.81	6.64
(% SE)	*7.3*	*12*	*8.7*	*10*
Variability CL (%)	30.4	35.4	35.9	40.1
(% SE)	*49*	*88*	*53*	*81*
V_1/F (L)	168	164	148	114
(% SE)	*6.3*	*6.8*	*6.1*	*11*
Variability V_1 (%)	25.6	30.6	26.7	41.1
(% SE)	*51*	*64*	*46*	*66*
V_2/F (L)	-		32.5	63.5
(% SE)	-		*15*	*17*
Variability V_2 (%)			10.2	28.0
(% SE)			*1854*	*89*
Q ($L\ h^{-1}$)	-		3.20	47.3
(% SE)	-		*16*	*40*
Variability in Q (%)			171	85.7
(% SE)			*50*	*49*
Tlag (h)	0.38	0.45	0.4	0.3
(% SE)	*13*	*5.8*	*11*	*20*
Variability Tlag (%)	54.9	6.65	35.6	49.8
(% SE)	*70*	*70*	*53*	*80*
Residual error				
at 20 ng ml^{-1}(%)	84.1	153.6	27.70	72.9
at 1200 ng ml^{-1}(%)	9.92	12.0	7.70	8.10
OFV	2039.449	2071.793	1989.896	1999.630

Key: SE denotes the standard error of the parameter estimate; ka - oral absorption rate constant; CL - clearance, V_1 - Volume of the central compartment; V_2 - Volume of distribution of the peripheral compartment; Q - intercompartmental clearance; OFV - objective function value

increased from 27.7% to 72.9% when the FOCE method was used (Table 4.6.1.a). Plots of weighted residuals against time did not suggest an improvement in the fit by using the FOCE method (Figures 4.6.1.a and 4.6.1.b). Considering the ten-fold increase in computing time and the lack of obvious improvement when FOCE was used, the FO method was applied to subsequent analyses.

Performing the Anderson-Darling normality test on POSTHOC parameter estimates checked the assumption in the model about the logarithmic normal distribution of the interindividual variability. The combined (proportional and additive) residual error structure proved to be superior to the additive, as judged by the drop in objective function value of 24.5 points.

It was concluded that the most appropriate model to describe the data was the two-compartment open model with a combined residual error model and that the FO method was satisfactory for parameter estimation.

Covariate Model – Only the baseline value for blood pressure and weight had an influence on clearance according to the generalised additive modelling (GAM) analysis (as shown in Table 4.6.1.b). The same covariates were selected when the POSTHOC estimates of the volume of the central compartment were analysed (Table 4.6.1.b). All covariates were subsequently evaluated in the nonlinear mixed effect model, testing each covariate individually on each parameter. The linear model for covariates wasinvestigated with GAM but when it was tested with NONMEM it did not improve the fit. No covariates showed a statistically significant influence either on clearance (CL/F) or on volume (V/F) when the stepwise procedure was implemented within NONMEM (Table 4.6.1.c).

Figure 4.6.1.b Weighted residuals versus time obtained from mono-exponential and bi-exponential decline models using the FOCE method with single dose mibefradil data

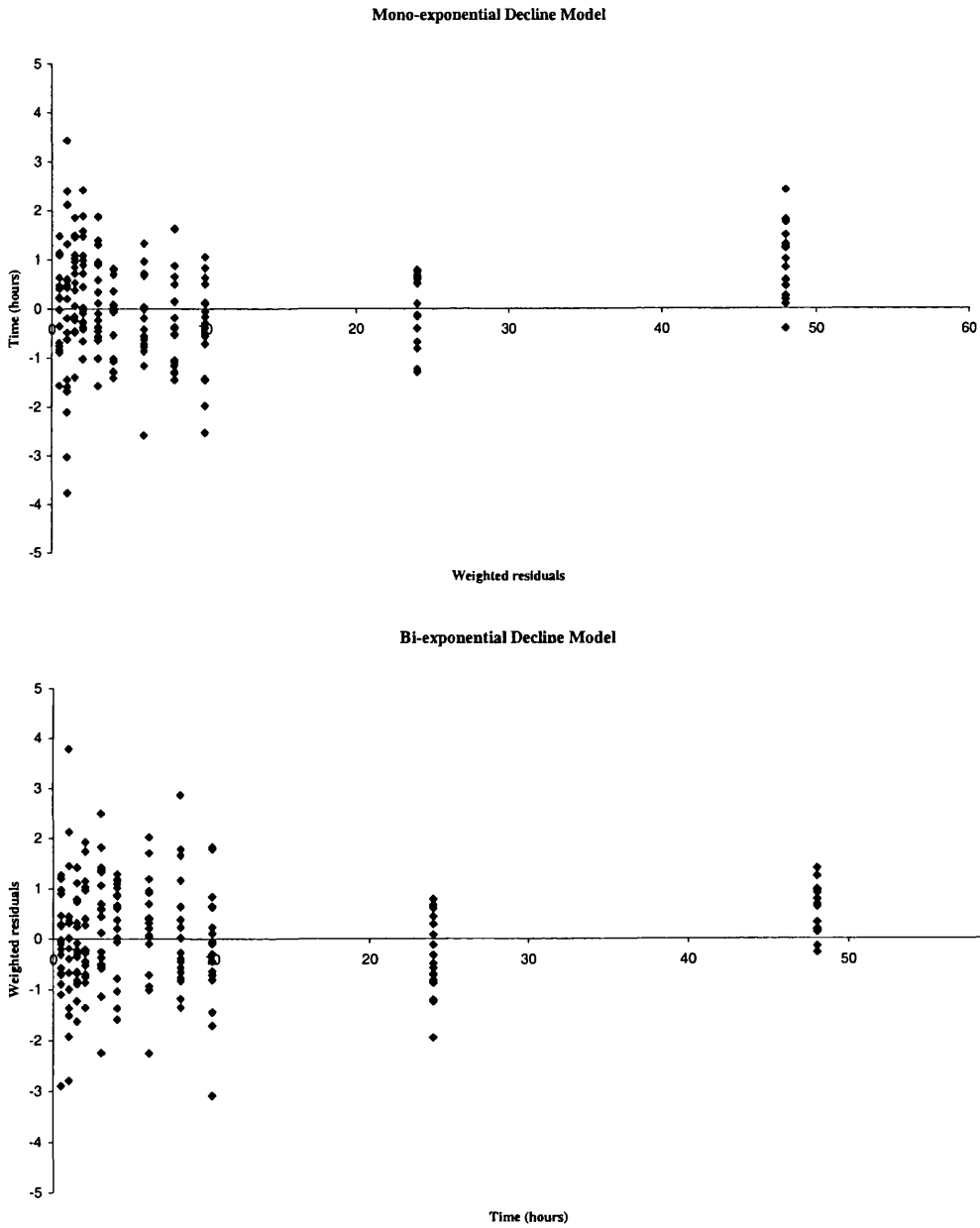

Table 4.6.1.b Results obtained from applying the generalised additive modelling approach to the POSTHOC pharmacokinetic parameter estimates after a single dose administration of mibefradil

Parameter	Model	AIC	DF
CL/F		446	17
	~Weight	361	16
	~BASB+Weight	337	15
	~ns(BASB,df=2)+Weight	274	14
	~ns(BASB,df=2)	261	15
V1/F		98542	17
	~Weight	77297	16
	~BASB + Weight	69591	15
	~ns(BASB,df=2) + Weight	61037	14
	~ns(BASB,df=2)	61008	15

Key: CL represents the clearance; F is the bioavailability; V1 is the volume of distribution of the central compartment; BASB is the baseline value for diastolic blood pressure, DF is the degrees of freedom; AIC is the Akaike Information Criterion and 'ns' represents the natural spline model.

Table 4.6.1.c Results of individual covariates tested by NONMEM in the pharmacokinetic parameter estimates from single dose administration of mibefradil

Parameter	Model	OBFV	ΔOBFV[a]
CL/F		1989.90	
	θ_3 * (Age/57)$^{\theta 7}$	1989.87	-0.03
	θ_3 * (Height/166)$^{\theta 7}$	1994.53	4.63
	θ_3 * (Weight/80)$^{\theta 7}$	1993.92	4.02
	θ_3 * (BASB/89)$^{\theta 7}$	1988.65	-1.25
V1/F	θ_8 * (Age/57)$^{\theta 9}$	1989.55	-0.35
	θ_8 * (Height/166)$^{\theta 9}$	1987.16	-2.74
	θ_8 * (Weight/80)$^{\theta 9}$	1986.75	-3.15
	θ_8 * (BASB/89)$^{\theta 9}$	1989.61	0.28

Key: OFV - Objective Function Value; V1 is the volume of distribution of the central compartment; CL/F is the clearance and F is the bioavailability. θ is a parameter estimate; BASB is the baseline value for diastolic blood pressure.

[a] *A reduction in objective function value of 7.9 points was considered statistically significant, at the 99.5% confidence level.*

4.6.1.2 Steady-State Study

Structural Model - One hundred and thirteen steady state concentrations were available for analysis, ranging from 9.1 to 1421.0 ng ml^{-1}. The number of data points per patient ranged from 9 to 12. The bi-exponential decline model fitted the data better than a mono-exponential decline model (objective function value drop of 23.5 points). Figure 4.6.1.d shows that with a bi-exponential decline model, the weighted residuals against time were more scattered around the abscissa-axis towards the late times than with one-compartment model. However, the parameter estimates of the bi-exponential decline model were associated with problems.

The oral absorption rate constant had a value of 0.167 h^{-1} and an error of 41% therefore could not be estimated satisfactorily. The interindividual variability on oral absorption rate was estimated at 30% with an error of 88.7%. Similar values of clearance were obtained with both models. The mono-exponential decline model estimated the volume of distribution of the central compartment to be 277 L with a degree of confidence of 8.7%. However, the interindividual variability on this parameter was indeterminate. The value of V_1 obtained with a bi-exponential decline model was poorly estimated and the interindividual variability in this parameter was high at 112%.

The interindividual variabilities on the volume of distribution of the peripheral compartment and on intercompartmental clearance were not well characterised by a bi-exponential decline model. However, due to the overall improvement in fit observed on the plots, the bi-exponential decline model was selected for future analysis.

The FOCE method offered no advantage over the FO method. Standard errors of the pharmacokinetic parameters were not estimated and the interindividual variability in V_2 and on Q was indeterminate (Table 4.6.1.d). Figures 4.6.1.c and 4.6.1.d show the plots of weighted residuals against time obtained from both approaches. No improvement in plots was observed using the bi-exponential decline model.

Figure 4.6.1.d Weighted residuals versus time obtained using mono-exponential and bi-exponential decline models using the FOCE method with steady state mibefradil data

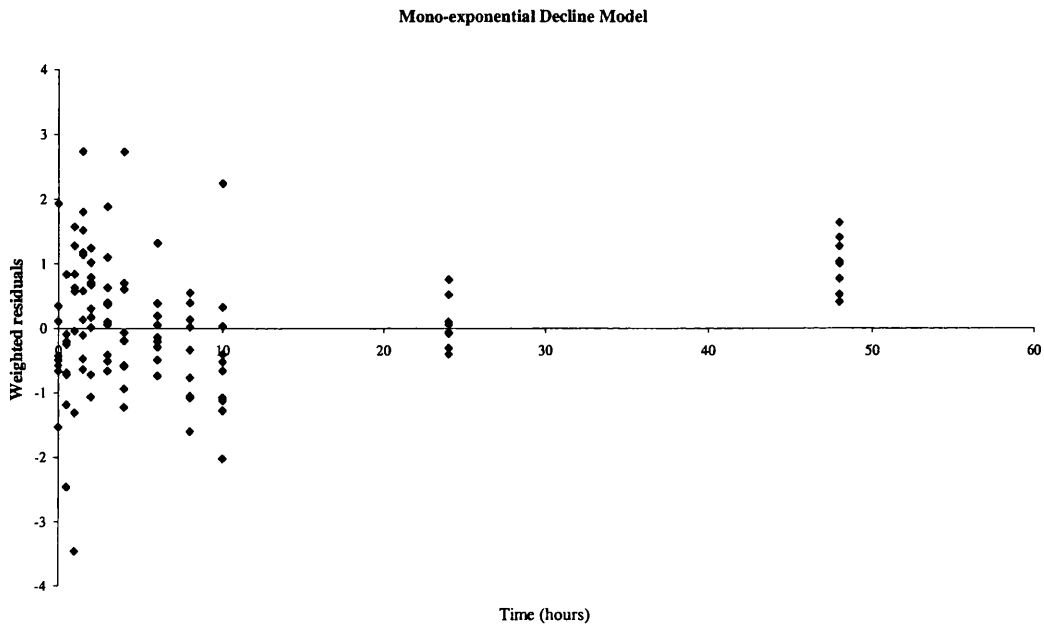

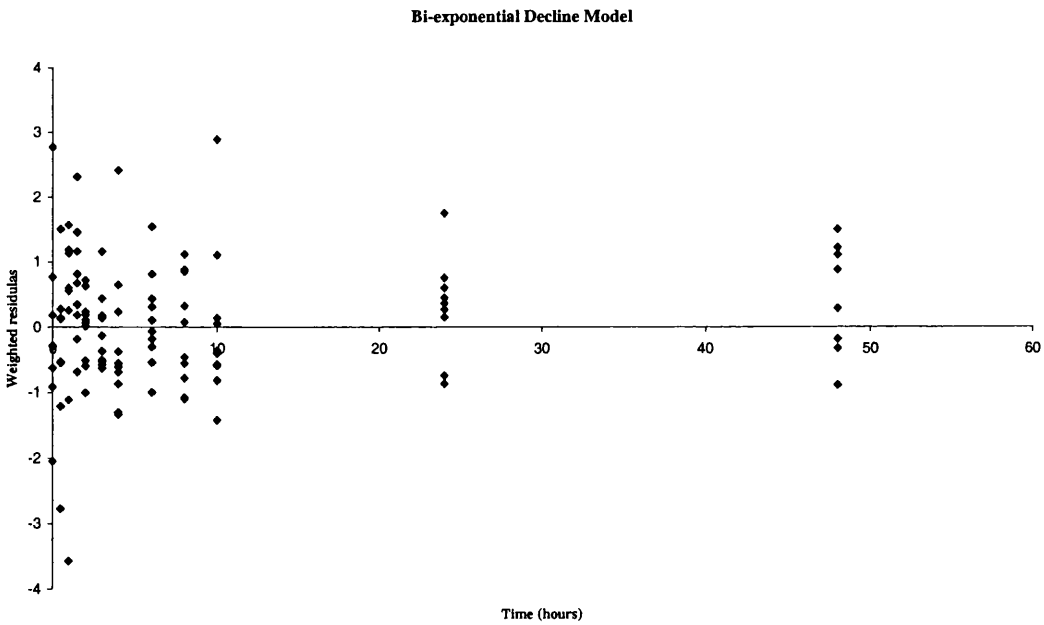

Figure 4.6.1.c Weighted residuals versus time obtained using mono-exponential and bi-exponential decline models and the FO method with steady state mibefradil data

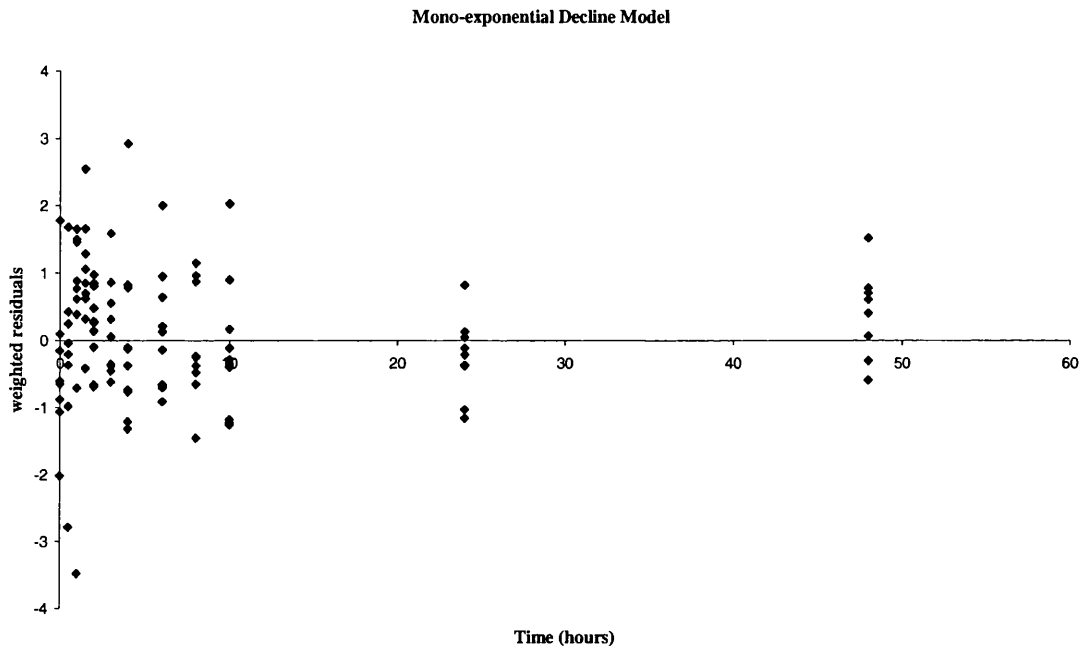

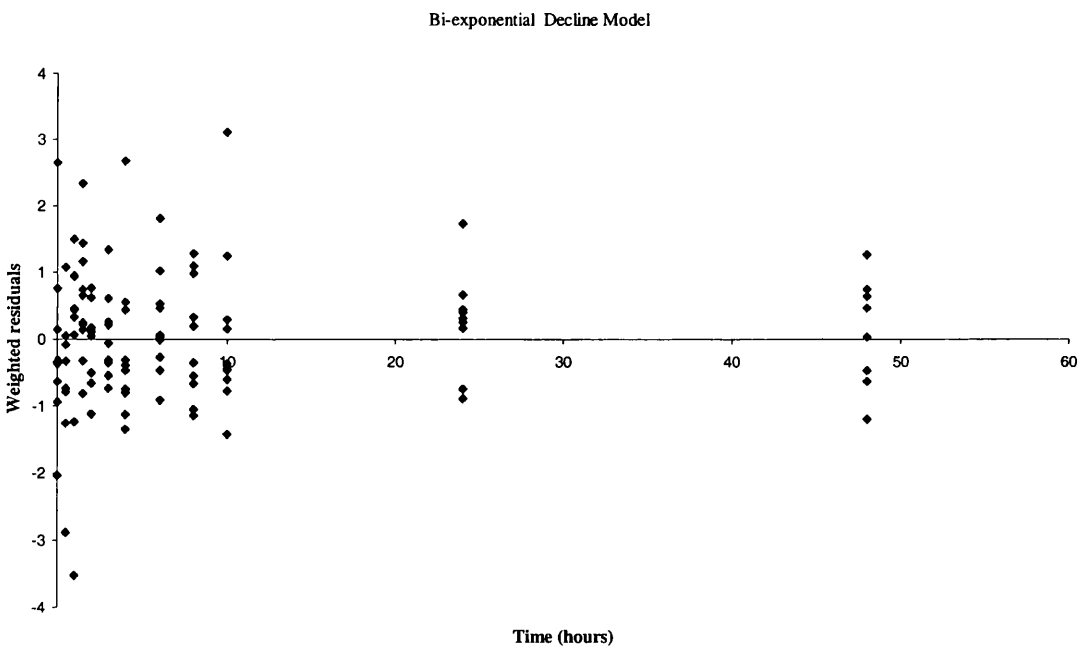

Table 4.6.1.d Pharmacokinetic parameter estimates obtained using mono- and bi-exponential decline models with multiple dose mibefradil data

	Mono-exponential		Bi-exponential	
Parameters	**FO**	**FOCE**	**FO**	**FOCE**
ka (h^{-1})	0.65	1.58	0.17	0.95
(% SE)	*20*	*16*	*41*	*
Variability ka (%)	185	51.3	29.6	42.4
(% SE)	*58*	*66*	*89*	*
CL/F (L h^{-1})	6.5	6.50	6.5	6.66
(% SE)	*13*	*14*	*14*	*
Variability CL (%)	37.3	43.5	37.5	42.7
(% SE)	*56*	*37*	*58*	*
V_1/F (L)	277	221	24.4	166
(% SE)	*8.7*	*11*	*47*	*
Variability V_1 (%)	indeterminate	22.4	56.3	35.2
(% SE)	*	*110*	*112*	*
V_2/F (L)	-		256	140
(% SE)	-		*11*	*
Variability V_2 (%)			indeterminate	indeterminate
(% SE)			*	*
Q (L h^{-1})	-		22.4	14.8
(% SE)	-		*39*	*
Variability in Q (%)	-		175	indeterminate
(% SE)	-		*420*	*
Residual error				
at 20 ng ml^{-1}	191.5	263.3	61.1	9.57
at 1200 ng ml^{-1}	8.29	9.91	8.90	9.57
OFV	1142.815	1158.181	1119.262	1125.580

*Key: SE denotes the standard error of the parameter estimate; ka - oral absorption rate constant; CL - clearance, V_1 - Volume of the central compartment; V_2 - Volume of distribution of the peripheral compartment; Q - intercompartmental clearance; OFV - objective function value; * not estimated.*

Although the objective function value dropped only 2 points with the combined structure (proportional and additive) compared to the additive model, the combined structure was selected for further analysis due to its flexibility.

Covariate Model – Volume of distribution of the central compartment and clearance were influenced by age, according to the GAM analysis results. After the inclusion of age as a covariate for V1, the AIC was 1709, (df=8), representing a decrease from the model without covariates. For clearance, the AIC decreased after the inclusion of age compared to the model without covariates. No covariates had an influence on volume of distribution of the peripheral compartment. The results of the GAM analysis are presented in Table 4.6.1.e.

No covariates had a statistically significant influence on any pharmacokinetic parameters when modelled using NONMEM. Similar conclusions were obtained by Welker (Welker, 1998).

Table 4.6.1.e Results obtained from applying the generalised additive modelling approach to the POSTHOC pharmacokinetic parameter estimates obtained after multiple dose administration of mibefradil

Parameter	Model	AIC	DF
CL/F		149	9
	~BASB	138	8
	~AGE	134	8
	~Height	158	8
	~Weight	151	8
V1/F		2213	9
	~BASB	1869	8
	~AGE	1709	8
	~Height	2552	8
	~Weight	2543	8

Key: CL represents the clearance; F the bioavailability; V1 is the volume of distribution of the central compartment; BASB is the baseline value for diastolic blood pressure, df is the degrees of freedom; AIC is the Akaike Information Criterion and ns represents the spline model.

4.6.2 PHARMACOKINETIC/PHARMACODYNAMIC RELATIONSHIPS

4.6.2.1.Single-Dose Study

Structural Model – The S0 model was fitted to the diastolic blood pressure data by fixing the pharmacokinetic parameters presented in section 4.6.1.1 while fitting the PD data. A full data set, comprising PK and PD measurements, was used in the analysis. (This corresponds to the method described in section 4.5.3).

Emax was estimated to be –22.4 mmgHg with an interindividual variability of 42.2%. The estimate of SO was –0.0225 mmHg/(ng/L) with a wide interindividual variability of 34.9 %. Figure 4.6.2 illustrates the weighted residuals plot obtained for predicted diastolic blood pressure and shows a scattered distribution.

Covariate Model – The GAM analysis identified the baseline value of blood pressure as a covariate that influenced Emax and two covariates, the baseline value of blood pressure and smoking status, that influenced the POSTHOC estimates of the S0 parameter. However, when baseline value was incorporated in the Emax parameter using NONMEM, only 5.1 points decrease ocurred whereas for the SO parameter the drop in objective function was 6.4 points. When smoking status was included in the model as a second covariate, the objective function decreased further 5 points. No covariates were therefore selected from the NONMEM runs.

Figure 4.6.2 Weighted residuals against predicted DBP obtained from the S0 model, fixing pharmacokinetic parameters (Method 2) and after the administration of a single dose of mibefradil

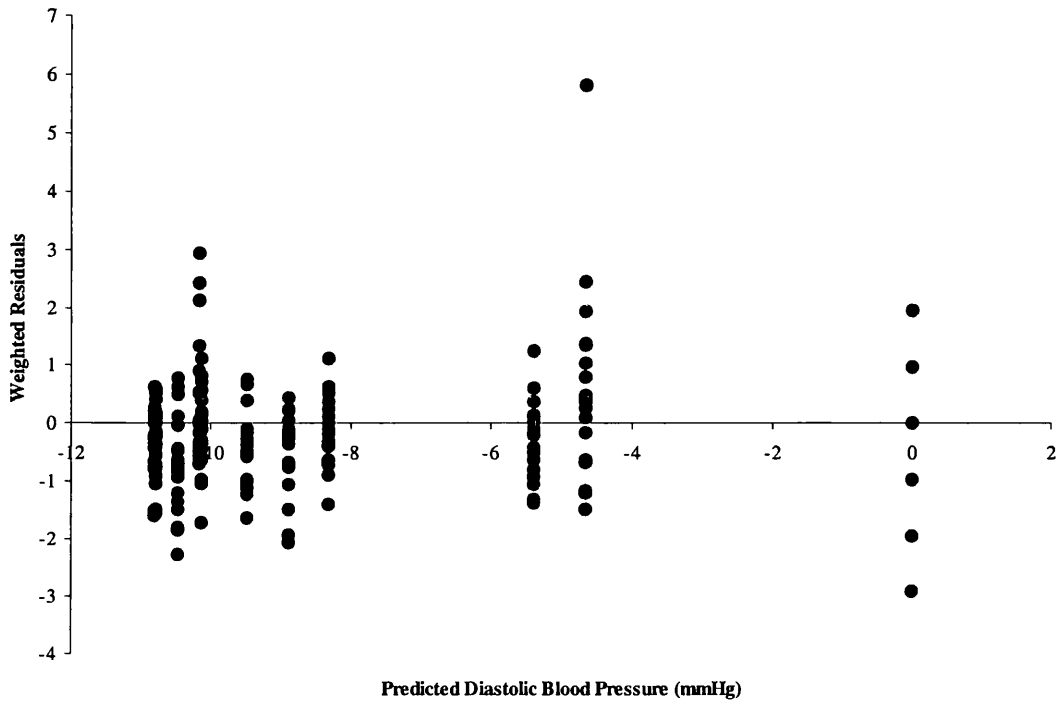

4.6.2.2 Steady-State Study

Structural Model – The parameter estimates obtained in the PD analys
in Table 4.6.2. It was not possible to obtain standard errors of these esti
steady-state analysis.

Covariate Model – Difficulties in the estimation step led to no covariat
identification. Interpatient variability in Emax was not estimated and th
step was aborted. It is likely that the small number of patients and the h
variability contributed to the problems with the parameter estimation.

4.6.2.2 Steady-State Study

Structural Model – The parameter estimates obtained in the PD analysis are presented in Table 4.6.2. It was not possible to obtain standard errors of these estimates in the steady-state analysis.

Covariate Model – Difficulties in the estimation step led to no covariate model identification. Interpatient variability in Emax was not estimated and the covariance step was aborted. It is likely that the small number of patients and the high interpatient variability contributed to the problems with the parameter estimation.

Table 4.6.2 Pharmacokinetic/pharmacodynamic parameter estimates obtained after the administration of multiple doses of mibefradil, for diastolic blood pressure (N=10)

	PK FIXED Full data set
PK parameters	
ka (h^{-1})	0.17
(% SE)	*40.*
Variability ka (%)	29.6
(%SE)	*89*
CL/F (L h^{-1})	6.5
(% SE)	*14*
Variability CL (%)	37.5
(% SE)	*58*
V_1/F (L)	24.4
(% SE)	*47*
Variability V_1 (%)	56.3
(% SE)	*112*
V_2/F (L)	256
(% SE)	*11*
Variability V_2 (%)	indeterminate
(% SE)	*
Q (L h^{-1})	22.4
(% SE)	*39*
Variability in Q (%)	175.0
(% SE)	*420*
Residual error	
at 20 ng ml^{-1}	61.1
at 1200 ng ml^{-1}	8.9
PD parameters	
Emax (mmHg)	-22.9
(% SE)	6.4
Variability Emax (%)	indeterminate
(% SE)	*
S0 (mmHg/(ng/L)	-0.0378
(% SE)	*
Variability S0 (%)	17.2
(% SE)	*53*
Residual error	42.5

*Key: SE denotes the standard error of the parameter estimates; ka oral absorption rate constant, CL clearance, V_1 Volume of the central compartment; V_2 Volume of distribution of the peripheral compartment; Q intercompartmental clearance; F is the bioavailability; OFV objective function value, * not estimated*

4.6.3. COMBINING PHARMACOKINETIC/PHARMACODYNAMIC DATA

The results from fitting the S0 model to the single-dose data using the four different approaches are presented in Table 4.6.3. Simultaneously fitting the PK and PD data led to difficulties in estimating the interpatient variability on V2. The remaining PK parameter estimates were similar across the three methods. The Emax estimates were slightly lower with Method 1 and 2 than with Method 3 and Method 4. The interpatient variability for Emax with Method 1 was indeterminate and with Method 2 was much higher than with the other two methods. For the S0 parameters, the estimates from the four methods were similar.

Table 4.6.3 Pharmacokinetic/pharmacodynamic parameter estimates obtained from four different methods, after the administration of a single dose of mibefradil, for diastolic blood pressure (N=17)

	METHOD 1 PK fixed (PD data set)	METHOD 2 PK fixed (FULL data set)	METHOD 3 Simultaneous PK/PD	METHOD 4 IPRED
PK parameters	**FIXED**	**FIXED**		
ka (h^{-1})	3.10	3.10	3.30	
(% SE)	*13*	*13*	*13*	
Variability ka (%)	92.0	92.0	86.0	
(% SE)	*33*	*33*	*37*	
CL/F (L h^{-1})	6.81	6.81	6.50	
(% SE)	*8.7*	*8.7*	*6.2*	
Variability CL (%)	35.9	35.9	33.0	
(% SE)	*53*	*53*	*42*	
V_1/F (L)	148	148	137.0	
(% SE)	*6.1*	*6.1*	*6.3*	
Variability V_1 (%)	26.7	26.7	26.4	
(% SE)	*46*	*46*	*42*	
V_2/F (L)	32.5	32.5	34.4	
(% SE)	*15*	*15*	*15*	
Variability V_2 (%)	10.2	10.2	0.43	
(% SE)	*1854*	*1854*	*	
Q (L h^{-1})	3.20	3.20	3.40	
(% SE)	*16*	*16*	*16*	
Variability in Q (%)	171	171	145	
(% SE)	*50*	*50*	*52*	
Tlag (h)	0.40	0.40	0.35	
(% SE)	*11*	*11*	*12*	
Variability Tlag (%)	35.6	35.6	45.1	
(% SE)	*53*	*53*	*62*	
Residual error				
at 20 ng ml^{-1}	27.7	27.7		
at 1200 ng ml^{-1}	7.7	7.7		
PD parameters	**ESTIMATED**			
Emax (mmHg)	-23.7	-22.4	-27.2	-26.0
(% SE)	*6.2*	*9.0*	*5.9*	*5.4*
Variability Emax (%)	*	42.2	10.9	8.40
(% SE)	indeterminate	*74*	*142*	*186*
S0 (mmHg/(ng/L)	-0.0294	-0.0225	-0.0300	-0.0300
(% SE)	*12*	*14*	*7.3*	*7.3*
Variability S0 (%)	37.9	34.9	32.4	34.5
(% SE)	*38*	*57*	*26*	*29*
Residual error	0.90	0.90	1.00	1.30

*Key: SE denotes the standard error of the parameter estimate; ka - oral absorption rate constant CL - clearance, V_1 - Volume of the central compartment; V_2 - Volume of distribution of the peripheral compartment; Q - intercompartmental clearance; OFV - objective function value; *not estimated*

4.7 DISCUSSION

The most appropriate model describing the pharmacokinetics of mibefradil after a single dose was the bi-exponential decline model with first-order absorption, and a lag time. The variability in V_2 was estimated to be very high. That can be explained in part by the fact that the drug concentrations were only sampled long enough to identify, but not define the second compartment. The results obtained here contrast with the results obtained in chapter 3, where a mono-exponential decline model was selected for the individual fits. The population approach allows the combination of information from each individual to be used simultaneously in the estimation of the mean population parameters. Problems encountered during the modelling process due to deficient sampling times where associated with limitations in the traditional approach. A mono-exponential decline model was selected in a previous population study of mibefradil using NONMEM (Welker and Banken, 1998), but they only had samples up to 24 hours after the last dose and were therefore unable to identify the second compartment. The pharmacokinetic parameters reported by these investigators were similar to the ones obtained in this study.

The GAM procedure selected the baseline value for diastolic blood pressure as a covariate correlated with Emax. The influence of the same covariate was selected by Welker et al. (1998) using NONMEM. However, NONMEM failed to detect such a relationship in the present study. This might be explained by the small number of patients. The use of GAM to identify relationships between POSTHOC parameter estimates and covariates was found to be useful, although in the present study, the amount of data available was limited therefore the methodology could not be fully explored. However, in the presence of a high number of covariates the time required to test all covariates individually in NONMEM can be very time consuming. GAM is an exploratory technique that can be used in conjunction with graphical analysis to reduce the time spent testing covariates within NONMEM. The preliminary results obtained in the present study indicate that the technique could offer potential advantages in covariate modelling.

The result obtained for the PK parameters when the PK/PD data were fitted simulaneously were similar to those obtained on sequential analysis. This indicated that the inclusion of PD data did not seriously compromise the PK parameter estimation on this occasion. However, the simultaneous approach failed to obtain an estimate of the standard error of interpatient variability on V2. This can be explained by the fact that the misspecification of PD model caused distortion in the PK parameters. Fixing the PK parameters is particular useful when the uncertainty on PD data is higher than with the PK data (Holford and Sheiner, 1981).

In contrast, for the PD parameters, the simultaneous fitting performed better than the sequential fitting as judged by the precision in the parameter estimates. The IPRED method yielded similar results to the simultaneous fitting. Fixing the PK parameters while fitting the PD data has the advantage of being faster than the simultaneous fitting. Fixing the PK parameters removes variability from the data that can affect the estimation of the PD parameters. In this study, the interindividual variability on Emax was indeterminate when the PK parameters were fixed. In contrast, the interindividual variability was estimated when the PK data were left in the data set while estimating PD parameters. Similar conclusions were reached in a preliminary simulation study by other investigators (Wade and Karlsson, 1999). They carried out a simulation study in PK and PD data from 30 data sets with 50 subjects each. The variability in PK and PD parameters were set to 10 and 30 % and NONMEM was used to analyse the data. These investigators discourage the practice of removing the PK data while estimating the PD parameters. Although the PK parameters are not being estimated in Method 2, the inclusion of the concentration measurements influences the estimation of PD parameters.

The results obtained in this study raised some points for discussion regarding the selection of the best approach of combining PK and PD data. Much work has however to be done before firm conclusions can be drawn.

CHAPTER 5 GENERAL DISCUSSION AND CONCLUSIONS

5.1 POPULATION PHARMACOKINETICS OF GENTAMICIN IN CANCER PATIENTS

Gentamicin is an antibiotic widely prescribed for the management of fever in neutropenic patients. Although efficacious, its utilisation in clinical practice is limited by its toxicity, in particular, nephrotoxicity and otoxicity, which are related to the trough concentration. Efficacy is determined by the early achievement of high peak concentrations, which are determined by the dose and the volume of distribution. In order to obtain an optimal dosage regimen, the clearance and volume of distribution estimates have to be tailored to the specific patient population.

The identification of gentamicin pharmacokinetics in this particular group of patients is crucial to the selection of a rational initial dosage regimen. This can be achieved by population modelling techniques. To date, no reports were available in the published literature characterising the population pharmacokinetics of gentamicin in adults with oncological disease using nonlinear mixed effects models. Such model was developed in this thesis, and used to evaluate the applicability of two common dosage regimens in this particular group of patients. Both dosage regimens should achieve satisfactory concentrations in this group of patients.

Although population-based methods provide an aid for initial dosage selection, data from this study indicate that a high-degree of variability in the pharmacokinetics of gentamicin in cancer patients is still present. It is therefore important to analyse individual gentamicin plasma concentrations and further dosage adjustment may be necessary to maximise efficacy and minimise toxicity.

The usefulness of the population model was extended to include an evaluation of creatinine clearance estimates as a measure of gentamicin clearance in cancer patients. The assessment of renal function is important for aminoglycosides because they are renally excreted. For that reason, creatinine clearance is one of the most widely used factors for adjustment in clinical settings. However, the accuracy of the nomograms to

estimate creatinine clearance depends on normal production and elimination of creatinine. Creatinine production in cancer patients is often reduced due to a reduction in muscle mass, thus the serum creatinine concentration is expected to be lower than normal, leading to an overestimation of creatinine clearance values, resulting in a potential drug overdose. This problem was confirmed in the population analysis. The study concluded that either setting the lower creatinine limit to 88.4 $\mu mol\ L^{-1}$, or using the measured creatinine concentration, provided inaccurate predictions of gentamicin clearance and concentrations. Better fits were obtained when the lower limit of creatinine was set to 60 or 70 $\mu mol\ L^{-1}$. These results were consistent with those obtained by other investigators.

One of the attractive aspects of the population pharmacokinetic approach is that all relevant pharmacokinetic parameters were estimated using routine data from therapeutic drug monitoring and therefore no extra costs were involved in the generation of the data. This technique is of value in the analysis of sparse sampling data with variable numbers of samples per patient, as was the case with gentamicin.

5.2 A PHARMACOKINETIC-PHARMACODYNAMIC COMPARISON OF MIBEFRADIL, DILTIAZEM AND VERAPAMIL

The data included in this analysis were obtained from phase II clinical trials. As it was a rich data set obtained under experimental conditions, the two-stage approach was used to characterise the pharmacokinetics and pharmacodynamics of mibefradil, verapamil and diltiazem. The results in this analysis agreed with previous studies reported in the literature (Welker, 1998). Peak plasma concentrations at steady state were reached within 2.5 hours after dose administration and at steady state mibefradil had a longer half-life than after single dose. The pharmacokinetics of mibefradil were characterised by low clearance. After single doses, the high values of clearance obtained for verapamil and diltiazem contrasted with the values obtained for mibefradil. The low clearance and long elimination half-life of mibefradil enabled once-daily dosing without the requirement to develop a slow-release formulation. In contrast, both verapamil and diltiazem require slow-release formulations to permit once daily dosing and this leads to the need for "brand" name prescribing to avoid variability in response due to formulation differences. Consequently, in contrast to verapamil and diltiazem, these favourable pharmacokinetic characteristics of mibefradil enable once-daily dosing without the requirement to develop a slow-release formulation.

The antihypertensive efficacy of mibefradil has been evaluated in several large placebo-controlled trials (Bernink et al., 1996; Bursztyn et al., 1997; Oparil et al., 1997; Carney et al., 1997). The results of these studies have shown mibefradil to be efficacious in the treatment of essential hypertension and doses of 50 and 100 mg once daily were recommended. At these doses mibefradil effectively reduced blood pressure over a 24-hour period with low trough/peak ratios and with a gradual onset, reaching maximum within 1-2 weeks. The findings in this thesis were that at steady state, 100 mg of mibefradil given once daily lowered the diastolic blood pressure smoothly for the 24-hour period. At steady state, the effect on blood pressure was more pronounced than in the single dose study.

Studies designed to compare the antihypertensive efficacy of mibefradil with that of other calcium antagonists are scarce. Although a series of comparisons have been made between mibefradil and diltiazem and mibefradil and nifedipine, there were no previous studies that compared mibefradil and verapamil. The findings of this analysis indicate that mibefradil has a longer-lasting antihypertensive action than verapamil and diltiazem.

At steady-state, no hysteresis loops occurred; this contrasted with single dose results. Like verapamil and diltiazem, a decrease in heart rate was observed with mibefradil, however as with verapamil and diltiazem, mibefradil prolonged PQ interval but much higher concentrations were needed to induce changes in PQ interval.

The complexities encountered in the PK/PD modelling of calcium antagonists warrant discussion. In vivo experiments are limited by the occurrence of side-effects when drug concentrations are increased. Consequently, in some cases, the drug concentration is not high enough to fully characterise the concentration-effect relationship. In the mibefradil study, the data did not permit an entirely satisfying determination of effect-concentration relationship. For blood pressure and heart rate, the Emax model was justified in some patients, while for other patients the linear model was more appropriate. The problem was more marked for mibefradil than for verapamil. As the aim of this analysis was to compare the pharmacokinetic/pharmacodynamic relationships of mibefradil with those of verapamil and diltiazem, the inability to select a uniform model for all patients rendered the analysis difficult. The S0 parameter was more accurately estimated than the EC50 parameter and this re-parameterization of the Emax model solved the problem by enabling the characterisation of effect-concentration relationships, when the Emax effect was not attained. This approach then permitted conclusions to be drawn about the relative therapeutic and adverse effects of each drug within the normal concentration range.

Individual fitting was appropriate for rich data as illustrated in mibefradil study. The PK analysis identified changes in PK parameters whereas the PK/PD analysis allowed

comparison of responses after single dose and steady state dosing. Additional and useful potential applications of the technique were the comparison of response/toxicity profiles among three drugs with similar clinical characteristics. The analysis was able to identify that mibefradil had a bigger separation between the decrease in blood pressure and the increase in PQ interval than diltiazem, however difficulties were encountered because of model differences.

Comparison of single dose and steady state pharmacodynamic parameters in individual patients suggested that the parameters were poorly correlated. This in part could be accounted for by the imprecise estimates in individual patients and by the relatively small population. The relative contribution of each of these factors could only be addressed in a larger study population.

5.3 COMBINING PHARMACOKINETIC AND PHARMACODYNAMIC DATA

The initial studies examined individual PK/PD relationships but an extension of the work investigating the influence of different techniques for analysing PK/PD data using a population approach was lacking in the literature. In this thesis, four different methods for combining PK and PD data were applied to the modelling of diastolic blood pressure data after the administration of a single dose of mibefradil. It was concluded that in those situations where the linking model between drug concentration and effect is known, the PK and PD modelling should be carried out simultaneously. However, most frequently, the PK model is better known than the pharmacodynamic model and more reliable estimates of the PK parameters can be obtained from drug concentration alone. So, the PD parameters should be estimated using a full data set while fixing PK parameters. Moreover, the use of full data set has the advantage of reducing the data manipulation. Due to the small number of patients the present analysis had some limitations which have been discussed previously, therefore caution is recommended before definitive conclusions can be drawn.

In this thesis the application of different modelling techniques were explored. The relevance of nonlinear mixed effect modelling to sparse data situations was demonstrated (Chapter 2). The nonlinear mixed effect modelling was applied to rich data (Chapter 4). Using nonlinear mixed effects modelling for full concentration-time profiles allowed the characterisation of the individual pharmacokinetic parameters as well as the mean population trend. Another advantage of nonlinear mixed effects modelling was the flexibility to handle error models to perform such analysis. This contrasts with the results obtained with the standard two-stage approach (Chapter 3) which did not differentiate between intra and interindividual variability. Combining pharmacokinetic and pharmacodynamic information using nonlinear mixed effects approach was also investigated (Chapter 4). The advantages and disadvantages of the techniques used in this work were applied and discussed. It can only be speculated that the use of these techniques would improve patient care.

APPENDICES

APPENDIX I

Equation 1 – Intravenous infusion administration with a bi-exponential decline

$$C_{(t)} = C_1 \left(e^{-\lambda_1 t} - e^{-\lambda_1 t'}\right) + C_2 \left(e^{-\lambda_2 t} - e^{-\lambda_2 t'}\right)$$

where

$$C_1 = \frac{R_0}{V_1}\left[\frac{(k_{21} - \lambda_1)}{\lambda_1(\lambda_1 - \lambda_2)}\right] \qquad \text{and} \qquad C_2 = \frac{R_0}{V_1}\left[\frac{(\lambda_2 - k_{21})}{\lambda_2(\lambda_1 - \lambda_2)}\right]$$

t' represents the time after the infusion is stopped, and t is the total time; V_1 is the volume of the central compartment; R_0 is the rate of administration, given by dose/time of infusion. λ_1 and λ_2 are distribution rate constants. K_{21} is a microconstant that represents the tranfer rate from compartment 2 to 1.

Equation 2 – Intravenous bolus administration with bi-exponential decline

$$C_{(t)} = C_1 e^{-\lambda_1 t} + C_2 e^{-\lambda_2 t}$$

where

$$C_1 = \frac{D(\lambda_1 - k_{21})}{V_1(\lambda_1 - \lambda_2)} \qquad \text{and} \qquad C_2 = \frac{D(k_{21} - \lambda_2)}{V_1(\lambda_1 - \lambda_2)}$$

V_1 is the volume of the central compartment; D is the dose; λ_1 and λ_2 are distribution rate constants. K_{21} is a microconstant that represents the tranfer rate from compartment 2 to 1.

Equation 3 – Mono-exponential decline with first-order absorption, with or without lag time.

$$C(t) = \frac{D * k01 * F}{V(k01 - k10)} \left(e^{-k10\ (t - tlag)} - e^{-k01(t - tlag)}\right)$$

$$C(t) = \frac{D\ k01}{V(k01 - k10)} \left(e^{-k10\,t} - e^{-k01\,t}\right)$$

Secondary parameters:

$$T_{max} = \frac{1}{(k01 - k10)} \ln \frac{k01}{k10} + tlag$$

For the model without a lag time the last term of the equation is not included

$$Cmax = \frac{D * F}{V} \left(e^{-k10(Tmax - tlag)}\right)$$

tlag is not included in the equation for models without lag time

$$AUC = \frac{D * F}{V\,k10}$$

$$T_{1/2} = \frac{0.693}{k10}$$

$$CL = V * k10$$

Key: k_{01} is the first-order absorption rate constant of drug into compartment 1; k_{10} is the first-order elimination rate constant of drug from compartment 1; D is the dose administered; t is the time from administration of drug; Tmax is the time to reach the maximum concentration; Cmax is the maximum concentration; AUC is the area under the concentration-time curve; tlag is the lag time, V is the volume of distribution, CL is the clearance and F is the bioavailability

Equation 4 - Zero-order absorption with bi-exponential decline during and after absorption, with or without lag time

With lag time:

$$C(t)=\frac{D}{T\,V_1}\left[\frac{(k_{21}-\lambda_1)}{(\lambda_1-\lambda_2)\lambda_1}(e^{-\lambda_1 T}-e^{-\lambda_1((t-tlag)-T)})-\frac{(k_{21}-\lambda_2)}{(\lambda_1-\lambda_2)\lambda_2}(e^{-\lambda_2 T}-e^{-\lambda_2((t-tlag)-T)})\right]$$

Without lag time

$$C(t)=\frac{D}{T\,V_1}\left[\frac{(k_{21}-\lambda_1)}{(\lambda_1-\lambda_2)\lambda_1}(e^{-\lambda_1 T}-e^{-\lambda_1(t-T)})-\frac{(k21-\lambda_2)}{(\lambda_1-\lambda_2)\lambda_2}(e^{-\lambda_2 T}-e^{-\lambda_2(t-T)})\right]$$

The relationships between k_{10}, the first-order elimination rate constant of drug from compartment 1, and λ_1 and λ_2 are described in the text, section 3.5.1.

Secondary parameters

$$AUC=\frac{FD}{V_1\,k10}$$

$$T_{1/2\lambda 2}=\frac{0.693}{\lambda_2}$$

$$CL=\frac{FD}{T*AUC}$$

Key: k01 is the first-order absorption rate constant of drug into compartment 1; D is the dose administered; t is the time from administration of drug; T is the time for the absorption to occur; Cmax is the maximum concentration; AUC is the area under the concentration-time curve; tlag is the lag time, V_1 is the volume of distribution of compartment 1 and CL is the clearance. λ_1 and λ_2 represent disposition rate constants.

Equation 5 - Effect-site concentration with first-order oral absorption, mono-exponential decline

$$Ce=\frac{D*k01*keo}{V}$$

$$\left[\frac{e^{-k01t}}{(k10-k01)(keo-k01)}+\frac{e^{-k10t}}{(k01-k10)(keo-k10)}+\frac{e^{-keot}}{(k01-keo)(k10-keo)}\right]$$

Equation 6 - Effect-site concentration with zero order oral absorption, bi-exponential decline

$$Ce=\frac{D*keo}{V_1*T}\left[\frac{(k_{21}-\lambda 1)}{(\lambda 1(\lambda 2-\lambda 1)(keo-\lambda 1)}(e^{-\lambda_1(t-T)}-e^{-\lambda_1 t})\right]+$$

$$\left[\frac{(k_{21}-\lambda_2)}{(\lambda_2(\lambda_1-\lambda_2)(keo-\lambda_2)}(e^{-\lambda_1(t-T)}-e^{-\lambda_2 t})\right]+$$

$$\left[\frac{(k_{21}-keo)}{(keo(\lambda_1-keo)(\lambda_2-keo)}(e^{-keo(t-T)}-e^{-keo\,t})\right]$$

Key: k01 is the first-order absorption rate constant of drug into compartment 1; D is the dose administered; t is the time from administration of drug; T is the time for the absorption to occur; Cmax is the maximum concentration; AUC is the area under the concentration-time curve; tlag is the lag time, V_1 is the volume of distribution of compartment 1 and CL is the clearance. λ_1 and λ_2 represent disposition rate constants from compartment 1 and 2, respectively. Keo is the first-order elimination rate constant from the effect-compatment.

APPENDIX II

Chapter 3 WinNonlin Model Commands

Commands for two compartment model; with zero-order absorption.

```
MODEL
remark   ****************************************************
remark   Developer: M.Rosario
remark   Date:      02-17-1998
remark   Version:   1.0
remark   Two-compartment; zero-order absorption
remark   ****************************************************
remark
remark - define model-specific commands
COMMANDS
NPARAMETERS 5
PNAMES  'V', 'k12', 'k21', 'k10', 'Tmax'
end
remark - define temporary variables
TEMPORARY
v=p(1)
k12=p(2)
k21=p(3)
k10=p(4)
tmax=p(5)
t=x
dos1=con(1)
E=dos1/Tmax
END
remark - define model equation
FUNCTION 1
F=0.0
r1=DSQRT((K12+K21+K10)**2-(4*K21*K10))
alpha=((K12+K21+K10)+r1)/2
beta=((K12+K21+K10)-r1)/2
if t<= tmax then
F=(E*(k21-alpha)*(dexp(-alpha*t)-1))/(V*alpha*(alpha-beta))&
  + (E*(beta-k21)*(dexp(-beta*t)-1))/(V*beta*(alpha-beta))
endif
if t>tmax then
F=(E*(k21-alpha)*(dexp(-alpha*Tmax)-1))&
/(V*alpha*(alpha-beta))*dexp(-alpha*(t-Tmax))&
 +(E*(beta-k21)*(dexp(-beta*Tmax)-1))&
/(V*beta*(alpha-beta))*dexp(-beta*(t-tmax))
endif
END
remark - end of model
EOM
```

Commands for a two-compartment model, zero-order absorption, with Tlag

```
MODEL
remark   ****************************************************
remark   Developer: M.Rosario
remark   Date:      02-17-1998
remark   Version:   1.0
remark   two-compartment; zero-order absorption; tlag
remark   ****************************************************
remark
remark - define model-specific commands
COMMANDS
NPARAMETERS 6
PNAMES  'V', 'k12', 'k21', 'k10', 'Tmax', 'Tlag'
end
remark - define temporary variables
TEMPORARY
v=p(1)
k12=p(2)
k21=p(3)
k10=p(4)
tmax=p(5)
Tlag=p(6)
t=x-tlag
dos1=con(1)
E=dos1/Tmax
END
remark - define model equation
FUNCTION 1
F=0.0
r1=DSQRT((K12+K21+K10)**2-(4*K21*K10))
alpha=((K12+K21+K10)+r1)/2
beta=((K12+K21+K10)-r1)/2
if t<= tmax then
F=(E*(k21-alpha)*(dexp(-alpha*(t+tlag))-1))/(V*alpha*(alpha-beta))&
  + (E*(beta-k21)*(dexp(-beta*(t+tlag))-1))/(V*beta*(alpha-beta))
endif
if t>tmax then
F=(E*(k21-alpha)*(dexp(-alpha*(Tmax+tlag))-1))&
/(V*alpha*(alpha-beta))*dexp(-alpha*(t+tlag-tmax))&
 +(E*(beta-k21)*(dexp(-beta*(Tmax+tlag))-1))&
/(V*beta*(alpha-beta))*dexp(-beta*(t+tlag-tmax))
endif
END
remark - end of model
EOM
```

Commands for S0 model

MODEL

```
remark   ******************************************************
remark   Developer: M Rosario
remark   Date:      06-25-1998
remark   Version:   1.0
remark   S0 model
remark   ******************************************************
remark
remark - define model-specific commands
COMMANDS
NPARAMETERS 2
PNAMES  'EMAX', 'S0'
END
FUNCTION 1
EMAX=p(1)
S0=p(2)
F=(EMAX*x*S0)/(x*S0+EMAX)
END
remark - end of model
EOM
```

Commands for link model between a two-compartment model with zero-order absorption and S0 model

```
MODEL
remark   ****************************************************
remark   Developer: M Rosario
remark   Date:      07-06-1998
remark   Version:   1.0
remark   S0 MOdel; Two-compartment; zero-order absorption
remark   ****************************************************
remark
remark - define model-specific commands
COMMANDS
NPARAMETERS 3
PNAMES  'emax', 'S0', 'keo'
ncon 1
END
remark - define temporary variables
TEMPORARY
V=450.84
k12=0.04
k21=0.12
k10=0.13
tabs=1
emax=p(1)
SO=p(2)
keo=p(3)
d=con(1)
t=x
del=t-tabs
tstar=max(0,del)
r1=dsqrt((k12+k21+k10)**2-(4*k21*k10))
alpha=((k12+k21+k10)+r1)/2
beta=((k12+k21+k10)-r1)/2
END
remark - define model equation
FUNCTION 1
coef=keo*d/(v*tabs)
ce1=((k21-alpha)/(alpha*(beta-alpha)*(keo-alpha)))
ce1=ce1*(exp(-alpha*tstar)-exp(-alpha*t))
ce2=((k21-beta)/(beta*(alpha-beta)*(keo-beta)))
ce2=ce2*(exp(-beta*tstar)-exp(-beta*t))
ce3=((k21-keo)/(keo*(alpha-keo)*(beta-keo)))
ce3=ce3*(exp(-keo*tstar)-exp(-keo*t))
amt=coef*(ce1+ce2+ce3)
sum=amt
ce=sum
F= emax*ce*S0/(ce*S0+emax)
END
remark - end of model
EOM
```

Commands For Linear model

```
MODEL
remark   ******************************************************
remark   Developer: M. Rosario
remark   Date:      02-10-1998
remark   Version:   1.0
remark   Linear model
remark   ******************************************************
remark
remark - LINEAR MODEL
COMMANDS
NPARAMETERS 1
PNAMES   'B1'
END
remark - define model equation
FUNCTION 1
F=  B1*x
END
remark - end of model
EOM
```

APPENDIX III

Chapter 4: The NMTRAM code file for the several methods of combining the PK and PD data.

METHOD 1 and 2

```
$PROB MIBEFRADIL PK/PD MODELLING - USING FIXED PK RUN15
$INPUT ID TIME AMT A=DROP DV HR=DROP PQ=DROP EVID TYPE CMT BASB BASH AGE HGT WGT SEX SMOK
$DATA MIBEFRA2.PRN IGNORE=#
$SUBROUTINE ADVAN4 TRANS4
$PK
    TVKA=THETA(1)
    TVV2=THETA(2)
    TVCL=THETA(3)
    TVQ=THETA(4)
    TVV3=THETA(5)
    TALAG1=THETA(6)
    KA=TVKA*EXP(ETA(1))
    V2=TVV2*EXP(ETA(2))
    CL=TVCL*EXP(ETA(3))
    Q=TVQ*EXP(ETA(4))
    V3=TVV3*EXP(ETA(5))
    ALAG1=TALAG1*EXP(ETA(6))
    S2=V2
    EMAX=THETA(7)*EXP(ETA(7))
    SO=THETA(8)*EXP(ETA(8))
$ERROR
    EFF=EMAX*F*SO/(EMAX+SO*F)
    Y=EFF+ERR(1)
$THETA
  3.05 FIXED      ;KA-FIXED TO PREV EST
  148 FIXED       ;V2-FIXED TO PREV EST
  6.81 FIXED      ;CL-FIXED TO PREV EST
  3.2 FIXED       ;Q-FIXED TO PREV EST
  32.5 FIXED      ;V3-FIXED TO PREV EST
  0.402 FIXED     ;ALAG-FIXED TO PREV EST
  (-40,-25.7,-10) ;EMAX-ESTIMATED
  (-1,-0.029,1)   ;S0-ESTIMATED
$OMEGA
  0.847 FIXED     ;KA-FIXED TO PREV EST
  0.0714 FIXED    ;V2-FIXED TO PREV EST
  0.129 FIXED     ;CL-FIXED TO PREV EST
  2.93 FIXED      ;Q-FIXED TO PREV EST
  0.0104 FIXED    ;V3-FIXED TO PREV EST
  0.127 FIXED     ;LAG-FIXED TO PREV EST
  0.0226          ;EMAX-ESTIMATED
  0.0294          ;S0-ESTIMATED
$SIGMA 1
$ESTIMATION PRINT=10 SIG=3 MAXEVALS=9000 NOABORT POSTHOC
$COVAR
$TABLE ID AMT TIME TYPE WRES FILE=MIBE15A.TAB NOPRINT ONEHEADER
```

METHOD 3

```
$PROB MIBEFRADIL SIMULTANEOUS PK/PD RUN12
$INPUT ID TIME AMT A=DROP DV HR=DROP PQ=DROP EVID TYPE CMT
    BASB=DROP BASH=DROP
$DATA MIBEFRA1.PRN IGNORE=#
$SUBROUTINE ADVAN4 TRANS4
$PK
     TVKA=THETA(1)
     TVV2=THETA(2)
     TVCL=THETA(3)
     TVQ=THETA(4)
     TVV3=THETA(5)
     TALAG1=THETA(6)
     KA=TVKA*EXP(ETA(1))
     V2=TVV2*EXP(ETA(2))
     CL=TVCL*EXP(ETA(3))
     Q=TVQ*EXP(ETA(4))
     V3=TVV3*EXP(ETA(5))
     ALAG1=TALAG1*EXP(ETA(6))
     S2=V2
$ERROR
     EMAX=THETA(7)*EXP(ETA(7))
     SO=THETA(8)*EXP(ETA(8))
     EFF=EMAX*F*SO/(EMAX+SO*F)
     W=(1+THETA(9)*THETA(9)*F*F)**0.5
     Y1=F+W*ERR(1)
     Y2=EFF+ERR(1)
     A=0
     IF (TYPE.EQ.0) A=1
     Y=A*Y1+(1-A)*Y2
$THETA (0,3.2,15) (0,140,500) (0,6.5,40) (0,3.2,60) (0,32.5,200) (0,0.4,5)
    (-60,-26,60) (-1,-0.01,5) (-5,0.07,5)
$OMEGA 0.3 0.3 0.3 0.3 0.3 0.3 0.3 0.3
$SIGMA 0.5
$ESTIMATION PRINT=10 SIG=3 MAXEVALS=9000 NOABORT POSTHOC
$COVAR
$TABLE ID AMT TIME WRES TYPE FILE=MIBE12.TAB NOPRINT ONEHEADER
```

METHOD 4

```
$PROB MIBEFRADIL IPRED PK/PD  RUN18
$INPUT ID TIME AMT DV HR=DROP PQ=DROP MDV EVID TYPE CMT BASB=DROP  BASH=DROP IPR
$DATA MIBEFRA3.PRN IGNORE=#
$PRED
     EMAX=THETA(1)*EXP(ETA(1))
     SO=THETA(2)*EXP(ETA(2))
     EFF=EMAX*IPR*SO/(EMAX+SO*IPR)
$ERROR
     Y=EFF+ERR(1)
$THETA (-60,-21,60) (-1,-0.05,5)
$OMEGA  0.3 0.3
$SIGMA  0.5
$ESTIMATION PRINT=10 SIG=3 MAXEVALS=9000 NOABORT POSTHOC
$COVAR
$TABLE ID AMT TIME FILE=MIBE18A.TAB NOPRINT ONEHEADER
```

PRESENTATIONS

- **Population pharmacokinetics of gentamicin in oncology patients.**

M. C. Rosario, C. A. Sharp, D. I. Jodrell., A. H. Thomson.

5th International Congress of Therapeutic Drug Monitoring and Clinical Toxicology, Vancouver, Canada, November 1997 (Poster).

- **A pharmacokinetic-pharmacodynamic comparison of mibefradil, diltiazem and verapamil.**

M. Rosario, P. A. Meredith, H. L. Elliott.

3rd International Symposium on Measurement and Kinetics of in Vivo Drug Effects Leiden, The Netherlands, May 1998 (Poster).

- **A pharmacokinetic-pharmacodynamic comparison of mibefradil, diltiazem and verapamil.**

M. Rosario, P.A. Meredith, A.H. Thomson, H.L. Elliott

Pharmacokinetics (UK), Manchester, UK, November 1998 (Poster).

PUBLICATIONS

- **Population pharmacokinetics of gentamicin in oncology patients.**

M. C. Rosario, C. A. Sharp, D. I. Jodrell, A. H. Thomson

Therapeutic Drug Monitoring 1997: 19 (5):599 (Abstract).

- **Population pharmacokinetics of gentamicin in patients with cancer.**

M. C. Rosario, A. H. Thomson, D. I. Jodrell, C. A. Sharp, H. L. Elliott

British Journal Clinical Pharmacology 1998; 46: 229-236.

BIBLIOGRAPHY

Minitab Statistical Package.(1996b) 11. Pennsylvania,USA: Minitab, Inc.

WinNonlin.(1996a) 1.1. Apex, USA: Scientific Consulting, Inc.

Splus Statistical Package.(1998) 4.5. MathSoft, Inc.

Aarons, L., Vozeh, S., Wenk, M., Follath, W. and Follath, F. (1989) Population pharmacokinetics of tobramycin. British Journal Of Clinical Pharmacology **28**, 305-314.

Ariens, E.J. and Simonis, A.M. (1964) A molecular basis for drug action. Journal Of Pharmacy And Pharmacology **16**, 137-157.

Bachman, W.J. and Gillespie, W.R. (1998) Truncated sigmoid Emax models: A reparameterization of the sigmoid Emax model for use with truncated PK/PD data. Clinical Pharmacology And Therapeutics **63**, 199(Abstract)

Barclay, M.L., Begg, E.J. and Chambers, S.T. (1992) Adaptive resistance following single doses of gentamicin in a dynamic in vitro model. Agents Chemotherapy **36**, 1951-1957.

Barriere, S.L. (1988) Aminoglycosides: A reassessment of their therapeutic role. Clinical Pharmacy **7**, 385-390.

Barza, M., Brown, R.B., Shen, D., Gibaldi, M. and Weinstein, L. (1975) Predictability of blood levels of gentamicin in man. Journal Of Infectious Diseases **132**, 165-174.

Beal, S.L. (1984) Population pharmacokinetic data and parameter estimation based on the first two statistical moments. Drug Metabolism Reviews **15**, 173-193.

Beal, S.L. and Sheiner, L.B. (1992) *NONMEM Users Guides, parts I - VII. Technical Report*, San Francisco: University of California.

Beal, S.L. and Sheiner, L.B. (1998) *NONMEM Users Guides. Technical Report*, San Francisco: University of California.

Bernink, P.J., Prager, G., Schelling, A. and Kobrin, I. (1996) Antihypertensive properties of the novel calcium antagonist mibefradil (Ro 40-5967). A new generation of calcium antagonists? Mibefradil International Study Group. Hypertension **27**, 426-432.

Bertino, J.S. (1993) Measured versus estimated creatinine clearance in patients with low serum creatinine values. Annals Of Pharmacotherapy **27**, 1439-1442.

Bertino, J.S., Booker, L.A., Franck, P. and Rybicki, B. (1991) Gentamicin pharmacokinetics in patients with malignancies. Antimicrobial Agents And Chemotherapy **35**, 1501-1503.

Boxenbaum, H.G. (1992) Pharmacokinetics: Philosophy of modeling. Drug Metabolism Reviews **24**, 89-120.

Boxenbaum, H.G., Riegelman, S. and Elashoff, R.M. (1974) Statistical estimations in pharmacokinetics. Journal Of Pharmacokinetics And Biopharmaceutics **2**, 123-148.

Brogden, R.N. and Marklam, A. (1997) Mibefradil. A review of its pharmacodynamic and pharmacokinetic properties, and therapeutic efficacy in the management of hypertension and angina pectoris. Drugs **54**, 774-793.

Buckley, M.M.T., Grant, S.M., Goa, K.L., McTavish, D. and Sorkin, E.M. (1990) Diltiazem. A reappraisal of its pharmacological properties and therapeutic use. Drugs **39**, 757-806.

Bursztyn, M., Kadr, H., Tilvis, R., Martina, B., Oigman, W., Talberg, J. and Kobrin, I. (1997) Mibefradil, a novel calcium antagonist, in elderly hypertensive: favourable haemodynamics and pharmacokinetics. American Heart Journal **134**, 238-247.

Burton, M.E., Vasko, M.R. and Brater, C. (1985) Comparison of drug dosing methods. Clinical Pharmacokinetics **10**, 1-37.

Carney, S., Ribeiro, A.B., Kallwellis, R., Zimlichman, R., Viskoper, R., Mion, D. and Kobrin, I. (1997) The addition of mibefradil to chronic hydrochlorothiazide therapy in hypertensive patients is associated with a significant antihypertensive effect. Journal Of Human Hypertension **11**, 459-466.

Chan, G.L.C. (1989) Alternative dosing strategy for aminoglycosides: Impact on efficacy, nephrotoxicity, and ototoxicity. Annals Of Pharmacotherapy **23**, 788-794.

Chan, R.A., Benner, E.J. and Hoeprich, P.D. (1972) Gentamicin therapy in renal failure: A nomogram for dosage. Annals Of Internal Medicine **76**, 773-778.

Chiou, W.L., Mohamed, A.F.G. and Peng, G.W. (1978) Method for the rapid estimation of the total body drug clearance and adjustment of dosage regimens in patients during a constant-rate intravenous infusion. Journal Of Pharmacokinetics And Biopharmaceutics **6**, 135-151.

Clozel, J.-P., Osterrieder, W. and Kleinbloesen, C.H. (1991) Ro-5967: A new nondihydropyridine calcium antagonist. Cardiovascular Drugs Review **9**, 4-17.

Clozel, J.-P., Veniant, M. and Osterrieder, W. (1990) The structurally novel Ca^{2+} channel blocker Ro 40-5697, which binds to the [3H] desmethoxyverapamil receptor is devoid of the negative inotropic effects of verapamil in normal and failing rat hearts. Cardiovascular Drugs And Therapy **4**, 731-736.

Cockcroft, D.W. and Gault, H. (1976) Prediction of creatinine clearance from serum creatinine. Nephron **16**, 31-41.

Dahlstrom, B.E., Paalzow, L.K., Segre, G. and Agren, A.J. (1978) Relation between morphine pharmacokinetics and analgesia. Journal Of Pharmacokinetics And Biopharmaceutics **6**, 41-53.

Daikos, G.L., Jackson, G.G. and Lolans, F.T. (1990) Adaptive resistance to aminoglycoside antibiotics from first-exposure down regulation. Journal Of Infectious Diseases **162**, 414-420.

Davidian, M. (1993) Some simple methods for estimating intraindividual variability in nonlinear mixed effects models. Biometrics **49**, 59-73.

Davidian, M. and Gallant, R. (1992) Smooth nonparametric maximum likelihood estimation for population pharmacokinetics, with application to quinidine. Journal Of Pharmacokinetics And Biopharmaceutics **20**, 529-556.

Davis, R.L., Lehmann, D., Stidley, C.A. and Neidhart, J. (1991) Amikacin pharmacokinetics in patients receiving high-dose cancer chemotherapy. Antimicrobial Agents And Chemotherapy **35**, 944-947.

Della Paschoa, O.E., Mandema, J.W. and Danhof, M. (1998) Pharmacokinetic-pharmacodynamic modeling of the anticonvulsant and electroencephalogram effects of phenytoin. Journal Of Pharmacology And Experimental Therapeutics **284**, 460-466.

Demczar, D.J., Nafziger, A.N. and Bertino, J.S. (1997) Pharmacokinetics of gentamicin at traditional versus high doses: implications for once-daily aminoglycoside dosing. Antimicrobial Agents And Chemotherapy **41**, 1115-1119.

Devine, B.J. (1974) Gentamicin therapy. Drug Intelligence And Clinical Pharmacy **8**, 650-655.

Donnelly, R., Elliott, H.L. and Meredith, P.A. (1994) Concentration-effect analysis of antihypertensive drug response. Application to calcium antagonists. Clinical Pharmacokinetics **26**, 472-485.

Du Bois, D. and Du Bois, E.F. (1916) Clinical calorimetry. A formula to estimate the approximate surface area if height and weight be known. Archives Of Internal Medicine **17**, 863-871.

Dube, L.M., Mousseau, N. and McGilveray, I.M. (1988) High performance liquid chromatographic determination of diltiazem and metabolites in plasma: evaluation of their stability. Journal Of Chromatography **430**, 103-111.

Duffull, S.B., Kirkpatrick, C.M.J. and Begg, E.J. (1997) Comparison of two Bayesian approaches to dose-individualization for once-daily aminoglycoside regimens. British Journal Of Clinical Pharmacology **43**, 125-135.

Egan, T.D., Lemmens, H.J., Fiset, P., Hermann, D., Muir, K.T., Stanski, D.R. and Shafer, S.L. (1993) The pharmacokinetics of the new short-acting opioid remifentanil (GI87084B) in healthy adult male volunteers. Anesthesiology **79**, 881-892.

Eggers, H., Kormer, S. and von Alter, R. (1990) Determination of the new calcium antagonist Ro 40-5967 in plasma by HPLC. Roche Research Report B-105981

Ette, E.I. and Ludden, T.M. (1995) Population pharmacokinetic modeling: The importance of informative graphics. Pharmaceutical Research **12**, 1845-1855.

Etzel, J.V., Nafziger, A.N. and Bertino, J.S. (1992) Variation in the pharmacokinetics of gentamicin and tobramycin in patients with pleural effusions and hypoalbuminemia. Antimicrobial Agents And Chemotherapy **36**, 679-681.

Fuseau, E. and Sheiner, L.B. (1984) Simultaneous modeling of pharmacokinetics and pharmacodynamics with a nonparametric pharmacodynamic model. Clinical Pharmacology And Therapeutics **35**, 733-741.

Garrison, M.W., Zaske, D.E. and Rostschafer, J.C. (1990) Aminoglycosides: Another perspective. Annals Of Pharmacotherapy **24**, 267-272.

Gibaldi, M. and Perrier, D. (1982) *Pharmacokinetics*, 2nd Edition. New York: Marcel Dekker, Inc.

Godfrey, K.R. and Fitch, W.R. (1984) On the identification of Michaelis-Menten elimination parameters from a single dose-response curve. Journal Of Pharmacokinetics And Biopharmaceutics **12**, 193-221.

Gomeni, R., Pineau, G. and Mentre, F. (1994) Population kinetics and conditional assessment of the optimal dosage regimen using the P-Pharm software package. Anticancer Research **14**, 2321-2326.

Hallynck, T.H., Soep, H.H., Thomis, J.A., Boelaert, J., Daneels, R. and Dettli, L. (1981) Should clearance be normalised to body surface area or to lean body mass? British Journal Of Clinical Pharmacology **11**, 523-525.

Hamann, S.R., Blouin, R.A. and McAllister, R.G. (1984) Clinical pharmacokinetics of verapamil. Clinical Pharmacokinetics **9**, 26-41.

Hashimoto, Y. and Sheiner, L.B. (1991) Designs for population pharmacodynamics: Value of pharmacokinetic data and population analysis. Journal Of Pharmacokinetics And Biopharmaceutics **9**, 333-353.

Hastie, T. and Tibshirani, R. (1996) *Generalized additive models*, 1st Edition. London: Chapman & Hall.

Higa, G.M. and Murray, W.E. (1987) Alterations in aminoglycoside pharmacokinetics in patients with cancer. Clinical Pharmacy **6**, 963-966.

Hill, A.V. (1910) The possible effects of the aggregation of the molecules of haemoglobin on its dissociation curves. Journal Of Physiology **40**, IV-VII.

Holford, N.H.G. and Sheiner, L.B. (1981) Understanding the dose-effect relationship: Clinical application of pharmacokinetic-pharmacodynamic models. Clinical Pharmacokinetics **6**, 429-453.

Holford, N.H.G. and Sheiner, L.B. (1982) Kinetics of pharmacologic response. Pharmacology And Therapeutics **16**, 143-166.

Hull, C.J., Van Beem, H.B.H., Mcleod, K., Sibbald, A. and Watson, M.J. (1978) A pharmacodynamic model for pancuronium. Bristish Journal Of Anesthesiology **50**, 1113-1123.

Inciardi, J.F. and Batra, K.K. (1993) Nonparametric approach to population pharmacokinetics in oncology patients receiving aminoglycoside therapy. Antimicrobial Agents And Chemotherapy **37**, 1025-1027.

Janknegt, R. (1990) Aminoglycoside therapy. Current use and future prospects. Pharmaceutisch Weekblad Scientific **12**, 81-90.

Jonsson, E.N. and Karlsson, M.O. (1999) Xpose- an Splus based population pharmacokinetic/pharmacodynamic model building aid for NONMEM. Computer Methods And Programs Biomedicine **58**, 51-64.

Jusko, W.J. (1971) Pharmacodynamics of chemotherapeutic effects: Dose-time-response relationships for phase-nonspecific agents. Journal Of Pharmaceutical Sciences **60**, 892-895.

Jusko, W.J. and Ko, H.C. (1994) Physiologic indirect response models characterize diverse types of pharmacodynamic effects. Clinical Pharmacology And Therapeutics **56**, 406-419.

Kahlmeter, G. and Kamme, C. (1975) Prolonged excretion of gentamicin in a patient with unimpaired renal function. Lancet **1**, 286-286.

Kataria, B.K., Ved, S.A., Nicodemus, H.F., Hoy, G.R., Lea, D., Dubois, M.Y., Mandema, J.W. and Shafer, S.L. (1994) The pharmacokinetics of propofol in children using three different data analysis approaches. Anesthesiology **80**, 104-122.

Katz, A.M. (1996) Calcium channel diversity in the cardiovascular system. Journal Of American College Cardiology **28**, 522-529.

Kaye, D., Levison, M.E. and Labovitz, E.D. (1974) The unpredictability of serum concentrations of gentamicin: pharmacokinetics of gentamicin in patients with normal and abnormal renal function. Journal Of Infectious Diseases **130**, 150-154.

Kelman, A.W., Whiting, B. and Bryson, S.M. (1982) Parameter optimisation in clinical pharmacokinetics. Computer Programs In Biomedicine **14**, 239-248.

Kirsten, R., Nelson, K., Kirsten, D. and Heintz, B. (1998) Clinical pharmacokinetics of vasodilators. Part I. Clinical Pharmacokinetics **35**, 457-482.

Klastersky, J., Daneau, D., Swings, G. and Weerts, D. (1974) Antibacterial activity in serum and urine as a therapeutic guide in bacterial infections. The Journal Of Infectious Diseases **129**, 187-193.

Laskin, O.L., Longstreth, J.A., Smith, C.R. and Lietman, P.S. (1983) Netilmicin and gentamicin multidose kinetics in normal subjects. Clinical Pharmacology And Therapeutics **34**, 644-650.

Levy, G. (1994) Mechanism-based pharmacodynamic modeling. Clinical Pharmacology And Therapeutics **56**, 356-358.

Lindstrom, M.J. and Bates, D.M. (1990) Nonlinear mixed effect models for repeated measures data. Biometrics **46**, 673-687.

Ludden, T.M., Beal, S.L. and Sheiner, L.B. (1994) Comparison of the Akaike Information Criterion, the Schwarz Criterion and the F-test as guides to model selection. Journal Of Pharmacokinetics And Biopharmaceutics **22**, 431-445.

MacGowan, A.P., Bedford, K.A., Blundell, E., Brown, N.M., Habib, F., Hows, J., Kirkpatrick, B., Korner, R.J., Slade, R.R., White, L.O. and Reeves, D.S. (1994) The pharmacokinetics of once daily gentamicin in neutropenic adults with haematological malignancy. Journal Of Antimicrobial Chemotherapy **34**, 809-812.

Maitre, P.O., Buhrer, M., Thomson, D. and Stanski, D.R. (1991) A three-step approach combining Bayesian regression and NONMEM population analysis: application to midazolam. Journal Of Pharmacokinetics And Biopharmaceutics **19**, 377-484.

Mallet, A. (1986) A maximum likelihood estimation method for random coefficient regression models. Biometrika **73**, 645-656.

Mallet, A., Mentre, F., Gilles, J., Kelman, A.W., Thomson, A.H., Bryson, S.M. and Whiting, B. (1988) Handling covariates in population pharmacokinetics, with an application to gentamicin. Biomedical Measurement Informatics And Control **2**, 138-146.

Mandema, J.W. and Stanski, D.R. (1996) Population pharmacodynamic model for ketorolac analgesia. Clinical Pharmacology And Therapeutics **60**, 619-635.

Mandema, J.W., Verotta, D. and Sheiner, L.B. (1992) Building population pharmacokinetic-pharmacodynamic models. I - Models for covariate effects. Journal Of Pharmacokinetics And Biopharmaceutics **20**, 511-528.

Manny, R.P. and Huston, P.R. (1986) Aminoglycoside volume of distribution in hematology-oncology patients. Clinical Pharmacy **5**, 629-632.

Mattie, H., Craig, W.A. and Pechere, J.C. (1989) Determinants of efficacy and toxicity of aminoglycosides. Journal Of Antimicrobial Chemotherapy **24**, 293

Mentre, F. and Mallet, A. (1994) Handling covariates in population pharmacokinetics. Biomedical Computing **36**, 25-33.

Metzler, C.M. (1987) Extended least squares (ELS) for pharmacokinetic models. Journal Of Pharmaceutical Sciences **76**, 565-571.

Mishra, S. and Hermsmeyer, K. (1994) Inhibition of signal Ca^{2+} in dog coronary arterial vascular muscle cells by Ro 40-5967. Journal Of Cardiovascular Pharmacology **24**, 1-7.

Moore, R.D., Lietman, P. and Smith, C.R. (1987) Clinical response to aminoglycoside therapy: Importance of the ratio of peak concentration to minimal inhibitory concentration. Journal Of Infectious Diseases **155**, 93-99.

Moore, R.D., Smith, C.R. and Lietman, P.S. (1984) The association of aminoglycoside plasma levels with mortality in patients with gram-negative bacteremia. Journal Of Infectious Diseases **149**, 443-448.

Nicolau, D.P., Freeman, C.D., Belliveau, P.P., Nightingale, C.H., Ross, J.W. and Quintiliani, R. (1995) Experience with a once-daily aminoglycoside program administered to 2184 adult patients. Antimicrobial Agents And Chemotherapy **39**, 650-655.

Oparil, S., Kobrin, I. and Abernethy, D.R. (1997) Dose-response characteristics of mibefradil, a novel calcium antagonists, in the treatment of essential hypertension. American Journal Of Hypertension **10**, 735-742.

Ordovas, J.P., Ronchera, C.L., Poveda, J.L., Jimenez, N.V. and Lopez, R. (1994) Selection of optimal prophylactic aminoglycoside dosage in cancer patients: population pharmacokinetic approaches. Journal Of Clinical Pharmacology And Therapeutics **19**, 47-56.

Peck, C., Barr, W.h., Benet, L.Z., Collins, J., Desjardins, R.E., Furst, D.E., Harter, J.G., Levy, G., Ludden, T., Rodman, J.H., Sanathanan, L., Schentag, J.J., Shah, V.P., Sheiner, L.B., Skelly, J.P., Stanski, D.R., Temple, R.J., Viswanathan, C.T., Weissinger, J. and Yacobi, A. (1992) Opportunities for integration of pharmacokinetics, pharmacodynamics, and toxicokinetics in rational drug development. Clinical Pharmacology And Therapeutics **51**, 465-473.

Peck, C. and Barret, B.B. (1979) Nonlinear Least-squares regression programs for microcomputers. Journal Of Pharmacokinetics And Biopharmaceutics **7**, 537-541.

Peck, C., Beal, S.L., Sheiner, L.B. and Nichols, A.I. (1984) Extended least squares nonlinear regression: a possible solution to the "choice of weights" problem in analysis of individual pharmacokinetic data. Journal Of Pharmacokinetics And Biopharmaceutics **12**, 545-558.

Peck, C., Brown, W.D., Sheiner, L.B., et al Personal Communication: O'Neill, J.T., 1980. A microcomputer drug (theophylline) dosing program which assists and teaches physicians.

Pennington, J.E., Dale, D.C., Reynolds, H.Y. and MacLowry, J.D. (1975) Gentamicin sulfate pharmacokinetics: Lower levels of gentamicin in blood during fever. Journal Of Infectious Diseases **132**, 270-275.

Phillips, J.K., Spearing, R.L., Crome, D.J. and Davies, J.M. (1988) Gentamicin volumes of distribution in patients with hematologic disorders. New England Journal Of Medicine **319**, 1290-1290.

Pinheiro and Bates, D.M. Department of Biostatistics, (Ed.) (1989) Technical Report 89. University of Wisconsin-Madison.

Racine-Poon, A. (1985) A Bayesian approach to nonlinear random effects models. Biometrics **41**, 1015-1023.

Ratkowsky, D.A. (1986) A suitable parameterization of the Michaelis-Menten enzyme reaction. Biochemistry Journal **240**, 357-360.

Regamey, C., Gordon, R.C. and Kirby, W.M.M. (1973) Comparative pharmacokinetics of tobramycin and gentamicin. Clinical Pharmacology And Therapeutics **14**, 396-403.

Reigner, B.G., Williams, P.E.O., Patel, I.H., Steimer, J.-L., Peck, C. and Brummelen, P.V. (1997) An evaluation of the integration of pharmacokinetic and pharmacodynamic principles in clinical drug development. Clinical Pharmacokinetics **33**, 142-152.

Robert, S., Zarowitz, B.J., Peterson, E.L. and Sastry, S. (1991) Renal function assessment in the critically ill. Pharmacotherapy **11**, 275-275.

Roe, D.J. (1997) Comparison of population pharmacokinetic modeling methods using simulated data: results from the population modeling workgroup. Statistics In Medicine **16**, 1241-1262.

Rosenquist, M., Brembilla-Perrot, B., Meinertz, T., Neugebauer, A., Crijns, H., Smeets, J., Van der Vring, J., Fromer, M. and Kobrin, I. (1997) The acute effects of intravenously administered mibefradil, a new calcium antagonist, on the electrophysiologic characteristics of the human heart. European Journal Of Clinical Pharmacology **52**, 7-12.

Sande, M.A. and Mandell, G.L. (1996) Antimicrobial Agents. The Aminoglycosides. In: Gilman, A.G., Rail, T.W., Nies, A.S. and Taylor, P., (Eds.) *The Pharmacological Basis of Therapeutics*, 9th Edition. pp. 1103-1121. New York: Pergamon Press.

Sawchuk, R.J., Zaske, D.E., Cipolle, R.J., Wargss, W.A. and Strate, R.G. (1977) Kinetic model for gentamicin dosing with the use of indidual patient parameters. Clinical Pharmacology And Therapeutics **21**, 362-369.

Schentag, J.J. and Jusko, W.J. (1977a) Gentamicin persistence in the body. Lancet **1**, 486-486.

Schentag, J.J. and Jusko, W.J. (1977b) Renal clearance and tissue accumulation of gentamicin in man. Clinical Pharmacology And Therapeutics **22**, 364-370.

Schentag, J.J., Jusko, W.J., Vance, J.W., Cumbo, T.J., Abrutyn, E., DeLattre, M. and Gerbracht, L.M. (1977) Gentamicin disposition and tissue accumulation on multiple dosing. Journal Of Pharmacokinetics And Biopharmaceutics **5**, 559-577.

Schmitt, R., Coenelis, H.K., Belz, G.G., Schroeter, V., Feifel, U., Pozenel, H., Kirch, W., Halabi, A., Woittiez, A.-J., Welker, H.A. and Brummelen, P. (1992) Hemodynamic and humoral effects of the novel calcium antagonist Ro 40-5967 in patients with hypertension. Clinical Pharmacology And Therapeutics **52**, 314-323.

Schoemaker, R.C., van Gerven, J.M. and Cohen, A.F. (1998) Estimating potency for the E_{max}-model without attaining maximal effects. Journal Of Pharmacokinetics And Biopharmaceutics **26**, 51:581-593.

Schumitzky, A. (1991) Nonparametric EM algorithms for estimating prior distributions. Applied Mathematics And Computation **45**, 141-157.

Schwartz, S.N., Pazin, G.J., Lyon, J.A., Ho, M. and Pascule, A.W. (1978) A controlled investigation of the pharmacokinetics of gentamicin and tobramycin in obese subjects. Journal Of Infectious Diseases **138**, 499-505.

Schwarz, G. (1978) Estimating the dimension of a model. The Annals Of Statistics **6**, 461-464.

Sculier, J.P. and Klastersky, J. (1984) Significance of serum bactericidal activity in gram-negative bacteremia in patients with and without granulocytopenia. American Journal Of Medicine **76**, 429-435.

Segre, G. (1968) Kinetics of interaction between drugs and biological systems. Il Farmaco **23**, 907-918.

Sheiner, L.B. (1984) The population approach to pharmacokinetic data analysis: Rationale and standard data analysis methods. Drug Metabolism Reviews **15**, 153-171.

Sheiner, L.B. and Beal, S.L. (1980) Evaluation of methods for estimating population pharmacokinetic parameters. I - Michaelis- Menten model: Routine clinical pharmacokinetic data. Journal Of Pharmacokinetics And Biopharmaceutics **8**, 553-651.

Sheiner, L.B. and Beal, S.L. (1981) Evaluation of methods for estimating population pharmacokinetic parameters. II - Bioexponential model and experimental pharmacokinetic data. Journal Of Pharmacokinetics And Biopharmaceutics **9**, 635-651.

Sheiner, L.B. and Beal, S.L. (1982) Bayesian individualization of pharmacokinetics: Simple implementation and of non-Bayesian methods. Journal Of Pharmaceutical Sciences **71**, 1344-1348.

Sheiner, L.B. and Beal, S.L. (1983) Evaluation of methods for estimating population pharmacokinetic parameters. III - Monoexponential model: routine pharmacokinetic data. Journal Of Pharmacokinetics And Biopharmaceutics **11**, 303-319.

Sheiner, L.B., Beal, S.L., Rosenberg, B. and Marathe, V.V. (1979b) Forecasting individual pharmacokinetics. Clinical Pharmacology And Therapeutics **26**, 294-305.

Sheiner, L.B. and Benet, L.Z. (1985) Premarketing observational studies of population pharmacokinetics of new drugs. Clinical Pharmacology And Therapeutics **38**, 481-487.

Sheiner, L.B. and Grasela, T.H. (1984) Experience with NONMEM: analysis of routine phenytoin clinical pharmacokinetic data. Drug Metabolism Reviews **15**, 293-303.

Sheiner, L.B., Rosenberg, B. and Marathe, V.V. (1977) Estimation of population characteristics of pharmacokinetic parameters from routine clinical data. Journal Of Pharmacokinetics And Biopharmaceutics **5**, 445-479.

Sheiner, L.B., Stanski, D.R., Vozeh, S., Miller, R.D. and Ham, J. (1979a) Simultaneous modeling of pharmacokinetics and pharmacodynamics: Application to d-tubocurarine. Clinical Pharmacology And Therapeutics **25**, 358-370.

Siber, G.R., Echeverria, P., Smith, A.L., Paisley, J.W. and Smith, D.H. (1975) Pharmacokinetics of gentamicin in children and adults. Journal Of Infectious Diseases **132**, 637-651.

Siersbaek-Nielsen, K., Hansen, J.M., Kampmann, J. and Kristensen, M. (1971) Rapid evaluation of creatinine clearances. Lancet **1**, 1133-1134.

Slattery, J. (1980) A pharmacokinetic model-independent approach for estimating dose required to give desired steady-state trough concentrations of drug in plasma. Journal Of Pharmacokinetics And Biopharmaceutics **8**, 105-110.

Smythe, M., Hoffman, J., Kizy, K. and Dmuchowski, C. (1994) Estimating creatinine clearance in elderly patients with low serum creatinine concentrations. American Journal Of Hospital Pharmacy **51**, 198-204.

Steimer, J.-L., Mallet, A., Golmard, J. and Boisvieux, J.-F. (1984) Alternative approaches to estimation of population pharmacokinetic parameters: Comparison with the Nonlinear Mixed-Effect model. Drug Metabolism Reviews **15**, 265-292.

Steimer, J.-L., Mallet, A. and Mentre, F. (1985) Estimating interindividual pharmacokinetic variability. In: M.Rowland, L.B.Sheiner and J.-L.Steimer, (Eds.) *Variability in Drug Therapy. Description, Estimation, and Control*, pp. 65-111. New York: Raven Press

Sun, H., Fadiran, E.O., Jones, C.D., Lesko, L., Huang, S., Higgins, K.M., Hu, C., Machado, S., Maldonado, S., Williams, R., Hossain, M. and Ette, E.I. (1999) Population pharmacokinetics. A regulatory perspective. Clinical Pharmacokinetics **37**, 41-58.

Thomson, A.H., Duncan, N., Silverstein, B., Alcock, S. and Jodrell, D. (1996) Development of guidelines for gentamicin dosing. Journal Of Antimicrobial Chemotherapy **38**, 885-893.

Unadkat, J.D., Bartha, F. and Sheiner, L.B. (1986) Simultaneous modeling of pharmacokinetics and pharmacodynamics with nonparametric kinetic and dynamic models. Clinical Pharmacology And Therapeutics **40**, 86-93.

Van Houwelingen, J.C. (1988) Use and abuse of variance models in regression. Biometrics **44**, 1073-1081.

Vozeh, S. and Steimer, J.-L. (1985) Feedback control methods for drug dosage optimisation. Concepts, classification and clinical application. Clinical Pharmacokinetics **10**, 457-476.

Vozeh, S., Steimer, J.-L., Rowland, M., Mentre, F., Balant, L.P. and Aarons, L. (1996) The use of population pharmacokinetics in drug development. Clinical Pharmacokinetics **30**, 81-93.

Wade, J.R. and Karlsson, M.O., 1999. Combining PK and PD data during population PK/PD analysis. In PAGE, Sants, France. Abstract on internet http://userpage.fu-berlin.de/~page/page99/.

Wakefield, J.C. and Racine-Poon, A. (1995) An application of Bayesian population pharmacokinetic/pharmacodynamic models to dose recommendation. Statistics In Medicine 971-986.

Welker, H.A. (1998) Single- and multiple-dose mibefradil pharmacokinetics in normal and hypertensive subjects. Journal Of Pharmacy And Pharmacology **50**, 983-987.

Welker, H.A., Eggers, H. and Kleinbloesen, C.H. (1989) Ro 40-5967: Pharmacokinetics of a new calcium antagonist. European Journal Of Clinical Pharmacology **36**, A304(Abstract).

Welker, H.A. and Banken, L. (1998) Mibefradil pharmacokinetic and pharmacodynamic population analysis. International Journal Of Clinical Pharmacology Research **XVIII**, 63-71.

Welker, H.A., Wiltshire, H.R. and Bullingham, R. (1998) Clinical pharmacokinetics of mibefradil. Clinical Pharmacokinetics **35**, 405-423.

Wenk, M., Spring, P., Vozeh, S. and Follath, F. (1979) Multicompartment pharmacokinetics of netilmicin. European Journal Of Clinical Pharmacology **16**, 331-334.

Wersall, J., Lundquist, P.-G. and Bjorkroth, B. (1969) Ototoxicity of gentamicin. Journal Of Infectious Diseases **119**, 410-415.

White, L.O., MacGowan, A.P., Lovering, A.M., Holt, H.A., Reeves, D.S. and Ryder, D. (1994) Assay of low trough serum gentamicin concentrations by fluorescence polarization immunoassay. Journal Of Antimicrobial Chemotherapy **33**, 1068-1070.

Wilson, T.W., Mahon, W.A., Inaba, T., Johnson, G.E. and Kadar, D. (1973) Elimination of tritiated gentamicin in normal human subjects and in patients with severely impaired renal function. Clinical Pharmacology And Therapeutics **14**, 814-822.

Winter, M.E. (1988) Basic principles: Creatinine Clearance. In: Koda-Kimble, M.A. and Young, L.Y., (Eds.) *Basic Clinical Pharmacokinetics*, Second Edition. pp. 78-86. Vancouver: Applied Therapeutics, Inc.

Yamaoka, K., Nakagawa, T. and Uno, T. (1978) Application of Akaike's Information Criterion (AIC) in the evaluation of linear pharmacokinetic equation. Journal Of Pharmacokinetics And Biopharmaceutics **6**, 165-175.

Zaske, D.E. (1992) Aminoglycosides. In: Evans, W.E., Schentag, J.J. and Jusko, W.J., (Eds.) *Applied Pharmacokinetics. Principles of therapeutic drug monitoring*, 3rd Edition. pp. 14.1-14.47 Vancouver: Applied Therapeutics, Inc.

Zaske, D.E., Cipolle, R.J., Rostschafer, J.C., Solem, L.D., Mosier, N.R. and Strate, R.G. (1982) Gentamicin pharmacokinetics in 1640 patients: Method for control of serum concentrations. Antimicrobial Agents And Chemotherapy **21**, 407-411.

Zeitany, R.G., Saghir, N.E., Santhosh-kumar, C.R. and Sigmon, M.A. (1990) Increased aminoglycoside dosage requirements in hematologic malignancy. Antimicrobial Agents And Chemotherapy **34**, 702-708.

Zhanel, G.G., Hoban, D.J. and Harding, G.K.M. (1991) The postantibiotic effect : A review of in vitro and in vivo data. Annals Of Pharmacotherapy **25**, 153-163.